Targeting CCL18 and its cognate receptor, CCR8 to treat hypertension-associated end-organ damage

Mingyu Zhu

Bachelor of Biomedical Science Advanced with Honours

A thesis submitted for the degree of Doctor of Philosophy at

Monash University in 2020

Cardiovascular Disease Program, Biomedicine Discovery Institute,

Department of Pharmacology

Table of Contents

Copyright notice

Summary

Hypertension is associated with end-organ damage in the vasculature, heart and kidneys. Patients with resistant hypertension have uncontrolled blood pressure (BP), despite concurrent use of 3 of more antihypertensive medications. Resistant hypertension leads to severe end-organ damage and a higher risk of a cardiovascular event as compared to patients with controlled hypertension. M2 macrophages contribute to hypertension associated end-organ damage, and such function may be mediated by the chemokine, C-C motif chemokine ligand 18 (CCL18). CCL18 activates its recently identified cognate receptor, C-C motif chemokine receptor 8 (CCR8). There is no current biomarker for resistant hypertension, and the CCL18-CCR8 axis has not been studied in the context of hypertension or the associated organ damage.

To assess the role of CCL18 in resistant hypertension, and its pro-fibrotic efficacy in the human vasculature, **Chapter 3** measured plasma CCL18 levels in resistant hypertensive patients, and treated human vascular cells with CCL18. This chapter provided the first evidence that resistant hypertension is associated with elevated plasma CCL18 levels. CCL18 also targeted aortic adventitial fibroblasts and endothelial cells in the vascular wall to promote collagen synthesis and endothelial-mesenchymal transition, respectively. Therefore, we have identified CCL18 as a potential biomarker and/or therapeutic target for resistant hypertension.

The role of the CCL18-CCR8 axis in hypertension was also investigated via global deletion of CCR8 in mice (CCR8 KO mice). In **Chapter 4**, the development of angiotensin II-induced hypertension (Ang II 0.7 mg/kg/d, 14d) and its associated end-organ damage were assessed in CCR8 KO male and female mice. We have found that the genetic deletion of CCR8 provides little protection for male and female mice from systolic BP elevation or the hypertension-associated end-organ damage, in this 14d Ang II model of hypertension. However, 14 days of Ang II infusion did not cause robust end-organ damage, suggesting that a longer Ang II infusion period was required to confirm our findings. As such, we utilised a 28d Ang II (0.7 mg/kg/d) model of hypertension in **Chapter 5**, to explore the effects of genetic and pharmacological targeting of CCR8 on hypertension and its associated end-organ damage in mice. Similar to the findings of Chapter 4, neither genetic deletion, nor pharmacological targeting (by a CCR8 antagonist, R243), of CCR8 provides protection from the development of

hypertension and the associated vascular remodelling or cardiac hypertrophy, in the 28d Ang II infusion model in mice. Although vascular expression of mouse CCL8, a recently identified functional analogue of human CCL18, was elevated in hypertension, its target remains to be determined as we found both human CCL18 and mouse CCL8 were unable to activate CCR8 in chinese hamster ovary cells.

In conclusion, although CCR8 signalling may not play a role in the development of hypertension, this thesis challenges the idea that CCR8 is the cognate receptor of CCL18. We have identified CCL18 as a potential biomarker of resistant hypertension and have demonstrated a pro-fibrotic capacity of CCL18 in the vasculature. Thus, the use of CCL18 as a biomarker, together with its therapeutic targeting, will contribute to the improvement of the clinical management of resistant hypertension.

Declaration

This thesis is an original work of my research and contains no material which has been accepted for the award of any other degree or diploma at any university or equivalent institution and that, to the best of my knowledge and belief, this thesis contains no material previously published or written by another person, except where due reference is made in the text of the thesis.

Signature:

Print Name: Mingyu Zhu

Date: 22 Dec 2020

Publications and awards during enrolment

Publication manuscripts

Huang C, Lewis C, Borg NA, Canals M, Diep H, Drummond GR, Goode RJ, Schittenhelm RB, Vinh A, **Zhu M**, Kemp-Harper B, Kleifeld O, & Stone MJ (2018). Proteomic Identification of Interferon-Induced Proteins with Tetratricopeptide Repeats as Markers of M1 Macrophage Polarization. J Proteome Res. 17: 1485-1499.

Conference abstracts

Oral presentations

Zhu M, Lewis CV, Finemore MJ, Christmas T, Eikelis N, Lambert GW, Schlaich MP, Widdop RE, Samuel CS, Drummond GR, Kemp-Harper BK. The M2 macrophage-derived chemokine, CCL18 is elevated in hypertension and promotes vascular fibrosis. *ASCEPT-PAGANZ Joint Scientific Meeting (2019):* ***finalist of the Garth McQueen Prize****.*

Zhu M, Lewis CV, Finemore MJ, Lieu M, Widdop RE, Samuel CS, Drummond GR, Kemp-Harper BK. CCL18 as a potential mediator of the pro-fibrotic actions of M2 macrophages in the vessel wall during hypertension. *American Heart Association Hypertension Scientific Meeting (2019):* ***oral presentation****.*

Zhu M, Lewis CV, Nguyen V, Lam M, Bourke JE, Samuel CS, Drummond GR, Kemp-Harper BK. CCL18 as a potential mediator of the pro-fibrotic actions of M2 macrophages in the vessel wall during hypertension. *Joint HBPRCA, AAS and AVBS Meeting (2018):* ***mini-oral presentation****.*

Poster presentations

Zhu M, Lewis CV, Finemore MJ, Christmas T, Eikelis N, Lambert GW, Schlaich MP, Widdop RE, Samuel CS, Drummond GR, Kemp-Harper BK. The M2 macrophage-derived chemokine, CCL18 is elevated in hypertension and promotes vascular fibrosis. *ASCEPT-PAGANZ Joint Scientific Meeting (2019):* ***Winner of the Cardiovascular Special Interest Group Poster Prize****.*

Zhu M, Lewis CV, Nguyen V, Lam M, Bourke JE, Samuel CS, Drummond GR, Kemp-Harper BK. CCL18 as a potential mediator of the pro-fibrotic actions of M2 macrophages in the vessel wall during hypertension. *Joint HBPRCA, AAS and AVBS Meeting (2018):* ***finalist in the HBPRCA Student Poster Award session****.*

Awards

2020 Monash University

Graduate Research Completion Award

2019 ASCEPT- PAGANZ Joint Scientific Meeting, Queenstown, New Zealand

Cardiovascular Special Interest Group Poster Prize Winner

Finalist, Garth McQueen Oral Prize (one of 6 finalists)

2017-2020 Monash University

Monash International Postgraduate Research Scholarship (MIPRS)

Monash Graduate Scholarship (MGS)

Acknowledgements

There are many people who I would like to acknowledge for their generous help, support and love throughout my PhD candidature. Firstly, I would like to express my sincere gratitude to my principal supervisor, A/Prof Barbara Kemp-Harper. It has been my absolute pleasure to work with you since the third year of my undergraduate studies. You are always approachable, energetic and compassionate, and I feel extremely lucky to have you as my supervisor. You have helped me with not only the conception and design of my research projects, but also the long myography experiments, data interpretation, and thesis revising. Your passion has inspired me throughout my research journey, and I have learnt so much from you in the aspects of being a scientist, a colleague and a mentor. I would also like to thank my co-supervisor, Prof Grant Drummond. Since my Honours year, I am always thrilled by your insightful scientific views and the brilliant questions to prompt my thinking process. You have been taking time to help me despite a busy schedule and being based at La Trobe, and I am very grateful for your support and guidance.

I have received an enormous amount of help and support from the Cardiovascular and Pulmonary Pharmacology Group (CPPG) and the Department of Pharmacology at Monash University (former and current members). In particular, I would like to thank Dr Caitlin Lewis, Ms Dorota Ferens, Dr John Ling, Ms Téa Christmas, Ms Meg Finemore, Prof Robert Widdop, Dr Bradley Broughton, Dr Tracey Gaspari, and Prof Chrishan Samuel. Caitlin has made major contribution to the conception of the CCL18 project, and has taught me nearly all the in vitro laboratory techniques required for this thesis. In the experimental point of view, Dot taught me all the required animal experimental techniques; John helped me with all aspects of flow cytometry; Téa and Meg assisted me with many experiments presented in this thesis. In the intellectual input perspective, Rob (head of the department), Brad, Tracey and Chrishan (panel members of my milestone reviews) have provided me with a large amount of invaluable advice and support. I would also like to acknowledge the following departmental members for their technical assistance and advice: Mr Cameron Hollands, Dr Chao Wang, Ms Iresha Spizzo, A/Prof Jane Bourke, Mr Levi Nguyen, Dr Matt Shen, Dr Maggie Lam, Ms Samoda Rupasinghe, Ms Shirley Truong, Ms Tara Scott, Dr Yan Wang and Dr Zoe Lok. Thank you everyone from the Pharmacology Department!

I am also delighted to have amazing collaborators across the country: A/Prof Martin Stone and Dr Herman Lim (Department of Biochemistry & Molecular Biology, Monash University), Prof Markus Schlaich (Dobney Hypertension Center, The University of Western Australia), Dr Nina Eikelis and Prof Gavin Lambert (Iverson Health Innovation Research Institute, Swinburne University of Technology), Dr Antony Vinh (Department of Physiology, Anatomy & Microbiology, La Trobe University). In addition, many thanks to Monash University for the financial support by awarding me the following PhD scholarships: Monash International Postgraduate Research Scholarship (MIPRS), Monash Graduate Scholarship (MGS), and Graduate Research Completion Award (GRCA).

Finally, I would like to thank my family, extended family, mentors and friends. Although we do not reside in the same country, my parents and grandparents always have their unconditional love for me. I also appreciate the encouragement from you to make my own decisions, which has made me a confident and independent person. My Aunts and Uncles who are family friends or relatives have made me feel cared for: Xiaohua, Xiangqing, Xiang, Lisa, Min, Hong, Michael Y. My career mentors, Dama and Yugeesh, have both provided me with priceless career advice. My friends in the department have made my PhD journey more enjoyable, especially Adriana, Chao, Emma, John, Kaki, Levi, Maggie L, Matt, Ray, Samoda, Shirley and Tommy. I would also like to acknowledge my friends outside of the department: Ana, Hakan, Richard, Jiayin, Jack, Esty, Yaqi, Nichole, Trista, Lydia, Qing Z, Yutong, Xiaocao, Cecelia, Elaine, Qian, Ken. Throughout these years, especially during the COVID-19 pandemic, I have growing appreciation to the preciousness of family, friends and mentors.

List of Abbreviations

%	Percentage
≈	Approximately
°C	Degree Celsius
ACE	Angiotensin converting enzyme
ACh	Acetylcholine
Ang II	Angiotensin II
ANOVA	Analysis of variance
AoAF	Aortic adventitial fibroblast
ARB	Angiotensin receptor blockers
AT_1	Angiotensin receptor type 1
BCA	Bicinchonic acid
BMI	Body mass index
BP	Blood pressure
CCL	C-C motif chemokine ligand
CCR	C-C motif chemokine receptor
CD	Cluster of differentiation
cDNA	Complementary DNA
CI	Confidence interval
CO_2	Carbon dioxide
CRISPR	Clustered regularly interspaced short palindromic repeats
CRP	C-reactive protein
Ct	Cycle threshold
d	Day
DAF-FM	4-amino-5-methylamino-2', 7'-difluorofluorescein
DAR	Diaminorhodamine
DEA-NO	Diethylamine NONOate
dH2O	Distilled water
DMSO	Dimethyl sulphoxide
DNA	Deoxyribonucleic acid

ECL	Enhanced chemiluminescence
ECM	Extracellular matrix
EDHF	Endothelium-derived hyperpolarising factor
ELISA	Enzyme linked immunosorbent assay
End-MT	Endothelial-mesenchymal transition
eNOS	Endothelial nitric oxide synthase
ERK	Extracellular signal-regulated kinase
ER-β	Estrogen receptor-beta
ET_1	Endothelin receptor type A
FBS	Fetal bovine serum
GAPDH	Glyceraldehyde 3-phophate dehydrogenase
h	Hour
H&E	Hematoxylin and eosin
HAEC	Human aortic endothelial cells
HBC	Hydroxypropyl-β-cyclodextrin
Het	Heterozygous
HFpEF	Heart failure with preserved ejection fraction
HFrEF	Heart failure with reduced ejection fraction
HRP	Horseradish peroxidase
HTN	Hypertensive
HUVEC	Human umbilical vein endothelial cells
IFNγ	Interferon gamma
IGF-1	Insulin-like growth factor 1
IQR	Interquartile range
KO	Knockout
L-NAME	N(ω)-nitro-L-arginine methyl ester
MAP	Mean arterial pressure
mmHg	Millimeters of mercury
M-CSF	Macrophage colony-stimulating factor
MMP	Matrix metalloproteinases
mRNA	Messenger RNA

NO	Nitric oxide
NOX	NADPH oxidase
PBS	Phosphate-buffered saline
PCA	Principal component analysis
PCR	Polymerase chain reaction
PGI_2	Prostacyclin
PKCα	Protein kinase C alpha
PMSF	Phenylmethylsulfonyl fluoride
RIPA	Radioimmunoprecipitation assay
ROS	Reactive oxygen species
s.c	Subcutaneous
scRNA	Single-cell RNA
SDS-PAGE	Sodium dodecyl sulfate-polyacrylamide gel electrophoresis
SEM	Standard error of the mean
SMAD	Mothers against decapentaplegic homolog
SOD	Superoxide dismutase
SP1	Specificity protein 1
TGF-β	Transforming growth factor beta
Th2 cells	Type 2 T helper cells
TIMP	Tissue inhibitors of metalloproteinases
TLR	Tool-like receptor
vs	Versus
VVG	Verhoeff-Van Gieson
WT	Wildtype
α-SMA	Alpha-smooth muscle actin

General COVID-19 impact statement

The COVID-19 pandemic has severely impacted my PhD research program. In March this year, I had 3 months of planned experimental work to complete for this thesis (March-June), and a subsequent 3-month period of writing (July-September) prior to thesis submission. As of March 30, my research was deemed non-essential and we were required to minimise our breeding colony of CCR8 knockout mice. Thus, I was unable to complete key chronic experiments in hypertensive mice (Chapter 4-5) nor perform chemokine assays in patient plasma samples (Chapter 3). During lockdown, the structure of these chapters has been extensively revised to accommodate the incomplete data sets and the unpredictable nature of this pandemic.

In recognition of these difficult circumstances, Monash University approved an extension of my candidature and scholarships until December 2020. Although a return to the laboratory in late May, and the candidature extension, allowed completion of essential short-term experiments for this thesis, chronic experiments for Chapters 4-5 could not be conducted due to restricted breeding and limited animal numbers, leading to insufficient statistical power of some datasets. In addition, as an overseas student, the financial implication of international tuition fees precluded further extension of my PhD candidature.

Among the incomplete datasets, those of Chapter 4 were the most impacted, due to the use of littermate control mice. Relevant impacts that are specific to each chapter are further detailed in **Sections 3.1, 4.1 and 5.1**.

Chapter 1

General Introduction

1.1 Introduction

Hypertension is a major risk factor for cardiovascular events, including ischemic heart disease, heart failure and stroke (Bromfield & Muntner, 2013). As a main characteristic of hypertension, fibrosis occurs in various organs including blood vessels, the heart and kidneys, which can lead to vascular stiffening and end-organ damage (Harvey et al., 2016). While current anti-hypertensive agents (e.g. angiotensin converting enzyme inhibitors, angiotensin receptor blockers) effectively lower blood pressure, they do not directly target hypertension-associated fibrosis. As such, many patients remain at risk of a cardiovascular event, despite adequate blood pressure control (Kannel, 2009), or are resistant to anti-hypertensive therapies per se (Achelrod et al., 2015). Therefore, treatment approaches which target the underlying disease mechanism are urgently required.

Our laboratory has recently published evidence that M2 polarised macrophages accumulate in the vascular wall and contribute to the elevated blood pressure, vascular stiffening and fibrosis associated with hypertension (Moore et al., 2015). M2 macrophages serve as a major source of the pro-fibrotic chemokine, C-C motif chemokine ligand 18 (CCL18) and we hypothesise that CCL18 activates its cognate receptor, C-C motif chemokine receptor 8 (CCR8) (Islam et al., 2013) to mediate the pro-fibrotic actions of M2 macrophages in hypertension. Indeed, CCL18 is a chemoattractant and has been implicated in inflammatory skin and lung diseases, promoting pulmonary fibrosis (Schutyser et al., 2005). While CCL18 has also been associated with cardiovascular pathologies in man, including atherosclerosis (Hägg et al., 2009) and unstable angina pectoris (Kraaijeveld et al., 2007), its role in hypertension-associated fibrosis is unknown.

This thesis aims to identify the mechanisms by which CCL18 promotes fibrosis and end-organ damage in the cardiovascular and renal system and to assess the therapeutic utility of targeting the CCL18-CCR8 axis in the treatment of hypertension and its associated complications.

1.2 Hypertension and fibrosis

1.2.1 Hypertension

Hypertension is generally defined as systolic blood pressure (BP) of no less than 140 mmHg and/or diastolic BP of no less than 90 mmHg (Australian Bureau of Statistics, 2018). Hypertension affects 23% of adult Australians (Australian Bureau of Statistics, 2018), and it increases the risk of ischemic heart disease, which is the leading cause of death in Australia (Australian Bureau of Statistics, 2020) and globally (World Health Organization, 2020). Due to its high prevalence and serious consequences, hypertension has become a major health issue worldwide (Bromfield & Muntner, 2013).

Under physiological conditions, BP is controlled via the interaction of the heart (cardiac output), vasculature (constrict and dilate to control total peripheral resistance) and kidney (Na^+/H_2O excretion and blood volume control) (Drummond et al., 2019) (**Figure 1**). Hypertension arises as a consequence of disturbances to these systems and in particular, increased activity of the sympathetic nervous system (SNS) and overactivation of the renin-angiotensin-aldosterone system (RAAS) contribute to elevated BP (Drummond et al., 2019). Specifically, the SNS innervates key BP controlling organs and will lead to in increase in heart rate, vasoconstriction and increased Na^+/H_2O reabsorption (Drummond et al., 2019). In addition, SNS activation of the kidney leads to the release of renin which, together with angiotensin converting enzyme (ACE), leads to the conversion of angiotensin I to angiotensin II (Ang II) (Justin Rucker & Crowley, 2017; Messerli et al., 2018). Ang II is a powerful vasoconstrictor and also targets the adrenal medulla to release aldosterone which increases Na^+/H_2O reabsorption in the kidney (Justin Rucker & Crowley, 2017).

Hypertension is associated with changes in the structure and function of multiple target organs (end-organ damage), including the vasculature, heart and kidneys (Drummond et al., 2019). End-organ damage leads to an increased risk of cardiovascular events and renal failure (Oparil et al., 2003), and may further exacerbate the rise in BP (Drummond et al., 2019), creating a vicious cycle in chronic hypertension. Hypertension-associated vascular damage includes endothelial dysfunction (impaired vascular relaxation) (McMaster et al., 2015), vascular contraction (Touyz et al., 2018), vessel wall thickening and elastin dysregulation (breakage, irregular structure, distension) (Humphrey Jay, 2008), fibrosis (adventitial collagen

deposition) and stiffening (Drummond et al., 2019). Cardiac hypertrophy and fibrosis also occur in hypertension (Weber, 2000), whilst renal damage in hypertension is mainly characterised by inflammation (Wei et al., 2014) and interstitial fibrosis (Mezzano Sergio et al., 2001).

There has been an increasing body of evidence highlighting that females are protected from the development of hypertension and its detrimental consequences, with a lower rate of hypertension-associated mortality observed in females before menopause (Go Alan et al., 2014). Although the gender difference in the pathophysiology of hypertension requires further investigation, it has been suggested that estrogen and estrogen receptor-beta (ER-β) protects women from cardiac damage (Kessler et al., 2019). Estrogen may also exert protective effects by downregulating the expression or activity of angiotensin receptor type 1 (AT_1) in kidneys and the vasculature, and/or by limiting endothelin receptor expression in blood vessels, kidneys and the heart (Colafella & Denton, 2018). By contrast, the Y chromosome is associated with a higher BP rise in the setting of hypertension (Sampson Amanda et al., 2012).

Current pharmacological treatments for hypertension include various drug classes, with the primary treatments being ACE inhibitors, angiotensin receptor blockers (ARBs), calcium channel blockers, and diuretics (Whelton et al., 2017). As ACE is required for the conversion of angiotensin I to Ang II, ACE inhibitors reduce Ang II production and hence decrease BP (Messerli et al., 2018). Via blockade of AT_1 receptors, ARBs limit vasoconstriction and the release of aldosterone/ vasopressin in hypertension (Wright et al., 2018). Calcium channels blockers inhibit the contraction of vascular smooth muscle and myocardium, leading to subsequent BP decrease (Wright et al., 2018). Furthermore, various subclasses of diuretics, such as thiazide diuretics, lower BP by limiting sodium and water retention via various mechanisms, such as blockade of the electroneutral sodium-chloride cotransporter or the Na-K-Cl cotransporter (Blowey, 2016).

Despite the large number of therapeutic options, 5-10% of patients have treatment resistant hypertension (de la Sierra et al., 2011), where treatment resistance is generally defined having uncontrolled BP (≥ 140/90 mmHg) with at least 3 classes of antihypertensive medications (de la Sierra et al., 2011). Of note, resistant hypertension may sometimes arise as patients are

nonadherent to anti-hypertensive medications (Achelrod et al., 2015), which may account for the variability in the reported prevalence of resistant hypertension. Nonetheless, after controlling for medication adherence, patients with resistant hypertension are still under increased risk of cardiovascular events, such as myocardial infarction, heart failure and stroke (Daugherty et al., 2012). Recently, researchers have reported renal denervation (surgical ablation of renal nerves) as a potential treatment option for resistant hypertension (Azizi et al., 2018; Townsend et al., 2017), where pharmacological therapies are ineffective. In addition, even with their BP well controlled, up to 25% patients are still at risk of a cardiovascular event (Kannel, 2009). This is due, to a large extent, to the inability of current anti-hypertensive medications to directly target the end-organ damage and fibrosis that is associated with hypertension. As such, new treatment approaches are needed which target the underlying disease mechanisms.

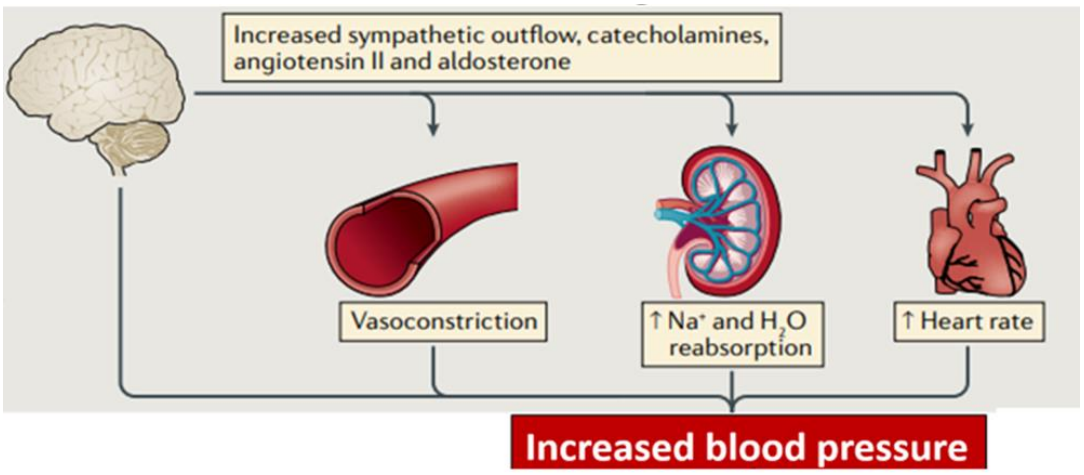

Figure 1. Schema of blood pressure controlling organs in hypertension (Adapted from Drummond et al., 2019).

1.2.2 Hypertension-associated fibrosis

A key role of the immune system in hypertension and its associated end-organ damage has recently been identified, with effector T cells and monocyte/ macrophages infiltrating into arteries, heart and kidney promoting cardiovascular and renal damage, fibrosis and associated dysfunction (Norlander et al., 2018). The proposed roles of T cells and

macrophages are summarised in **Table 1**. Thus effector CD4+ helper T cells and CD8+ T cells both accumulate in target organs and release inflammatory cytokines, such as Interferon gamma (IFNγ), to stimulate inflammation in hypertension (Drummond et al., 2019). T cell-derived cytokines promote infiltration of other immune cells, including monocytes/ macrophages, into target organs to potentiate hypertension-associated inflammation and fibrosis (Drummond et al., 2019). In addition, CD4+ T cells may stimulate autoantibody production from B cells, which can in turn exacerbate BP elevation. Of note, the role of T cells in hypertension has not been fully elucidated, and other T cell subtypes may also play integral roles in the disease pathophysiology (Drummond et al., 2019), a concept which will not be the focus of this thesis. During hypertension, monocytes also infiltrate into the vessel wall, and they undergo differentiation followed by polarisation (Chinetti-Gbaguidi et al., 2015; Hilgers, 2002). This process results in the accumulation of both the pro-inflammatory "M1" and the pro-fibrotic "M2" subtypes of macrophages in the vasculature, with the M2 macrophages being the predominant subtype in chronic hypertension (Moore et al., 2015). M1 macrophages promote vascular inflammation and endothelial dysfunction in hypertension, via the generation of reactive oxygen species (ROS) and inflammatory cytokines (Kossmann et al., 2014). By contrast, M2 macrophages release pro-fibrotic cytokines and chemokines (e.g. transforming growth factor-β; TGF-β), causing not only endothelial dysfunction, vascular remodelling and fibrosis, but also diastolic dysfunction in the heart (Chinetti-Gbaguidi et al., 2015; Drummond et al., 2019). The M2 macrophage subtype will be the main focus of this thesis due to the finding that M2 macrophages are the key player in chronic hypertension (Moore et al., 2015). The role of M2 macrophages in hypertension-associated fibrosis is further described in **Section 1.2.3**.

A main characteristic of hypertension is vascular stiffening, which mainly occurs in conduit arteries such as the common carotid artery and the aorta (Oparil et al., 2003). Stiffened arteries have lowered capacity to buffer cardiac pulse, leading to increased cardiac afterload (resistance) and higher pulse waves in the periphery (**Figure 2**) (Briet et al., 2012). The high pulse pressure can cause target organ damage (including left ventricular hypertrophy) and impaired coronary perfusion, which increases the risks of myocardial infarction, heart failure and stroke (Oparil et al., 2003). Stiffening in the hypertensive vasculature can arise as a consequence of elastin fibre loss and the replacement with rigid collagen (fibrosis) (Oparil et

al., 2003). Hypertension is associated with the disorganisation and breakage of elastin fibers, and the loss of elastin content in the vasculature (Oparil et al., 2003). Such changes reduce elasticity of conduit arteries and hence contribute to arterial stiffness, which has been suggested to precede hypertension (Le et al., 2011). In addition, in response to inflammation associated vascular injury during the development of hypertension, myofibroblasts, vascular smooth muscle cells (VSMCs) and fibrocytes (a monocyte-derived myofibroblast precursor) generate collagen to promote tissue healing (An et al., 2015; Wanjare et al., 2015; Wu et al., 2016). Whilst an acute wound healing response is necessary to maintain tissue integrity and function, persistent and chronic immune activation can stimulate excessive collagen generation, which can lead to fibrosis and end-organ damage (Harvey et al., 2016). Therefore, chronic inflammation might be responsible for the excessive collagen deposition and subsequent vessel stiffening in hypertension.

Specifically, hypertension causes increased release of pro-fibrotic mediators, such as TGF-β (Harvey et al., 2016), which target collagen-producing vascular cells to stimulate fibrosis. TGF-β has been reported to promote the differentiation of monocyte-derived fibrocytes and resident fibroblasts into myofibroblasts (Mori et al., 2005). Myofibroblasts are characterised by increased expression of α-smooth muscle actin (α-SMA), and they possess a high capacity to generate collagen (Wang et al., 2017) (**Figure 3**). Endothelial cells can also undergo endothelial-mesenchymal transition (End-MT) in response to TGF-β, and the resultant mesenchymal progenitors adopt a myofibroblast-like phenotype to produce collagen (Zhang et al., 2016). The process of End-MT is characterised by the loss of endothelial markers (such as VE-cadherin and von Wilebrand factor), and the up-regulation of myofibroblast markers (such as α-SMA and vimentin) (Sánchez-Duffhues et al., 2018).

The above-mentioned pro-fibrotic processes may increase the generation of different collagen types. In the vasculature, the fibrillary collagen types I, III and V, and the basement membrane collagen type IV are present (Osidak et al., 2015). Collagen I, III, and, to a lesser extent, V, are produced by VSMCs and myofibroblasts in the media and adventitia, respectively (Osidak et al., 2015). Collagen I and III are the major contributors to the vascular stiffness in hypertension, with collagen I being the most abundant among all types, constituting approximately two thirds of total collagen mass in the aorta (Osidak et al., 2015). Thus collagen producing cells synthesize pro-collagen chains with N- and C-propeptides at

either end, such as two collagen 1A1 and one collagen 1A2 chains for collagen I (Canty & Kadler, 2005). These pro-collagen chains are cleaved by specific N- and C-proteinases to generate collagen fibrils, which subsequently assemble to form collagen fibres the key component of extracellular matrix (ECM) (Canty & Kadler, 2005). Moreover, collagen fibres can be degraded into fragments by matrix metalloproteinases (MMPs), which also play a complex role (pro-fibrotic or anti-fibrotic depending on MMP subtypes) in ECM remodelling (Giannandrea & Parks, 2014).

Arterial stiffness is an independent risk factor for cardiovascular diseases and hypertension (Dumor et al., 2018). In fact, there is growing evidence that vascular stiffening precedes hypertension (Golob et al., 2015; Herrera et al., 2014; Kaess et al., 2012; Le et al., 2011). On the other hand, cardiac and renal fibrosis normally occur subsequent to the chronic elevation in blood pressure. In the heart, interstitial and perivascular fibrosis are both associated with hypertension, which might arise due to exposure of the heart to high pulse pressure as a consequence of arterial stiffening (Diez, 2007). It is also proposed that inflammation and oxidative stress contribute to cardiac fibrosis in hypertension, by chronically stimulating tissue reparative mechanisms (Diez, 2007). Similarly, it has been suggested that glomerular and tubulointerstitial fibrosis in kidneys may be promoted by arterial stiffening and/or oxidative stress (Jia et al., 2014; Zhao et al., 2008). Therefore, it is not surprising that hypertension-associated fibrosis is closely linked to inflammation, where macrophages play a crucial role.

Current anti-hypertensive therapies do not directly target hypertension-associated fibrosis (Whelton et al., 2017). While ACE inhibitors and ARBs effectively lower BP, they may only delay the progression of fibrosis and end-organ damage by a matter of months (Yu, 2003). In general, the number of approved anti-fibrotic medications are limited, and the first anti-fibrotic drug pirfenidone was approved recently by the American Food and Drug Administration in 2014 (Margaritopoulos et al., 2016; Tsou et al., 2014). Pirfenidone is a treatment for idiopathic pulmonary fibrosis, targeting TGF-β mediated lung fibrosis via unclear mechanisms (Margaritopoulos et al., 2016; Tsou et al., 2014). However, pirfenidone produces various off-target side effects including gastrointestinal symptoms and photosensitivity reactions (Margaritopoulos et al., 2016). As such, new therapeutic strategies for hypertension and the associated fibrosis are urgently required and targeting the immune component of the disease may represent a novel approach.

Table 1. The roles of M1 and M2 macrophages, CD4+ T helper cells and CD8+ T cells in hypertension.

Cell type	Function	Evidence of contribution to hypertension
M1 Macrophages	Production of inflammatory cytokine (e.g. IL-1β) and ROS	Promote vascular inflammation and endothelial dysfunction
M2 Macrophages	Production of pro-fibrotic and inflammatory cytokines, such as TGF-β and CCL18	Cause endothelial dysfunction, vascular remodelling and fibrosis, and promote diastolic dysfunction in the heart *Role of CCL18 in hypertension has not been studied*
CD4+ T helper cells	Release of inflammatory cytokines, such as IFNγ, in target organs; Activation of B cells	Attract and activate other immune cells, such as monocytes/ macrophages, may impact vascular and cardiac function as described for M1 and M2 macrophages above Promote inflammation of the target organs; May further elevate BP via B cell-derived autoantibodies
CD8+ cytotoxic T cells	Release of inflammatory cytokines, such as IFNγ and TNF, in target organs	Attract and activate other immune cells, such as monocytes/ macrophages, may impact vascular and cardiac function as described for M1 and M2 macrophages above Impair renal tubular sodium transport and promote endothelial dysfunction

ROS = reactive oxygen species, IFNγ = Interferon gamma, TNF = tumour necrosis factor, BP = blood pressure. Relevant evidence of contribution to hypertension is based on data published from experimental models of hypertension. Summarised from (Drummond et al., 2019) and (Chinetti-Gbaguidi et al., 2015).

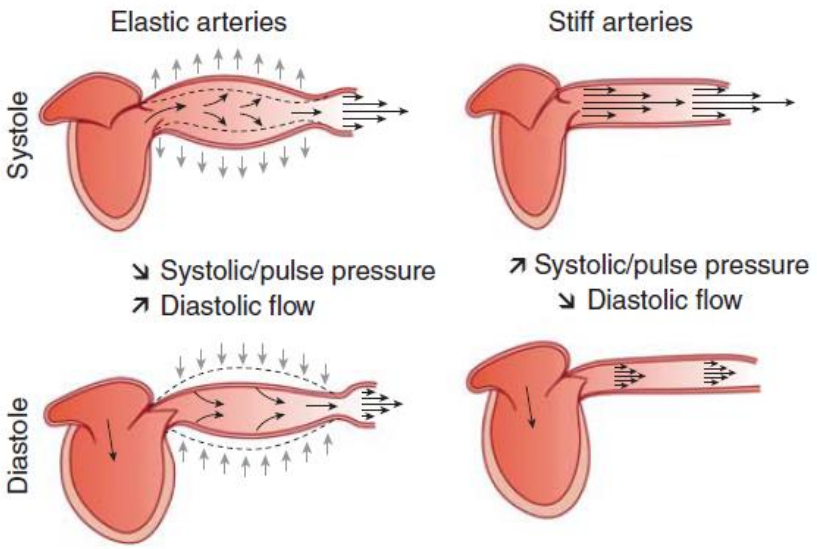

Figure 2. Schema of arterial stiffening, and its impacts on pulse pressure and diastolic flow (Briet et al., 2012).

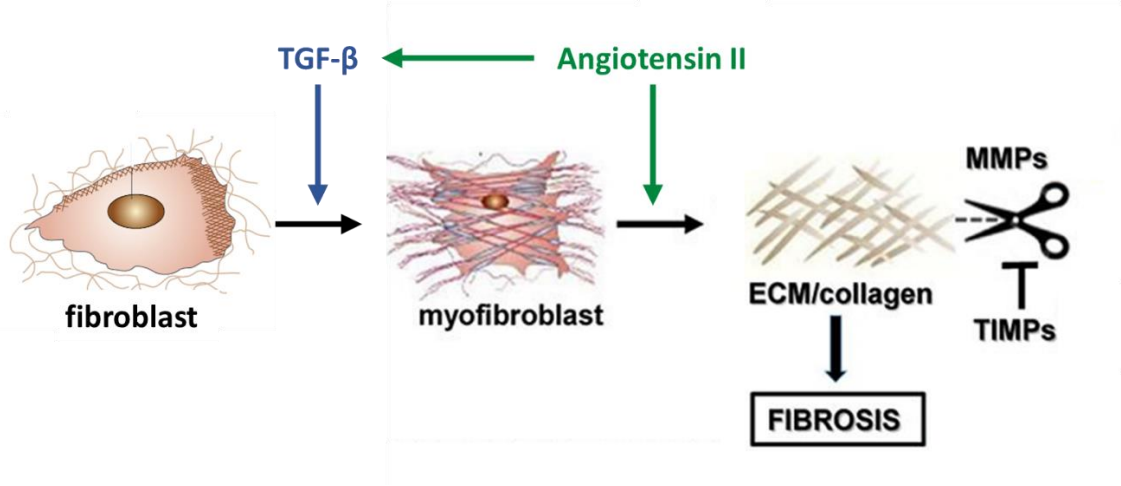

Figure 3. Schema of the general fibrotic pathways. ECM = extracellular matrix, MMP = matrix metalloproteinases, TIMP = tissue inhibitors of matrix metalloproteinases. Adapted from (Wang et al., 2017).

1.2.3 Role of M2 macrophages in hypertension-associated fibrosis

As mentioned in **Section 1.1**, it is believed that pathological fibrosis is the primary cause of vascular stiffening in hypertension and contributes to cardiac and renal dysfunction. Fibrosis

occurs to assist in tissue healing, whilst pathological fibrosis usually involves chronic excessive production of collagen that forms ECM, predominantly from fibroblasts /myofibroblasts (Harvey et al., 2016). This process is initiated by chronic inflammation with unsolved tissue injury, mediated by pro-fibrotic stimuli (such as Ang II and TGF-β) and counteracted by MMPs, while MMPs can also be inhibited by tissue inhibitors of metalloproteinases (TIMPs) (Harvey et al., 2016) (**Figure 3**).

It has been suggested that macrophages play a key role in not only hypertension but also its associated fibrosis. Thus the loss of macrophage colony-stimulating factor (M-CSF) in mice limits macrophage accumulation in the vessel wall, which in turn protects mice from Ang II-induced hypertension and the associated vascular remodelling (De Ciuceis et al., 2005). Similarly, M-CSF deficient mice are also protected in a one kidney/deoxycorticosterone acetate (DOCA)-salt model of hypertension (Ko et al., 2007). In addition, selective depletion of circulating monocytes markedly reduced macrophage numbers in the vessel wall and attenuated Ang II-induced hypertension as well as vascular dysfunction (Wenzel et al., 2011). Such protective effects in hypertension were lost with adoptive transfer of Ly6C^{high} monocytes, suggesting a key role of monocytes/macrophages in hypertension (Wenzel et al., 2011). As mentioned in **Section 1.2.2**, the subsets of macrophages in hypertension are of interest. Macrophages can be polarised to multiple phenotypes by different cytokines, with the two ends of the spectrum being M1 and M2 macrophages (Chinetti-Gbaguidi et al., 2015). The M1 phenotype is promoted by type 1 T helper (Th1) cytokines such as IFN-γ, and M1 macrophages are key contributors to vascular damage in the early stages of hypertension, via the secretion of pro-inflammatory cytokines, ROS and MMPs (Chinetti-Gbaguidi et al., 2015; Kossmann et al., 2014). On the other hand, Th2 cytokines such as interleukin- (IL)-4 and IL-13 polarise macrophages towards the M2 phenotype, which oppose the effects of M1 macrophages (Chinetti-Gbaguidi et al., 2015) (**Figure 4**). M2 macrophages promote resolution of inflammation by releasing anti-inflammatory cytokines, whilst in the later stages of hypertension, they contribute to vascular fibrosis (Chinetti-Gbaguidi et al., 2015; Moore et al., 2015). Thus, M2 macrophages have been reported to accumulate in the vessel wall during the later stages of hypertension in mice (0.7 mg/kg/d Ang II, 28-day infusion) (Moore et al., 2015). The infiltration of Ly6C^{high} monocytes in this hypertension model is also blocked with a CCR2 antagonist, INCB3344, which led to a subsequent decrease in aortic M2 macrophages (Moore

et al., 2015). As such, findings that INCB3344 reduces systolic BP, reverses aberrant collagen deposition and vascular stiffening further support a causal role of M2 macrophages in hypertension-associated vascular fibrosis. Moreover, M2 macrophages have been implicated in myocardial and renal fibrosis in hypertension (Falkenham et al., 2015; Guiteras et al., 2016).

Collectively, these findings suggest that targeting M2 macrophage accumulation and/or function may represent a novel approach for reducing blood pressure and associated end-organ fibrosis and damage. Indeed, it is well recognised that M2 macrophages release growth factors such as insulin-like growth factor 1 (IGF-1) to promote VSMC proliferation and subsequent vascular remodelling, and they also produce pro-fibrotic agents such as TGF-β to induce collagen deposition (Chinetti-Gbaguidi et al., 2015). Interestingly, M2 macrophages also generate a pro-fibrotic chemokine known as C-C motif chemokine ligand 18 (CCL18) (Schutyser et al., 2005), and we have shown that they release much higher levels of CCL18 than TGF-β (Lewis, 2017) (**Figure 5A-B**). Currently, the role of CCL18 in hypertension-associated fibrosis remains to be explored.

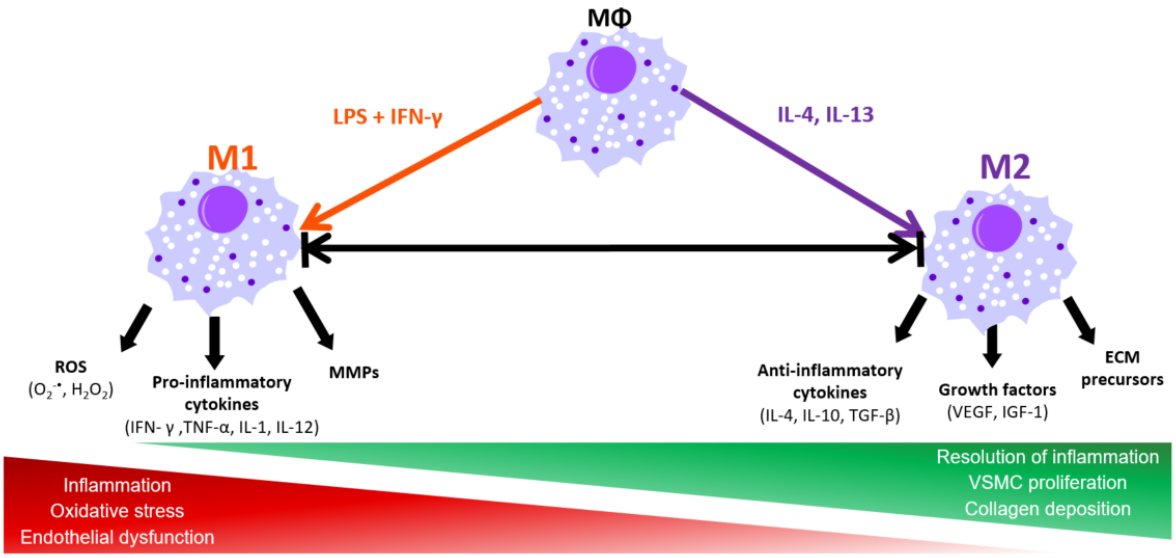

Figure 4. Characteristics and functions of M1 and M2 macrophages. IFN-γ: interferon-γ, ROS: reactive oxygen species, TNF: tumour necrosis factor, MMPs: matrix metalloproteinases, TGF-β: transforming growth factor-β, VEGF: Vascular endothelial growth factor, IGF-1: insulin-like growth factor 1, ECM: extracellular matrix, VSMC: vascular smooth muscle cell. (Courtesy of McConaghy TE, 2015).

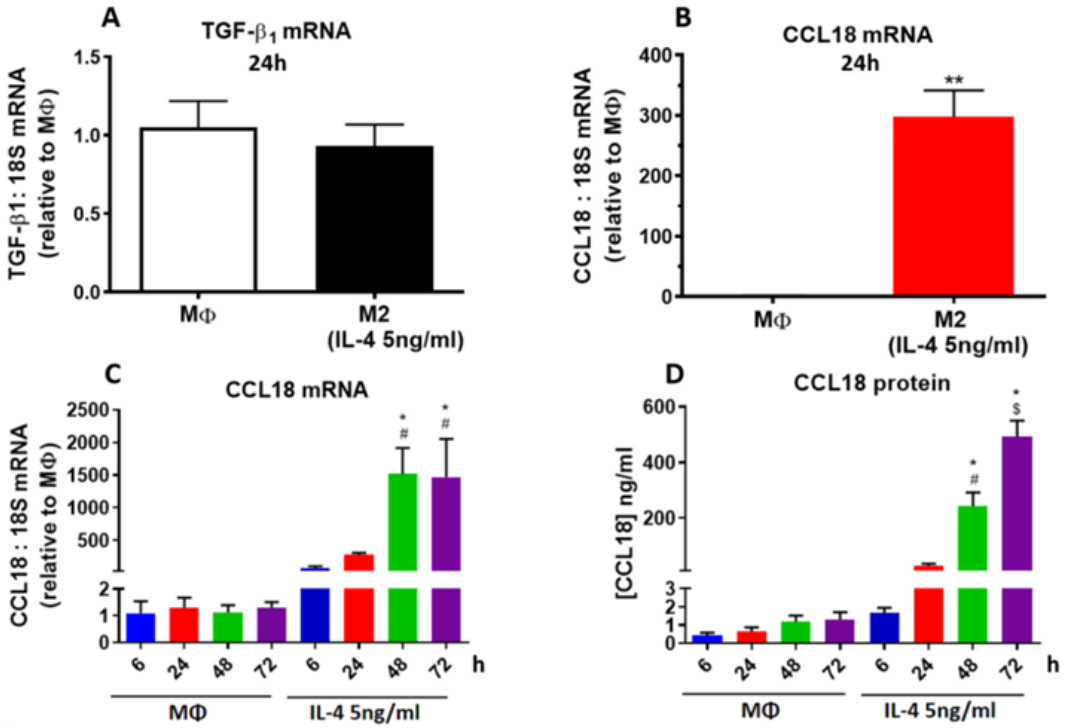

Figure 5. Effects of IL-4 (M2 stimulus) on the expression of TGF-β1 and CCL18 in human primary macrophages. TGF-β1 mRNA (A), CCL18 mRNA (B-C) and CCL18 protein (D) expression following treatment of M-CSF (50ng/ml) differentiated human primary macrophages with IL-4 (5ng/ml; 6-24h). Data presented as mean ± SEM, mRNA fold changes expressed relative to MΦ (untreated), n= 4-7. * $p<0.05$ vs. MΦ (at the same time point); # $p<0.05$ vs. 6h and 24h; $ $p<0.05$ vs. 6h, 24h and 48h (One-way ANOVA, Sidak's post hoc test). (Lewis, 2017; Zhu, 2016)

1.3 CCL18, a pro-fibrotic chemokine

1.3.1 General actions and signalling of CCL18

CCL18, also known as pulmonary and activation-regulated chemokine (PARC) or macrophage inflammatory protein-4 (MIP-4), is generated predominantly by monocytes/macrophages. Other cellular sources of CCL18 include dendritic cells, dermal fibroblasts and leukaemia cells (Schutyser et al., 2005). Alveolar macrophages constitutively express high levels of CCL18 (Schraufstatter et al., 2012), and while the constitutive expression of CCL18 in other monocytes/macrophages is low, the expression can be up-regulated by LPS (pro-inflammatory) and Th2 cytokines (promotes M2 macrophage polarisation) (Schutyser et al., 2005). Consistent with the published findings, studies in our laboratory have shown that in human primary macrophages, the M2 stimulus IL-4 substantially increased CCL18 mRNA and protein expression by up to 400- and 1500-fold, respectively (Lewis, 2017; Zhu, 2016) (**Figure 5C-D below Section 1.2**).

The human CCL18 gene is located on chromosome 17q11.2 (Hieshima et al., 1997), which encodes a precursor protein of 89 amino acids, followed by cleavage of 29 amino acids to produce mature CCL18 (60 amino acid) (Hieshima et al., 1997). To date, three isoforms of human CCL18 have been identified: 1-68, 3-69 and 4-69 (Schutyser et al., 2002; Schutyser et al., 2001), all of which contain two-disulfide bonds (Cys10-Cys34 and Cys11-Cys50), with the Cys10-Cys34 disulfide bond key to CCL18-mediated chemotaxis (Legendre et al., 2013). Whilst the CCL18 gene and protein in rhesus macaque are approximately 90% similar to human CCL18 (Basu et al., 2002), no rodent ortholog has been identified (Chenivesse & Tsicopoulos, 2018). Despite being only 31% identical to human CCL18, mouse CCL8 has been identified as the functional analogue of human CCL18 (Islam et al., 2013) (**detailed in Section 1.3.2**).

Chemotactic and inflammatory effects of CCL18

CCL18 plays an important role in various inflammatory and fibrotic pathways. It has a chemotactic effect on human naïve T cells (Günther et al., 2005) and to a lesser extent Th2 cells, memory T cells, B cells, immature dendritic cells and bone marrow progenitor cells (Chenivesse & Tsicopoulos, 2018; Günther et al., 2005; Schutyser et al., 2005). CCL18 also acts on monocytes /macrophages to promote chemotactic responses, as well as M2 polarisation,

calcium mobilization and actin polymerization (Schraufstatter et al., 2012; Schutyser et al., 2005). In addition, human CCL18 is found to attract mouse memory T cells (Günther et al., 2005) and mouse splenocytes (Bruna-Romero et al., 2003).

Of note, the chemotactic actions of CCL18 are not as strong as many other chemokines, such as CXCL12 (Chenivesse & Tsicopoulos, 2018). Whilst it attracts regulatory T cells and Th2 cells, CCL18 simulates generation of IL-10 from dendritic cells (Azzaoui et al., 2011), which in turn inhibits proliferation of effector T cells and hence may limit excessive inflammation (Chenivesse et al., 2012). This process is suggested to maintain tolerance of the human body to environmental stimuli, protecting healthy humans from allergy (Azzaoui et al., 2011). CCL18 may also inhibit chemotaxis by antagonising CCR3 and negating the chemoattractant response to CCL11 and CCL13 (Nibbs et al., 2000). In addition, it inhibits CCR1-, CCR2-, CCR4- and CCR5-mediated chemotactic responses, via binding to glycosaminoglycans, resulting in the displacement of Cis-presented glycosaminoglycan-bound chemokines (Krohn et al., 2013) (further described in **Section 1.3.3**). As such, CCL18 is generally considered to have a regulatory role under physiological conditions.

To further support the regulatory role of CCL18, this chemokine, as mentioned previously, promotes monocyte differentiation to the M2 macrophage phenotype (as mentioned above) (Schraufstatter et al., 2012). M2 macrophages have a high capacity of for phago/pinocytosis and led to up-regulation of the expression of inflammatory chemokines such as CXCL8, CCL2, CCL3 and CCL22, was well as anti-inflammatory cytokines such as IL-10 (Chinetti-Gbaguidi et al., 2015). Although not tested to date, CCL18 may also promote inflammation via stimulating ROS generation from immune cells. As will be discussed subsequently, CCL18 can activate PKCα (protein kinase C alpha) (Luzina et al., 2006a), a key activator of NADPH oxidase 2 (NOX2) (Brandes et al., 2014). The primary function of NOX2 is the generation of the ROS, superoxide ($\cdot O_2^-$) (Paik et al., 2014). Moreover, NOX2 is the predominant isoform in macrophages and is involved in pathogen removal as well as organ damage (Lewis et al., 2019). Indeed our laboratory has shown that M2 macrophages generate H_2O_2 to promote fibrosis (Lewis et al., 2019). These findings collectively suggest complex roles of CCL18 in chemotactic, inflammatory and fibrotic responses.

Pro-fibrotic activity of CCL18

The pro-fibrotic actions of CCL18 have been demonstrated in the healthy lung and skin (Atamas et al., 2003). CCL18 may also facilitate the recovery of burn injury (Ridiandries et al., 2018), and is substantially elevated in chronic skin wounds (Kroeze et al., 2012). The pro-fibrotic actions of CCL18 are due, in part to its ability to stimulate T cell infiltration (Pochetuhen et al., 2007; Wynn & Ramalingam, 2012). Thus, CCL18 overexpression induces pulmonary fibrosis in mice, via the recruitment of α5 integrin-expressing T cells and the subsequent increase in collagen production from lung fibroblasts (Luzina et al., 2009). CCL18 can also directly stimulate collagen production from healthy lung fibroblasts, via activation of an unidentified G-protein coupled receptor and the subsequent phosphorylation and activation of the extracellular signal-regulated kinase (ERK) pathway (ERK1 or ERK2) (Atamas et al., 2003; Schutyser et al., 2005). Phosphorylated ERK1/2 modulates the expression of cell cycle regulator genes and hence leads to increased proliferation of fibroblasts and myofibroblasts (Fujiwara et al., 2014), which will be further described in **Section 1.3.3**. Importantly, anti-fibrotic effects of CCL18 have also been reported in a bleomycin-induced pulmonary fibrosis model (Pochetuhen et al., 2007). As such, CCL18 might have biphasic effects on fibrosis depending on different milieu (Pochetuhen et al., 2007), a concept that remains to be investigated.

In the vasculature, CCL18 promotes End-MT in human umbilical vein endothelial cells (HUVECs) (further details in **Section 1.3.2**), an action that is particularly relevant in the context of cancer angiogenesis and metastasis (Lin et al., 2015). In fact, tumour associated macrophages, as well as cancer cells themselves, generate high levels of CCL18 (Leung et al., 2004; Meng et al., 2015). In cancer, CCL18 also promotes the transition of epithelial cells to a mesenchymal phenotype (epithelial-mesenchymal transition), which is associated with tumour metastasis (Meng et al., 2015). Other than their ability to migrate, endothelial or epithelial-derived mesenchymal cells gain the ability to generate collagen (Goldmann et al., 2018; Lin et al., 2015), and hence may promote fibrosis in other disease states, a concept yet to be explored.

1.3.2 CCL18 receptor and functional analogue

Until recently, research on CCL18 has been limited by the lack of identified receptors and a murine orthologue. In 2013, a G-protein coupled receptor, CCR8 was found to be activated by CCL18 (Islam et al., 2013). Islam et al. (2013) showed that CCL18 induced calcium influx and the migration (chemotaxis) of CCR8-transfected 4DE4 cells (mouse pre-B cell line) in a concentration-dependent manner. CCL18 also causes internalisation of CCR8 following activation. Researchers have reported CCR8 expression on various subtypes of T cells, including Th2 cells, skin homing CLA+ T cells and regulatory T cells, but not naïve T cells (Chenivesse & Tsicopoulos, 2018). To date, a role of CCR8 in mediating the pro-fibrotic actions of CCL18 has not been reported. It should also be noted that CCL1 can also activate CCR8 on leukocytes (mainly Th2 cells) (Connolly et al., 2012; Zingoni et al., 1998), mediating the migration and infiltration of these immune cells to sites of inflammation, in an ERK1/2-dependent manner (Connolly et al., 2012; Louahed et al., 2003). Furthermore, consistent with the chemotactic effects of CCL18, CCL1 activates CCR8 to promote monocyte/macrophage chemotaxis (Haque et al., 2004; Islam et al., 2013). Despite the ability of both chemokines to activate CCR8, the chemotactic actions of CCL1 are greater than those of CCL18 (Islam et al., 2013). However, as CCL18 is more highly expressed in inflammation (Islam et al., 2011), it is likely to be the key modulator of CCR8 function in diseases such as hypertension.

In addition to T cells and monocytes/macrophages, CCR8 is also expressed on cultured VSMCs and human umbilical vein endothelial cells (HUVECs) (Haque et al., 2004). Preliminary research from our laboratory has demonstrated CCR8 expression in intact mouse aorta (both normotensive and hypertensive), in the adventitia and perivascular fat (Zhu, 2016; **Figure 6**). Although CCR8 mRNA has been found in chicken adipose tissue (Hausman et al., 2014), there is little evidence supporting a role of adipocytes in hypertension-associated fibrosis. Rather, cells that have pro-fibrotic capacities in the perivascular fat include T cells, fibroblasts and fibrocytes. We anticipate that CCL18 may target CCR8 on these cell types, thereby promoting collagen deposition and leading to vascular fibrosis (Atamas et al., 2003; Wanjare et al., 2015; Yeager et al., 2011). We have also found co-localisation of CCR8 and endothelial cells in mouse aorta (Zhu, 2016; **Figure 6**). Interestingly, it has been reported that CCL18 can promote endothelial-mesenchymal transition (End-MT) in HUVECs (Lin et al., 2015), and by undergoing End-MT, endothelial cells gain the ability to produce collagen and stimulate hypertension-

associated fibrosis (Wu et al., 2016). Collectively, VSMCs, T cells, fibroblasts, fibrocytes, and endothelial cells are potential cellular targets of CCL18 in the vasculature, which might promote hypertension-associated fibrosis following CCR8 activation.

In addition to CCR8 activation, CCL18 can also competitively antagonise CCR3 (Krohn et al., 2013). Such antagonism might limit inflammation as CCR3 mediates leukocyte (mainly Th2 cells and eosinophils) infiltration into inflammatory sites in the setting of allergy (Nibbs et al., 2000). Furthermore, CCR3 activation contributes to pulmonary fibrosis (Komai et al., 2010), possibly via ERK1/2 signalling (Shamri et al., 2013) and subsequent modulation of collagen-producing fibroblasts (Huber et al., 2002). These relevant studies suggest that the pro-fibrotic effects of CCL18 might be tempered by its ability to antagonise CCR3.

Furthermore, an ability of CCL18 to modulate CCR1, CCR2, CCR4 or CCR5 may counter its pro-fibrotic actions. Thus, although CCL18 is not a ligand for these chemokine receptors, it inhibits their activation by displacing glycosaminoglycan-bound chemokines on these receptors (Krohn et al., 2013). These receptors promote infiltration of monocytes/macrophages (expressing CCR1, 2 and 5) and T cells (expressing CCR4) into sites of inflammation, and are also expressed on collagen producing VSMCs (CCR1 and 2) (Hayes et al., 1998). In addition, given that CCR1, 2, 4 and 5 are all pro-fibrotic (Pignatti et al., 2006; Seki et al., 2009a; Seki et al., 2009b), the inhibitory action of CCL18 is likely to reduce its ability to stimulate fibrosis via CCR8. Collectively, the ability of CCL18 to activate CCR8 and to inhibit CCR1-5 might account for its previously mentioned biphasic effects on pulmonary fibrosis (Pochetuhen et al., 2007) (**Table 2**).

In addition to CCR8, CCL18 has been shown to activate two other receptors under pathophysiological conditions, namely PITPNM3 (Chen et al., 2011) and G protein-coupled receptor 30 (GPR30) (Catusse et al., 2010). PITPNM3 is overexpressed in cancer cells, mediating CCL18-induced migration of breast cancer cells as well as tumour-associated naive T cells (Su et al., 2017). CCL18 also inhibits the migration and proliferation of lymphocytes by activating GPR30 on acute lymphocytic leukemia B cells (Catusse et al., 2010). However, the agonist action of CCL18 on PITPNM3 and GPR30 has only been reported in cancer or tumour-associated cells.

Together with the identification of CCR8 as the cognate receptor for CCL18, mouse CCL8 (mCCL8) has also recently been identified as functional analogue of human CCL18 (hCCL18) (Islam et al., 2013). Thus, like macrophage-derived hCCL18, mCCL8 mRNA expression in mouse macrophages is up-regulated by the M2 stimuli, IL-4 and IL-10 (Islam et al., 2013). Both hCCL18 and mCCL8 activate CCR8, and produce similar concentration-dependent chemotactic effects on polarised Th2 cells that have elevated CCR8 expression (Islam et al., 2011; Islam et al., 2013). The identification of the CCL18 receptors and mouse functional analogue allows the physiological and pathophysiological roles of CCL18 to be more thoroughly investigated. For example, genetic and pharmacological tools can be used to delineate the role of the hCCL18/mCCL8-CCR8 axis in health and disease. CCR8 knockout mice have been used to investigate the role of CCR8 in acute colitis, with mice being viable and without reported phenotypic changes (Oshio et al., 2014). Furthermore, treatment of mice with a small molecule CCR8 antagonist, R243, has been used to explore the role of CCR8 in acute colitis (Oshio et al., 2014) and extracellular vesicle uptake mechanisms in cancer (Berenguer et al., 2018). AZ084, another small molecule CCR8 antagonist, has been shown to inhibit in vitro leukocyte infiltration mediated by CCR8 (Connolly et al., 2012). However, AZ084 was not commercially available when this research program commenced.

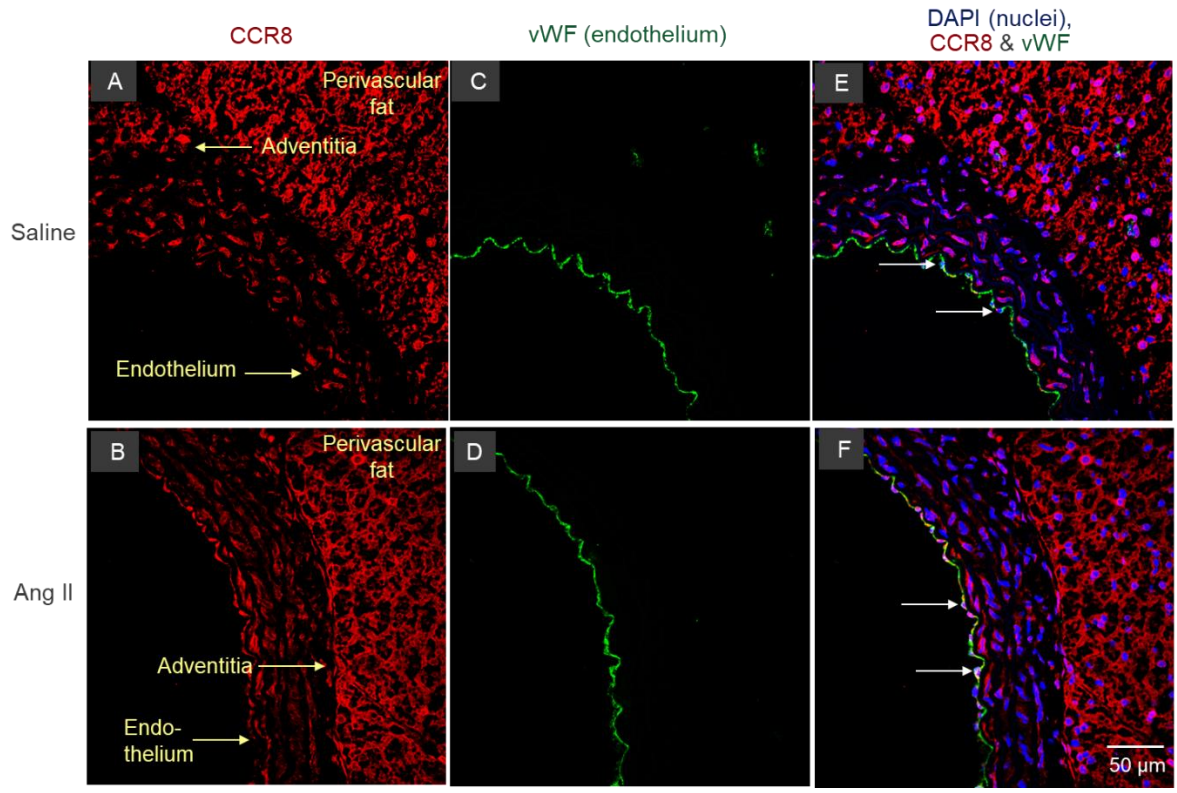

Figure 6. Localization of CCR8 and endothelial cells in the aorta from normotensive and Angiotensin II-induced hypertensive mice. Localization of (A-B) CCR8 and (C-D) von Willebrand Factor (vWF, endothelial marker), and (E-F) co-localization of DAPI (nucleated cells), CCR8 and vWF in the aorta, from 28d saline (top panels) or Angiotensin II (bottom panels) treated mice. Images were taken at a magnification of X40. Representative images from n=6 are shown. (Zhu, 2016)

Table 2. Characteristics of chemokine receptors targeted by CCL18.

Receptors	Stimulated/ Inhibited by CCL18	Cell types expressing receptors	Actions of receptors	References
CCR8	Stimulated	Leukocytes, VSMCs, HUVECs	Chemotaxis, possibly pro-fibrotic	(Haque et al., 2004; Islam et al., 2013)
CCR3	Inhibited (antagonism)	Mainly eosinophils, Th2 cells and fibroblasts	Chemotaxis, pro-fibrotic	(Huber et al., 2002; Komai et al., 2010; Krohn et al., 2013)
CCR1, 2, 4, 5	Inhibited (via displacement of bound GAG chemokines)	CCR1 and CCR2: monocytes, macrophages, VSMCs CCR4: mainly T cells CCR5: monocytes, macrophages	Chemotaxis, pro-fibrotic	(Krohn et al., 2013; Matsuo et al., 2016; Pignatti et al., 2006; Seki et al., 2009a; Seki et al., 2009b; Vestergaard et al., 2004)

VSMCs: vascular smooth muscle cells, HUVECs: human umbilical vein endothelial cells, Th2 cells: type 2 T helper cells, GAG= glycosaminoglycan.

1.3.3 Mechanisms via which CCL18 regulates fibrosis

Given the CCL18 receptor and murine functional analogue have only been recently identified (Islam et al., 2013), the mechanism(s) via which CCL18 promotes fibrosis remain unclear. However, studies to date have proposed the potential involvement of several signalling pathways (**Figure 7**).

First, in the setting of pulmonary fibrosis, CCL18 was found to increase the phosphorylation and activity of a transcription factor, specificity protein 1 (SP1) (Luzina et al., 2006b). SP1 functions in conjunction with the basal activity of another transcription factor, mothers against decapentaplegic homolog 3 (SMAD3), although SMAD3 is not directly modulated by

CCL18 (Luzina et al., 2006b). Following activation, SMAD3 and phosphorylated SP1 translocate from the cytosol to the nucleus (Tan & Khachigian, 2009), where they bind to specific DNA regions to regulate gene transcription. This results in increased alpha-smooth muscle actin (α-SMA) expression, as well as collagen from fibroblasts, myofibroblasts, and End-MT derived cells, all of which promote fibrosis (Ghosh et al., 2013). Importantly, this signalling pathway is thought to be independent of TGF-β (Luzina et al., 2006b).

Second, as mentioned in **Section 1.3.1**, extracellular signal-regulated kinases 1 and 2 (ERK1/2) might also play a role in CCL18 signalling (Atamas et al., 2003). Luzina et al. (2006a) found that CCL18 upregulated collagen synthesis in lung fibroblasts via protein kinase C alpha (PKCα) activation, followed by the downstream ERK1/2 phosphorylation. Phosphorylated ERK1/2 serves as a transcription factor, changing the expression of cell cycle regulator genes (Fujiwara et al., 2014). Consequently, the proliferation rates of fibroblasts and myofibroblasts can be elevated (Benelli et al., 2013; Fujiwara et al., 2014). Moreover, studies have demonstrated interactions between ERK1/2 and the SMAD3-SP1 signalling. Thus ERK1/2 contributes to TGF-β induced SMAD3 activation in human mesangial cells (pericytes in the glomerulus), although this does not occur in all cell types, being absent in mouse mammary epithelial cells (Hayashida et al., 2003). Yan et al. (2013) also reported reduced binding capacity of SP1 following inhibition of ERK1/2, which suggests that ERK1/2 can modulate SP1 activity.

Third, CCL18 might also regulate fibrosis by modulating matrix metalloproteinase (MMP)-2 and MMP-9, enzymes that promote the breakdown of extracellular matrix (ECM). Overexpression of CCL18 in mouse lungs was found to increase the levels of MMP-2 and MMP-9, via unknown mechanisms (Pochetuhen et al., 2007). MMP-2 is generally anti-fibrotic in various fibrosis models, whilst MMP9 can be pro-fibrotic, anti-fibrotic, or neither, depending on the nature of the fibrosis model studied (Giannandrea & Parks, 2014). The anti-fibrotic effects of MMPs are thought to be a result of ECM breakdown, however the relevant pro-fibrotic mechanisms remain unidentified (Giannandrea & Parks, 2014).

It is important to note that the role of the signalling pathways mentioned above, in pro-fibrotic actions of CCL18, were elucidated prior to the identification of the CCL18 cognate receptor, CCR8. As such, it remains to be confirmed whether these mechanisms are downstream of CCR8 activation.

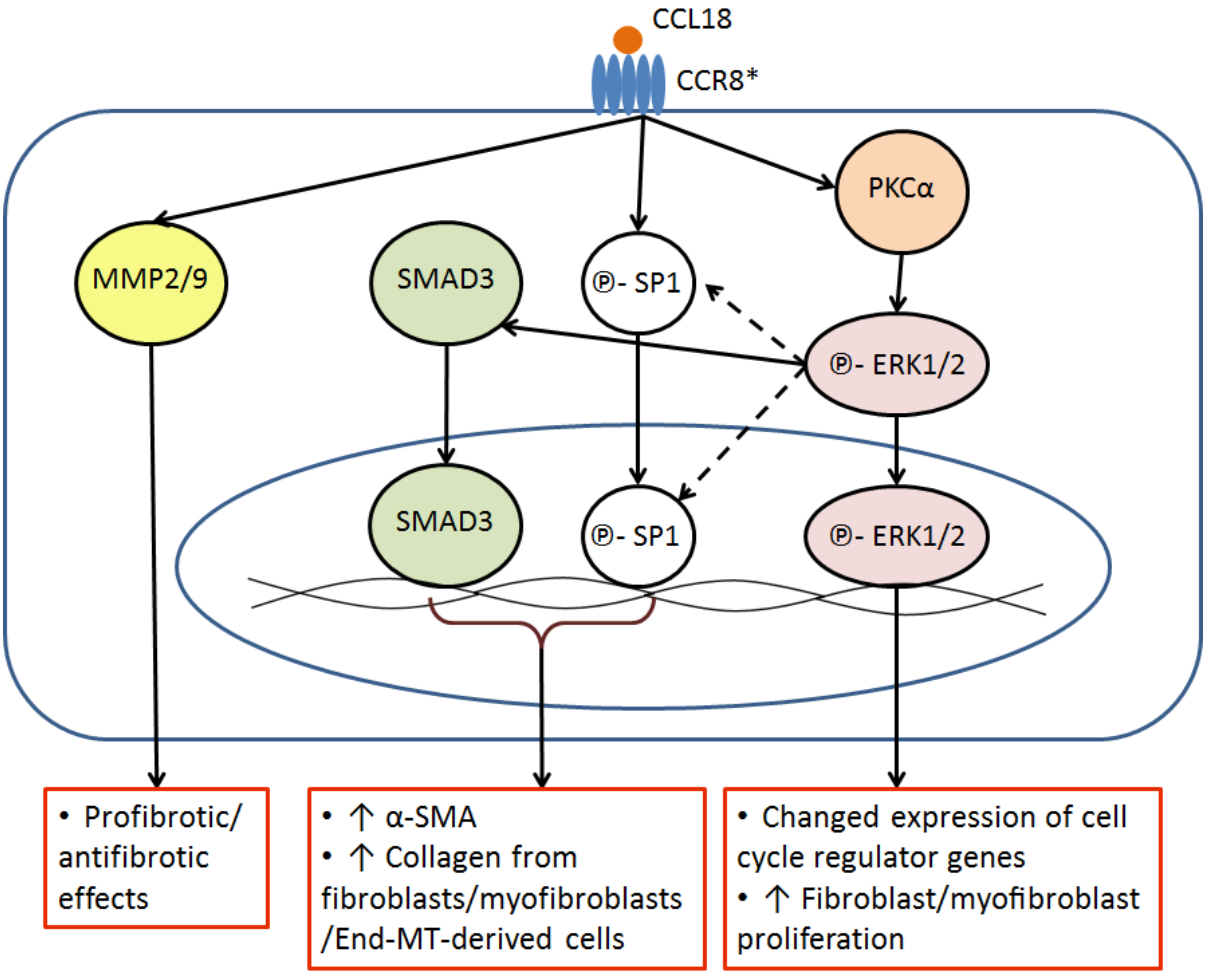

Figure 7. Proposed CCL18 signalling pathways involved in fibrosis. Summarized from (Benelli et al., 2013; Fujiwara et al., 2014; Ghosh et al., 2013; Hayashida et al., 2003; Luzina et al., 2006a; Luzina et al., 2006b; Pochetuhen et al., 2007; Yan et al., 2013). Dotted lines: effects have not been confirmed. MMP: matrix metalloproteinase, SMAD3: Mothers against decapentaplegic homolog 3, Ⓟ- SP1: phosphorylated specificity protein 1, PKCα: protein kinase C alpha, Ⓟ- ERK: phosphorylated extracellular signal-regulated kinase, α-SMA: alpha-smooth muscle actin, End-MT-derived cells: endothelial-mesenchymal transition derived cells. * Role of CCR8 in pro-fibrotic action yet to be confirmed.

1.4 CCL18 in disease states

Given its pro-fibrotic capacity, it is likely that CCL18 contributes to fibrosis in pathological settings. Indeed, elevated levels of M2 macrophage-derived hCCL18/ mCCL8 have been reported to be associated with cancer angiogenesis, pulmonary fibrosis, inflammatory disorders, and cardiovascular diseases (Schutyser et al., 2005). A pro-fibrotic role of CCL18 in these conditions is anticipated given the ability of the chemokine to increase collagen production from healthy human dermal and lung fibroblasts (Atamas et al., 2003), stimulate T cell recruitment (Günther et al., 2014), and promote polarisation of macrophages towards the pro-fibrotic M2 phenotype (Schraufstatter et al., 2012). Indeed, in patients with idiopathic pulmonary fibrosis, high bronchoalveolar lavage fluid levels of CCL18 are associated with collagen accumulation (Prasse et al., 2006), and serum CCL18 levels positively correlates with the impairment of lung function (Prasse et al., 2009). In addition, in patients with systemic sclerosis, an immune disorder characterised by marked fibrosis, elevated serum CCL18 levels may predict progression of lung fibrosis, lung function, and mortality at 5 and 10 years since diagnosis (Hoffmann-Vold et al., 2016).

While a role for CCL18 in lung disease is clearly recognised, there is a growing body of evidence to suggest that CCL18 may also play a pathological role in cardiovascular diseases, including coronary artery disease (acute coronary syndrome and angina), atherosclerosis, and aneurysm. Thus, plasma levels of CCL18 are elevated in patients with acute coronary syndrome such that those with high serum CCL18 (>70.9 ng/ml) have a 3 times greater risk of having a future fatal cardiovascular event, compared to those with low CCL18 levels (< 43.0 ng/ml) (de Jager et al., 2012). Plasma levels of CCL18 are also elevated in patients with obstructive coronary artery disease (Versteylen et al., 2016) and transiently increased during unstable angina pectoris episodes; thereby serving as a marker of refractory unstable angina pectoris (Kraaijeveld et al., 2007). In addition, CCL18 is co-localised with macrophages in human carotid atherosclerotic lesions (Hägg et al., 2009), and interestingly its expression here is 10-fold higher than that in the lung (Hägg et al., 2009), a site where CCL18 is the most abundant.

Elevated serum CCL18 has also been observed in aneurysm patients, especially in those with metabolic active aneurysms (Courtois et al., 2014). Since metabolic active aneurysms present

greater inflammatory responses and a higher risk of aneurysm rupture, it has been suggested that CCL18 may serve as a marker of aneurysm rupture risk (Courtois et al., 2014). Together, these data point to a clinically significant role of CCL18 in cardiovascular disease.

1.5 CCL18 in hypertension

1.5.1 Potential role of CCL18 in hypertension

Although the association between CCL18 and the cardiovascular diseases discussed above has been established, little is known about the role of CCL18 in hypertension. Nonetheless, several lines of evidence support a potential contribution of CCL18 to hypertension. First, Günther et al. (2014) reported that autoantibodies (IgG) from systemic sclerosis patients activated AT_1 and endothelin receptor type A (ET_A) to increase CCL18 expression in peripheral blood mononuclear cells (PBMCs), especially monocytes. This effect was inhibited by the AT_1 antagonist valsartan and the ET_A antagonist sitaxsentan, further confirming the role of AT_1 and ET_A receptors in promoting CCL18 generation (Günther et al., 2014). In general, autoantibodies act as ligands to activate receptors, typically in bivalent forms (Bradbury et al., 2011). Autoantibodies are also elevated in hypertensive patients, and can target AT_1 receptors on the endothelium and VSMCs (Chen et al., 2009; Yang et al., 2014), leading to downstream ERK1/2 activation which may promote fibrosis (Lu et al., 2020). In addition, autoantibodies as well as the cognate ligands themselves (Ang II and endothelin 1), may activate AT_1 and ET_A receptors on macrophages (Günther et al., 2014) to promote CCL18 generation, a concept which remains to be explored.

The potential contribution of CCL18 to hypertension is further supported by findings utilising the angiotensin II-infusion model of hypertension in mice (Moore et al., 2015). Thus, mCCL8 mRNA expression and M2 macrophage accumulation are both elevated in the aorta of hypertensive, as compared to normotensive, mice (Moore et al., 2015). Moreover, macrophage depletion leads to a reduction in systolic blood pressure, and a reduction in aberrant aortic collagen deposition and stiffening (Moore et al., 2015), suggesting that M2 macrophage-derived mCCL8 promotes hypertension-associated fibrosis. Consistent with the published data, our laboratory has recently shown an increased number of mCCL8 expressing M2 macrophages in the vascular wall of hypertensive mice (**Figure 8**). In addition, we have confirmed expression of the CCL18 receptor, CCR8 in the aorta from hypertensive mice (**Figure 6 under Section 1.3**).

Collectively, these findings suggest that CCL18 may play a role in pathogenesis of hypertension, yet it remains to be determined if CCL18 is elevated in hypertensive patients.

In addition, while CCL18 may modulate VSMCs, T cells, fibroblasts, fibrocytes, or endothelial cells to promote fibrosis (**see Section 1.3**), confirmation of the cellular targets of CCL18 and interrogation of the relevant signalling pathways in the setting of hypertension are required. Moreover, the role of the cognate receptor CCR8 in hypertension and the associated fibrosis and end-organ damage remains unknown, and the effects of pharmacologically targeting the CCL18-CCR8 axis are yet to be explored.

1.5.2 Animal models to study the role of CCL18-CCR8 axis in hypertension

The identification of the cognate receptor (CCR8) and mouse functional analogue (CCL8) of CCL18 (Islam et al., 2013), has made it possible to study the role of CCL18 in animal models of hypertension. In particular, Ang II infusion (typically ≈ 0.7 mg/kg/d, 14- or 28-day) models of hypertension in mice, which are based on the well recognised overactivation of the RAAS in hypertension, cause robust BP elevation, cardiac hypertrophy, and vascular remodelling/ dysfunction/ fibrosis in mice (Li et al., 2007; Madhur et al., 2010; Moore et al., 2015). These models are commonly used to study the pathophysiology of hypertension and demonstrate the efficacy of antihypertensive medications.

To our knowledge, studies using the above-mentioned Ang II models have not investigated the prevalence of cardiac or renal fibrosis in this setting. Although higher doses of Ang II (typically > 2.1 mg/kg/d) have been found to induce cardiac and renal fibrosis (Yu et al., 2018; Zhao et al., 2018), such doses represent models of abdominal aortic aneurysm, which can cause high mortality rates (Amin et al., 2019). Moreover, whilst DOCA-salt models of hypertension also cause robust fibrosis in the kidneys (Krishnan et al., 2019), they may not lead to cardiac or vascular fibrosis (Omarjee et al., 2019).

In the current thesis, we wished to examine the impact of targeting the CCL18-CCR8 axis on the elevation in BP and vascular, cardiac and renal remodelling and fibrosis. As such the Ang II model of hypertension in mice (0.7 mg/kg/d, 14- and 28-day) was chosen due to ability to induce hypertension without the need for addition surgical intervention (e.g. removal of a kidney) and the key vascular and immune component to the disease pathophysiology. This was of particular importance, given our hypothesis that M2 macrophages in the vascular wall

generate CCL18 which targets CCR8 on vascular cell types to contribute to hypertension and associated end-organ damage.

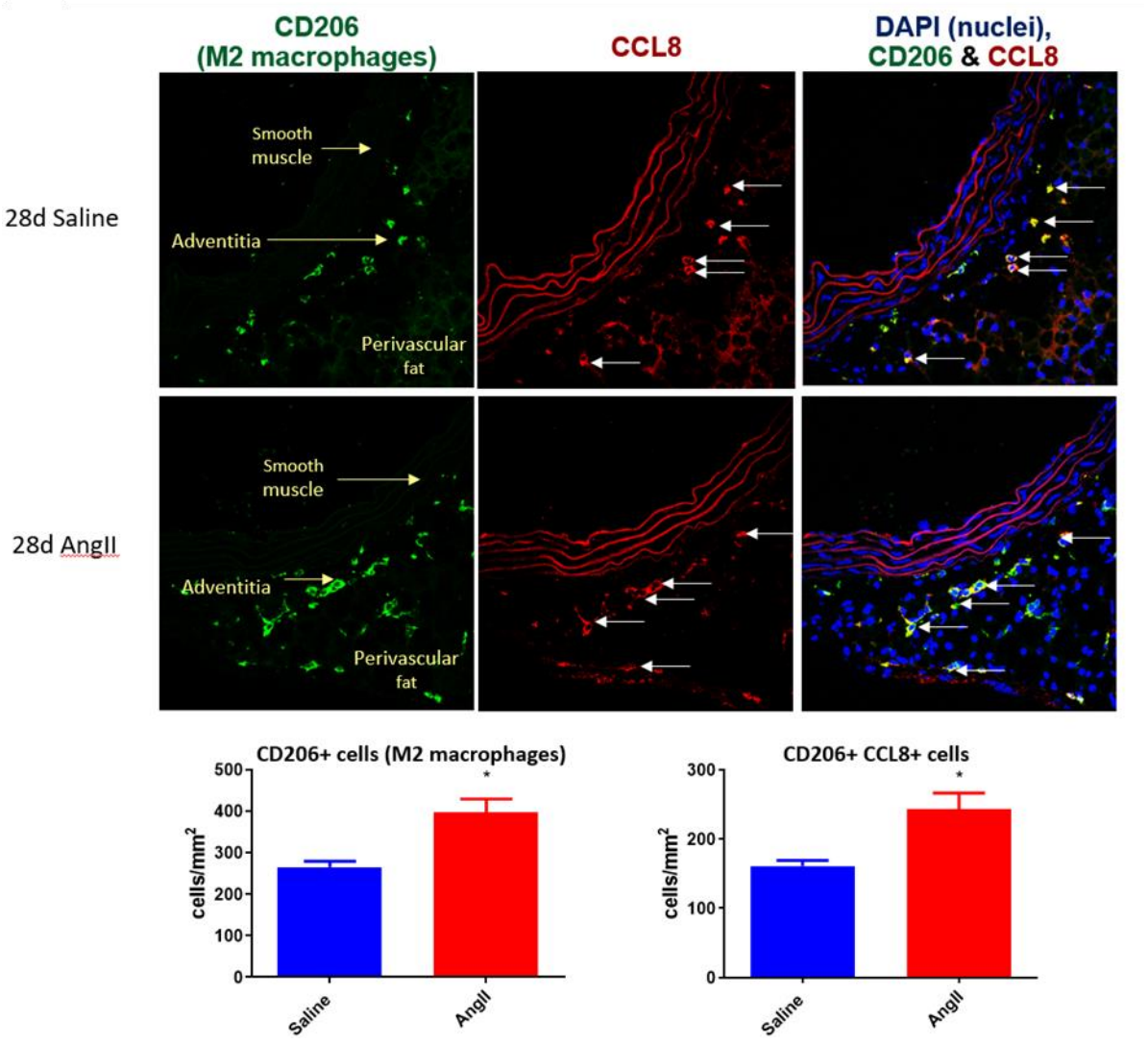

Figure 8. Localization of M2 macrophages and CCL8 in the aorta from normotensive and Ang II-induced hypertensive mice. Immunohistochemical staining for CD206 (M2 marker, green), CCL8 (red), and DAPI (nucleated cells, blue) in the aorta, from 28d saline (top panels) or Ang II (bottom panels) treated mice. Representative images from n=6 shown and quantified below. Data normalized to area (mm^2) and presented as mean ± SEM, n=5-6. * $p<0.05$ vs. saline (Student's unpaired t-test). (Zhu, 2016)

1.6 Summary and aims

CCL18, which activates its cognate receptor CCR8 (Islam et al., 2013), is a key contributor to fibrosis in various pathological conditions, and is implicated in several types of cardiovascular diseases (Courtois et al., 2014; de Jager et al., 2012; Hägg et al., 2009; Kraaijeveld et al., 2007; Versteylen et al., 2016). However, the cellular targets and signalling pathways of CCL18 in hypertension are yet to be determined, and the role of the CCL18-CCR8 axis in hypertension-associated fibrosis is unknown.

Based on the current literature and the preliminary data from our lab, we hypothesise that targeting the CCL18-CCR8 axis can reverse hypertension and associated cardiovascular and renal fibrosis, and protect against end-organ damage (**Figure 9**). To address this hypothesis, the research program aims to:

1) determine if CCL18 serves as a biomarker of hypertension and evaluate the pro-fibrotic effects of CCL18, using clinically-relevant human cells/cell lines (**Chapter 3**);

2) investigate the role of CCL18-CCR8 axis in the development of hypertension in male and female mice (**Chapter 4**);

3) assess the therapeutic utility of targeting the CCL18-CCR8 axis via genetic and pharmacological approaches to protect against hypertension and the associated end-organ damage (**Chapter 5**).

This project will provide essential pre-clinical data on the therapeutic utility of targeting CCL18-CCR8 to control blood pressure and end-organ damage, and hence may provide a novel therapeutic option for hypertension and its associated cardiovascular complications.

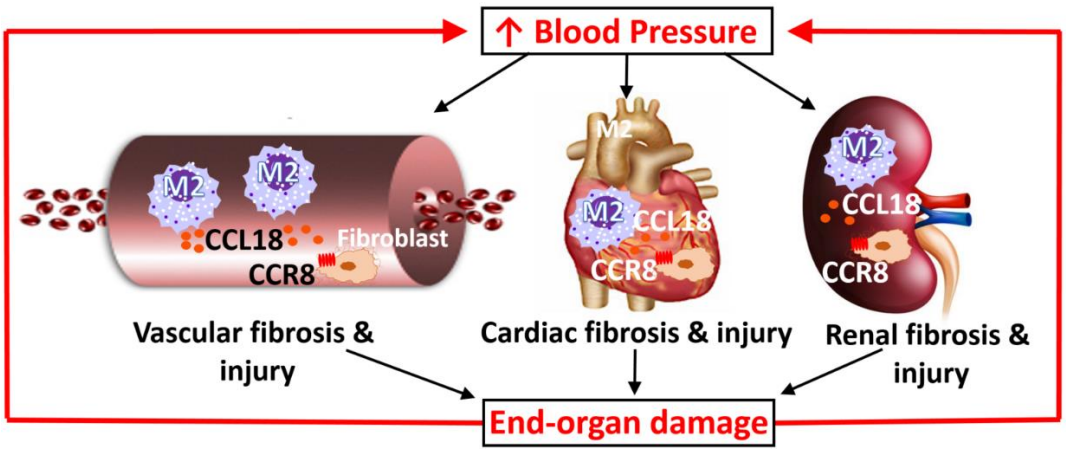

Figure 8. Proposed role of the CCL18-CCR8 axis in hypertension-associated fibrosis and end-organ damage. (Courtesy of Kemp-Harper B, 2018).

1.7 References

Achelrod D, Wenzel U, & Frey S (2015). Systematic review and meta-analysis of the prevalence of resistant hypertension in treated hypertensive populations. Am J Hypertens 28**:** 355-361.

Amin HZ, Sasaki N, Yamashita T, Mizoguchi T, Hayashi T, Emoto T, Matsumoto T, Yoshida N, Tabata T, Horibe S, Kawauchi S, Rikitake Y, & Hirata K-i (2019). CTLA-4 Protects against Angiotensin II-Induced Abdominal Aortic Aneurysm Formation in Mice. Sci Rep 9**:** 8065.

An SJ, Liu P, Shao TM, Wang ZJ, Lu HG, Jiao Z, Li X, & Fu JQ (2015). Characterization and functions of vascular adventitial fibroblast subpopulations. Cell Physiol Biochem 35**:** 1137-1150.

Atamas SP, Luzina IG, Choi J, Tsymbalyuk N, Carbonetti NH, Singh IS, Trojanowska M, Jimenez SA, & White B (2003). Pulmonary and Activation-Regulated Chemokine Stimulates Collagen Production in Lung Fibroblasts. Am J Respir Cell Mol Biol 29**:** 743-749.

Australian Bureau of Statistics (2018). Hypertension and measured high blood pressure. https://www.abs.gov.au/statistics/health/health-conditions-and-risks/hypertension-and-measured-high-blood-pressure/2017-2018#endnotes.

Australian Bureau of Statistics (2020). Causes of Death, Australia. https://www.abs.gov.au/statistics/health/causes-death/causes-death-australia/2019.

Azizi M, Schmieder RE, Mahfoud F, Weber MA, Daemen J, Davies J, Basile J, Kirtane AJ, Wang Y, Lobo MD, Saxena M, Feyz L, Rader F, Lurz P, Sayer J, Sapoval M, Levy T, Sanghvi K, Abraham J, Sharp ASP, Fisher NDL, Bloch MJ, Reeve-Stoffer H, Coleman L, Mullin C, & Mauri L (2018). Endovascular ultrasound renal denervation to treat hypertension (RADIANCE-HTN SOLO): a multicentre, international, single-blind, randomised, sham-controlled trial. Lancet 391**:** 2335-2345.

Azzaoui I, Yahia SA, Chang Y, Vorng H, Morales O, Fan Y, Delhem N, Ple C, Tonnel AB, Wallaert B, & Tsicopoulos A (2011). CCL18 differentiates dendritic cells in tolerogenic cells able to prime regulatory T cells in healthy subjects. Blood 118**:** 3549-3558.

Basu S, Schaefer TM, Ghosh M, Fuller CL, & Reinhart TA (2002). MOLECULAR CLONING AND SEQUENCING OF 25 DIFFERENT RHESUS MACAQUE CHEMOKINE cDNAS REVEALS EVOLUTIONARY CONSERVATION AMONG C, CC, CXC, AND CX3C FAMILIES OF CHEMOKINES. Cytokine 18**:** 140-148.

Benelli R, Vene R, Minghelli S, Carlone S, Gatteschi B, & Ferrari N (2013). Celecoxib induces proliferation and Amphiregulin production in colon subepithelial myofibroblasts, activating erk1-2 signaling in synergy with EGFR. Cancer Lett 328**:** 73-82.

Berenguer J, Lagerweij T, Zhao XW, Dusoswa S, van der Stoop P, Westerman B, de Gooijer MC, Zoetemelk M, Zomer A, Crommentuijn MHW, Wedekind LE, López-López À, Giovanazzi A, Bruch-Oms M, van der Meulen-Muileman IH, Reijmers RM, van Kuppevelt TH, García-Vallejo JJ, van Kooyk Y, Tannous BA, Wesseling P, Koppers-Lalic D, Vandertop WP, Noske DP, van Beusechem VW, van

Rheenen J, Pegtel DM, van Tellingen O, & Wurdinger T (2018). Glycosylated extracellular vesicles released by glioblastoma cells are decorated by CCL18 allowing for cellular uptake via chemokine receptor CCR8. Journal of extracellular vesicles 7**:** 1446660.

Blowey DL (2016). Diuretics in the treatment of hypertension. Pediatr Nephrol 31**:** 2223-2233.

Bradbury AR, Sidhu S, Dubel S, & McCafferty J (2011). Beyond natural antibodies: the power of in vitro display technologies. Nat Biotechnol 29**:** 245-254.

Brandes RP, Weissmann N, & Schröder K (2014). Nox family NADPH oxidases: Molecular mechanisms of activation. Free Radic Biol Med 76**:** 208-226.

Briet M, Boutouyrie P, Laurent S, & London GM (2012). Arterial stiffness and pulse pressure in CKD and ESRD. Kidney Int 82**:** 388-400.

Bromfield S, & Muntner P (2013). High Blood Pressure: The Leading Global Burden of Disease Risk Factor and the Need for Worldwide Prevention Programs. Curr Hypertens Rep 15**:** 134-136.

Bruna-Romero O, Schmieg J, Del Val M, Buschle M, & Tsuji M (2003). The dendritic cell-specific chemokine, dendritic cell-derived CC chemokine 1, enhances protective cell-mediated immunity to murine malaria. J Immunol 170**:** 3195-3203.

Canty EG, & Kadler KE (2005). Procollagen trafficking, processing and fibrillogenesis. J Cell Sci 118**:** 1341.

Catusse J, Wollner S, Leick M, Schröttner P, Schraufstätter I, & Burger M (2010). Attenuation of CXCR4 responses by CCL18 in acute lymphocytic leukemia B cells. J Cell Physiol 225**:** 792-800.

Chen J, Yao Y, Gong C, Yu F, Su S, Chen J, Liu B, Deng H, Wang F, Lin L, Yao H, Su F, Anderson Karen S, Liu Q, Ewen Mark E, Yao X, & Song E (2011). CCL18 from Tumor-Associated Macrophages Promotes Breast Cancer Metastasis via PITPNM3. Cancer Cell 19**:** 541-555.

Chen QW, Edvinsson L, & Xu CB (2009). Role of ERK/MAPK in endothelin receptor signaling in human aortic smooth muscle cells. BMC Cell Biol 10**:** 52.

Chenivesse C, Chang Y, Azzaoui I, Ait Yahia S, Morales O, Plé C, Foussat A, Tonnel A-B, Delhem N, Yssel H, Vorng H, Wallaert B, & Tsicopoulos A (2012). Pulmonary CCL18 Recruits Human Regulatory T Cells. The Journal of Immunology 189**:** 128.

Chenivesse C, & Tsicopoulos A (2018). CCL18 - Beyond chemotaxis. Cytokine 109**:** 52-56.

Chinetti-Gbaguidi G, Colin S, & Staels B (2015). Macrophage subsets in atherosclerosis. Nat Rev Cardiol 12**:** 10-17.

Colafella KMM, & Denton KM (2018). Sex-specific differences in hypertension and associated cardiovascular disease. Nature Reviews Nephrology 14**:** 185-201.

Connolly S, Skrinjar M, & Rosendahl A (2012). Orally bioavailable allosteric CCR8 antagonists inhibit dendritic cell, T cell and eosinophil migration. Biochem Pharmacol 83**:** 778-787.

Courtois A, Nusgens BV, Hustinx R, Namur G, Gomez P, Kuivaniemi H, Defraigne J-O, Colige AC, & Sakalihasan N (2014). Gene Expression Study in Positron Emission Tomography–Positive Abdominal Aortic Aneurysms Identifies CCL18 as a Potential Biomarker for Rupture Risk. Mol Med 20**:** 697-706.

Daugherty SL, Powers JD, Magid DJ, Tavel HM, Masoudi FA, Margolis KL, O'Connor PJ, Selby JV, & Ho PM (2012). Incidence and prognosis of resistant hypertension in hypertensive patients. Circulation 125**:** 1635-1642.

De Ciuceis C, Amiri F, Brassard P, Endemann DH, Touyz RM, & Schiffrin EL (2005). Reduced vascular remodeling, endothelial dysfunction, and oxidative stress in resistance arteries of angiotensin II-infused macrophage colony-stimulating factor-deficient mice: evidence for a role in inflammation in angiotensin-induced vascular injury. Arterioscler Thromb Vasc Biol 25**:** 2106-2113.

de Jager SCA, Bongaerts BWC, Weber M, Kraaijeveld AO, Rousch M, Dimmeler S, van Dieijen-Visser MP, Cleutjens KBJM, Nelemans PJ, van Berkel TJC, & Biessen EAL (2012). Chemokines CCL3/MIP1α, CCL5/RANTES and CCL18/PARC are Independent Risk Predictors of Short-Term Mortality in Patients with Acute Coronary Syndromes. PLoS One 7**:** e45804.

de la Sierra A, Segura J, Banegas JR, Gorostidi M, de la Cruz JJ, Armario P, Oliveras A, & Ruilope LM (2011). Clinical features of 8295 patients with resistant hypertension classified on the basis of ambulatory blood pressure monitoring. Hypertension 57**:** 898-902.

Diez J (2007). Mechanisms of cardiac fibrosis in hypertension. J Clin Hypertens (Greenwich) 9**:** 546-550.

Drummond GR, Vinh A, Guzik TJ, & Sobey CG (2019). Immune mechanisms of hypertension. Nat Rev Immunol 19**:** 517-532.

Dumor K, Shoemaker-Moyle M, Nistala R, & Whaley-Connell A (2018). Arterial Stiffness in Hypertension: an Update. Curr Hypertens Rep 20**:** 72.

Falkenham A, de Antueno R, Rosin N, Betsch D, Lee TD, Duncan R, & Legare JF (2015). Nonclassical resident macrophages are important determinants in the development of myocardial fibrosis. Am J Pathol 185**:** 927-942.

Fujiwara T, Kanazawa S, Ichibori R, Tanigawa T, Magome T, Shingaki K, Miyata S, Tohyama M, & Hosokawa K (2014). L-arginine stimulates fibroblast proliferation through the GPRC6A-ERK1/2 and PI3K/Akt pathway. PLoS One 9**:** e92168.

Ghosh AK, Quaggin SE, & Vaughan DE (2013). Molecular basis of organ fibrosis: potential therapeutic approaches. Exp Biol Med 238**:** 461-481.

Giannandrea M, & Parks WC (2014). Diverse functions of matrix metalloproteinases during fibrosis. Dis Model Mech 7**:** 193-203.

Go Alan S, Mozaffarian D, Roger Véronique L, Benjamin Emelia J, Berry Jarett D, Blaha Michael J, Dai S, Ford Earl S, Fox Caroline S, Franco S, Fullerton Heather J, Gillespie C, Hailpern Susan M, Heit John A, Howard Virginia J, Huffman Mark D, Judd Suzanne E, Kissela Brett M, Kittner Steven J, Lackland Daniel T, Lichtman Judith H, Lisabeth Lynda D, Mackey Rachel H, Magid David J, Marcus Gregory M, Marelli A, Matchar David B, McGuire Darren K, Mohler Emile R, Moy Claudia S, Mussolino Michael E, Neumar Robert W, Nichol G, Pandey Dilip K, Paynter Nina P, Reeves Matthew J, Sorlie Paul D, Stein J, Towfighi A, Turan Tanya N, Virani Salim S, Wong Nathan D, Woo D, & Turner Melanie B (2014). Heart Disease and Stroke Statistics—2014 Update. Circulation 129**:** e28-e292.

Goldmann T, Zissel G, Watz H, Drömann D, Reck M, Kugler C, Rabe KF, & Marwitz S (2018). Human alveolar epithelial cells type II are capable of TGFβ-dependent epithelial-mesenchymal-transition and collagen-synthesis. Respir Res 19**:** 138.

Golob MJ, Tian L, Wang Z, Zimmerman TA, Caneba CA, Hacker TA, Song G, & Chesler NC (2015). Mitochondria DNA mutations cause sex-dependent development of hypertension and alterations in cardiovascular function. J Biomech 48**:** 405-412.

Guiteras R, Flaquer M, & Cruzado JM (2016). Macrophage in chronic kidney disease. Clin Kidney J 9**:** 765-771.

Günther C, Bello-Fernandez C, Kopp T, Kund J, Carballido-Perrig N, Hinteregger S, Fassl S, Schwärzler C, Lametschwandtner G, Stingl G, Biedermann T, & Carballido JM (2005). CCL18 Is Expressed in Atopic Dermatitis and Mediates Skin Homing of Human Memory T Cells. The Journal of Immunology 174**:** 1723.

Günther J, Kill A, Becker MO, Heidecke H, Rademacher J, Siegert E, Radić M, Burmester GR, Dragun D, & Riemekasten G (2014). Angiotensin receptor type 1 and endothelin receptor type A on immune cells mediate migration and the expression of IL-8 and CCL18 when stimulated by autoantibodies from systemic sclerosis patients. Arthritis Res Ther 16**:** R65.

Hägg DA, Olson FJ, Kjelldahl J, Jernås M, Thelle DS, Carlsson LMS, Fagerberg B, & Svensson PA (2009). Expression of chemokine (C-C motif) ligand 18 in human macrophages and atherosclerotic plaques. Atherosclerosis 204**:** e15-e20.

Haque NS, Fallon JT, Pan JJ, Taubman MB, & Harpel PC (2004). Chemokine receptor-8 (CCR8) mediates human vascular smooth muscle cell chemotaxis and metalloproteinase-2 secretion. Blood 103**:** 1296-1304.

Harvey A, Montezano AC, Lopes RA, Rios F, & Touyz RM (2016). Vascular Fibrosis in Aging and Hypertension: Molecular Mechanisms and Clinical Implications. Can J Cardiol 32**:** 659-668.

Hausman GJ, Barb CR, Fairchild BD, Gamble J, & Lee-Rutherford L (2014). Gene expression profiling in adipose tissue from growing broiler chickens. Adipocyte 3**:** 297-303.

Hayashida T, Decaestecker M, & Schnaper HW (2003). Cross-talk between ERK MAP kinase and Smad signaling pathways enhances TGF-beta-dependent responses in human mesangial cells. FASEB J 17**:** 1576-1578.

Hayes IM, Jordan NJ, Towers S, Smith G, Paterson JR, Earnshaw JJ, Roach AG, Westwick J, & Williams RJ (1998). Human vascular smooth muscle cells express receptors for CC chemokines. Arterioscler Thromb Vasc Biol 18**:** 397-403.

Herrera VL, Decano JL, Giordano N, Moran AM, & Ruiz-Opazo N (2014). Aortic and carotid arterial stiffness and epigenetic regulator gene expression changes precede blood pressure rise in stroke-prone Dahl salt-sensitive hypertensive rats. PLoS One 9**:** e107888.

Hieshima K, Imai T, Baba M, Shoudai K, Ishizuka K, Nakagawa T, Tsuruta J, Takeya M, Sakaki Y, Takatsuki K, Miura R, Opdenakker G, Van Damme J, Yoshie O, & Nomiyama H (1997). A novel human CC chemokine PARC that is most homologous to macrophage-inflammatory protein-1 alpha/LD78 alpha and chemotactic for T lymphocytes, but not for monocytes. J Immunol 159**:** 1140-1149.

Hilgers KF (2002). Monocytes/macrophages in hypertension. J Hypertens 20**:** 593-596.

Hoffmann-Vold AM, Tennøe AH, Garen T, Midtvedt Ø, Abraityte A, Aaløkken TM, Lund MB, Brunborg C, Aukrust P, Ueland T, & Molberg Ø (2016). High Level of Chemokine CCL18 Is Associated With Pulmonary Function Deterioration, Lung Fibrosis Progression, and Reduced Survival in Systemic Sclerosis. Chest 150**:** 299-306.

Huber MA, Denk A, Peter RU, Weber L, Kraut N, & Wirth T (2002). The IKK-2/Ikappa Balpha /NF-kappa B pathway plays a key role in the regulation of CCR3 and eotaxin-1 in fibroblasts. A critical link to dermatitis in Ikappa Balpha -deficient mice. J Biol Chem 277**:** 1268-1275.

Humphrey Jay D (2008). Mechanisms of Arterial Remodeling in Hypertension. Hypertension 52**:** 195-200.

Islam SA, Chang DS, Colvin RA, Byrne MH, McCully ML, Moser B, Lira SA, Charo IF, & Luster AD (2011). Mouse CCL8, a CCR8 agonist, promotes atopic dermatitis by recruiting IL-5+ TH2 cells. Nat Immunol 12**:** 167-177.

Islam SA, Ling MF, Leung J, Shreffler WG, & Luster AD (2013). Identification of human CCR8 as a CCL18 receptor. J Exp Med 210**:** 1889-1898.

Jia G, Aroor AR, & Sowers JR (2014). Arterial Stiffness: A Nexus between Cardiac and Renal Disease. Cardiorenal Med 4**:** 60-71.

Justin Rucker A, & Crowley SD (2017). The role of macrophages in hypertension and its complications. Pflugers Archiv : European journal of physiology 469**:** 419-430.

Kaess BM, Rong J, Larson MG, Hamburg NM, Vita JA, Levy D, Benjamin EJ, Vasan RS, & Mitchell GF (2012). Aortic stiffness, blood pressure progression, and incident hypertension. JAMA 308**:** 875-881.

Kannel WB (2009). Hypertension: reflections on risks and prognostication. Med Clin North Am 93**:** 541-558, Table of Contents.

Kessler EL, Rivaud MR, Vos MA, & van Veen TAB (2019). Sex-specific influence on cardiac structural remodeling and therapy in cardiovascular disease. Biol Sex Differ 10**:** 7-7.

Ko EA, Amiri F, Pandey NR, Javeshghani D, Leibovitz E, Touyz RM, & Schiffrin EL (2007). Resistance artery remodeling in deoxycorticosterone acetate-salt hypertension is dependent on vascular inflammation: evidence from m-CSF-deficient mice. American Journal of Physiology-Heart and Circulatory Physiology 292**:** H1789-H1795.

Komai M, Tanaka H, Nagao K, Ishizaki M, Kajiwara D, Miura T, Ohashi H, Haba T, Kawakami K, Sawa E, Yoshie O, Inagaki N, & Nagai H (2010). A novel CC-chemokine receptor 3 antagonist, Ki19003, inhibits airway eosinophilia and subepithelial/peribronchial fibrosis induced by repeated antigen challenge in mice. J Pharmacol Sci 112**:** 203-213.

Kossmann S, Hu H, Steven S, Schonfelder T, Fraccarollo D, Mikhed Y, Brahler M, Knorr M, Brandt M, Karbach SH, Becker C, Oelze M, Bauersachs J, Widder J, Munzel T, Daiber A, & Wenzel P (2014). Inflammatory monocytes determine endothelial nitric-oxide synthase uncoupling and nitro-oxidative stress induced by angiotensin II. J Biol Chem 289**:** 27540-27550.

Kraaijeveld AO, de Jager SC, de Jager WJ, Prakken BJ, McColl SR, Haspels I, Putter H, van Berkel TJ, Nagelkerken L, Jukema JW, & Biessen EA (2007). CC chemokine ligand-5 (CCL5/RANTES) and CC chemokine ligand-18 (CCL18/PARC) are specific markers of refractory unstable angina pectoris and are transiently raised during severe ischemic symptoms. Circulation 116**:** 1931-1941.

Krishnan SM, Ling YH, Huuskes BM, Ferens DM, Saini N, Chan CT, Diep H, Kett MM, Samuel CS, Kemp-Harper BK, Robertson AAB, Cooper MA, Peter K, Latz E, Mansell AS, Sobey CG, Drummond GR, & Vinh A (2019). Pharmacological inhibition of the NLRP3 inflammasome reduces blood pressure, renal damage, and dysfunction in salt-sensitive hypertension. Cardiovasc Res 115**:** 776-787.

Kroeze K, Pronk J, Kirtschig G, Boer ED, Middelkoop E, Scheper R, & Gibbs S Chapter 4 Comparison of cytokine , chemokine and growth factor profiles in burn wounds , chronic wounds and surgical excision wounds.

Krohn SC, Bonvin P, & Proudfoot AE (2013). CCL18 exhibits a regulatory role through inhibition of receptor and glycosaminoglycan binding. PLoS One 8**:** e72321.

Le VP, Knutsen RH, Mecham RP, & Wagenseil JE (2011). Decreased aortic diameter and compliance precedes blood pressure increases in postnatal development of elastin-insufficient mice. Am J Physiol Heart Circ Physiol 301**:** H221-229.

Legendre B, Tokarski C, Chang Y, De Freitas Caires N, Lortat-Jacob H, Nadaï PD, Rolando C, Duez C, Tsicopoulos A, & Lassalle P (2013). The disulfide bond between cysteine 10 and cysteine 34 is required for CCL18 activity. Cytokine 64**:** 463-470.

Leung SY, Yuen ST, Chu KM, Mathy JA, Li R, Chan AS, Law S, Wong J, Chen X, & So S (2004). Expression profiling identifies chemokine (C-C motif) ligand 18 as an independent prognostic indicator in gastric cancer. Gastroenterology 127**:** 457-469.

Lewis C (2017). Investigating the roles of distinct macrophage phenotypes in cardiovascular disease. PhD thesis: Monash University, Melbourne.

Lewis CV, Vinh A, Diep H, Samuel CS, Drummond GR, & Kemp-Harper BK (2019). Distinct Redox Signalling following Macrophage Activation Influences Profibrotic Activity. Journal of immunology research 2019**:** 1278301.

Li HL, She ZG, Li TB, Wang AB, Yang Q, Wei YS, Wang YG, & Liu DP (2007). Overexpression of myofibrillogenesis regulator-1 aggravates cardiac hypertrophy induced by angiotensin II in mice. Hypertension 49**:** 1399-1408.

Lin L, Chen YS, Yao YD, Chen JQ, Chen JN, Huang SY, Zeng YJ, Yao HR, Zeng SH, Fu YS, & Song EW (2015). CCL18 from tumor-associated macrophages promotes angiogenesis in breast cancer. Oncotarget 6**:** 34758-34773.

Louahed J, Struyf S, Demoulin JB, Parmentier M, Van Snick J, Van Damme J, & Renauld JC (2003). CCR8-dependent activation of the RAS/MAPK pathway mediates anti-apoptotic activity of I-309/ CCL1 and vMIP-I. Eur J Immunol 33**:** 494-501.

Lu Y, Sun X, Peng L, Jiang W, Li W, Yuan H, & Cai J (2020). Angiotensin II-Induced vascular remodeling and hypertension involves cathepsin L/V- MEK/ERK mediated mechanism. Int J Cardiol 298**:** 98-106.

Luzina IG, Highsmith K, Pochetuhen K, Nacu N, Rao JN, & Atamas SP (2006a). PKCα Mediates CCL18-Stimulated Collagen Production in Pulmonary Fibroblasts. Am J Respir Cell Mol Biol 35**:** 298-305.

Luzina IG, Todd NW, Nacu N, Lockatell V, Choi J, Hummers LK, & Atamas SP (2009). Regulation of pulmonary inflammation and fibrosis through expression of integrins alphaVbeta3 and alphaVbeta5 on pulmonary T lymphocytes. Arthritis Rheum 60**:** 1530-1539.

Luzina IG, Tsymbalyuk N, Choi J, Hasday JD, & Atamas SP (2006b). CCL18-stimulated upregulation of collagen production in lung fibroblasts requires Sp1 signaling and basal Smad3 activity. J Cell Physiol 206**:** 221-228.

Madhur MS, Lob HE, McCann LA, Iwakura Y, Blinder Y, Guzik TJ, & Harrison DG (2010). Interleukin 17 promotes angiotensin II-induced hypertension and vascular dysfunction. Hypertension 55**:** 500-507.

Margaritopoulos GA, Vasarmidi E, & Antoniou KM (2016). Pirfenidone in the treatment of idiopathic pulmonary fibrosis: an evidence-based review of its place in therapy. Core Evidence 11**:** 11-22.

Matsuo K, Itoh T, Koyama A, Imamura R, Kawai S, Nishiwaki K, Oiso N, Kawada A, Yoshie O, & Nakayama T (2016). CCR4 is critically involved in effective antitumor immunity in mice bearing intradermal B16 melanoma. Cancer Lett 378**:** 16-22.

McMaster WG, Kirabo A, Madhur MS, & Harrison DG (2015). Inflammation, immunity, and hypertensive end-organ damage. Circ Res 116**:** 1022-1033.

Meng F, Li W, Li C, Gao Z, Guo K, & Song S (2015). CCL18 promotes epithelial-mesenchymal transition, invasion and migration of pancreatic cancer cells in pancreatic ductal adenocarcinoma. Int J Oncol 46**:** 1109-1120.

Messerli FH, Bangalore S, Bavishi C, & Rimoldi SF (2018). Angiotensin-Converting Enzyme Inhibitors in Hypertension: To Use or Not to Use? J Am Coll Cardiol 71**:** 1474-1482.

Mezzano Sergio A, Ruiz-Ortega M, & Egido J (2001). Angiotensin II and Renal Fibrosis. Hypertension 38**:** 635-638.

Moore JP, Vinh A, Tuck KL, Sakkal S, Krishnan SM, Chan CT, Lieu M, Samuel CS, Diep H, Kemp-Harper BK, Tare M, Ricardo SD, Guzik TJ, Sobey CG, & Drummond GR (2015). M2 macrophage accumulation in the aortic wall during angiotensin ii infusion in mice is associated with fibrosis, elastin loss, and elevated blood pressure. Am J Physiol Heart Circ Physiol 309**:** H906-H917.

Mori L, Bellini A, Stacey MA, Schmidt M, & Mattoli S (2005). Fibrocytes contribute to the myofibroblast population in wounded skin and originate from the bone marrow. Exp Cell Res 304**:** 81-90.

Nibbs RJ, Salcedo TW, Campbell JD, Yao XT, Li Y, Nardelli B, Olsen HS, Morris TS, Proudfoot AE, Patel VP, & Graham GJ (2000). C-C chemokine receptor 3 antagonism by the beta-chemokine macrophage inflammatory protein 4, a property strongly enhanced by an amino-terminal alanine-methionine swap. J Immunol 164**:** 1488-1497.

Norlander AE, Madhur MS, & Harrison DG (2018). The immunology of hypertension. The Journal of experimental medicine 215**:** 21-33.

Omarjee L, Roy C, Leboeuf C, Favre J, Henrion D, Mahe G, Leftheriotis G, Martin L, Janin A, & Kauffenstein G (2019). Evidence of Cardiovascular Calcification and Fibrosis in Pseudoxanthoma Elasticum Mouse Models Subjected to DOCA-Salt Hypertension. Sci Rep 9**:** 16327.

Oparil S, Zaman MA, & Calhoun DA (2003). Pathogenesis of Hypertension. Ann Intern Med 139**:** 761-776.

Oshio T, Kawashima R, Kawamura YI, Hagiwara T, Mizutani N, Okada T, Otsubo T, Inagaki-Ohara K, Matsukawa A, Haga T, Kakuta S, Iwakura Y, Hosokawa S, & Dohi T (2014). Chemokine receptor CCR8 is required for lipopolysaccharide-triggered cytokine production in mouse peritoneal macrophages. PLoS One 9**:** e94445.

Osidak MS, Osidak EO, Akhmanova MA, Domogatsky SP, & Domogatskaya AS (2015). Fibrillar, Fibril-associated and Basement Membrane Collagens of the Arterial Wall: Architecture, Elasticity and Remodeling Under Stress. Curr Pharm Des 21**:** 1124-1133.

Paik Y-H, Kim J, Aoyama T, De Minicis S, Bataller R, & Brenner DA (2014). Role of NADPH oxidases in liver fibrosis. Antioxid Redox Signal 20**:** 2854-2872.

Pignatti P, Brunetti G, Moretto D, Yacoub MR, Fiori M, Balbi B, Balestrino A, Cervio G, Nava S, & Moscato G (2006). Role of the chemokine receptors CXCR3 and CCR4 in human pulmonary fibrosis. Am J Respir Crit Care Med 173**:** 310-317.

Pochetuhen K, Luzina IG, Lockatell V, Choi J, Todd NW, & Atamas SP (2007). Complex regulation of pulmonary inflammation and fibrosis by CCL18. Am J Pathol 171**:** 428-437.

Prasse A, Pechkovsky DV, Toews GB, Jungraithmayr W, Kollert F, Goldmann T, Vollmer E, Müller-Quernheim J, & Zissel G (2006). A vicious circle of alveolar macrophages and fibroblasts perpetuates pulmonary fibrosis via CCL18. Am J Respir Crit Care Med 173**:** 781-792.

Prasse A, Probst C, Bargagli E, Zissel G, Toews GB, Flaherty KR, Olschewski M, Rottoli P, & Müller-Quernheim J (2009). Serum CC-chemokine ligand 18 concentration predicts outcome in idiopathic pulmonary fibrosis. Am J Respir Crit Care Med 179**:** 717-723.

Ridiandries A, Tan JTM, & Bursill CA (2018). The Role of Chemokines in Wound Healing. Int J Mol Sci 19**:** 3217.

Sampson Amanda K, Jennings Garry LR, & Chin-Dusting Jaye PF (2012). Y Are Males So Difficult to Understand? Hypertension 59**:** 525-531.

Sánchez-Duffhues G, García de Vinuesa A, & Ten Dijke P (2018). Endothelial-to-mesenchymal transition in cardiovascular diseases: Developmental signaling pathways gone awry. Dev Dyn 247**:** 492-508.

Schraufstatter IU, Zhao M, Khaldoyanidi SK, & Discipio RG (2012). The chemokine CCL18 causes maturation of cultured monocytes to macrophages in the M2 spectrum. Immunology 135**:** 287-298.

Schutyser E, Richmond A, & Van Damme J (2005). Involvement of CC chemokine ligand 18 (CCL18) in normal and pathological processes. J Leukoc Biol 78**:** 14-26.

Schutyser E, Struyf S, Proost P, Opdenakker G, Laureys G, Verhasselt B, Peperstraete L, Van de Putte I, Saccani A, Allavena P, Mantovani A, & Van Damme J (2002). Identification of biologically active chemokine isoforms from ascitic fluid and elevated levels of CCL18/pulmonary and activation-regulated chemokine in ovarian carcinoma. J Biol Chem 277**:** 24584-24593.

Schutyser E, Struyf S, Wuyts A, Put W, Geboes K, Grillet B, Opdenakker G, & Van Damme J (2001). Selective induction of CCL18/PARC by staphylococcal enterotoxins in mononuclear cells and enhanced levels in septic and rheumatoid arthritis. Eur J Immunol 31**:** 3755-3762.

Seki E, De Minicis S, Gwak GY, Kluwe J, Inokuchi S, Bursill CA, Llovet JM, Brenner DA, & Schwabe RF (2009a). CCR1 and CCR5 promote hepatic fibrosis in mice. J Clin Invest 119**:** 1858-1870.

Seki E, de Minicis S, Inokuchi S, Taura K, Miyai K, van Rooijen N, Schwabe RF, & Brenner DA (2009b). CCR2 promotes hepatic fibrosis in mice. Hepatology 50**:** 185-197.

Shamri R, Young KM, & Weller PF (2013). PI3K, ERK, p38 MAPK and integrins regulate CCR3-mediated secretion of mouse and human eosinophil-associated RNases. Allergy 68**:** 880-889.

Su S, Liao J, Liu J, Huang D, He C, Chen F, Yang L, Wu W, Chen J, Lin L, Zeng Y, Ouyang N, Cui X, Yao H, Su F, Huang J-d, Lieberman J, Liu Q, & Song E (2017). Blocking the recruitment of naive CD4+ T cells reverses immunosuppression in breast cancer. Cell Res 27**:** 461-482.

Tan NY, & Khachigian LM (2009). Sp1 phosphorylation and its regulation of gene transcription. Mol Cell Biol 29**:** 2483-2488.

Touyz RM, Alves-Lopes R, Rios FJ, Camargo LL, Anagnostopoulou A, Arner A, & Montezano AC (2018). Vascular smooth muscle contraction in hypertension. Cardiovasc Res 114**:** 529-539.

Townsend RR, Mahfoud F, Kandzari DE, Kario K, Pocock S, Weber MA, Ewen S, Tsioufis K, Tousoulis D, Sharp ASP, Watkinson AF, Schmieder RE, Schmid A, Choi JW, East C, Walton A, Hopper I, Cohen DL, Wilensky R, Lee DP, Ma A, Devireddy CM, Lea JP, Lurz PC, Fengler K, Davies J, Chapman N, Cohen SA, DeBruin V, Fahy M, Jones DE, Rothman M, & Böhm M (2017). Catheter-based renal denervation in patients with uncontrolled hypertension in the absence of antihypertensive medications (SPYRAL HTN-OFF MED): a randomised, sham-controlled, proof-of-concept trial. Lancet 390**:** 2160-2170.

Tsou P-S, Haak AJ, Khanna D, & Neubig RR (2014). Cellular Mechanisms of Tissue Fibrosis. 8. Current and future drug targets in fibrosis: focus on Rho GTPase-regulated gene transcription. American Journal of Physiology - Cell Physiology 307**:** C2-C13.

Versteylen MO, Manca M, Joosen IA, Schmidt DE, Das M, Hofstra L, Crijns HJ, Biessen EA, & Kietselaer BL (2016). CC chemokine ligands in patients presenting with stable chest pain: association with atherosclerosis and future cardiovascular events. Neth Heart J 24**:** 722-729.

Vestergaard C, Just H, Baumgartner Nielsen J, Thestrup-Pedersen K, & Deleuran M (2004). Expression of CCR2 on monocytes and macrophages in chronically inflamed skin in atopic dermatitis and psoriasis. Acta Derm Venereol 84**:** 353-358.

Wang Y, Del Borgo M, Lee HW, Baraldi D, Hirmiz B, Gaspari TA, Denton KM, Aguilar M-I, Samuel CS, & Widdop RE (2017). Anti-fibrotic Potential of AT(2) Receptor Agonists. Front Pharmacol 8**:** 564.

Wanjare M, Agarwal N, & Gerecht S (2015). Biomechanical strain induces elastin and collagen production in human pluripotent stem cell-derived vascular smooth muscle cells. Am J Physiol Cell Physiol 309**:** C271-281.

Weber KT (2000). Fibrosis and hypertensive heart disease. Curr Opin Cardiol 15**:** 264-272.

Wei Z, Spizzo I, Diep H, Drummond GR, Widdop RE, & Vinh A (2014). Differential Phenotypes of Tissue-Infiltrating T Cells during Angiotensin II-Induced Hypertension in Mice. PLoS One 9**:** e114895.

Wenzel P, Knorr M, Kossmann S, Stratmann J, Hausding M, Schuhmacher S, Karbach SH, Schwenk M, Yogev N, Schulz E, Oelze M, Grabbe S, Jonuleit H, Becker C, Daiber A, Waisman A, & Münzel T (2011). Lysozyme M-positive monocytes mediate angiotensin II-induced arterial hypertension and vascular dysfunction. Circulation 124**:** 1370-1381.

Whelton PK, Carey RM, Aronow WS, Casey DE, Collins KJ, Dennison Himmelfarb C, DePalma SM, Gidding S, Jamerson KA, Jones DW, MacLaughlin EJ, Muntner P, Ovbiagele B, Smith SC, Spencer CC, Stafford RS, Taler SJ, Thomas RJ, Williams KA, Williamson JD, & Wright JT (2017). 2017 ACC/AHA/AAPA/ABC/ACPM/AGS/APhA/ASH/ASPC/NMA/PCNA Guideline for the Prevention, Detection, Evaluation, and Management of High Blood Pressure in Adults. Hypertension. 71(6): 1269-1324.

World Health Organization (2020). The top 10 causes of death. https://www.who.int/news-room/fact-sheets/detail/the-top-10-causes-of-death.

Wright JM, Musini VM, & Gill R (2018). First-line drugs for hypertension. The Cochrane database of systematic reviews 4**:** Cd001841.

Wu J, Montaniel KR, Saleh MA, Xiao L, Chen W, Owens GK, Humphrey JD, Majesky MW, Paik DT, Hatzopoulos AK, Madhur MS, & Harrison DG (2016). Origin of Matrix-Producing Cells That Contribute to Aortic Fibrosis in Hypertension. Hypertension 67**:** 461-468.

Wynn TA, & Ramalingam TR (2012). Mechanisms of fibrosis: therapeutic translation for fibrotic disease. Nat Med 18**:** 1028-1040.

Yan D, Chen D, Hawse JR, van Wijnen AJ, & Im HJ (2013). Bovine lactoferricin induces TIMP-3 via the ERK1/2-Sp1 axis in human articular chondrocytes. Gene 517**:** 12-18.

Yang S, Zhong Q, Qiu Z, Chen X, Chen F, Mustafa K, Ding D, Zhou Y, Lin J, Yan S, Deng Y, Wang M, Zhou Y, Liao Y, & Zhou Z (2014). Angiotensin II receptor type 1 autoantibodies promote endothelial microparticles formation through activating p38 MAPK pathway. J Hypertens 32**:** 762-770.

Yeager ME, Frid MG, & Stenmark KR (2011). Progenitor cells in pulmonary vascular remodeling. Pulmonary Circulation 1**:** 3-16.

Yu HT (2003). Progression of chronic renal failure. Arch Intern Med 163**:** 1417-1429.

Yu X, Xia Y, Zeng L, Zhang X, Chen L, Yan S, Zhang R, Zhao C, Zeng Z, Shu Y, Huang S, Lei J, Yuan C, Zhang L, Feng Y, Liu W, Huang B, Zhang B, Luo W, Wang X, Zhang H, Haydon RC, Luu HH, He TC, & Gan H (2018). A blockade of PI3Kγ signaling effectively mitigates angiotensin II-induced renal injury and fibrosis in a mouse model. Sci Rep 8**:** 10988.

Zhang Y, Wu X, Li Y, Zhang H, Li Z, Zhang Y, Zhang L, Ju J, Liu X, Chen X, Glybochko PV, Nikolenko V, Kopylov P, Xu C, & Yang B (2016). Endothelial to mesenchymal transition contributes to arsenic-trioxide-induced cardiac fibrosis. Sci Rep 6**:** 33787.

Zhao W, Chen SS, Chen Y, Ahokas RA, & Sun Y (2008). Kidney fibrosis in hypertensive rats: role of oxidative stress. Am J Nephrol 28**:** 548-554.

Zhao W, Zhao T, Chen Y, Bhattacharya SK, Lu L, & Sun Y (2018). Differential Expression of Hypertensive Phenotypes in BXD Mouse Strains in Response to Angiotensin II. Am J Hypertens 31**:** 108-114.

Zhu M (2016). CCL18 as a mediator of the pro-fibrotic actions of M2 macrophages in the vessel wall during hypertension. Honours thesis: Monash University, Melbourne.

Zingoni A, Soto H, Hedrick JA, Stoppacciaro A, Storlazzi CT, Sinigaglia F, D'Ambrosio D, O'Garra A, Robinson D, Rocchi M, Santoni A, Zlotnik A, & Napolitano M (1998). Cutting Edge: The Chemokine Receptor CCR8 Is Preferentially Expressed in Th2 But Not Th1 Cells. The Journal of Immunology 161**:** 547.

Chapter 2

General Methods

2.1 Ethics approval

Human plasma

Human plasma samples were collected during studies conducted at the Heart Centre of Alfred Hospital (2001-2017), under ethics numbers 92/00, 51/03, 7/05, 8/12, 87/12 and 215/12. Relevant studies were conducted in collaboration with Prof Markus Schlaich (Dobney Hypertension Center, The University of Western Australia), Dr Nina Eikelis and Prof Gavin Lambert (Iverson Health Innovation Research Institute, Swinburne University of Technology), where ambulatory BP, body mass index (BMI), heart rate, age, medication history and C-reactive protein (CRP; from the plasma of some patients) were measured or recorded. Plasma from the subjects was collected and stored by Dr Nina Eikelis and Prof Gavin Lambert.

The study cohort consisted of 14 normotensive subjects (control, male: female = 11:3), 20 untreated essential hypertensive patients (male: female = 10:10) and 20 resistant hypertensive patients (male: female = 14:7).

Animal studies

Studies were approved by the Monash Animal Research Platform Ethics Committee (Ethics Number: MARP/2017/104), and were conducted in accordance with the "Australian Code for the Care and Use of Animals for Scientific Purposes 8th Edition".

2.2 Animals and genotype identification

Animals

All mice in this project were of a C57BL/6J background. $CCR8^{-/-}$ (CCR8 KO) mice were generated via CRISPR/Cas9, by the Australian Phenomics Network, Monash University.

In the 14-day angiotensin infusion model (for Chapter 4), CCR8 KO male and female mice, and their wildtype (WT) littermates were used (generated via $CCR8^{+/-}$ x $CCR8^{+/-}$ breeding). Female mice were at the age of 10-14 weeks, and male mice were 8-13 weeks old.

In the 28-day angiotensin infusion model (for Chapter 5), CCR8 KO male mice were used (generated via $CCR8^{+/-}$ x $CCR8^{+/-}$ breeding or straight $CCR8^{-/-}$ x $CCR8^{-/-}$ mating). WT male mice were either bred from the CCR8 KO colony ($CCR8^{+/-}$ x $CCR8^{+/-}$ or WT x WT breeding) or obtained from Monash Animal Research Platform (MARP; Monash University, Clayton, Australia). These CCR8 KO and WT mice were 10-12 weeks old.

All above-mentioned mice were bred and housed at the Animal Research Laboratories, MARP or Pharmacology Mouse Room (Monash University, Clayton, Australia). Mice were maintained on a 12-hour light-dark cycle and provided with free access to chow diet and drinking water. When required, mice were transported in high barrier SPF containers.

Genotyping

A REDExtract-N-Amp™ Tissue PCR Kit (Sigma-Aldrich, Germany) was used to identify the genotype of each mouse, as per manufacturer's instructions. The extraction mixture was added into 1.5 ml Eppendorf tubes, each of which contained a tip of mouse tail. DNA was extracted from these samples by a 10-minute incubation at room temperature followed by a 3-minute incubation at 95 °C. Reaction was stopped by Neutralization Solution B, and the extracted DNA was amplified with REDExtract-N-Amp PCR Reaction Mix and 100 ng custom-made primers for CCR8 (Sigma-Aldrich, Germany). Sequences of custom-made primers were as follows: 5'-CTTGCCGCACACTAACACCC 3' (Forward primer), 5' TCTTTTAAAGTAGGATGGTGCTGG 3' and 5' CTGGCCGTCCTCACCTTGAT 3' (Reverse primers). DNA amplification was performed using a thermal cycler (Bio-Rad Laboratories MyCycler; Bio-Rad Laboratories, USA), with annealing temperature set at 59 °C. Amplified DNA was then loaded into 5% agarose gels that contained SYBR safe dye (ThermoScientific, USA) for electrophoresis. 1x Tris-acetate-EDTA (TAE) buffer was used as a solvent for agarose and the running buffer for electrophoresis at 100 V. Resultant DNA bands were visualised by a ChemiDoc MP system (Bio-Rad Laboratories, USA) to determine the genotype of each mouse.

2.3 Angiotensin infusion models of hypertension in mice

14-day and 28-day models

In the 14-day angiotensin II (Ang II) infusion model of hypertension, male and female WT mice were randomly assigned to a saline or Ang II (0.7 mg/kg/d, 14 days; GL Biochem, China) treatment group. Male and female CCR8 KO mice were all treated with Ang II (0.7 mg/kg/d) for 14 days. WT and CCR8 KO mice were littermates. In the 28-day Ang II infusion model of hypertension, male WT and CCR8 KO mice were randomly assigned to a saline or Ang II infusion (0.7 mg/kg/d, 28 days) group, and mice were not littermates. Treatments were administered subcutaneously via osmotic minipumps (Model 2002 for 14 days or Model 2004 for 28 days; Alzet, USA). Treated animals per group: n= 3-10 for the 14-day model (highly impacted by COVID-19 as mentioned in **Chapter 4, Section 4.1**), and 9-13 for the 28-day model.

All mice were under isoflurane anaesthesia (0.4 L/min, 2% inhaled with oxygen) during minipump implantation, where a lateral incision of ≈10 mm was made through the skin at the neck. A subcutaneous pouch was created through this incision, in which minipumps were inserted, followed by the closing of incision with monofilament sutures and the application of topical antibiotics (Tribactril; Jurox, Australia). During the surgery, mice were monitored for hind paw withdrawal, blink reflexes and respiratory rate. After the surgery, mice were allowed to recover and then returned to home cages, followed by daily monitoring for 2 days and twice weekly thereafter.

R243 treatment protocol (for Chapter 5)

Using the 28-day Ang II hypertension model, a cohort of WT male mice were further treated with R243 (CCR8 antagonist, 1.1 mg/kg/d; Glixx Laboratories, USA) or vehicle (2:1 warm mixture of 30% hydroxypropyl-β-cyclodextrin: 100% DMSO). Treatment commenced 14 days after the hypertension induction surgeries and continued for a further 14 days. For each of these mice, R243 or vehicle was administrated via another osmotic minipump (Model 2002; Alzet, USA). The dose and vehicle of R243 were chosen and adapted based on a study by Berenguer et al. (2018), and the minipump implantation procedures and health monitoring

are as described above. Treated animals per group: n= 4-6 (COVID-19 impact stated in **Chapter 5, Section 5.1**).

Body weights and monitoring

During the course of treatments, all mice were monitored twice weekly to assess their state of health. They were also weighed weekly, with additional weighing and monitoring when there were signs of abnormality or weight loss.

2.4 Tail cuff plethysmography

Systolic blood pressure (BP) of mice was measured using tail cuff plethysmography (MC4000 multi-channel blood pressure analysis system; Hatteras Instruments, USA). After mice were acclimatised to the BP monitoring equipment, BP was recorded 3 days before, 1 day before, and just prior to surgeries (Day 0) to obtain an average baseline BP. During the 14-day treatment period, BP was measured on Days 3, 7, 10 and 14; for the 28-day model of hypertension, BP was further monitored on Days 17, 21, 24 and 28. BP was recorded for 25-30 measurement cycles on each day of measurement, where mice were placed in restraints on a heated platform (40°C), with an inflatable cuff around the base of each tail. The pulse was detected using a sensor with an LED light source, and systolic BP was recorded as the cuff inflation pressure required to fully occlude blood flow in the tail.

At the end of the treatment periods, mice were killed by CO_2 overdose. Mice assigned to the 28-day hypertension model were then perfused through the left ventricle using phosphate-buffered saline (PBS) with 0.2% clexane (400 IU, Sanofi, Australia), in preparation for flow cytometric analysis (section 2.6). The aorta (thoracic and abdominal), kidneys, heart, spleen, liver and lungs of each mouse were removed and weighed before being processed for end point measures.

2.5 Wire myography

To assess vascular function, abdominal aortae were isolated from CCR8 KO and WT mice, the fat and connective tissues removed and aortae cut into 2 mm sections. Aortic sections were mounted in a small vessel myograph (Danish Myo Technology A/S, Denmark) on pin mounts (200 µm diameter) and changes in isometric tension recorded (LabChart 8, ADI Instruments, New Zealand). Vessels were kept at a resting tension of 5mN at 37 °C in Kreb's solution (in mM: 118 NaCl, 4.5 KCl, 0.5 $MgSO_4$, 1 KH_2PO_4, 25 $NaHCO_3$, 11.1 glucose, 2.5 $CaCl_2$; pH 7.4), and bubbled with carbogen (5% CO_2, 95% oxygen). Arteries were contracted maximally with the thromboxane A_2 mimetic, U46619 (0.3 µM). Once the contraction had reached a plateau, vessels were washed, tension allowed to return to baseline and then arteries were rechallenged with U46619 (0.3 µM; F_{max}).

Endothelium-dependent and -independent vasorelaxation responses were assessed by constructing cumulative concentration-response (CR) curves to acetylcholine (ACh; 1 nM- 30 µM) and the NO donor, diethylamine NONOate (DEA-NO; 0.3 nM- 30 µM), respectively in aortae pre-contracted to ≈65 % F_{max} with titrated concentrations of U46619. In separate aortic sections, cumulative CR curves to phenylephrine (PE; 1 nM-30 µM), were constructed. Arteries were then washed with Krebs', pre-contracted to ≈20-30 % F_{max} with U46619 prior to the addition of N(ω)-nitro-L-arginine methyl ester (L-NAME, 100 µM) to assess endogenous NO bioavailability.

2.6 Flow cytometry

Isolation of leukocytes from aortae, kidneys and spleens

Flow cytometry was performed to characterise the effects of genetic deletion of CCR8 on infiltration of inflammatory cells into target organs. Following euthanasia, mice were perfused through the left ventricle with phosphate-buffered saline (PBS; with 137 mM NaCl, 2.7 mM KCl, 10.1 mM Na_2HPO_4 and 1.8 mM KH_2PO_4, pH = 7.4) containing 0.2% Clexane (400 IU/ml; Sanofi Aventis, France). The thoracic aorta (with perivascular fat intact), left kidney (cut in half along the transverse plane, the cranial half used), and spleen were then excised for flow

cytometry. These samples were mechanically disrupted using scissors, where aortae and kidneys were further digested via the addition of 1 ml of digestion buffer for 45 minutes at 37 °C. The digestion buffer contained collagenase I-S (450 U/ml), collagenase XI (125 U/ml) and hyaluronidase (450 U/ml), which were dissolved in PBS containing calcium and magnesium (Sigma, USA).

Processed samples were passed through 70 µm filters (BD Bioscience, USA), followed by centrifugation (all centrifugation for flow cytometry was at 4 °C, 1500 rpm for 5 minutes unless otherwise specified). Cell pellets were resuspended in 0.8 ml FACS buffer (PBS containing 1% bovine serum albumin) for aortae, 30% Percoll (GE Healthcare Life Science, UK) for kidneys, or Red Blood Cell Lysis Buffer (5-minute incubation on ice; BD Biosciences, USA) for spleens. Kidney samples were then under-laid with 70% Percoll and centrifuged at 25 °C, 2500 rpm for 25 minutes. The mononuclear cell layer between the Percoll gradients were collected, centrifuged and re-suspended in FACS buffer (1 ml). For spleen samples, lysis buffer was neutralised with PBS after the incubation, followed by centrifugation and re-suspension in FACS buffer (30 ml).

Antibody staining and sample analysis

Single cell suspensions in FACS buffer were pelleted onto 96 U-bottom plates, and then stained using an antibody cocktail (20 minutes incubation on ice). The cocktail included AF-700 anti-CD45, BV605 anti-CD11b, PE-Cy7 anti-F4/80, PE anti-CD206, APC anti-CD3, FITC anti-CD4, BV785 anti-CD8, all were of rat anti-mouse isotype (anti-CD11b from Invitrogen, USA; anti-CD3 from eBioscience, USA; others from BioLegend, USA) (**Table 1**). Each antibody was also individually incubated with UltraComp eBeads® (eBioscience, USA) for single-colour compensation. After the antibody incubation, cells were washed by FACS buffer, centrifuged, and pellets resuspended with 200 µl FACS buffer. Prior to sample running, CountBright counting beads (Invitrogen, USA) were added for data normalisation, and 7-AAD (BioLegend, USA) was used as a viability stain.

Table 1. Antibodies used for flow cytometry and their sources.

Antigen	Fluorophore Tag	Source
CD45	AF-700	BioLegend, USA
CD11b	BV605	Invitrogen, USA
F4/80	PE-Cy7	BioLegend, USA
CD206	PE	BioLegend, USA
CD3	APC	eBioscience, USA
CD4	FITC	BioLegend, USA
CD8	BV785	BioLegend, USA

Gating strategy

Data from stained samples were obtained using a Fortessa X-20 instrument controlled by the FlowDiva software (BD Biosciences, USA) and processed using FlowJo software v10 (FlowJo, USA). Gating was performed as shown in **Figure 1**, where non-cellular debris were excluded by having low forward scatter area (FSC-A) and low side scatter area (SSC-A). Then singlets with similar FSC-A as compared to forward scatter height (FSC-H) values were selected, followed by the selection of live cells that were 7AAD-negative (7AAD-). Subsequently, leukocytes, myeloid cells and total T cells were gated by CD45+, CD11b+ CD3- and CD11b- CD3+ events, respectively. Myeloid cells were further gated by F4/80+ events (total macrophages) and F4/80+ CD206+ events ("M2"-like macrophages), whereas T cells were further gated for CD4+ CD8- and CD4- CD8+ T cells (**Figure 1**).

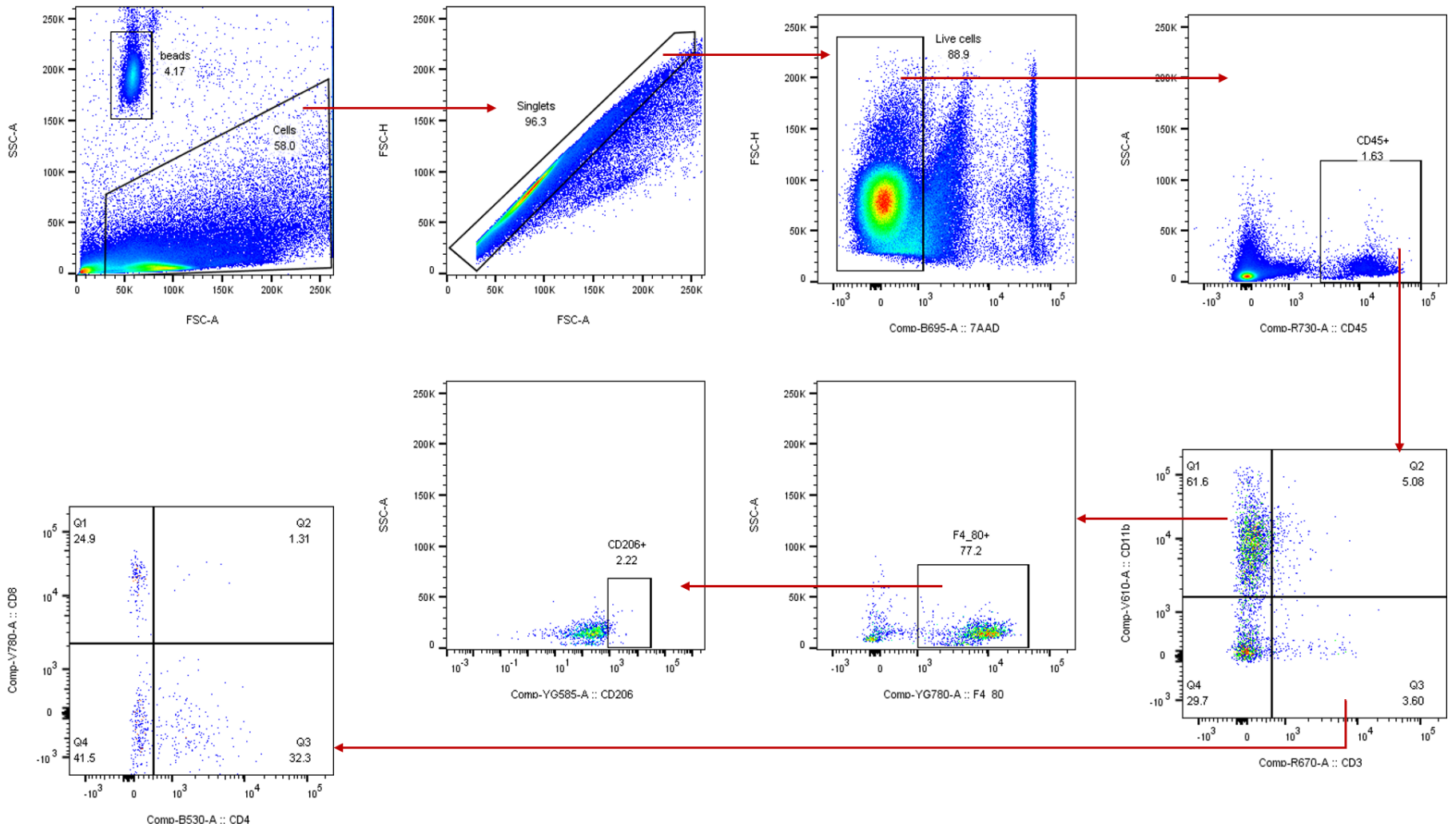

Figure 1. Example of gating strategies used for flow cytometric analysis. FSC-A = forward scatter area, SSC-A = side scatter area, FSC-H = forward scatter height.

2.7 Histological studies

A distal section of mouse thoracic aorta (≈4 mm; for **Chapters 4-5**), a transverse section of the heart (representing 1/3 of the heart taken near the basal region) (for **Chapter 5**), and the cranial half of each right kidney (for **Chapter 5**) was fixed in 10 % neutral buffered formalin for 3 days. Fixed tissues were then embedded in paraffin and cut into transverse sections for kidney and heart (4 μm), or cross sections of 4-5 μm for aortae. 4 μm aortic sections were stained with Verhoeff-Van Gieson (VVG), 5 μm sections were stained with hematoxylin and eosin (H&E) or Picrosirius red staining. Heart sections were stained with H&E and Picrosirius red, and kidney sections underwent Masson's Trichrome staining. The embedding and cutting of tissues were performed by Monash Histology Services (Monash University, Clayton, Australia).

Picrosirius red staining was used to measure the collagen content in the target organs. For **Chapter 4**, aortic sections were firstly de-waxed by being submerged in xylene and a series of graded ethanol solutions (2 washes in 100% then one in 70%). The de-waxed sections were rinsed with water, followed by immersion in Bouin's fixative (9.7% formaldehyde, 71% aqueous picric acid, 5% acetic acid) for 1 hour at 60 °C. Fixed slides were washed in water and stained by picrosirius red (0.01%; Sigma-Aldrich, USA) for 1 hour. After staining, sections were washed with tap water, 3 changes of 80% ethanol, and 3 changes of xylene, successively. To prepare slides for imaging, non-aqueous DPX (VWR International, USA) was used as a mounting medium for cover-slipping. For **Chapter 5**, aortic and cardiac sections were stained using the above-mentioned protocol by Monash Histology Services (Monash University, Clayton, Australia). For both **Chapters 4 and 5**, aortic slides were imaged at x10 and x20 magnification using both bright-field and polarised microscopy (Olympus BX51, Olympus Life Science, Australia). Images for hearts were captured at up to x40 magnification by a slide scanner (Aperio Scanscope AT Turbo, Leica Biosystems, Germany).

VVG and H&E stains were also performed assess elastin dysregulation and the structure of mouse aortae, respectively (Chapters 4-5), or the structure of heart (H&E for Chapter 5). Masson's Trichrome was used to assess collagen deposition in the kidneys (Chapter 5). The above-mentioned stains were performed by Monash Histology Services (Monash University,

Clayton, Australia) (See **Appendices 1-3** for detailed protocols). Images for these stains were captured at up to x40 magnification by a slide scanner (Aperio Scanscope AT Turbo, Leica Biosystems, Germany).

Each section of the above-mentioned staining was analysed in a blinded manner, with 6-8 fields of view (1 section per animal) (aortic picrosirius staining of the 14-day model and assessment of renal/ cardiac fibrosis), or as a whole with data averaged from 3 sections per animal (all other measures).

2.8 Cell culturing and treatments

Aortic adventitial fibroblasts (AoAFs)

Human aortic adventitial fibroblasts (AoAFs; Cell Applications, Australia) were used to explore the effects of CCL18 on vascular fibrosis. AoAFs were cultured in Stromal Cell Growth Medium (SCGM; Lonza, Switzerland) with 5% FBS, and passages 2 to 8 were used in this study. Cells were grown in T-75 flasks, incubated in a humidified incubator (5% CO_2; Sanyo MCO-18AIC CO_2 incubator, Quantum Scientific, USA) at 37 °C. Confluent cells were passaged using Trypsin-EDTA (Lonza, Switzerland), or seeded on 6-well plates at 10^5 cells/well with serum free SCGM. Cells were either left untreated (control), or treated with TGF-β1 (10 ng/ml; R&D systems, USA), or CCL18 (3, 10, 30, 300 ng/ml; R&D systems, USA). Time courses of treatments were used for AoAFs: 3, 6, 24 hours (h) for mRNA measurements and 24, 48, 72 h for western blotting. At the end of the treatment periods, AoAFs were rinsed with PBS (Sigma-Aldrich, USA). For protein extraction, cells were then incubated with Accutase (Sigma-Aldrich, USA) for 5 minutes at 37 °C for detachment. Detached cells underwent centrifugation of 7000 rpm, 5 minutes at 37 °C. Cell pellets were re-suspended in radioimmunoprecipitation assay lysis and extraction buffer (RIPA buffer; Cell Signalling Technology, USA), followed by protein extraction and western blotting (**Section 2.9**). For mRNA measurements, Buffer RLT (Qiagen, Germany) with 1% β-mercaptoethanol (β-ME; Sigma-Aldrich, USA) were added in the wells of rinsed AoAFs to lyse the cells, followed by RNA extraction and measurements (**Section 2.10**).

Human aortic endothelial cells (HAECs)

Human aortic endothelial cells (HAECs; Cell Applications, Australia) were used to assess the pro-fibrotic effects of CCL18. These cells were grown in endothelial growth serum (Sigma-Aldrich, USA), and passages 3 to 8 were used. Cells were grown in T-75 flasks, incubated in a humidified incubator (5% CO_2; Sanyo MCO-18AIC CO_2 incubator, Quantum Scientific, USA) at 37 °C. Confluent cells were passaged using Trypsin-EDTA (Lonza, Switzerland), and seeded on 6-well plates at 10^5 cells/well. Cells were either left untreated (control), or treated with TGF-β1 (10 ng/ml; R&D systems, USA), or CCL18 (3, 10, 30, 300 ng/ml; R&D systems, USA). Cells were treated for 7 days (treatments replaced on day 3) for subsequent protein extraction and western blot analysis. HAECs were detached, pelleted and re-suspended, using the same procedures as described for AoAFs.

2.9 Western blotting

Protein was extracted from AoAFs and HAECs by incubation (30-60 minutes on ice) with the RIPA buffer, containing 1mM phenylmethylsulfonyl fluoride (PMSF) and 1x protease/ phosphatase inhibitor cocktail (Cell Signalling Technology, USA). Following the incubation, cells debris were pelleted by centrifugation (13000 rpm, 10 minutes, 4 °C), and supernatants (containing cellular proteins from the membrane, nuclear and cytoplasm) were collected and stored at -20 °C for western blotting.

Prior to western blotting, total concentrations of the extracted protein samples were measured via a bicinchonic acid (BCA) assay according to manufacturer's instructions (PierceTM BCA Protein Assay, ThermoScientific, USA). In each sample, equivalent amounts of protein were then topped up to the same volume by 1.5x Laemmli buffer (7.5% glycerol, 3.75% β-ME, 2.25% SDS, 75 mM Tris-HCl pH 6.8, 0.004% bromophenol blue), heated at 95 °C for 3 minutes, and loaded into 7.5% or 10% polyacrylamide gels with molecular weight markers (Precision Plus Protein Standards, Dual Color ladder, Bio-Rad Laboratories, USA). Proteins

were separated by Sodium dodecyl sulfate-polyacrylamide gel electrophoresis (SDS-PAGE; 200V; ChemiDoc MP system, Bio-Rad Laboratories, USA), and then transferred onto low fluorescence polyscreen polycinylidene fluoride (LF PVDF) membranes via the Bio-Rad Trans Blot Turbo transfer system (USA).

Following the transfer, membranes were blocked by 5% skim milk in Tris-Buffered Saline (TBS; 200 mM Tris, 150 mM NaCl, pH 7.5) with 0.1 % tween-20, for 1h. Subsequently, membranes were probed with primary antibodies overnight at 4 °C. Primary antibodies included α-SMA (1:2500 dilution; Abcam, ab5694), GAPDH (housekeeping protein, 1:20000; Abcam, ab8245) and CCR8 (1:500; suitable for human and mouse samples; Novus Biologicals, novnb100709, USA) for both cell types, collagen I (1:1000; Abcam, ab34710) for AoAFs, and VE-cadherin (1:1000; Cell Signalling Technology, D87F2) for HAECs. On the next day, membranes were washed and incubated with secondary antibodies for 1h, including horseradish peroxidase (HRP)-conjugated anti-mouse (1:10000; Jackson ImmunoResearch Laboratories, USA) for GAPDH, and anti-rabbit HRP (1:10000; Dako, Denmark) for all other markers. Resultant protein bands were visualised by Clarity ECL substrates and the ChemiDoc MP system, with densitometries quantified using Image Lab Software (Bio-Rad Laboratories, USA).

2.10 RNA measurements

RNA extraction from human AoAFs

RNA was extracted from human AoAFs using the RNeasy Mini Kit (Qiagen, Germany). Cells were firstly lysed using Buffer RLT, as described in **Section 2.8**, and then scraped with the base of RNase-free 1 ml pipette tips. Scraped lysates were mixed with 70% ethanol (1:1 volume) and transferred to RNeasy spin columns (RNeasy Minikit; Qiagen, Germany). After centrifugation at 10000 rpm for 15s (flow-through discarded), RNA samples were purified using a series of washing buffers (Buffer RW1 and RPE from the Minikit) and one DNase incubation (5µl per sample, in 35µl Buffer RDD; RNase-free DNase Kit; Qiagen, Germany), according to manufacturer's instructions. Purified RNA was eluted from spin columns with RNase-free H_2O, and 2µl of the eluted RNA was used for the assessment of yield and purity

by the QIAxpert system (Qiagen, Germany). The system measured samples at absorbances (A) of 260nm and 280nm, where an A260: A280 ratio of ≥ 2 was considered sufficiently pure.

RNA extraction from mouse aortae

The top third section of thoracic aorta from each mouse was snap frozen in liquid nitrogen for mRNA measurements. Aortic samples were placed in Buffer RLT with 1% β-ME (150 µl per sample), and minced with fine scissors. Minced samples were further disrupted by a sonicator (UP50H; Hielscher, Germany), followed by the digestion of proteins by an incubation with proteinase K (55°C for 10 minutes; Qiagen, Germany). Following centrifugation at 10000 rpm for 5 minutes, the supernatants were mixed with 100% ethanol (2 sample: 1 ethanol by volume). Subsequent RNA purification was performed using the RNeasy Micro Kit (Qiagen, Germany) according to manufacturer's instructions, with RNA yield and purity assessed by QiaExpert (Qiagen, Germany). Procedures of RNA purification, yield measurement and purity assessment has been described in the paragraph above (for RNA extraction from AoAFs).

cDNA conversion and RT-qPCR

1 µg or 0.5 µg (depending on yields) of each AoAF RNA and aortic RNA sample was converted to cDNA, using a High-capacity cDNA reverse transcription kit (as per the manufacturer's instructions; Applied Biosystems, Australia), and a thermal cycler (BioRad MyCycler; BioRad, USA). On the thermal cycler, the reaction parameters were set as follows for four steps: 25 °C for 10 minutes, 37 °C for 2h, 85 °C for 5 minutes, and 4 °C for holding. Resultant cDNA samples were used for RT-qPCR or stored at -20 °C until ready for use.

RT-qPCR where were then used to determine mRNA expression, with all Taqman primers purchased from Life Technologies, USA. For human AoAFs, genes of interest included collagen I, III, V (COL1A1, COL3A1, COL5A1) and α-SMA (ACTA2); 18S was used as a house-keeping gene. For mouse aortae, gene expression of CD206 (M2 macrophage marker), CCL8, CCR8, and the oxidative stress markers NOX2 (NADPH oxidase 2), eNOS (endothelial nitric oxide synthase), SOD1 and SOD3 (superoxide dismutase 1 and 3) were measured; GAPDH was used as the

house-keeping gene. AoAF and aortic cDNA samples were loaded in triplicates with the above-mentioned primers and Taqman Universal PCR Master Mix (Applied Biosystems, USA) into 96-well plates. These plates were run in the Bio-Rad CFX96 Real-Time PCR Detection System (Bio-Rad Laboratories, USA), with the following cycling conditions: 50°C initiation for 2min, subsequent denaturation at 95°C for 10min, and 40 cycles of 95°C denaturation (15s) with 60°C annealing and extension (1min). Fluorescence was recorded at the end of each PCR cycle, allowing mRNA expression to be determined by the comparative cycle threshold (Ct) method (Schmittgen & Livak, 2008), normalised to 18S or GAPDH and expressed relative to the control values (from untreated AoAFs or saline-treated WT mice).

2.11 Enzyme-Linked Immunosorbent Assay (ELISA)

CCL18 levels from human plasma samples were measured using a CCL18 ELISA kit (Human CCL18/PARC DuoSet ELISA; R&D Systems, USA), and CCL8 levels from mouse plasma samples were measured using a CCL8 ELISA kit (Mouse CCL8/MCP-2 DuoSet ELISA; R&D Systems, USA). The ELISA kits contained capture antibody, detection antibody, standards (all specific to CCL18 or CCL8), and Streptavidin conjugated to horseradish-peroxidase (Streptavidin-HRP). Other reagents (PBS, wash buffer, reagent diluent, substrate solution, and stop solution) were included in an ancillary kit (DuoSet Ancillary Reagent Kit 2; R&D Systems, USA). ELISA was performed as per manufacturer's instructions, with all relevant incubations at room temperature, and every washing step involved 3 washes with the working concentration of wash buffer.

Prior to the assay, working concentrations of the capture antibody (specific for CCL18 or CCL8) were used to coat the ELISA plate (100 µl/well, overnight incubation). On the day of assay, the capture antibody was aspirated, and the ELISA plate washed. To prevent non-specific binding, the plates were blocked by 1x reagent diluent (300 µl/well, 30-60 minutes incubation), followed by aspiration and washing. During the incubation period, CCL18 or CCL8 standards were prepared by 1:2 serial dilutions in reagent diluent supplemented with 30% fetal bovine serum (FBS; Life technologies, USA), to concentrations ranging from 7.81 pg/ml

to 1 ng/ml. Plasma samples were diluted in the same FBS-supplemented diluent, using 1:150 dilution for human plasma and 1:2000 dilution for mouse plasma.

After blocking, samples, standards or FBS-supplemented diluent (blank control) were added to the plates (100 µl/well, in duplicates), which were then incubated for 2h before being aspirated and washed. To allow detection of the target protein in samples, working concentration of CCL18 or CCL8 detection antibody was added to the wells (100 µl/well, 2h incubation), followed by aspiration and washes. Subsequently, Streptavidin-HRP (diluted 1:200 in reagent diluent) was added to the plates (100 µl/well, 20-minute incubation in the dark). After the incubation, plates were aspirated and washed, followed by a final 20-minute incubation in substrate solution (1:1 mixture of hydrogen peroxide and tetramethylbenzidine; 100 µl/well). In this time the substrate solution was converted by the enzyme to a coloured product.

The enzymatic reactions were terminated by the addition of stop solution (50 µl/well), with gentle tapping of the plate for thorough mixing. Finally, the colour density was determined using a micro-plate reader at 450 nm wavelength, and a CCL18 or CCL8 standard curve was created with a 4-parameter logistic (4-PL) curve-fit. The intensity of the coloured product was directly proportional to the [CCL18] or [CCL8] in the sample. The amount of CCL18 or CCL8 was therefore estimated by comparing the optical density (OD) values of the samples with the OD values of the standards.

2.12 Single-cell RNA sequencing (scRNA-Seq)

ScRNA-Seq and relevant analysis were performed by Dr. Antony Vinh, Prof. Grant Drummond and Dr. Alexander Pinto at La Trobe University, using the aortae of a cohort of WT saline- or Ang II- treated mice, as described by McLellan et al. (2020). In brief, metabolically active nucleated aortic cells were isolated by Fluorescence-Activated Cell Sorting (FACS) to form a single cell preparation. This preparation was processed by a Chromium controller with the Chromium Single Cell 3’ v2 reagent kit (10X Genomics, USA), and then sequenced using HiSeq 4000 (Illumina, USA).

2.13 Bioluminescence resonance energy transfer (BRET) assays

BRET assays were performed by Dr. Herman Lim (Department of Biochemistry, Monash University), as described by Lim et al. (2021). Briefly, Flp-In Chinese hamster ovary (CHO) cells were transfected by human CCR8 (hCCR8) or mouse CCR8 (mCCR8). CHO cells were then stimulated with human- or mouse- CCL1 (hCC1/ mCCL1; established CCR8 agonists), or hCC18/ mCCL8 (chemokines of interest). G-protein activation was assessed by measuring activation of different G-protein subunits: $G\alpha_{i2}$+ $G\beta_1$ tagged by $venus^{156-229}$, $G\gamma_2$ tagged by $venus^{1-155}$, GRKct tagged by Rluc, with CCR8 constructed by PCR amplification and tagged by myc. cAMP inhibition assay was performed using 10μM forskolin, where CCR8 was tagged by myc. β-arrestin2 recruitment was measured with CCR8 tagged by Rluc and β-arrestin tagged by YFP. The BRET signal was measured as a ratio of fluorescence at 450-500 nm: 515-560 nm, and expressed as a percentage of maximal response to CCL1.

2.14 Statistical analysis

All data were presented as mean ± standard error of the mean (SEM), or individual points with correlation analysis. RT-qPCR data were expressed as fold changes relative to the control group (untreated cells or saline-treated WT mice). Organ weights were expressed as % of body weight. Vasorelaxation responses to ACh or DEA-NO were expressed as % reversal of pre-contraction to U46619, and vasoconstriction responses to phenylephrine or L-NAME were expressed as % of maximal response to U46619 (F_{max}). Quantification of histological staining was performed in a blinded manner, with picrosirius red staining expressed as % of adventitial area. Elastin dysregulation was assessed using a scoring system, with a score of 1= no dysregulation, 2= mild dysregulation, 3= moderate dysregulation, 4= severe dysregulation.

Linear regression analysis was used to investigate the correlation of plasma CCL18 levels with systolic BP, age, body mass index (BMI), or number of anti-hypertensive medications taken.

Student's unpaired t-test was used to compare the baseline BP of WT and CCR8 KO mice. 2-way ANOVA (with Tukey's post-hoc test) was used to compare systolic BP or body weight measurements in multiple treatment groups over the 14-day or 28-day treatment period. scRNA data were analysed by principal component analysis (PCA), using Cell Ranger (version 2.1.1) and R (version 3.4 or 3.6) as described by McLellan et al. (2020). Other data were analysed by 1-way ANOVA with Dunnett's post-hoc test (vs untreated control AoAFs or HAECs) or Tukey's post-hoc test (all other comparisons). Statistical tests were performed using GraphPad Prism 8 (USA) unless otherwise specified, with $p < 0.05$ considered statistically significant.

2.15 References

Berenguer J, Lagerweij T, Zhao XW, Dusoswa S, van der Stoop P, Westerman B, de Gooijer MC, Zoetemelk M, Zomer A, Crommentuijn MHW, Wedekind LE, López-López À, Giovanazzi A, Bruch-Oms M, van der Meulen-Muileman IH, Reijmers RM, van Kuppevelt TH, García-Vallejo JJ, van Kooyk Y, Tannous BA, Wesseling P, Koppers-Lalic D, Vandertop WP, Noske DP, van Beusechem VW, van Rheenen J, Pegtel DM, van Tellingen O, & Wurdinger T (2018). Glycosylated extracellular vesicles released by glioblastoma cells are decorated by CCL18 allowing for cellular uptake via chemokine receptor CCR8. Journal of extracellular vesicles 7**:** 1446660.

Lim HD, Lane JR, Canals M, & Stone MJ (2021). Systematic Assessment of Chemokine Signaling at Chemokine Receptors CCR4, CCR7 and CCR10. Int J Mol Sci 22.

McLellan MA, Skelly DA, Dona MSI, Squiers GT, Farrugia GE, Gaynor TL, Cohen CD, Pandey R, Diep H, Vinh A, Rosenthal NA, & Pinto AR (2020). High-Resolution Transcriptomic Profiling of the Heart During Chronic Stress Reveals Cellular Drivers of Cardiac Fibrosis and Hypertrophy. Circulation 142: 1448-1463.

Schmittgen TD, & Livak KJ (2008). Analyzing real-time PCR data by the comparative CT method. Nat Protocols 3**:** 1101-1108.

Chapter 3

CCL18 is elevated in resistant hypertension and promotes vascular fibrosis

CCL18 is elevated in resistant hypertension and promotes vascular fibrosis

Authors:

Mingyu Zhu[1], Caitlin V. Lewis[1], Meghan J. Finemore[1], Tea Christmas[1], Nina Eikelis[2], Gavin W. Lambert[2], Markus P. Schlaich[3], Robert E. Widdop[1], Chrishan S. Samuel[1], Grant R. Drummond[4], Barbara K. Kemp-Harper[1].

Affiliations:

[1]Biomedicine Discovery Institute, Department of Pharmacology, Monash University, Clayton, VIC, Australia.

[2]Iverson Health Innovation Research Institute, Swinburne University of Technology, VIC, Australia.

[3]Dobney Hypertension Centre, The University of Western Australia, Perth, WA, Australia.

[2]Department of Physiology, Anatomy & Microbiology, La Trobe University, Bundoora, VIC, Australia.

3.1 COVID-19 impact statement

Essential experiments for Chapter 3 were completed either before the COVID-19 pandemic or during the period of eased restriction (mid-May to early July). A small number of other experiments, such as measuring levels of (pro-)collagen I and matrix metalloproteinases in the aortic fibroblast culture media, would have provided additional data. However, these non-essential experiments were not performed due to time being lost under the impact of the COVID-19 pandemic.

3.2 Abstract

Introduction: Patients with resistant hypertension have uncontrolled blood pressure (BP), despite concurrent use of 3 of more antihypertensive medications. Resistant hypertension leads to severe end-organ damage and a higher risk of a cardiovascular event as compared to patients with controlled hypertension. M2 macrophages contribute to hypertension associated end-organ damage, and may promote fibrosis via the release of the pro-fibrotic chemokine, C-C motif chemokine ligand 18 (CCL18). There is no current biomarker for resistant hypertension, and CCL18 has not been studied in the context of hypertension or the associated vascular fibrosis. As such, this study aimed to assess the role of CCL18 in resistant hypertension, and its pro-fibrotic efficacy in the human vasculature.

Methods: Plasma CCL18 levels from normotensive (Systolic BP: 119 ±2 mmHg), essential (155 ±3 mmHg) or resistant (156 ±5 mmHg) hypertensive patients were measured by ELISA. Human aortic adventitial fibroblasts (AoAFs) and endothelial cells were treated with the pro-fibrotic agent TGF-β1 (10 ng/ml) or CCL18 (3-300 ng/ml) for 3-72h and 7d, respectively. In human AoAFs, expression of pro-collagen I, mature collagen I and α-SMA and were measured (qRT-PCR, Western blotting). Endothelial-mesenchymal transition was measured via VE-cadherin and α-SMA protein expression.

Results: Plasma CCL18 levels were 49% higher in patients with resistant hypertension as compared to normotensive subjects (64 ± 6 vs 43 ± 6 ng/ml; $p<0.05$). In human AoAFs, TGF-β1 caused a 2-fold increase in protein expression of collagen I (24h, $p<0.01$) and a 2-3-fold increase of α-SMA (24-72h, $p<0.05$). CCL18 did not change α-SMA expression, but increased the protein expression of pro-collagen I by 2-fold (300 ng/ml, 24h; $p<0.01$), and elevated mature collagen I by 3-fold (72h; $p<0.05$). In human aortic endothelial cells, CCL18 (10 ng/ml) increased α-SMA (1.5-fold, $p<0.05$) and showed a trend to decrease VE-cadherin.

Discussion: Resistant hypertension is associated with elevated plasma CCL18 levels. CCL18 targets adventitial fibroblasts and endothelial cells in the vascular wall to promote collagen synthesis and endothelial-mesenchymal transition, respectively. Therefore, CCL18 is a potential biomarker and/or therapeutic target for resistant hypertension.

3.3 Introduction

Chronic hypertension is associated with end-organ damage, to which the immune system is a key contributor (Drummond et al., 2019). In particular, the "M2" subset of macrophages has been found to play an important role in hypertension-associated vascular, cardiac, and renal damage by promoting fibrosis (Falkenham et al., 2015; Guiteras et al., 2016; Moore et al., 2015). Despite a multitude of available anti-hypertensive treatments, 5-10 % of hypertensive patients are resistant to therapies, i.e. their blood pressure (BP) remains uncontrolled (systolic BP ≥ 140 mmHg and/or diastolic BP ≥ 90 mmHg) when treated with at least three different classes of anti-hypertensive medications (de la Sierra et al., 2011). Resistant hypertensive patients are at a greater risk of a cardiovascular event, such as myocardial infarction, heart failure, and stroke (Daugherty et al., 2012). As such, reliable biomarkers to identify patients unlikely to respond to conventional therapies and effective treatments are urgently required to achieve better clinical management for resistant hypertension.

Given the key role of M2 macrophages in hypertension (Drummond et al., 2019), these immune cells may serve as a source of a biomarker and/or treatment target for resistant hypertension. Preliminary data from our laboratory showed that when macrophages are polarised to the M2 phenotype, the production of a pro-fibrotic chemokine, C-C motif chemokine ligand 18 (CCL18) is increased substantially, whereas expression of TGF-β1 (another major pro-fibrotic factor) remains unchanged. CCL18 has been found to stimulate chemotaxis of leukocytes, including T and B lymphocytes and immature dendritic cells, into sites of inflammation (Schutyser et al., 2005). CCL18 promotes fibrosis not only by recruiting T cells, but also by directly increasing collagen generation from pulmonary fibroblasts (Atamas et al., 2003; Pochetuhen et al., 2007; Wynn & Ramalingam, 2012).

CCL18 has been implicated in various cardiovascular diseases. For example, in patients with acute coronary syndrome, high levels of plasma CCL18 are associated with a higher risk of fatal cardiovascular events (de Jager et al., 2012). CCL18 is also elevated in serum from patients with abdominal aortic aneurysm (Courtois et al., 2014), and it is co-localised with macrophages in carotid atherosclerotic lesions (Hägg et al., 2009). Furthermore, in a pilot study of our laboratory, CCL18 is found to promote collagen generation from cardiac

fibroblasts, although it has not been studied in the context of hypertension or the associated vascular fibrosis.

Considering the published studies and our preliminary data, we hypothesized that the macrophage-derived profibrotic chemokine, CCL18 is a biomarker in patients with resistant hypertension and mediates the pro-fibrotic actions of M2 macrophages in this disease setting. This study aimed to evaluate the role of CCL18 in patients with resistant hypertension, and to investigate the pro-fibrotic effects of CCL18 on human vascular cells (including aortic adventitial fibroblasts and aortic endothelial cells).

3.4 Methods

Enzyme-Linked Immunosorbent Assay (ELISA)

Human plasma samples were collected during studies conducted at the Heart Centre of Alfred Hospital (2001-2017), under ethics numbers 92/00, 51/03, 7/05, 8/12, 87/12 and 215/12. The study cohort comprised normotensive subjects (control, n= 14), untreated essential hypertensive patients (n= 20) and resistant hypertensive patients (n= 20).

CCL18 levels from human plasma samples were measured using a CCL18 ELISA kit (Human CCL18/PARC DuoSet ELISA; R&D Systems, USA) and an ancillary kit (DuoSet Ancillary Reagent Kit 2; R&D Systems, USA). ELISA was performed as per manufacturer's instructions, and plasma sample diluent was supplemented with 30% fetal bovine serum (FBS; Life technologies, USA) according to manufacturer's recommendation. Detailed procedures are described in General Methods (**Section 2.11**). CCL18 concentration was calculated by constructing a fitted standard curve of optical density against the concentrations of serially diluted CCL18.

Cell culturing and treatments

Human aortic adventitial fibroblasts (AoAFs; Cell Applications, Australia) were cultured in Stromal Cell Growth Medium (SCGM; Lonza, Switzerland) with 5% FBS, and passages 2 to 8 were used in this study. Human aortic endothelial cells (HAECs; Cell Applications, Australia) were grown in endothelial growth serum (Sigma-Aldrich, USA), and passages 3 to 8 were used. AoAFs and HAECs were grown in T-75 flasks, incubated in a humidified incubator (5% CO_2; Sanyo MCO-18AIC CO_2 incubator, Quantum Scientific, USA) at 37 °C. Both cell types were passaged using Trypsin-EDTA (Lonza, Switzerland), and seeded on 6-well plates at 10^5 cells/well. Cells were either left untreated (control), or treated with TGF-β1 (10 ng/ml; R&D systems, USA), or CCL18 (3-300 ng/ml; R&D systems, USA). Treatment periods for AoAFs were 3-24 hours (h) for mRNA measurements and 24-72 h for western blotting, whilst HAECs were treated for 7 days (treatments replaced on day 3) for subsequent western blot analysis. At the end of treatments, cells were detached from wells and lysed as detailed in General Methods (**Section 2.8**).

mRNA measurements

RNA was extracted from AoAFs using the RNeasy Mini Kit according to manufacturer's instructions (Qiagen, Germany), with the yield and purity assessed by the QiaExpert system (Qiagen, Germany). Extracted RNA was then converted to cDNA using a High-capacity cDNA reverse transcription kit (as per manufacturer's instructions; Applied Biosystems, Australia), and a thermal cycler (Bio-Rad Laboratories MyCycler; Bio-Rad Laboratories, USA). Resultant cDNA samples were used to measure gene expression of collagen I, III, V (COL1A1, COL3A1, COL5A1) and α-SMA (ACTA2) (primers purchased from Life Technologies, USA). 18S was used as a house-keeping gene, relevant real-time quantitative reverse transcription polymerase chain reaction (RT-qPCR) was run in triplicates in the Bio-Rad CFX96 Real-Time PCR Detection System (USA). mRNA expression was determined by the comparative cycle threshold (Ct) method (Schmittgen & Livak, 2008), being normalised to 18S and expressed relative to the control values from untreated AoAFs. More detailed procedures are outlined in General Methods (**Section 2.10**).

Protein extraction and western blotting

Protein was extracted from AoAFs and HAECs by incubation (30-60 minutes) with the radioimmunoprecipitation assay (RIPA) lysis and extraction buffer, containing 1mM phenylmethylsulfonyl fluoride (PMSF) and 1x protease/phosphatase inhibitor cocktail (Cell Signalling Technology, USA). Following the incubation, cells debris were pelleted by centrifugation (13000 rpm, 10 minutes, 4 °C), and supernatants were collected for western blotting.

Prior to western blotting, total concentrations of the extracted protein samples were measured via a bicinchonic acid (BCA) assay according to manufacturer's instructions (Pierce™ BCA Protein Assay, ThermoScientific, USA). In each sample, equivalent amounts of protein were then topped up to the same volume by 1.5x Laemmli buffer and loaded into 7.5% or 10% polyacrylamide gels with molecular weight markers (Precision Plus Protein Standards, Dual Color ladder, Bio-Rad Laboratories, USA). Proteins were separated by Sodium dodecyl

sulfate-polyacrylamide gel electrophoresis (SDS-PAGE; 200V; ChemiDoc MP system, Bio-Rad Laboratories, USA), and then transferred onto low fluorescence polyscreen polycinylidene fluoride (LF PVDF) membranes via the Bio-Rad Trans Blot Turbo transfer system (USA).

Following the transfer, membranes were blocked by 5% skim milk in Tris-Buffered Saline (TBS; 200 mM Tris, 150 mM NaCl, pH 7.5) with 0.1 % tween-20, for 1h. Subsequently, membranes were probed with primary antibodies overnight at 4 °C. Primary antibodies included α-SMA (1:2500 dilution; Abcam, ab5694), GAPDH (1:20000; Abcam, ab8245) and CCR8 (1:500; suitable for human and mouse samples; Novus Biologicals, novnb100709, USA) for both cell types, collagen I (1:1000; Abcam, ab34710) for AoAFs, and VE-cadherin (1:1000; Cell Signalling Technology, D87F2) for HAECs. Membranes were then washed and incubated with secondary antibodies for 1h, including horseradish peroxidase (HRP)-conjugated anti-mouse (1:10000; Jackson ImmunoResearch Laboratories, USA) for GAPDH, and anti-rabbit HRP (1:10000; Dako, Denmark) for all other markers. Resultant protein bands were visualised by Clarity ECL substrates and the ChemiDoc MP system, with densitometries quantified using Image Lab Software (Bio-Rad Laboratories, USA).

Statistical analysis

All data were presented as mean ± standard error of the mean (SEM), or individual points with correlation analysis. RT-qPCR data were expressed as fold changes relative to the control group (untreated cells). Multiple groups were compared via 1-way ANOVA with Tukey's post-hoc test (for experiments using human plasma) or Dunnett's post-hoc test (vs untreated control AoAFs or HAECs). Linear regression analysis was used to investigate the correlation of plasma CCL18 levels with systolic blood pressure, age, body mass index (BMI), or number of anti-hypertensive medications taken. All statistical tests were performed using GraphPad Prism 8 (USA), with $p < 0.05$ considered statistically significant.

3.5 Results

Plasma CCL18 is elevated in resistant hypertension

In this study, the systolic blood pressure (SBP) of patients with essential hypertension (untreated) and resistant hypertension was elevated to a similar level (155 ± 3 and 157 ± 5 mmHg, respectively) compared to normotensive participants (119 ± 2 mmHg; $p< 0.05$) (**Figure 1A**). Resistant hypertensive (resistant HTN) patients also had 49 % higher plasma CCL18 level than normotensive subjects (64 ± 6 vs 43 ± 6 ng/ml; $p<0.05$) (**Figure 1B**). No correlation was found between plasma CCL18 levels and systolic BP (**Figure 1 C**).

When potential confounding factors were investigated, female resistant HTN patients had significantly higher plasma CCL18 levels than normotensive female participants (68 ± 8 ng/ml vs normotensive 18 ± 5 ng/ml; $p< 0.05$), whilst no difference was found among the three groups of male subjects (**Figure 2A**). CCL18 levels of female normotensive subjects tended to be lower than those of male subjects (normotensive female vs male: 18 ± 5 vs 51 ± 6 ng/ml), but these changes failed to reach statistical significance due to the low sample size (**Figure 2A**). In addition, the resistant HTN cohort (male and female data combined) was older (61 ± 3 years vs normotensive 46 ± 4 years) and had a higher BMI (33 ± 1 kg/m^2 vs normotensive 27 ± 1 kg/m^2) (**Figure 2B**). Further analysis found no correlation of plasma CCL18 levels with age, and weak correlation between plasma CCL18 and BMI (**Figure 2C-D**). In the resistant HTN group, expression of C-reactive protein (CRP; inflammatory marker) was not significantly changed compared to normotensive subjects, and the number of anti-HTN medications taken was not associated with plasma CCL18 (**Supplementary Figure 1, Supplementary Tables 1-2**).

CCL18 does not change α-SMA expression in human aortic adventitial fibroblasts (AoAFs)

To investigate the pro-fibrotic effects of CCL18 on human vascular cells, human AoAFs were treated with TGF-β1 (10ng/ml; positive control) or CCL18 (3-300 ng/ml), after which mRNA (3-24h treatments) and protein (24-72h treatments) expression of α-SMA (ACTA2 gene; myofibroblast marker) were measured. TGF-β1 increased ACTA2 mRNA expression by 6-fold at 24h ($p< 0.01$ vs untreated control) but not at 3h or 6h (**Figure 3D**). α-SMA protein expression was also increased by TGF-β1 (2-3 fold, 24-72h treatments; $p< 0.05$) (**Figure 4**). As

compared to untreated human AoAFs, no change was observed on the mRNA or protein expression of α-SMA in CCL18 treated cells (**Figures 3D, 4B-G**).

CCL18 increases collagen protein generation from human AoAFs

Following TGF-β1 or CCL18 treatment of human AoAFs, collagen generation was also measured. TGF-β1 (10 ng/ml, 24h)-treated AoAFs had increased mRNA expression of collagen I (COL1A1) and collagen V (COL5A1) (by 1.5-fold and 2.5-fold vs untreated control, respectively; $p< 0.01$), whilst no difference was seen in collagen III (COL3A1) expression (**Figure 3A-C**). Increased collagen I protein (doublet at ≈130 and 115 kDa) expression was also observed in TGF-β1 (24h)-treated human AoAFs (2-fold, $p< 0.01$), with no significant change at 48h or 72h (**Figure 5**). By contrast, pro-collagen I expression (doublet at ≈235 and 215 kDa) remained unchanged following 24-48h of TGF-β1 treatment, and was reduced at 72h ($p< 0.01$ vs control) (**Figure 5**).

CCL18 treatment (3-300 ng/ml, 3-24 h) did not alter the mRNA expression of collagen I, III or V in human AoAFs (**Figure 3A-C**). However, when protein expression was measured, 300 ng/ml of CCL18 caused a 2-fold increase in pro-collagen I generation (at 24h) and a 3-fold increase in mature collagen I production (at 72h) ($p< 0.05$ vs control; **Figure 5**). Expression of the CCL18 receptor, CCR8 could not be confirmed in AoAFs due to the low specificity of available antibodies. However, CCR3 (antagonised by CCL18) expression was confirmed in AoAF (**Supplementary Figure 2**).

CCL18 promotes α-SMA expression and may reduce VE-cadherin expression in human aortic endothelial cells (HAECs)

Pro-fibrotic effects of CCL18 were further studied using HAECs, which were treated with TGF-β1 (10ng/ml) or CCL18 (3-300 ng/ml) for 7 days, and markers of endothelial-mesenchymal transition (End-MT) were measured. TGF-β1 did not lead to changes in the protein expression of α-SMA (myofibroblast marker) or VE-cadherin (endothelium marker) (**Figure 6**). CCL18 had a biphasic effect on the protein expression of α-SMA (myofibroblast marker), where 10 ng/ml

treatment significantly increased α-SMA by 1.5-fold ($p < 0.05$ vs untreated control) (**Figure 6B-C**), yet α-SMA levels were unchanged at CCL18 concentrations $\geq$ 30ng/ml. Changes in the protein expression of VE-cadherin may also be biphasic, where 10 ng/ml of CCL18 showed a trend to decrease VE-cadherin (**Figure 6D-E**).

3.6 Figures

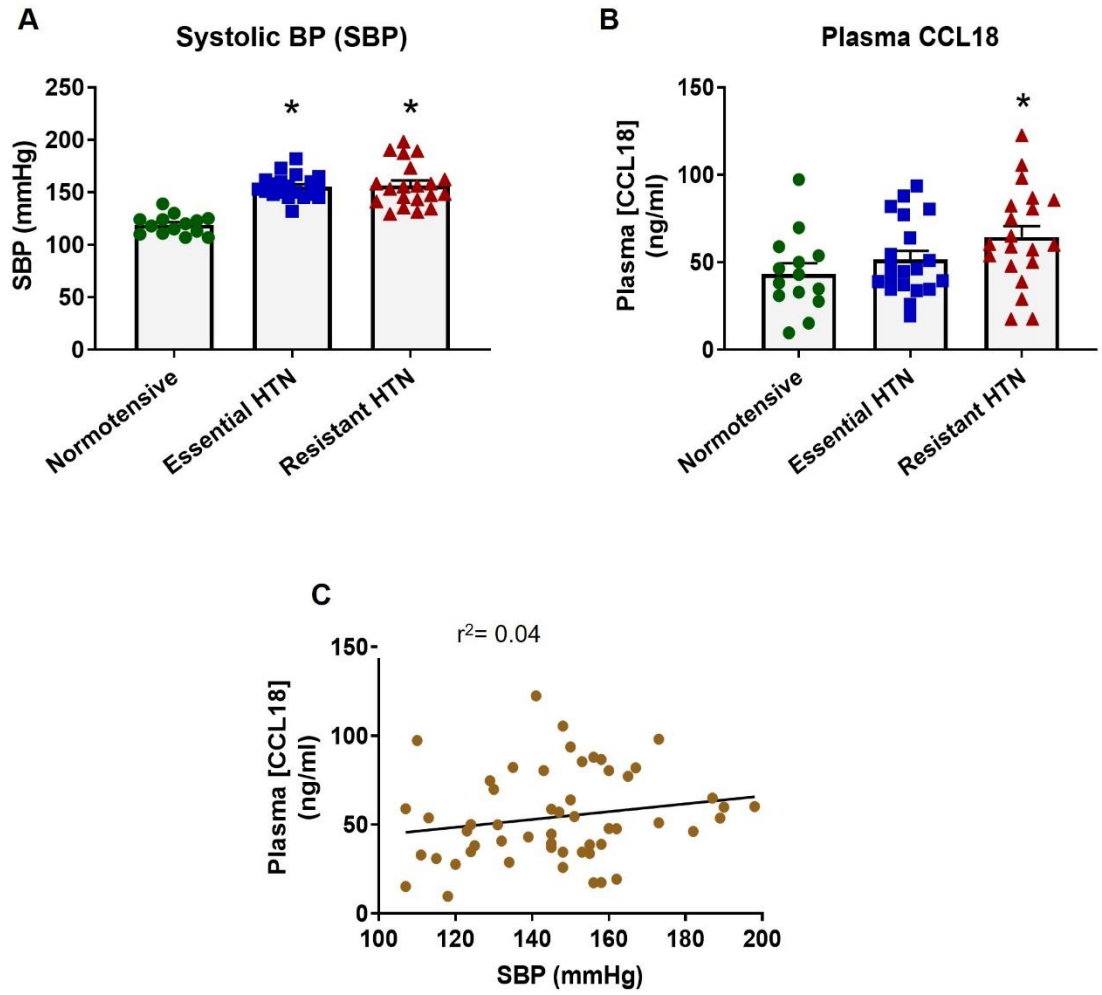

Figure 1. Plasma CCL18 and systolic blood pressure (SBP) of normotensive, essential hypertensive (HTN), and resistant HTN subjects. Essential HTN patients were untreated; Resistant HTN patients were on at least 3 different classes of anti-HTN medications. SBP (**A**) and plasma CCL18 levels (**B**) were measured in the three subject groups. (**C**) Correlation analysis between plasma CCL18 and SBP in the whole cohort (**C**).

Data presented as mean ± SEM, dots depict individual data points (**A-B**) or individual points (**C**), n= 14-20 per group or 54 in total. (**A-B**) *p<0.05 vs normotensive subjects, 1-way ANOVA, Tukey's post hoc test. (**C**) Linear regression analysis.

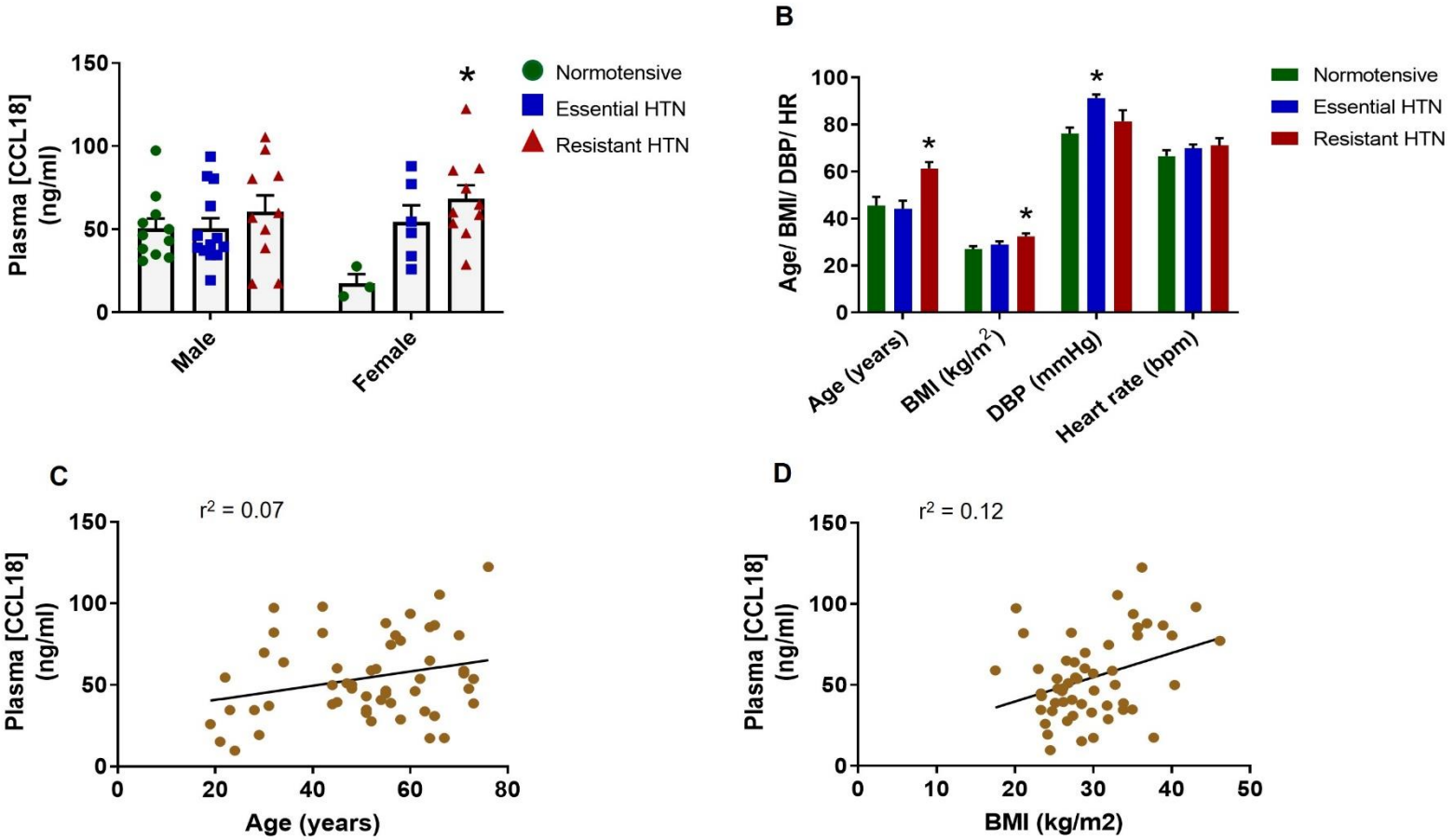

Figure 2. Association of plasma CCL18 with gender, age, BMI, diastolic blood pressure (DBP) and heart rate (HR). (**A**) Plasma CCL18 levels in different genders. (**B**) Age, BMI, DBP, and HR measurements in the three subject groups. (**C-D**) Correlation of CCL18 with age (**C**) and BMI (**D**), in resistant hypertensive (HTN) patients compared to normotensive subjects. Data presented as mean ± SEM, dots depict individual data points (**A-B**) or individual points (**C-D**), n= 3-20 per group. (**A-B**) *p<0.05 vs normotensive subjects, 1-way ANOVA, Tukey's post hoc test. (**C-D**) Linear regression analysis.

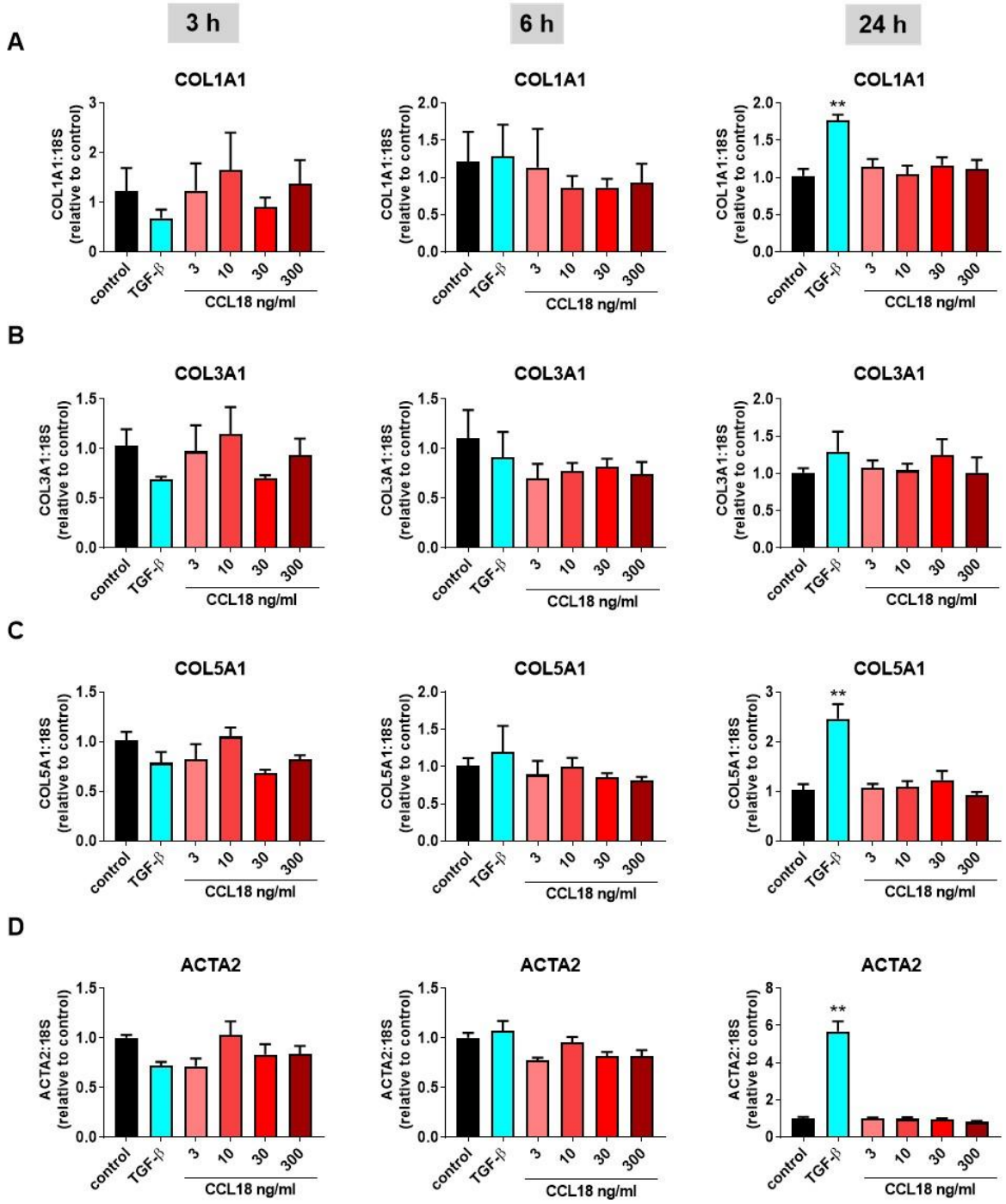

Figure 3. Effects of CCL18 on mRNA expression of collagen (COL) and α-smooth muscle actin (α-SMA) in human aortic adventitial fibroblasts (AoAFs). Concentration- and time-dependent effects on COL1A1 (**A**), COL3A1 (**B**), COL5A1 (**C**) and ACTA2 (**D**; α-SMA) mRNA expression following 3 to 24 hours of CCL18 (3-300 ng/ml) or TGF-β1 (10ng/ml) treatment.

Data presented as mean ± SEM, n= 3-6. MRNA fold changes expressed relative to control (untreated). ** $p<0.01$ vs control, 1-way ANOVA, Dunnett's post hoc test.

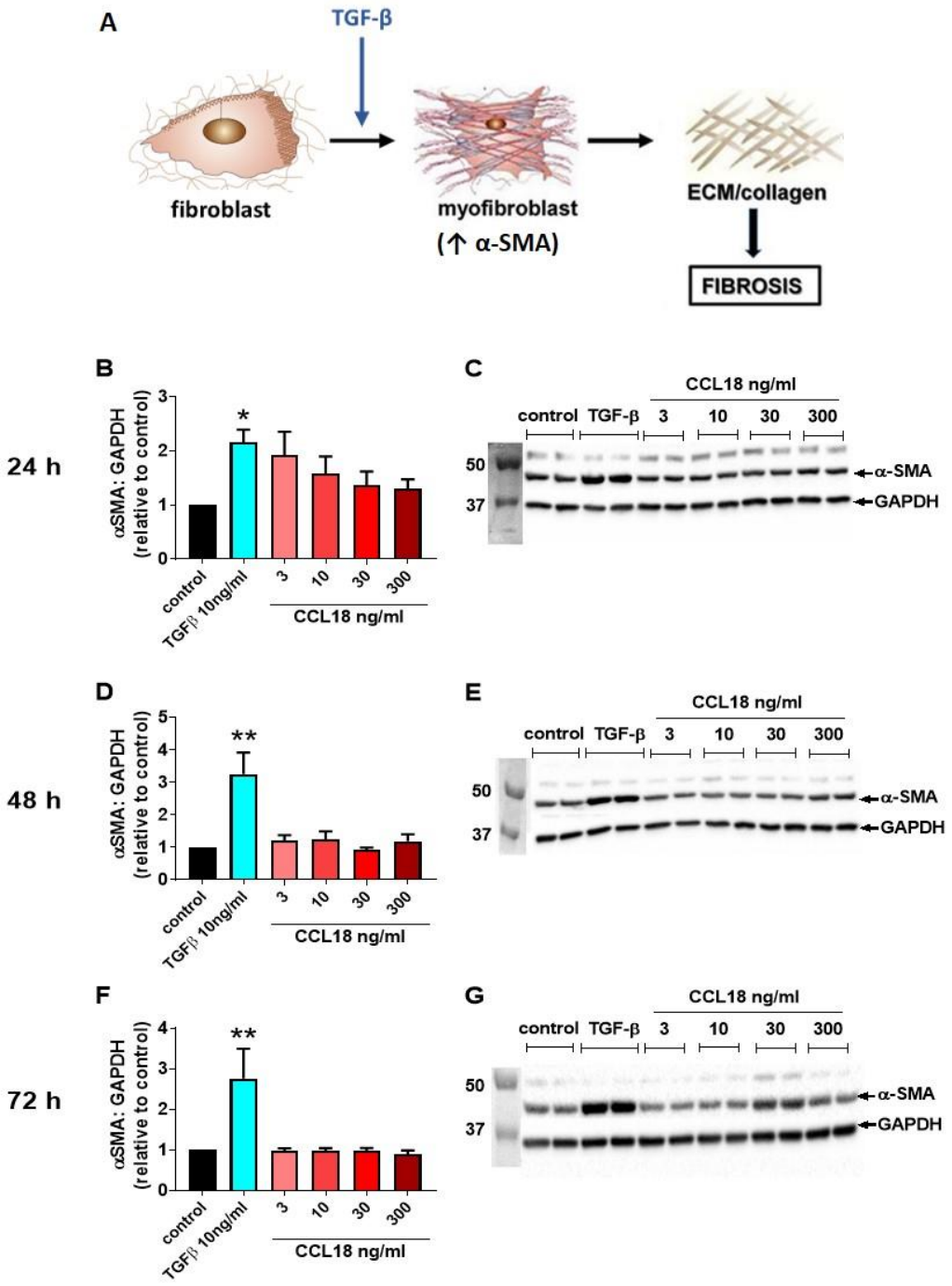

Figure 4. Effects of CCL18 on protein expression of α-SMA in human AoAFs. (**A**) Schema depicting the steps involved in fibrosis, highlighting the differentiation of fibroblasts to myofibroblasts (express α-SMA) and subsequent generation of collagen. Concentration- and time-dependent effects on α-SMA expression following 24h (**B-C**), 48h (**D-E**), and 72h (**F-G**) treatment with CCL18 (3-300 ng/ml) or TGF-β1 (10ng/ml). Left panel: quantification data; right panel: representative western blots. Data presented as mean ± SEM, n= 7-9. Fold changes expressed relative to untreated control. *p<0.05 vs control, **p<0.01 vs control, 1-way ANOVA, Dunnett's post hoc test.

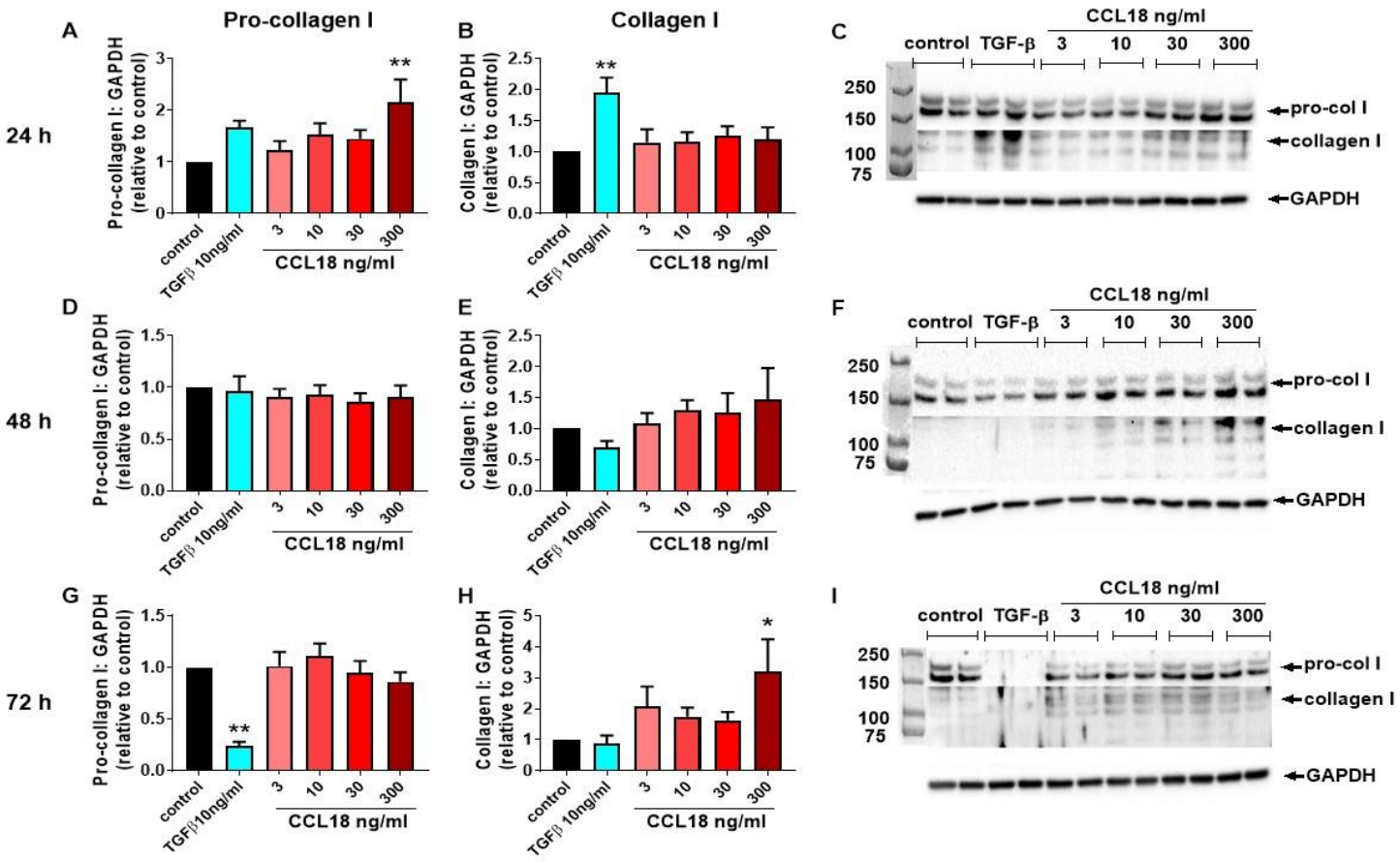

Figure 5. Effects of CCL18 on protein expression of pro-collagen I (pro-col I) and collagen I in human AoAFs. Concentration- and time-dependent effects on pro-collagen I and collagen I expression following 24h (**A-C**), 48h (**D-F**), and 72h (**G-I**) of CCL18 (3-300 ng/ml) or TGF-β1 (10ng/ml) treatment. Left panel: quantified pro-col I expression; middle panel: quantified collagen I expression; right panel: representative western blots. Data presented as mean ± SEM, n= 6-11. Fold changes expressed relative to untreated control. *p<0.05 vs control, **p<0.01 vs control, 1-way ANOVA, Dunnett's post hoc test.

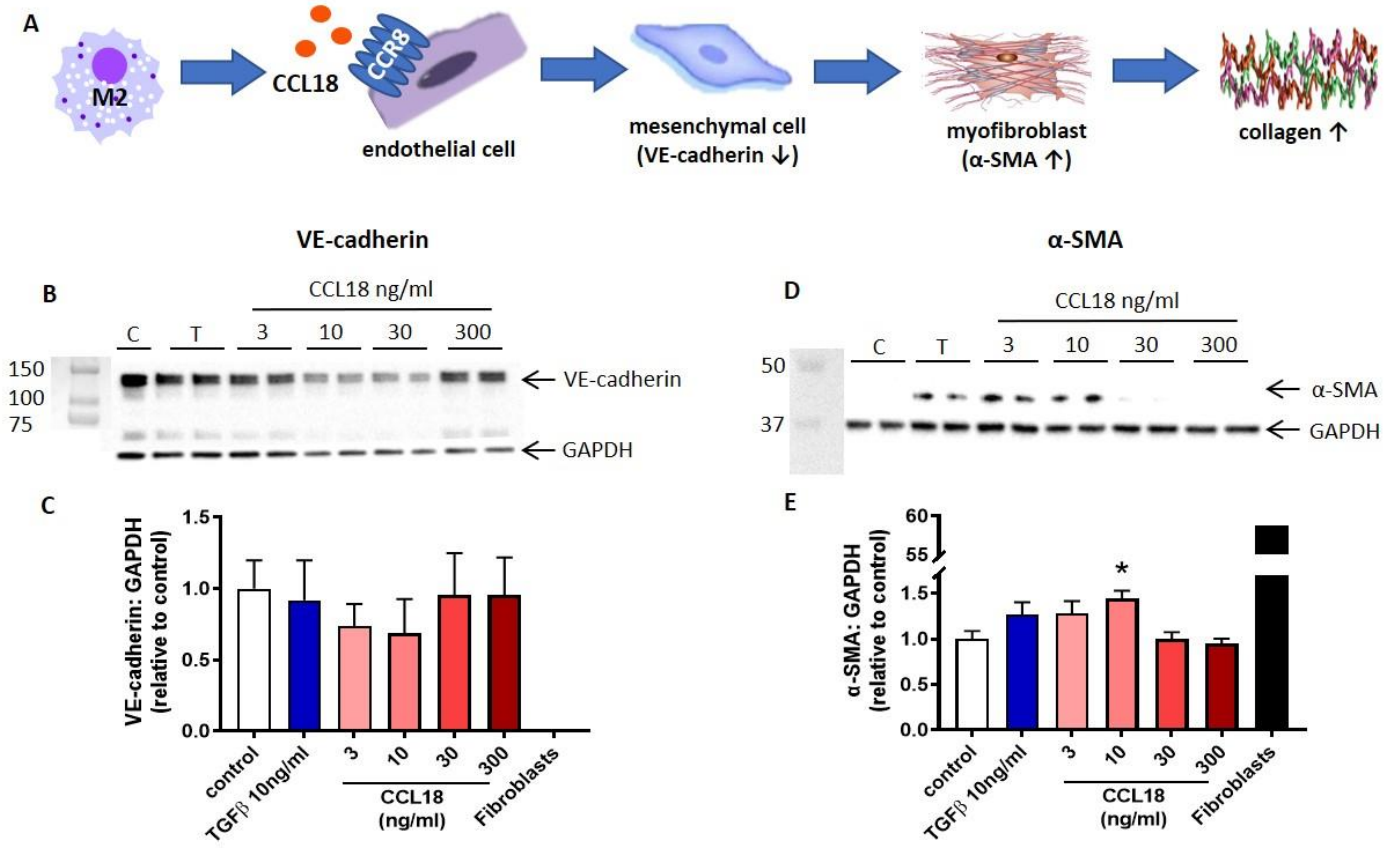

Figure 6. Effects of CCL18 on protein expression of α-SMA and VE-cadherin in human aortic endothelial cells (HAECs). Concentration-dependent effects on VE-cadherin (**B-C**) and α-SMA (**D-E**) expression following 7 days treatment with CCL18 (3-300 ng/ml) or TGF-β1 (T; 10ng/ml). Fibroblast samples (n= 2) were included as a positive control for α-SMA and negative control for VE-cadherin. Top panel (**A**): schema of proposed mechanism by which CCL18 acts on endothelial cells to promote endothelial-mesenchymal transition and fibrosis; middle panel: representative western blots (C= control); bottom panel: quantified data. Data presented as mean ±SEM, n= 4-10. Fold changes expressed relative to untreated control. *p<0.05 vs control, 1-way ANOVA, Dunnett's post hoc test.

3.7 Discussion

Resistant hypertension is characterised by chronic uncontrolled high blood pressure, and end-organ damage. M2 macrophages play a key role in the end-organ fibrosis/damage associated with hypertension (Moore et al., 2015). Since the pro-fibrotic chemokine CCL18 is highly expressed in M2 macrophages, this study explored the potential of CCL18 to be a biomarker and/or a treatment target for resistant hypertension. We have provided the first evidence that plasma CCL18 is elevated in resistant hypertensive (HTN) patients, and that CCL18 contributes to aortic fibrosis by stimulating collagen generation from human aortic adventitial fibroblasts (AoAFs) and by promoting endothelial-mesenchymal transition (End-MT). This study highlights an important role of CCL18 in resistant hypertension.

Patients with resistant hypertension are at a 50% greater risk of a cardiovascular event than patients with controlled hypertension (Daugherty et al., 2012). To improve outcomes for this high-risk patient group, early identification of patients at risk of resistant hypertension is essential. The establishment of a novel biomarker to enable identification of patients unlikely to respond to conventional therapies, will allow clinicians to distinguish patients who are likely to be resistant HTN and expedite alternative treatments (e.g. renal denervation) to lower BP, thereby reducing the risk of a cardiovascular event. Our findings indicate that CCL18 may be such a biomarker. Whilst CCL18 levels have been measured in a number of cardiovascular diseases, to our knowledge this is the first study to measure CCL18 in hypertensive patients. We have made the novel finding that CCL18 is elevated in patients with resistant, but not essential (untreated) hypertension. The validity of this finding is supported by the observation that plasma levels of CCL18 in healthy (normotensive) subjects (43 [10-97] ng/ml) were similar to those reported in other studies (42.5 [IQR 31-54] ng/ml) (Ziliotto et al., 2018). In addition, plasma CCL18 levels in resistant HTN patients (63 [17-122] ng/ml) were similar to those of high-risk acute coronary syndrome patients (67 [IQR 43–105] ng/ml) (de Jager et al., 2012). A correlation between BP and CCL18 was not apparent and indeed systolic BP did not differ between patients with essential and resistant hypertension, with only resistant HTN patients have elevated CCL18. Collectively these data suggest that plasma CCL18 levels may be used to distinguish between essential HTN and resistant HTN patients. Although CCL18 levels appeared to be elevated in some patients with essential hypertension (>50mg/ml), it must be noted that these patients were newly diagnosed and untreated. We

do not know if these patients were subsequently diagnosed with resistant hypertension and the future identification, and exclusion, of such patients from this cohort may lead to a clearer difference in plasma CCL18 between essential and resistant hypertension.

Despite resistant HTN subjects being older and having a higher BMI, further correlational analysis shows no or very weak correlation of CCL18 with these factors. However, our finding that female normotensive subjects appeared to have lower plasma CCL18 levels than their normotensive male counterparts, yet plasma CCL18 levels were similar between female and male HTN patients, is of interest. de Torres et al. (2011) demonstrated that plasma CCL18 does not differ between male and female smokers, but to our knowledge, no studies have compared relevant sex differences in the general healthy population. As such, the underlying reason for this observed sex difference in CCL18 plasma level remains unclear. CCL18 plasma levels may also be related to pre- and post- menopausal status of the female participants, since two of the three normotensive females in our study were in their 20s. However, due to the small number of normotensive female participants, this hypothesis is yet to be explored. Collectively, the use of CCL18 as a marker for resistant hypertension may be more relevant in females than males, which requires confirmation with a larger female cohort.

To confirm whether CCL18 can serve as a biomarker for resistant hypertension, further investigation is required. Thus, a more accurate determination of the predictive value of CCL18 will be obtained by increasing the sample size and recruiting more female patients, as well as determining if those recently diagnosed essential HTN patients are responsive to anti-HTN treatments or have resistant hypertension. In addition, the correlation of plasma CCL18 with clinical outcome measures, including pulse wave velocity (measure of aortic stiffness), left ventricular hypertrophy, and glomerular filtration rate will be key to assess the predictive value of CCL18 for hypertension-associated organ damage. Moreover, combining measures of CCL18 with those of systemic inflammation, such as C-reactive protein (CRP), tumour necrosis factor-α (TNF-α) and IL-1β, will further establish its predictive value. In particular, our preliminary data show a trend for CRP elevation in the plasma of resistant HTN patients (as compared to normotensive subjects). In line with this, another study has found that CRP is significantly higher in patients with resistant hypertension as compared to those with controlled hypertension (Magen et al., 2008). As a general marker of inflammation, CRP elevation alone may be an indicator, or risk predictor, of various inflammatory diseases and

cardiovascular events, such as acute coronary syndrome (de Jager et al., 2012). Therefore, CCL18 in combination with CRP may serve as a more selective marker of resistant hypertension. Similarly, measures of TNF-α and IL-1β may also be combined with CCL18 to predict resistant hypertension, due to the upregulation of these inflammatory cytokines in peripheral blood monocytes from hypertensive patients (Dörffel et al., 1999). Relevant future directions and clinical implications will be further explored in the General Discussion (**Chapter 6**).

Our finding that CCL18 is elevated in patients with resistant hypertension and generated by human M2 macrophages, led us to hypothesise that CCL18 is a key mediator of the pro-fibrotic actions of M2 macrophages in resistant hypertension. Indeed, CCL18 has been shown to have pro-fibrotic actions in the lung, promoting collagen generation from pulmonary fibroblasts and leading to T cell recruitment (Atamas et al., 2003; Pochetuhen et al., 2007). Moreover, our laboratory has provided evidence that CCL18 can promote fibrosis in the cardiovascular system, promoting collagen generation from human cardiac fibroblasts (Lewis et al., unpublished). Here we have extended these studies to investigate the ability of CCL18 to promote collagen generation in human vascular cell types, namely aortic adventitial fibroblasts (AoAFs) and aortic endothelial cells (HAECs). The chosen concentration range of CCL18 treatments (3-300 ng/ml) is in relevance to the levels measured in the patients with resistant hypertension. In human AoAFs, pro-collagen chains are initially synthesized with N- and C-propeptides at either end (Canty & Kadler, 2005). These propeptides are then secreted and cleaved by specific N- or C-proteinases to form collagen fibrils, which contribute to fibrosis (Canty & Kadler, 2005). Since collagen I is the most abundant (67%) type of collagen in the aorta (Osidak et al., 2015), pro-collagen I, mature collagen I and α-SMA (myofibroblast marker) have been measured in this study. It was found that TGF-β1 (pro-fibrotic factor, positive control) increases α-SMA and collagen protein expression at 24h, which is consistent with previous studies performed on other types of fibroblasts (Jester et al., 1996; Lijnen & Petrov, 2002). Whilst α-SMA expression, the measure of fibroblast to myofibroblast differentiation, remained elevated following 72h of treatment with TGF-β1, modulation of both pro-collagen I and collagen I appeared to be time-dependent with expression attenuated or unchanged, respectively as compared to untreated fibroblasts at 72h. The reasons underlying the lack of effect of TGF-β1 on AoAF collagen generation at this time point, are

unclear. However, collagen I may be predominantly released into the cell culture media by this stage (Baranyi et al., 2019), which cannot be detected by measuring intracellular proteins. Another possible explanation is that there may be higher levels of matrix metalloproteinases (MMPs) present to counter the pro-fibrotic effects of TGF-β1. As such, future studies are required to measure collagen and/or MMP levels in supernatants of relevant cell cultures.

Unlike TGF-β1, CCL18 did not change α-SMA expression at the mRNA or protein level, and no previous studies have investigated the effects of CCL18 on α-SMA expression from fibroblasts. Nonetheless, CCL18 leads to an increase in pro-collagen I production (at 24h), followed by an increase in mature collagen I (at 72h). The concentration- and time-dependent effects of CCL18 are consistent with the previously observed actions of CCL18 on pulmonary fibroblasts (Atamas et al., 2003). These data collectively suggest that instead of promoting myofibroblast differentiation, CCL18 can directly simulate collagen production from AoAFs.

CCL18 has recently been reported to induce endothelial to mesenchymal transition (End-MT) in human umbilical vein endothelial cells (HUVECs) (Lin et al., 2015), raising the interesting possibility that CCL18 may also induce End-MT in HAECs and contribute to the vascular stiffening that is evident in hypertension (Wu et al., 2016). As a positive control in this experiment, TGF-β1 is most commonly used to induce pro-fibrotic effects (including End-MT) (Wang et al., 2017; Zhang et al., 2016). Of note, data with regard to TGF-β and End-MT are conflicting with a previous study reporting an inability of TGF-β1 to reduce VE-cadherin (endothelial marker) expression in HUVECs (Maleszewska et al., 2013). One study has also suggested that TGF-β2, rather than TGF-β1 or TGF-β3, is the predominant TGF-β isoform responsible for End-MT (Medici et al., 2011). In our study, TGF-β1 indeed increased α-SMA (myofibroblast marker) expression. Although such an increase was modest, it concurs with a previous report and as such the effects of CCL18 on End-MT could be investigated (Kokudo et al., 2008). This study showed that CCL18 leads to increased expression of α-SMA and a trend for a decrease in VE-cadherin expression in HAECs. Interestingly, CCL18 also had biphasic effects on measures of End-MT in HAECs, with the increase in α-SMA and decrease in VE-cadherin peaking at 10 ng/ml and higher concentrations ($\geq$ 30ng/ml) having no impact. Such observations may reflect the ability of CCL18 to both activate CCR8 and also antagonise CCR3 (Nibbs et al., 2000). Specifically, studies measuring the chemoattractant potency of CCL18 at CCR8, reported an EC_{50} value of approximately 3 ng/ml (Atamas et al., 2003), and a pA_2 value

at CCR3 of -7.3 (equating to an antagonist concentration of approximately 300 ng/ml) (Krohn et al., 2013). Therefore, higher concentrations of CCL18 may antagonise CCR3 and lead to anti-inflammatory and/or anti-fibrotic effects (Komai et al., 2010; Nibbs et al., 2000), which counteract the pro-fibrotic actions of CCR8. Collectively, our data suggest that an ability of CCL18 to promote End-MT may represent another mechanism by which CCL18 contributes to vascular fibrosis in hypertension.

To further explore the pro-fibrotic functions of CCL18 in the vasculature, future studies can measure pro-collagen I and collagen I in samples of AoAF culture media, and use additional markers to confirm the ability of CCL18 to promote End-MT. One of the potential End-MT markers is a transcription factor, SNAIL. In the context of cancer, where End-MT is well established, studies have shown that CCL18 increases the expression of SNAIL, which mediates a loss of cell-cell adhesion, a property characteristic of epithelial-mesenchymal transition and End-MT (Kokudo et al., 2008). SNAIL also facilitates downregulation of VE-cadherin expression (Medici et al., 2011), and hence may represent a more sensitive marker of End-MT. In addition, elevated collagen I levels may occur via enhancing tissue inhibitor of metalloproteinases (TIMPs), or reducing MMPs, expression and activity. As such, measurements of MMPs and TIMPs in AoAF culture media will allow us to further determine the mechanisms by which CCL18 promotes vascular fibrosis. In addition, the effects of CCL18 may be studied on other pro-fibrotic cell types in the human vasculature, including vascular smooth muscle cells and fibrocytes (Wanjare et al., 2015; Yeager et al., 2011). The pro-fibrotic role of CCL18 may also be related to its ability to attract monocytes and T cells (Broxmeyer et al., 1999; Pochetuhen et al., 2007), into the heart or vasculature. T cells play a key role in hypertension-associated organ damage via the production of various mediators, such as reactive oxygen species and IFNγ (Drummond et al., 2019), and CCL18 can act in an autocrine fashion on macrophages to further promote the pro-fibrotic M2 phenotype (Schraufstatter et al., 2012). Furthermore, although CCR8 has been proposed as the cognate receptor of CCL18, its role in the pro-fibrotic actions of CCL18 in both the lung and cardiovascular cell types remains to be elucidated. CCR8 antagonists or siRNA will be useful tools to confirm whether the effects of CCL18 are mediated by CCR8, and to determine the relevant downstream signalling.

In conclusion, our findings provide evidence that CCL18 is elevated in patients with resistant hypertension and promotes vascular fibrosis. We suggest that M2 macrophages serve as the predominant source of CCL18 and this chemokine plays a key role in the end-organ damage associated with resistant hypertension. Moreover, from a clinical perspective, CCL18 may serve as a potential biomarker and/or treatment target for resistant hypertension. The early identification of resistant HTN patients using biomarkers will provide an opportunity for clinicians to lower cardiovascular event risks in these patients, by early implementation of traditional multi-drug combination therapies or invasive treatments such as renal denervation (Zaldivia et al., 2017). Therefore, CCL18 serving as a biomarker and/or a novel pharmacological treatment target, may lead to a substantial improvement in the clinical management of resistant hypertension.

3.8 References

Atamas SP, Luzina IG, Choi J, Tsymbalyuk N, Carbonetti NH, Singh IS, Trojanowska M, Jimenez SA, & White B (2003). Pulmonary and Activation-Regulated Chemokine Stimulates Collagen Production in Lung Fibroblasts. Am J Respir Cell Mol Biol 29**:** 743-749.

Baranyi U, Winter B, Gugerell A, Hegedus B, Brostjan C, Laufer G, & Messner B (2019). Primary Human Fibroblasts in Culture Switch to a Myofibroblast-Like Phenotype Independently of TGF Beta. Cells 8**:** 721.

Broxmeyer HE, Kim CH, Cooper SH, Hangoc G, Hromas R, & Pelus LM (1999). Effects of CC, CXC, C, and CX3C chemokines on proliferation of myeloid progenitor cells, and insights into SDF-1-induced chemotaxis of progenitors. Ann N Y Acad Sci 872**:** 142-162.

Canty EG, & Kadler KE (2005). Procollagen trafficking, processing and fibrillogenesis. J Cell Sci 118**:** 1341.

Courtois A, Nusgens BV, Hustinx R, Namur G, Gomez P, Kuivaniemi H, Defraigne J-O, Colige AC, & Sakalihasan N (2014). Gene Expression Study in Positron Emission Tomography–Positive Abdominal Aortic Aneurysms Identifies CCL18 as a Potential Biomarker for Rupture Risk. Mol Med 20**:** 697-706.

Daugherty SL, Powers JD, Magid DJ, Tavel HM, Masoudi FA, Margolis KL, O'Connor PJ, Selby JV, & Ho PM (2012). Incidence and prognosis of resistant hypertension in hypertensive patients. Circulation 125**:** 1635-1642.

de Jager SCA, Bongaerts BWC, Weber M, Kraaijeveld AO, Rousch M, Dimmeler S, van Dieijen-Visser MP, Cleutjens KBJM, Nelemans PJ, van Berkel TJC, & Biessen EAL (2012). Chemokines CCL3/MIP1α, CCL5/RANTES and CCL18/PARC are Independent Risk Predictors of Short-Term Mortality in Patients with Acute Coronary Syndromes. PLoS One 7**:** e45804.

de la Sierra A, Segura J, Banegas JR, Gorostidi M, de la Cruz JJ, Armario P, Oliveras A, & Ruilope LM (2011). Clinical features of 8295 patients with resistant hypertension classified on the basis of ambulatory blood pressure monitoring. Hypertension 57**:** 898-902.

de Torres JP, Casanova C, Pinto-Plata V, Varo N, Restituto P, Cordoba-Lanus E, Baz-Dávila R, Aguirre-Jaime A, & Celli BR (2011). Gender differences in plasma biomarker levels in a cohort of COPD patients: a pilot study. PLoS One 6**:** e16021-e16021.

Dörffel Y, Lätsch C, Stuhlmüller B, Schreiber S, Scholze S, Burmester GR, & Scholze J (1999). Preactivated peripheral blood monocytes in patients with essential hypertension. Hypertension 34**:** 113-117.

Drummond GR, Vinh A, Guzik TJ, & Sobey CG (2019). Immune mechanisms of hypertension. Nat Rev Immunol 19**:** 517-532.

Falkenham A, de Antueno R, Rosin N, Betsch D, Lee TDG, Duncan R, & Légaré J-F (2015). Nonclassical Resident Macrophages Are Important Determinants in the Development of Myocardial Fibrosis. The American Journal of Pathology 185**:** 927-942.

Guiteras R, Flaquer M, & Cruzado JM (2016). Macrophage in chronic kidney disease. Clin Kidney J 9**:** 765-771.

Hägg DA, Olson FJ, Kjelldahl J, Jernås M, Thelle DS, Carlsson LMS, Fagerberg B, & Svensson PA (2009). Expression of chemokine (C-C motif) ligand 18 in human macrophages and atherosclerotic plaques. Atherosclerosis 204**:** e15-e20.

Jester JV, Barry-Lane PA, Cavanagh HD, & Petroll WM (1996). Induction of alpha-smooth muscle actin expression and myofibroblast transformation in cultured corneal keratocytes. Cornea 15**:** 505-516.

Kokudo T, Suzuki Y, Yoshimatsu Y, Yamazaki T, Watabe T, & Miyazono K (2008). Snail is required for TGFbeta-induced endothelial-mesenchymal transition of embryonic stem cell-derived endothelial cells. J Cell Sci 121**:** 3317-3324.

Komai M, Tanaka H, Nagao K, Ishizaki M, Kajiwara D, Miura T, Ohashi H, Haba T, Kawakami K, Sawa E, Yoshie O, Inagaki N, & Nagai H (2010). A novel CC-chemokine receptor 3 antagonist, Ki19003, inhibits airway eosinophilia and subepithelial/peribronchial fibrosis induced by repeated antigen challenge in mice. J Pharmacol Sci 112**:** 203-213.

Krohn SC, Bonvin P, & Proudfoot AE (2013). CCL18 exhibits a regulatory role through inhibition of receptor and glycosaminoglycan binding. PLoS One 8**:** e72321.

Lijnen P, & Petrov V (2002). Transforming growth factor-beta 1-induced collagen production in cultures of cardiac fibroblasts is the result of the appearance of myofibroblasts. Methods Find Exp Clin Pharmacol 24**:** 333-344.

Lin L, Chen YS, Yao YD, Chen JQ, Chen JN, Huang SY, Zeng YJ, Yao HR, Zeng SH, Fu YS, & Song EW (2015). CCL18 from tumor-associated macrophages promotes angiogenesis in breast cancer. Oncotarget 6**:** 34758-34773.

Magen E, Mishal J, Paskin J, Glick Z, Yosefy C, Kidon M, & Schlesinger M (2008). Resistant Arterial Hypertension Is Associated With Higher Blood Levels of Complement C3 and C-Reactive Protein. The Journal of Clinical Hypertension 10**:** 677-683.

Maleszewska M, Moonen JR, Huijkman N, van de Sluis B, Krenning G, & Harmsen MC (2013). IL-1β and TGFβ2 synergistically induce endothelial to mesenchymal transition in an NFκB-dependent manner. Immunobiology 218**:** 443-454.

Medici D, Potenta S, & Kalluri R (2011). Transforming growth factor-β2 promotes Snail-mediated endothelial-mesenchymal transition through convergence of Smad-dependent and Smad-independent signalling. The Biochemical journal 437**:** 515-520.

Moore JP, Vinh A, Tuck KL, Sakkal S, Krishnan SM, Chan CT, Lieu M, Samuel CS, Diep H, Kemp-Harper BK, Tare M, Ricardo SD, Guzik TJ, Sobey CG, & Drummond GR (2015). M2 macrophage accumulation in the aortic wall during angiotensin ii infusion in mice is associated with fibrosis, elastin loss, and elevated blood pressure. Am J Physiol Heart Circ Physiol 309**:** H906-H917.

Nibbs RJ, Salcedo TW, Campbell JD, Yao XT, Li Y, Nardelli B, Olsen HS, Morris TS, Proudfoot AE, Patel VP, & Graham GJ (2000). C-C chemokine receptor 3 antagonism by the beta-chemokine macrophage inflammatory protein 4, a property strongly enhanced by an amino-terminal alanine-methionine swap. J Immunol 164**:** 1488-1497.

Osidak MS, Osidak EO, Akhmanova MA, Domogatsky SP, & Domogatskaya AS (2015). Fibrillar, Fibril-associated and Basement Membrane Collagens of the Arterial Wall: Architecture, Elasticity and Remodeling Under Stress. Curr Pharm Des 21**:** 1124-1133.

Pochetuhen K, Luzina IG, Lockatell V, Choi J, Todd NW, & Atamas SP (2007). Complex regulation of pulmonary inflammation and fibrosis by CCL18. Am J Pathol 171**:** 428-437.

Schmittgen TD, & Livak KJ (2008). Analyzing real-time PCR data by the comparative CT method. Nat Protocols 3**:** 1101-1108.

Schraufstatter IU, Zhao M, Khaldoyanidi SK, & Discipio RG (2012). The chemokine CCL18 causes maturation of cultured monocytes to macrophages in the M2 spectrum. Immunology 135**:** 287-298.

Schutyser E, Richmond A, & Van Damme J (2005). Involvement of CC chemokine ligand 18 (CCL18) in normal and pathological processes. J Leukoc Biol 78**:** 14-26.

Wang Z, Han Z, Tao J, Wang J, Liu X, Zhou W, Xu Z, Zhao C, Wang Z, Tan R, & Gu M (2017). Role of endothelial-to-mesenchymal transition induced by TGF-β1 in transplant kidney interstitial fibrosis. J Cell Mol Med 21**:** 2359-2369.

Wanjare M, Agarwal N, & Gerecht S (2015). Biomechanical strain induces elastin and collagen production in human pluripotent stem cell-derived vascular smooth muscle cells. Am J Physiol Cell Physiol 309**:** C271-281.

Wu J, Montaniel KR, Saleh MA, Xiao L, Chen W, Owens GK, Humphrey JD, Majesky MW, Paik DT, Hatzopoulos AK, Madhur MS, & Harrison DG (2016). Origin of Matrix-Producing Cells That Contribute to Aortic Fibrosis in Hypertension. Hypertension 67**:** 461-468.

Wynn TA, & Ramalingam TR (2012). Mechanisms of fibrosis: therapeutic translation for fibrotic disease. Nat Med 18**:** 1028-1040.

Yeager ME, Frid MG, & Stenmark KR (2011). Progenitor cells in pulmonary vascular remodeling. Pulmonary Circulation 1**:** 3-16.

Zaldivia MT, Rivera J, Hering D, Marusic P, Sata Y, Lim B, Eikelis N, Lee R, Lambert GW, Esler MD, Htun NM, Duval J, Hammond L, Eisenhardt SU, Flierl U, Schlaich MP, & Peter K (2017). Renal Denervation Reduces Monocyte Activation and Monocyte-Platelet Aggregate Formation: An Anti-Inflammatory Effect Relevant for Cardiovascular Risk. Hypertension 69**:** 323-331.

Zhang Y, Wu X, Li Y, Zhang H, Li Z, Zhang Y, Zhang L, Ju J, Liu X, Chen X, Glybochko PV, Nikolenko V, Kopylov P, Xu C, & Yang B (2016). Endothelial to mesenchymal transition contributes to arsenic-trioxide-induced cardiac fibrosis. Sci Rep 6**:** 33787.

Ziliotto N, Bernardi F, Jakimovski D, Baroni M, Bergsland N, Ramasamy DP, Weinstock-Guttman B, Zamboni P, Marchetti G, Zivadinov R, & Ramanathan M (2018). Increased CCL18 plasma levels are associated with neurodegenerative MRI outcomes in multiple sclerosis patients. Multiple Sclerosis and Related Disorders 25**:** 37-42.

3.9 Supplementary figures and tables

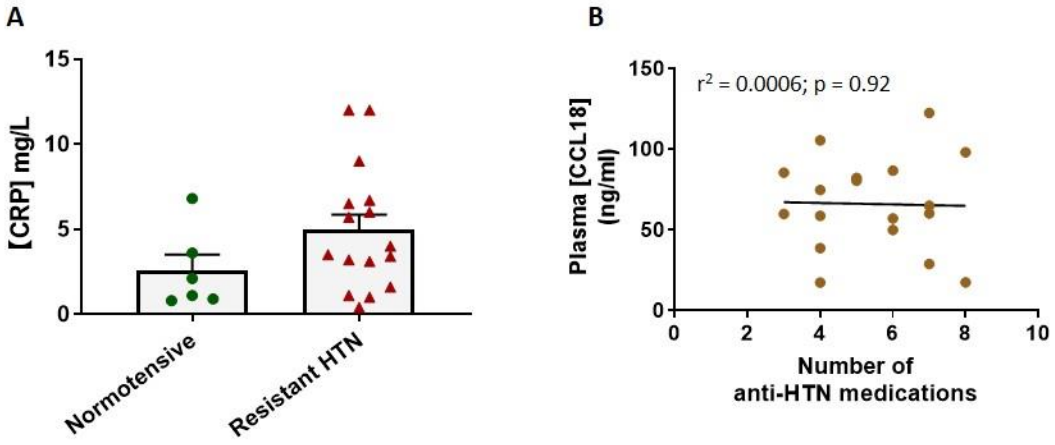

Supplementary Figure 1. C-reactive protein (CRP), anti-hypertensive (-HTN) medications and plasma CCL18 in resistant HTN subjects. Resistant HTN patients were on at least 3 different classes of anti-HTN medications. CRP levels in normotensive and resistant HTN patients (**A**), and correlation analysis between plasma CCL18 and number of anti-HTN medications taken by resistant HTN subjects (**B**) were shown.

Data presented as mean ± SEM, dots depict individual data points (**A**) or individual points (**B**), n= 6-20 per group. (**A**) Student's t-test; (**B**) Linear regression analysis.

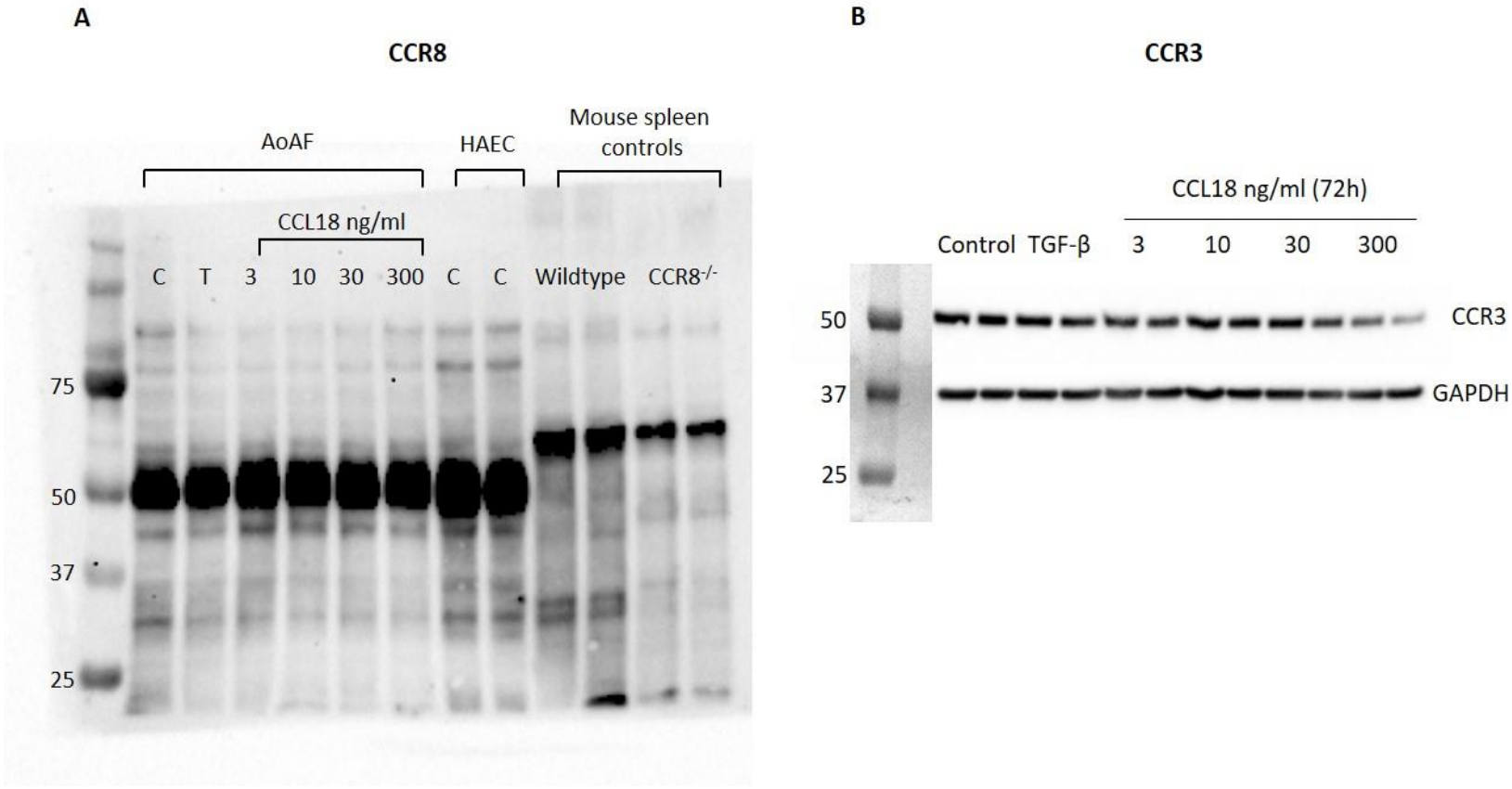

Supplementary Figure 2. Detection of CCR8 and CCR3 expression in human AoAFs and/or HAECs. (**A**) Representative western blot of CCR8 expression in AoAF treated with CCL18 (3-300 ng/ml) or TGF-β1 (10ng/ml) for 72h, or in untreated HAECs. C= untreated control; T= TGF-β1; spleen samples from wildtype and CCR8$^{-/-}$ mice were included as positive and negative controls, respectively. (**B**) Representative western blot of CCR3 expression in AoAF treated with CCL18 (3-300 ng/ml) or TGF-β1 (10ng/ml) for 72h. Sizes of CCR8 in kDa: 40 for human samples, 41 for mouse samples, 50 for expected band according to manufacturer of the anti-CCR8 antibody.

Supplementary Table 1. Anti-hypertensive (anti-HTN) medications taken by each resistant HTN patient in the study. # Patient noted to be "intolerant to virtually all anti-HTN drugs"; *Less than 3 anti-HTN medications recorded.

Patient ID	CCL18 (ng/ml)	Anti-hypertensive (anti-HTN) medications							
35	80.399	spironolactone (25 mg 1-0-0)	karvezide (25 mg 1-0-0)	norvasc (10 mg 1-0-0)	sotalol hydrochloride (40 mg 1-0-1)	physiotens (0.4 mg 0-0-1)			
36	82.21	Avapro (300 mg)	Minax (100 mg)	Physiotens (0.4 mg)	Cordilox (240 mg)	Spironolactone (25 mg)			
37	59.864	Ramipril (5 mg 1-0-1)	avapro (300 mg 1-0-0)	natrilix (1.5 mg 1/2-0-0)					
38	74.629	Avapro (300 mg)	Natrilix (1.5 mg)	Verapamil (240 mg)	Moxonidine (400 mg)				
39	85.43	Lasix (40 mg)	Micardis (80 mg)	Aldomet (250 mg)					
40	49.948	Coveram 10/10	Hydralazine (25 mg)	Minax (100 mg)	Physiotens (400 mg)	Prazosin (5 mg)	Indapamide (2.5 mg)		
41	64.895	AtacandPlus (32/25 mg)	Betaloc (100 mg)	Zanidip (20 mg)	Hydralazine (25 mg)	Fruozemide (60 mg)	Minipress (15 mg)	Loniten (15 mg)	
42	86.675	Forusemide (20 mg)	Methyldopa (500ng)	Micardis PLUS 80 (12.5 mg)	Transderm patch (50mcg)	Spiranolactone (25 mg)	Felodipine (2.5 mg)		
43	17.333	Transiderm Nitropatch (50 mg)	Physiotens (0.2 mg)	Pressin (7.5 mg)	Lasix (40 mg)				
44 #	53.656								
45	57.018	Anginine (rarely)	Caduet (10/20 mg)	Noten (100 mg)	Methyldopa (250 mg)	Olmetec Plus (40/25 mg)	Spironolactone (25 mg)		
46	58.691	Physiotens (400 mg)	Norvasc (10 mg)	Avapro HCT (300/25 mg)	Aldactone (25 mg)				
47	122.39	Atenolol (50 mg)	Netrilix XR (1.5 mg)	Nitro-Dur Patch (10 mg/24hrs)	Prazosin (1 mg)	Teveten (600 mg)	Spironolactone (25 mg)	Zanidip (20 mg)	
48 *	47.675	Minipress (0.5 mg)							
49	105.39	Zanidip (20 mg)	Avapro HCT (300/25 mg)	Physiotens (400mcg)	Coversyl (10 mg)				
50	38.675	Avapro (300/25 mg)	Hydopa (50 mg)	Metropdol (50 mg)	Aldactone (12.5 mg)				
51	98.028	Eplerenone (25 mg)	Spironolactone (25 mg)	Irbesartan (300 mg)	Metoprolol (100 mg)	Physiotens (200 mg)	Prazosin (5 mg)	Frusemide (40 mg)	Lercanidipine (20 mg)
52	60.129	Coversyl Plus (5/1.25 mg)	Metoprolol (50 mg)	Prazosin (5 mg)	Minoxidil (10 mg)	Norvasc (10 mg)	Moxonidine (0.4 mg)	Spironolactone (100 mg)	
53	17.48	Metoprolol (50 mg)	Amlodipine 10	Glyceryl Trinitrate 10 mg patch	Prazosin (1 mg)	Ramipril 10	Atacand 32	Lasix 40	Chlorthalidone 25
54	28.79	Aldomet (250 mg)	Coversyl (5 mg)	Coversyl Plus (5/1.25 mg)	Sotalol (40 mg)	Exforge (10/160 mg)	Physiotens (400 mg)	Tegretol (300 mg)	

Supplementary Table 2. Non-anti-HTN medications taken by each resistant HTN patient in the study. # Patient noted to be "intolerant to virtually all anti-HTN drugs"; *Less than 3 anti-HTN medications recorded.

Patient ID	CCL18 (ng/ml)	Other medications								
35	80.399	Aspirin (100 mg 1-0-0)	crestor (5 mg 1-0-0)	effexor (75 mg 1-0-0)						
36	82.21									
37	59.864									
38	74.629	Nexium (40 mg)	Osteovit (75 mg)	Caltrate (600 mg)	Effexor XR (150 mg)	Thyroxin (100 mg)	Lipitor (10 mg)			
39	85.43	Aspirin (100 mg)	Metformin (500 mg)							
40	49.948	Lipidil (145 mg)								
41	64.895	Nexium (40 mg)								
42	86.675	Aspirin (100 mg)	Clopidogrel (75 mg)	Endep (25 mg)	Metformin (500 mg)	Ostelin 1000	Targin (10/5 mg)			
43	17.333	Astrix (100 mg)	Aropax (20 mg)	Zocor (40 mg)	Janumet (metformin) (50 mg)					
44 #	53.656	Endep (30 mg)	mogadon (5 mg)	Serepax	Oroxine (150 mg)					
45	57.018	Xalatan eye drops (50 mcg/ml per eye)	Glyade (40 mg)	Diaformin (500 mg)	Aspirin (100 mg)					
46	58.691	Crestor (20 mg)	Novomix 30 Flexpen							
47	122.39	Seretole MDI Inhaler	Somac (40 mg)	Tegretol (100 mg)						
48 *	47.675	Astrix (100 mg)	Crestor (20 mg)	Symbicort (200 mg)						
49	105.39	Nexium (20 mg)	Lipitor (20 mg)	Tegretol (200 mg)	Diabex (1000 mg)	Lantus	Novorapid	OsteoVit Vitamin D		
50	38.675	Novomix	Diaformin 1000	Diamicron MR (60 mg)						
51	98.028	Aspirin (100 mg)	Atorvastatin (40 mg)	Mianserin (20 mg)	Oxycontin (40 mg)	Clopidogrel (75 mg)				
52	60.129									
53	17.48	Novomix30 FlexiPen	Diabex 1000	Nytorin (10/80)						
54	28.79	Aspirin (100 mg)	Crestor (20 mg)	Diaformin (850 mg)	Amaryl (4 mg)	NovoRapid	Levemir	Effexor (150 mg)	Zyprexa (5 mg)	Spironolectone (12.5 mg)

Chapter 4

Genetic deletion of CCR8 does not modulate the development of angiotensin II (14-day)-induced hypertension in mice

Genetic deletion of CCR8 does not modulate the development of angiotensin II (14-day)-induced hypertension in mice

Authors:

Mingyu Zhu[1], Meghan J. Finemore[1], Dorota Ferens[1], Grant R. Drummond[2], Barbara K. Kemp-Harper[1].

Affiliations:

[1]Biomedicine Discovery Institute, Department of Pharmacology, Monash University, Clayton, VIC, Australia.

[2]Department of Physiology, Anatomy & Microbiology, La Trobe University, Bundoora, VIC, Australia.

4.1 COVID-19 impact statement

In **Chapter 4**, sample sizes are low in some animal cohorts, particularly for saline-treated wildtype mice (n=2 in histological studies, n=3-6 in other studies). This is due to the COVID-19 pandemic, during which several mice (mainly wildtype mice assigned to the saline treatment group) could not be treated for blood pressure or end-point measurements. The unpredictable nature of littermate generation, together with the need to reduce the colony size in preparation for the first COVID-19 related lockdown in Melbourne, has further prevented relevant experiments from being conducted during the short period of restriction relaxation (mid-May to early July).

4.2 Abstract

Introduction: M2 macrophages contribute to vascular fibrosis and stiffening in hypertension. M2 macrophages are also the major source of a pro-fibrotic chemokine, C-C motif chemokine ligand 18 (CCL18), which activates its cognate receptor, C-C motif chemokine receptor 8 (CCR8). However, the role of CCL18 or CCR8 in hypertension has not been investigated. This study aimed to explore the effects of global CCR8 deletion on hypertension and its associated end-organ damage in male and female mice.

Methods: CCR8 knockout (CCR8 KO; C57BL/6J background) male and female mice, and their wildtype (WT) littermate controls were treated with saline or angiotensin II (Ang II; 0.7 mg/kg/d, 14d, s.c). Blood pressure was measured via tail cuff plethysmography, organs (including heart and kidneys) weighed, and vascular function assessed by wire myography. In the aortae of male mice, mRNA expression of CCL8, CCR8, CD206 (M2 macrophage marker) and oxidative stress markers were measured via qRT-PCR. Aortic structure, elastin regulation and adventitial fibrosis were assessed by staining with Haematoxylin and Eosin, Verhoeff–Van Gieson and picrosirius red, respectively.

Results: In both male and female CCR8 KO mice the hypertensive response to angiotensin II and associated cardiac hypertrophy, were unchanged. The augmented contraction to phenylephrine in the aorta from male hypertensive mice, was maintained in angiotensin II-treated CCR8 KO mice. By contrast, endothelium-dependent relaxation to ACh was enhanced in the aorta of male hypertensive CCR8 KO mice as compared to wild-type hypertensive mice. Genetic deletion of CCR8 appeared to reduce the hypertension-associated increase in aortic CCL8 mRNA expression to levels seen in saline-infused wild-type mice. CCR8 KO hypertensive aortae had unchanged expression of oxidative stress markers as compared to WT hypertensive mice, and no improvements were seen on vascular remodelling or fibrosis.

Discussion: Genetic deletion of CCR8 provides little protection for male and female mice from systolic blood pressure elevation or the hypertension-associated end-organ damage, in a 14d Ang II model of hypertension. Therefore, the CCL8-CCR8 axis may not serve as a key contributor to the short-term development of hypertension.

4.3 Introduction

Hypertension associated end-organ damage involves the remodelling, stiffening and fibrosis in the vasculature, heart, and kidneys (Diez, 2007; Oparil et al., 2003; Zhao et al., 2008). Inflammation and in particular, the "M2" subset of macrophages play an important role in hypertension and its associated end-organ damage. Specifically, when hypertension is induced by 14 days of angiotensin II (Ang II) treatment in mice, M2 macrophages infiltrate and accumulate in the hypertensive vasculature (Moore et al., 2015). This M2 macrophage accumulation is associated with an increase in heart weight, vascular fibrosis, and vascular remodelling, evident following 28 days of treatment with Ang II, and reversed by the inhibition of macrophage infiltration (Moore et al., 2015).

Whilst the mechanisms via which M2 macrophages promote vascular fibrosis remain unknown, the pro-fibrotic chemokine, C-C motif chemokine ligand 18 (CCL18) (Schutyser et al., 2005) may play a key role. Thus, M2 macrophages generate large amounts of CCL18 (Zhu, 2016), which has a chemotactic effect on several types of inflammatory cells, including T and B lymphocytes and immature dendritic cells, and promotes lung remodelling (Schutyser et al., 2005). Whilst the pro-fibrotic effect of CCL18 is due in part to its ability to promote T cell infiltration (Pochetuhen et al., 2007; Wynn & Ramalingam, 2012), it can also directly stimulate collagen generation from pulmonary fibroblasts (Atamas et al., 2003). To date, no studies have been published to explore the potential role of CCL18 in hypertension and/or its associated end-organ damage. However, there is evidence suggesting that CCL18 contributes to cardiovascular diseases, including coronary artery disease (acute coronary syndrome and angina), atherosclerosis, and aneurysm (de Jager et al., 2012; Kraaijeveld et al., 2007; Versteylen et al., 2016). These findings raise the interesting possibility that CCL18 may also contribute to the pathophysiology of hypertension and the associated fibrosis.

In further support of this hypothesis, the recently identified cognate receptor of CCL18, C-C motif chemokine receptor 8 (CCR8) (Islam et al., 2013) is expressed on cardiovascular relevant cell types such as vascular smooth muscle cells and human umbilical vein endothelial cells (HUVECs) (Haque et al., 2004), together with immune cells (Connolly et al., 2012). Thus, CCR8 promotes the chemotaxis of leukocytes into sites of inflammation, including type 2 T helper cells (Th2 cells), monocytes and macrophages (Connolly et al., 2012). Although CCR8 has

another ligand, CCL1, CCL18 is more highly expressed in inflammation (Islam et al., 2011). As such, CCL18 is more likely to be the key modulator of CCR8 function in diseases that are associated with inflammation, such as hypertension. Like CCL18, the role of CCR8 in hypertension also remains to be explored.

It is difficult to study the role of CCL18-CCR8 axis using animal models, because CCL18 does not have orthologues in rodents. However, Islam et al. (2013) suggested that human CCL18 (hCCL18) and mouse CCL8 (mCCL8) are functional analogues, both of which activate CCR8. Indeed, the expression of mCCL8 is increased in the hypertensive vasculature of mice (Moore et al., 2015), and preliminary findings from our laboratory suggest that mCCL8 is co-localised with M2 macrophages in the vascular wall. Collectively, these data suggest that the hCCL18- or mCCL8-CCR8 axis may play a key role in hypertension and genetic deletion of CCR8 may serve as a useful tool to delineate the contribution of this signalling pathway in this disease setting.

We hypothesized that genetic deletion of CCR8 would limit the increase in blood pressure (BP) and/or end-organ damage in hypertension. Utilising a 14-day Ang II infusion model of hypertension, this study aimed to explore the effects of globally knocking out CCR8 on BP, heart and kidney weights, and vascular function in male and female mice. Since female hypertensive mice were protected from vascular dysfunction per se, we further investigated the effects of CCR8 genetic deletion on vascular inflammation, remodelling and fibrosis in male Ang II-treated mice.

4.4 Methods

Animals and genotyping

CCR8 knockout (CCR8 KO) mice, and their wildtype (WT) littermates used in this study were generated via $CCR8^{+/-}$ x $CCR8^{+/-}$ breeding (all with a C57BL/6J background). Female and male mice were used at 10-14 weeks and 8-13 weeks of age, respectively. CCR8 KO mice were generated via CRISPR/Cas9, by the Australian Phenomics Network, Monash University. Mice were bred and housed at the Animal Research Laboratories or Pharmacology Mouse Room (Monash University, Clayton, Australia), on a 12-hour light-dark cycle and provided with free access to chow diet and drinking water. A REDExtract-N-Amp™ Tissue PCR Kit (Sigma-Aldrich, Germany) was used to identify the genotype of each mouse, as per manufacturer's instructions (detailed in **Chapter 2, Section 2.2**). In this procedure, DNA was extracted from the tip of each mouse tail, and 100 ng DNA from each mouse was amplified with custom made primers for CCR8 (Sigma-Aldrich, Germany), followed by the loading of DNA into agarose gels for electrophoresis. All procedures were approved by the Monash Animal Research Platform Ethics Committee (Ethics Number: MARP/2017/104).

Angiotensin infusion model of hypertension

WT mice were randomly assigned to a vehicle (saline) or angiotensin II (Ang II, 0.7 mg/kg/d, GL Biochem, China) infusion group, and all CCR8 KO mice were treated with Ang II (0.7 mg/kg/d). Treatments were administered via osmotic minipumps (Model 2002, Alzet, USA) for 14 days. All mice were under isoflurane anaesthesia (0.4 L/min, 2% inhaled with oxygen) during minipump implantation, where a lateral incision of ≈10 mm was made through the skin at the neck. A subcutaneous pouch was created through this incision, in which minipumps were inserted, followed by the closing of incision with monofilament sutures. After the surgery, mice were allowed to recover and then returned to home cages.

Tail cuff plethysmography

Systolic blood pressure (BP) was measured using tail cuff plethysmography (MC4000 multi-channel blood pressure analysis system; Hatteras Instruments, USA). After mice were

acclimatised to the BP monitoring equipment, BP was recorded 3 days before surgeries, 1 day before surgeries, and just prior to surgeries (Day 0) to form an average baseline BP. During the 14-day treatment period, BP was measured on Days 3, 7, 10 and 14. BP was recorded for 25-30 measurement cycles on each day of measurement, where mice were placed in restraints on a heated platform (40°C), with an inflatable cuff around the base of each tail. Systolic BP was recorded as the cuff inflation pressure required to fully occlude blood flow in the tail. At the end of the treatment period, mice were killed via overdose of CO_2, with the aorta, kidneys, heart, spleen, liver and lungs of each mouse removed and weighed before being processed for end point measures.

Wire myography

To assess vascular function, abdominal aortae were isolated from CCR8 KO and WT mice, the fat and connective tissues removed and aortae cut into 2 mm sections. Aortic sections were mounted in a small vessel myograph (Danish Myo Technology A/S, Denmark) on pin mounts (200 µm diameter) and changes in isometric tension recorded (LabChart 8, ADI Instruments, New Zealand). Vessels were kept at a resting tension of 5mN at 37 °C in Kreb's solution (in mM: 118 NaCl, 4.5 KCl, 0.5 $MgSO_4$, 1 KH_2PO_4, 25 $NaHCO_3$, 11.1 glucose, 2.5 $CaCl_2$; pH 7.4), and bubbled with carbogen (5% CO_2, 95% oxygen). Arteries were contracted maximally with the thromboxane A_2 mimetic, U46619 (0.3 µM). Once the contraction had reached a plateau, vessels were washed, tension allowed to return to baseline and then arteries were rechallenged with U46619 (0.3 µM; F_{max}).

Endothelium-dependent and -independent vasorelaxation responses were assessed by constructing cumulative concentration-response (CR) curves to acetylcholine (ACh; 1 nM- 30 µM) and the NO donor, diethylamine NONOate (DEA-NO; 0.3 nM- 30 µM), respectively in aortae pre-contracted to ≈65 % F_{max} with titrated concentrations of U46619. In separate aortic sections, cumulative CR curves to phenylephrine (PE; 1 nM-30 µM), were constructed. Arteries were then washed with Krebs', pre-contracted to ≈20-30 % F_{max} with U46619 prior to the addition of N(ω)-nitro-L-arginine methyl ester (L-NAME, 100 µM) to assess endogenous NO bioavailability.

mRNA measurements in aortae

The top third section of thoracic aorta from each mouse was snap frozen in liquid nitrogen for mRNA measurements via real-time quantitative reverse transcription polymerase chain reaction (RT-qPCR). RNA was extracted from thoracic aortae using the RNeasy Micro Kit according to manufacturer's instructions (Qiagen, Germany), with its yield and purity assessed by QiaExpert (Qiagen, Germany) (protocols detailed in **Chapter 2, Section 2.10**). The extracted RNA was then converted to cDNA using a High-capacity cDNA reverse transcription kit (as per the manufacturer's instructions; Applied Biosystems, Australia), and a thermal cycler (BioRad MyCycler; BioRad, USA) (as detailed in **Chapter 2, Section 2.10**).

Resultant cDNA samples were used to measure gene expression of CD206 (M2 macrophage marker), CCL8, CCR8, and the oxidative stress markers NOX2 (NADPH oxidase 2), eNOS (endothelial nitric oxide synthase), SOD1 and SOD3 (superoxide dismutase 1 and 3) (primers were from Life Technologies, USA). GAPDH was used as the house-keeping gene, and relevant RT-qPCR was run in triplicates, as described in **Chapter 2, Section 2.10,** in the Bio-Rad CFX96 Real-Time PCR Detection System (Bio-Rad Laboratories, USA). mRNA expression was determined by the comparative cycle threshold (Ct) method (Schmittgen & Livak, 2008), being normalised to GAPDH and expressed relative to the average control values from saline-treated WT mice.

Histological studies

The bottom section of thoracic aorta (≈4 mm) from each mouse was fixed in 10 % neutral buffered formalin for 3 days. Aorta segments were then embedded in paraffin and cut into cross sections of 4 µm for Verhoeff-Van Gieson (VVG) staining, or 5 µm for hematoxylin and eosin (H&E) and Picrosirius red staining. The embedding and cutting of aortic segments, VVG and H&E staining were performed by Monash Histology Services (Monash University, Clayton, Australia).

Aortic segments were stained with H&E or VVG to assess the structure and elastin content of mouse aortae, respectively, as per protocols developed by Monash Histology Services (Monash University, Clayton, Australia) (**Appendices 1-2**). Images for these stains were captured at up to x40 magnification by a slide scanner (Aperio Scanscope AT Turbo, Leica Biosystems, Germany). Each section was analysed as a whole, with data averaged from 3 sections per animal.

Picrosirius red stain was used to measure the collagen content in the vasculature. In brief, aortic sections were de-waxed by being submerged in xylene and a series of graded ethanol solutions. The sections were then rinsed with water, followed by immersion in Bouin's fixative for 1 hour at 60 °C. Fixed slides were washed in water and stained with picrosirius red (0.01%; Sigma-Aldrich, USA) for 1 hour. After staining, sections were washed with water, 80% ethanol, and xylene, successively. To prepare slides for imaging, non-aqueous DPX (VWR International, USA) was used as a mounting medium for cover-slipping. Slides were imaged at x10 and x20 magnification using both bright-field and polarised microscopy (Olympus BX51, Olympus Life Science, Australia). 6 fields of views of each section (1 section per animal) were analysed.

Statistical analysis

All data were presented as mean ± standard error of the mean (SEM). Organ weights were expressed as % of body weight. Vasorelaxation responses to ACh or DEA-NO were expressed as % reversal of pre-contraction to U46619, and vasoconstriction responses to PE or L-NAME were expressed as % of F_{max}. RT-qPCR data were expressed as fold changes relative to the control group (saline-treated WT mice). Quantification of histological staining was performed in a blinded manner, with picrosirius red staining expressed as % of adventitial area. Elastin dysregulation was assessed using a scoring system, with a score of 1= no dysregulation, 2= mild dysregulation, 3= moderate dysregulation, 4= severe dysregulation.

Student's unpaired t-test was used to compare the baseline BP of WT and CCR8 KO mice. 2-way ANOVA (with Tukey's post-hoc test) was used to compare systolic BP or body weight measurements in multiple treatment groups over the 14-day treatment period. All other data

were analysed by 1-way ANOVA with Tukey's post-hoc test. All statistical tests were performed using GraphPad Prism 8 (USA), with $p < 0.05$ considered statistically significant.

4.5 Results

Genetic deletion of CCR8 does not lower systolic blood pressure in male and female mice with angiotensin II (14d)-induced hypertension

$CCR8^{-/-}$ (CCR8 KO) mice and their littermate $CCR8^{+/+}$ (wildtype; WT) controls were identified by genotyping (**Figure 1**). When designed Forward Primer and Reverse Primer 1 were used to amplify mouse tail DNA, PCR product from WT mice was a single band of 1401 bp, whilst $CCR8^{+/-}$ (heterozygous; Het) or CCR8 KO mice produced a single band of 405-432 bp. To further distinguish the genotypes, a second reverse primer (Reverse Primer 2) was used, with a single band of 563 bp produced from WT or Het mice, and no PCR products from CCR8 KO mice.

Identified CCR8 KO and WT littermates were used to investigate the potential role of CCR8 in hypertension. Mean baseline systolic blood pressure (BP) in male CCR8 KO mice was slightly lower than that in male WT mice, but this difference did not reach statistical significance (114 ± 1.3 vs 120 ± 2.6 mmHg, p= 0.055) (**Figure 2A**). In addition, baseline systolic BP remained unchanged in female CCR8 KO (117 ± 6.1 mmHg) as compared to female WT (116 ± 3.5 mmHg) mice (**Figure 2B**). In male WT mice, angiotensin II (Ang II) infusion caused a significant elevation in systolic BP by day 7 (148 ± 6.8 mmHg, n= 6, $p<0.05$) which was maintained at day 10 and then modestly attenuated at day 14 (136 ± 8 mmHg, **Figure 2C**). The pressor response to Ang II was unchanged in male CCR8 KO mice. In contrast to male WT mice, the pressor response to Ang II in female WT mice was delayed such that a significant increase in systolic BP was not observed until day 14 (155 ± 5.7 mmHg vs 120 ± 5.5 mmHg in saline-treated females, n= 3-8, $p<0.05$) (**Figure 2D**). In CCR8 KO female mice, a more rapid rise in systolic BP was observed following infusion with Ang II with a significant increase observed at day 7 (148 ± 4.8 mmHg, n= 3-7, $p<0.05$) which was sustained until day 14 (**Figure 2D**).

Genetic deletion of CCR8 does not affect organ weights in male and female mice with angiotensin II (14d)-induced hypertension

Organ weights were measured to provide an initial assessment of organ damage associated with hypertension. The body weight (BW), of male (8-13 weeks old on Day 0) and female (10-

14 weeks old on Day 0) mice, over the 14-day treatment period, did not differ among the treatment groups (WT+ saline, WT+ Ang II, CCR8 KO+ Ang II) (**Figure 3A-B**). Ang II infusion in male WT and CCR8 KO mice did not lead to significant changes in kidney, liver, spleen, or heart weights (**Figure 3C**). Cardiac hypertrophy, assessed by heart weight/body weight ratio was apparent in WT female mice following Ang II treatment (WT+ Ang II: 0.55 ± 0.02 vs WT+ saline: 0.42 ± 0.03 %BW; n= 3-8, $p<0.05$), yet the magnitude of Ang II-induced hypertrophy was unchanged in female CCR8 KO mice (0.53 ± 0.02 %BW) (**Figure 3D**).

CCR8 KO male mice have improved endothelium-dependent vasorelaxation in response to acetylcholine

Preliminary experiments in untreated, naïve male and female CCR8 KO mice, demonstrated that genetic deletion of CCR8 did not alter endothelium-dependent (ACh), or -independent (DEA/NO) vasorelaxation in isolated abdominal aorta (**Supplementary Figure 1 & 2**). In male WT and CCR8 KO mice, vasorelaxation to ACh was markedly attenuated by the NOS inhibitor, L-NAME. By contrast, in female CCR8 KO mice a L-NAME resistant component to ACh-induced relaxation was apparent at concentrations >3 µM (**Supplementary Figure 2A**). Genetic deletion of CCR8 did not change contractile responses to the thromboxane A_2 mimetic, U46619 in abdominal aorta from either male or female mice (**Supplementary Figure 1 & 2).** By contrast, in male mice the maximal contraction to phenylephrine (PE) appeared to be enhanced in aorta from CCR8 KO (F_{max}: 47 ± 5 %) versus WT (F_{max}: 24 ± 6 %, $p=0.06$) mice (**Supplementary Figure 1C**). In both male WT and CCR8 KO mice, the maximum contraction to PE was further augmented following treatment with L-NAME (WT + L-NAME: F_{max} = 86 ±4 %; CCR8 KO + L-NAME: F_{max} = 81 ± 6 %). Whilst contractile responses to PE did not differ significantly between WT and CCR8 KO female mice (WT: pEC_{50} = 5.70 ± 0.13, F_{max} = 52 ± 16 %; CCR8 KO: pEC_{50} = 5.73 ± 0.09, F_{max} = 69 ± 9 %), L-NAME increased the potency to PE by ≈10-fold ($p<0.05$) with a trend for an increase in maximum response, in both genotypes (**Supplementary Figure 2C)**.

In WT male and female mice, Ang II treatment did not alter endothelium-dependent vasorelaxation to acetylcholine (ACh), endothelium-independent vasorelaxation to DEA-NO, or L-NAME-induced contraction (a measure of endogenous NO bioavailability) in the isolated

aortae (**Figures 4A-4C, 5A-5C**). The maximum contraction to PE was significantly increased in male WT mice following Ang II infusion (F_{max}: 61 ± 9 % in WT + Ang II vs 33 ± 9 % in WT + saline, $p< 0.05$), whilst no significant change in the contractile response to PE was observed in hypertensive female WT mice (**Figures 4D, 5D; Table 1**). Of note, a positive correlation between the maximum contraction to PE and BP in male WT mice was apparent 14 days after Ang II infusion ($r^2= 0.42$, $p< 0.05$; **Supplementary Figure 4A-B**). No positive correlation between the contraction to the thromboxane A_2 mimetic, U46619 and BP was observed (**Supplementary Figure 4A-B**) with the maximal contraction to U46619 similar between aortae from saline- (1.4 ± 0.2 mN) and Ang II-treated (1.3 ± 0.1 mN) mice.

Whilst the development of Ang II-induced hypertension was not associated with endothelial dysfunction, the genetic deletion of CCR8 augmented the maximal response to ACh in the aorta from male mice following Ang II infusion (CCR8 KO + Ang II: R_{max} = 90 ± 0.4 % vs WT + Ang II: R_{max} = 72 ± 5 %, $p<0.05$). Although a cohort of 14d saline-treated CCR8 KO mice was not included in this study, vasorelaxation to ACh in hypertensive CCR8 KO mice was similar to that in 28d saline-treated CCR8 KO mice included in **Chapter 5** (CCR8 KO + saline: R_{max} = 86 ± 3 %; 28d treatment) (**Figure 4A**). Vasorelaxation to DEA/NO and L-NAME-induced contraction were unchanged in hypertensive CCR8 KO mice as compared to saline- and Ang II-treated WT mice (**Figure 4B-C**). Relative to saline-treated WT mice, saline- and Ang II- treated CCR8 KO mice displayed augmented contractions to PE (CCR8 KO + saline 28d: F_{max} = 50 ± 4 %; CCR8 KO + Ang II: F_{max} = 66 ±7 %), that were similar in magnitude to those observed in the aortae from hypertensive WT mice (**Figure D**). The positive correlation between the maximal contraction to PE and BP, observed in WT mice was not apparent in CCR8 KO mice ($r^2= 0.02$, $p= 0.74$) (**Supplementary Figure 4A-B**).

Following Ang II infusion in CCR8 KO female mice, responses to ACh, L-NAME and DEA-NO remained unchanged. Although as compared to WT, vasorelaxation to DEA/NO tended to be less potent in both WT + Ang II and CCR8KO + Ang II these changes were not statistically significant. Also, similar to their male counterparts, the maximum contraction to PE in female hypertensive CCR8KO mice showed a tendency to increase (CCR8 KO + Ang II F_{max}: 58 ± 7 % vs. WT + Ang II: 33 ± 5 %) but these differences were not statistically significant (**Figure 5, Table 2**).

In isolated mesenteric arteries from male mice, neither Ang II treatment or genetic deletion of CCR8, appeared to change the response to ACh, DEA-NO or PE (**Supplementary Figure 3**).

Genetic deletion of CCR8 may limit the increase in CCL8 mRNA expression in the hypertensive vasculature of male mice

In male mouse aortae, mRNA expression of CD206 (marker of M2 macrophages), CCL8, CCR8 and oxidative stress markers were measured. Hypertensive WT mice showed a trend for an increase in CD206 and CCL8 mRNA expression, with no change in CCR8 expression (**Figure 6B-D**). CCR8 expression was not detected in aortae from CCR8 KO hypertensive mice (**Figure 6D**). Whilst genetic deletion of CCR8 did not change the expression of CD206 in the hypertensive vasculature, it led to an apparent reduction in CCL8 mRNA expression in the aortae of CCR8 KO + Ang II mice, yet these changes did not reach statistical significance (**Figure 6C-D**).

Among the oxidative stress markers studies, NOX2 (NADPH oxidase 2) mRNA expression showed a trend for elevation in the vasculature of WT hypertensive mice as compared to saline treated WT mice (**Figure 7A**) and this was sustained following genetic deletion of CCR8. The mRNA expression of eNOS (endothelial nitric oxide synthase), and the antioxidants SOD1 (superoxide dismutase 1) and SOD3 remained unchanged in the aortae of hypertensive WT and CCR8 KO mice (**Figure 7B-D**).

Genetic deletion of CCR8 does not limit the structural remodelling of the aorta in Ang II-treated mice.

Vascular remodelling, elastin structure and adventitial collagen deposition were also assessed in male mice. In the hypertensive WT vasculature, there was a trend for a modest increase in media: lumen ratio (25 % increase), and adventitial collagen content (26 % increase) (**Figures 8-10**), however due to the low sample size in the WT + saline treatment group (n=2), statistical comparisons could not be made. Although elastin dysregulation was apparent in two of the four aortae from hypertensive WT mice, dysregulation was also apparent in one of the aortae from a saline-treated WT mouse, with the limited sample size contributing to this variability

in elastin dysregulation scores. Genetic deletion of CCR8 did not appear to prevent the medial thickening, elastin dysregulation or increased collagen content in aortae of Ang II-treated mice (**Figures 8-10**).

4.6 Figures

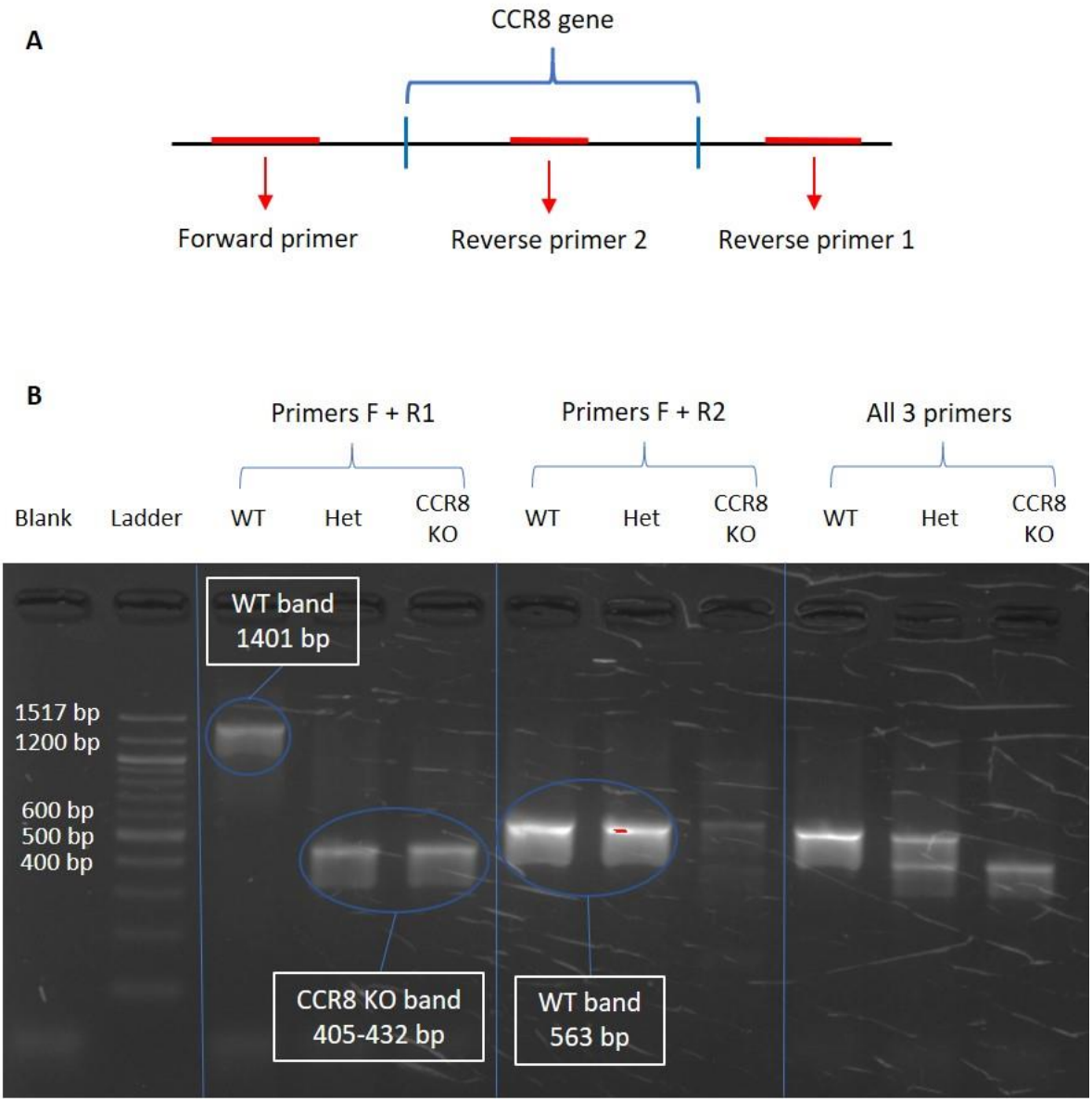

Figure 1. Genotype identification of CCR8$^{+/+}$ (WT), CCR8$^{+/-}$ (Het) and CCR8$^{-/-}$ (CCR8 KO) mice. **(A)** Schema illustrating the relative locations of designed primers. **(B)** Representative image of PCR products generated using Forward primer with Reverse primer 1 (F + R1), Forward primer with Reverse primer 2 (F + R2), or all three primers. DNA was extracted from the tips of mouse tails, and the designed primers were used to amplify relevant fragments via PCR. PCR products were then loaded onto agarose gels for electrophoresis.

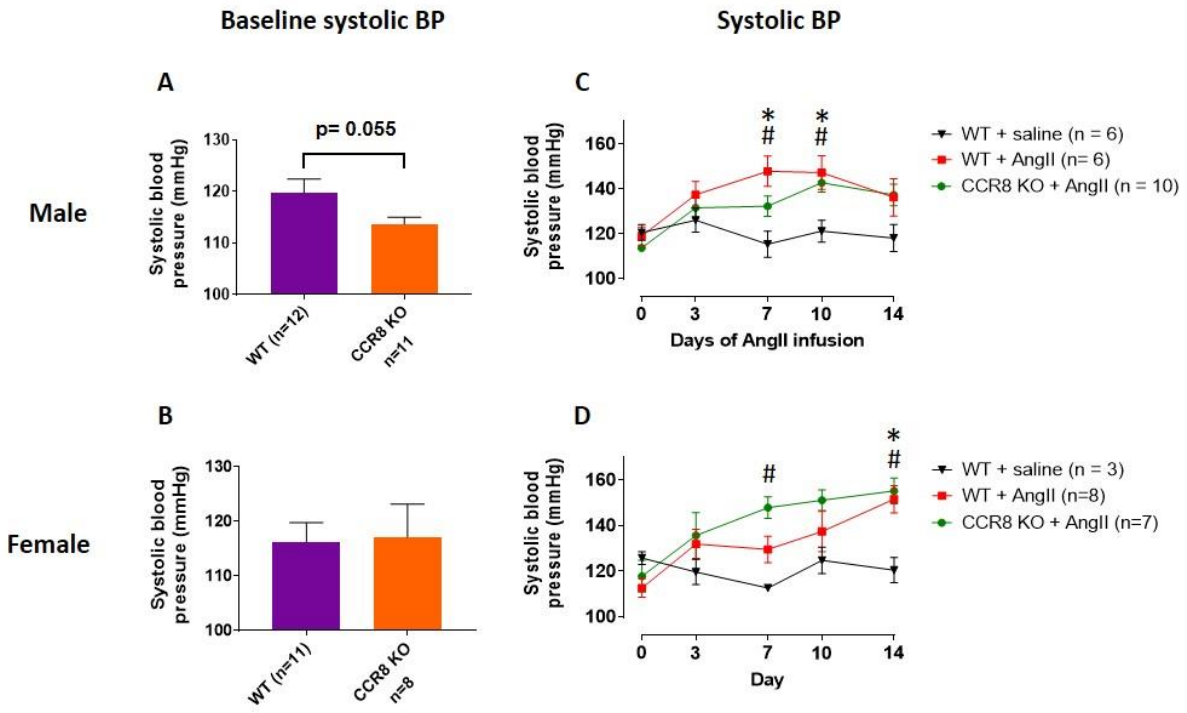

Figure 2. Effect of 14-day angiotensin II infusion on systolic blood pressure (BP) of male and female WT and CCR8 KO mice. **(A-B)** Baseline systolic BP of wildtype (WT) and CCR8 knockout (KO) mice, in males (**A**) and females (**B**). **(C-D)** Systolic BP over 14 days where male (**C**) and female (**D**) mice were treated with saline or Ang II (0.7 mg/kg/d). BP was measured by tail cuff plethysmography.

Data presented as mean ± SEM, where n = number of animals. (A-B) Student's unpaired t-test. (C-D) *p<0.05 WT + Ang II vs. WT + Saline, # p<0.05 CCR8 KO + Ang II vs. WT + Saline; 2-way ANOVA, Tukey's post hoc test.

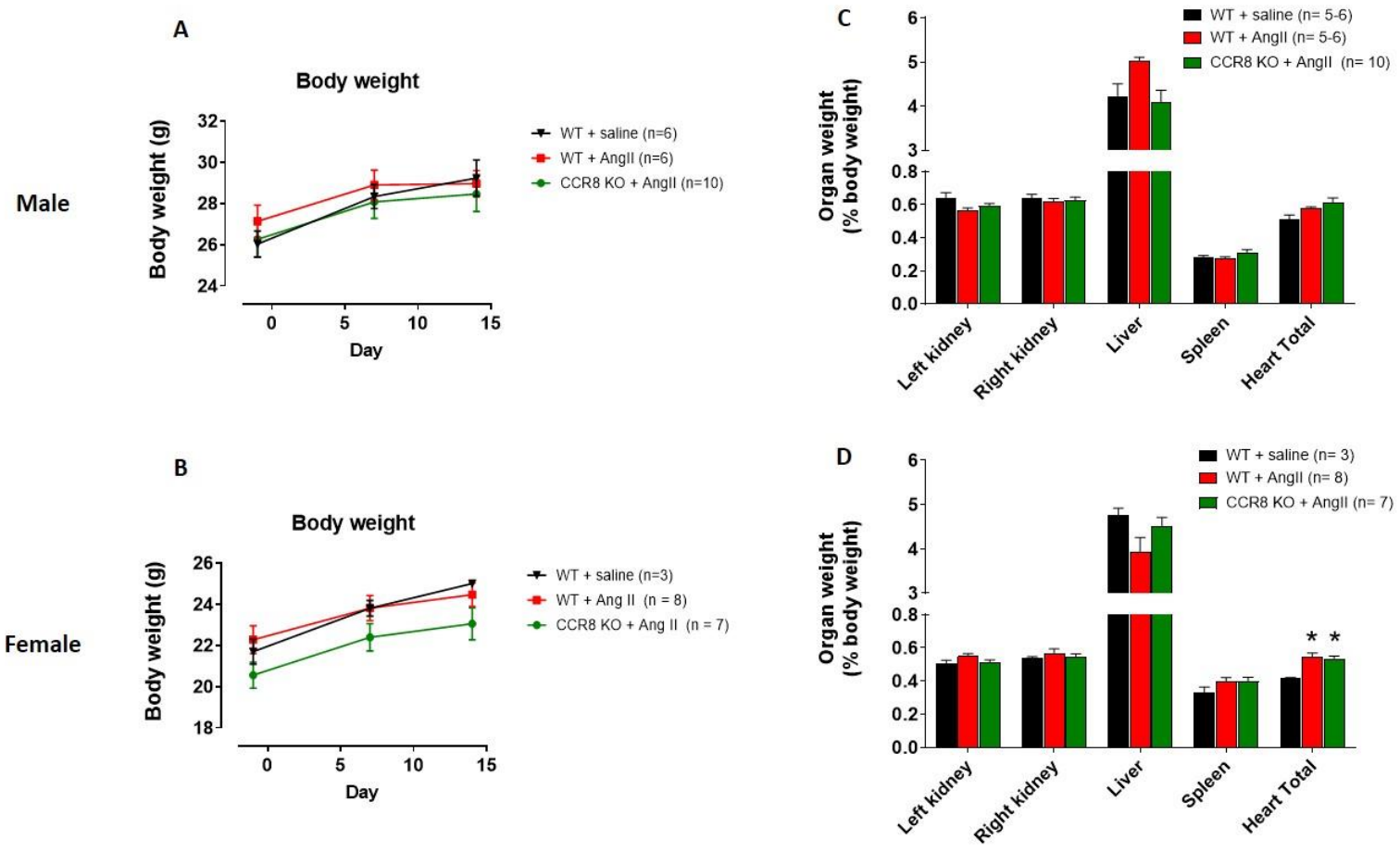

Figure 3. Effects of 14-day angiotensin II infusion on the body and organ weights of male WT and CCR8 KO mice (A-B) Body weights of wildtype (WT) and CCR8 knockout (KO) mice over 14 days, where male (**A**) and female (**B**) mice were treated with with saline or Ang II (0.7 mg/kg/d). (**C-D**) Organ weights of WT and CCR8 KO mice (relative to body weights), at the end of the saline or Ang II (0.7 mg/kg/d) treatment. Data presented as mean ± SEM, where n= number of animals. (A-B) 2-way ANOVA, Tukey's post hoc test. (C-D) *p<0.05 vs. WT + Saline; 1-way ANOVA, Tukey's post hoc test.

Male

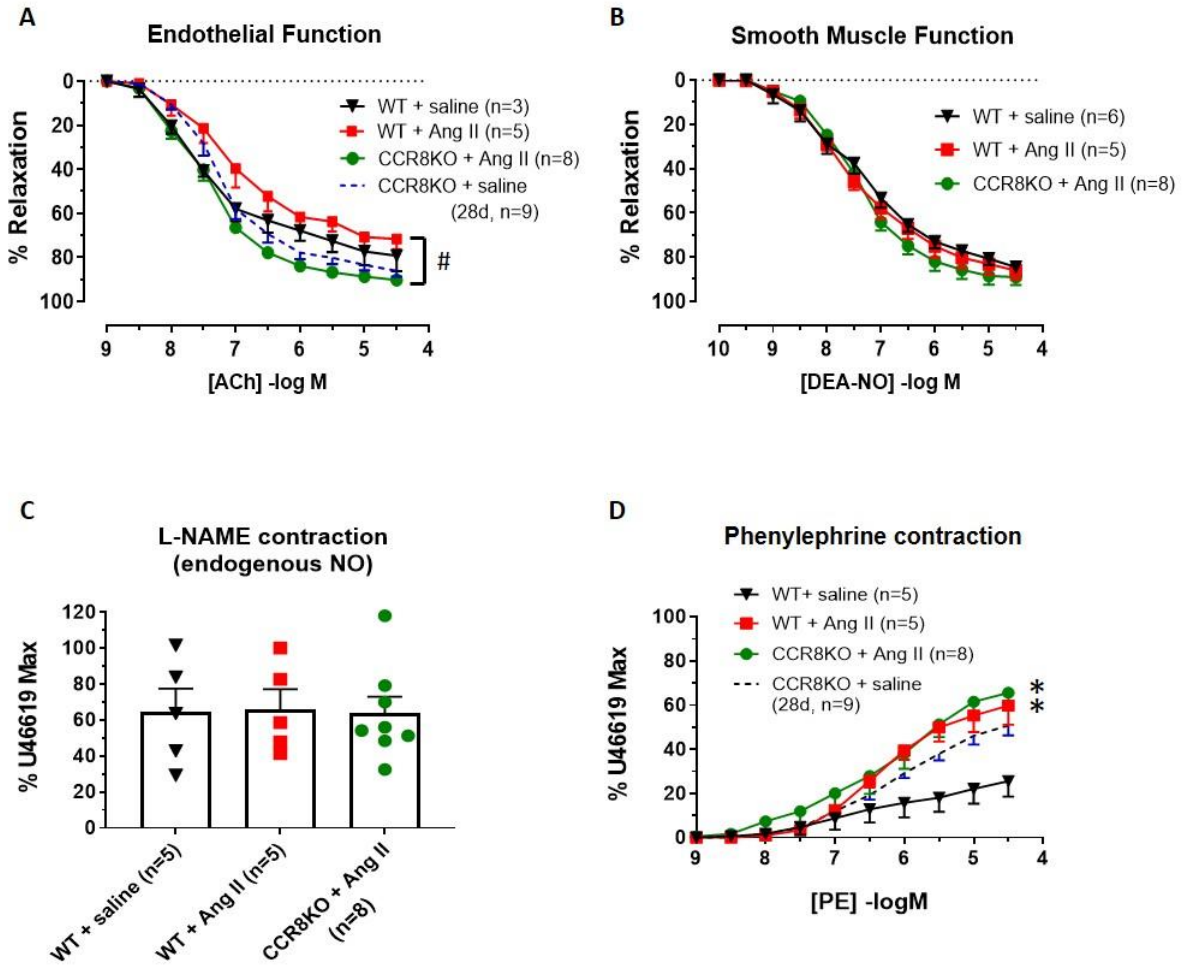

Figure 4. Effect of 14-day angiotensin II infusion on the function of the abdominal aorta in male WT and CCR8 KO mice. Cumulative concentration response curves to acetylcholine (ACh) (**A**), DEA-NO (**B**) and phenylephrine (PE) (**D**) and L-NAME (100µM)-induced contraction (**C**) in isolated abdominal aortae from wildtype (WT) and CCR8 knockout (KO) mice treated with either saline or Ang II (0.7 mg/kg/d) for 14 days. A CCR8 KO group treated with saline for 28 days was included in (A) and (D) for comparison and interpretation purposes.

Data expressed as % reversal of pre-contraction to U46619 (A-B) or % of the maximal U46619 contraction (C-D). Data presented as mean ± SEM, where n = number of animals. *p<0.05 vs. WT + saline (maximal contraction to PE), #p<0.05 vs. WT + Ang II (maximal relaxation to ACh); 1-way ANOVA, Tukey's post hoc test.

Female

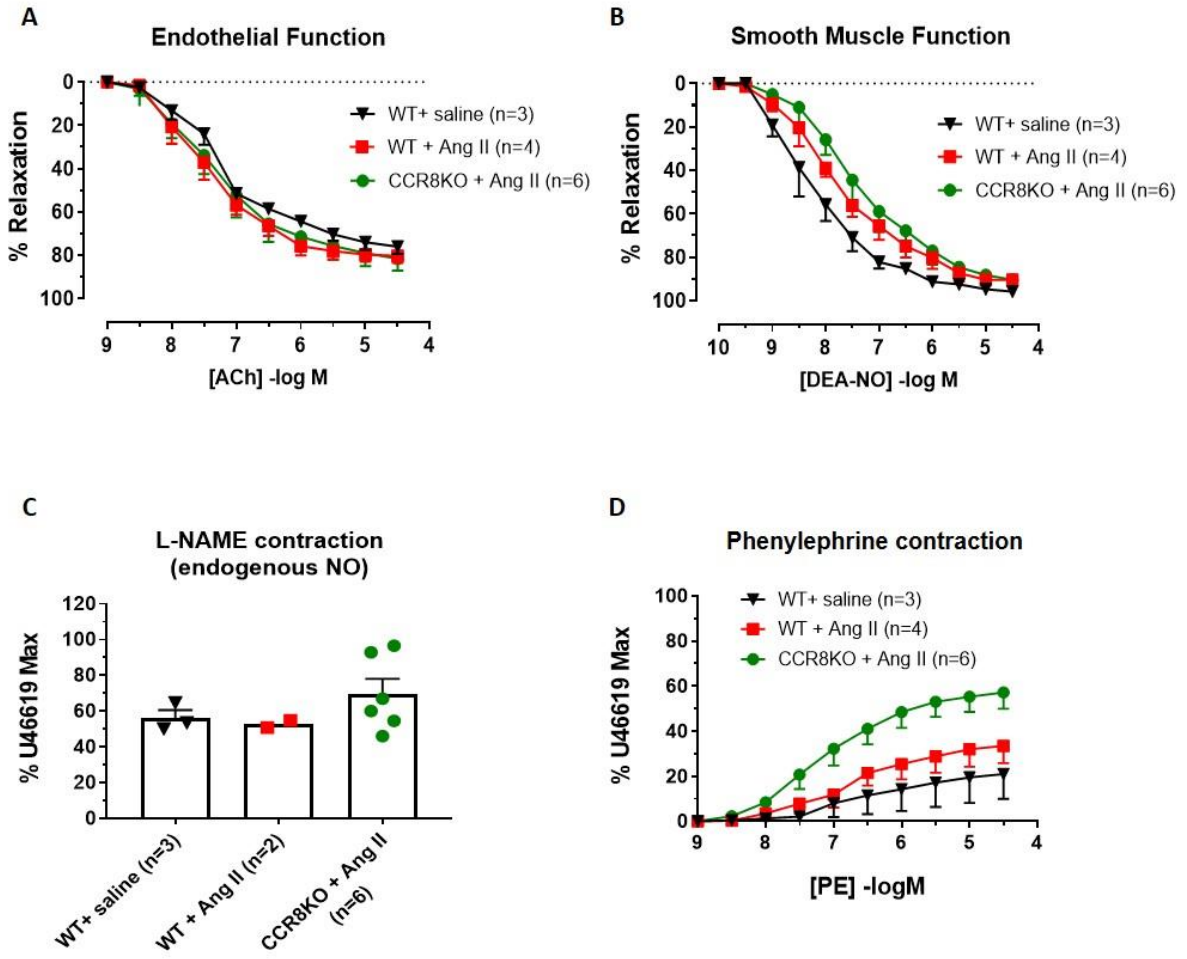

Figure 5. Effect of 14-day angiotensin II infusion on the function of the abdominal aorta in female WT and CCR8 KO mice. Cumulative concentration response curves to acetylcholine (ACh) (**A**), DEA-NO (**B**) and phenylephrine (PE) (**D**) and L-NAME (100µM)-induced contraction (**C**) in isolated abdominal aortae from wildtype (WT) and CCR8 knockout (KO) mice treated with either saline or Ang II (0.7 mg/kg/d) for 14 days.

Data expressed as % reversal of pre-contraction to U46619 (A-B) or % of the maximal U46619 contraction (C-D). Data presented as mean ± SEM (when n> 2) or mean (when n= 2), n= number of animals. 1-way ANOVA, Tukey's post hoc test (when n> 2).

Table 1. Effect of genetic deletion of CCR8 on relaxation to ACh and DEA/NO and contraction to PE in isolated aortae from saline- and Ang II-treated male mice.

Group	Vasodilator/ Vasoconstrictor							
	ACh			**DEA-NO**			**PE**	
	pEC_{50} (-log M)	**R_{max} (%)**	**Pre-contraction (% U4 max)**	**pEC_{50} (-log M)**	**R_{max} (%)**	**Pre-contraction (% U4 max)**	**pEC_{50} (-log M)**	**F_{max} (%)**
WT + saline	7.72 ± 0.22	79 ± 7	65 ± 1	7.87 ± 0.31	82 ± 4	59 ± 0.4	5.93 ± 0.6	34 ± 10
WT + Ang II	7.2 ± 0.09	72 ± 5	68 ± 3	7.58 ± 0.18	83 ± 5	69 ± 4	6.39 ± 0.22	61 ± 9 *
CCR8 KO + saline (28d model, for comparison)	7.45 ± 0.15	86 ± 3	64 ± 2	ND	ND	58 ± 2	6.17 ± 0.11	50 ± 4
CCR8 KO + Ang II	7.54 ± 0.07	90 ± 0.4 #	68 ± 3	7.51 ± 0.07	87 ± 4	56 ± 4	6.35 ± 0.32	66 ± 7 *

pEC_{50} values expressed as -log M, R_{max} values as % reversal of the level of pre-contraction to U46619, and F_{max} values as % contraction to U46619 (0.3 µM). Values given as mean ± SEM. n= 3-9. *p<0.05 vs. WT + saline (maximal contraction to PE), #p<0.05 vs. WT + Ang II (maximal relaxation to ACh); 1-way ANOVA, Tukey's post hoc test.

WT + saline: WT mice treated with saline for 14 days; **WT + Ang II**: WT mice treated with Ang II (0.7mg/kg/d) for 14 days; **CCR8 KO + saline**: CCR8 KO mice treated with saline for 28 days, included for comparative purposes as data was not obtained for a 14-day saline treatment; **CCR8 KO + Ang II**: CCR8 KO mice treated with Ang II (0.7mg/kg/d) for 14 days. **ACh**: acetylcholine; **DEA/NO**: diethylamine NONOate; **PE**: phenylephrine; **ND**: not determined.

Table 2. Effect of genetic deletion of CCR8 on relaxation to ACh and DEA/NO and contraction to PE in isolated aortae from Ang II-treated female mice.

Group	Vasodilator/ Vasoconstrictor							
	ACh			**DEA-NO**			**PE**	
	pEC_{50} (-log M)	**R_{max} (%)**	**Pre-contraction (% U4 max)**	**pEC_{50} (-log M)**	**R_{max} (%)**	**Pre-contraction (% U4 max)**	**pEC_{50} (-log M)**	**F_{max} (%)**
WT + saline	7.36 ± 0.13	79 ± 1	58 ± 3	8.33 ± 0.27	93 ± 0.9	62 ± 1	6.08 ± 0.8	11 ± 7
WT + Ang II	7.6 ± 0.16	80 ± 3	66 ± 2*	7.84 ± 0.22	88 ± 2	58 ± 5	6.89 ± 0.22	33 ± 5
CCR8 KO + Ang II	7.31 ± 0.18	78 ± 4	67 ± 0.5*	7.41 ± 0.31	86 ± 3	59 ± 1	7.28 ± 0.27	58 ± 7

pEC_{50} values expressed as -log M, R_{max} values as % reversal of the level of pre-contraction to U46619, and F_{max} values as % contraction to U46619 (0.3 μM). Values given as mean ± SEM. n= 3-6. *p<0.05 vs. WT + saline (pre-contraction), 1-way ANOVA, Tukey's post hoc test.

WT + saline: WT mice treated with saline for 14 days; **WT + Ang II**: WT mice treated with Ang II (0.7mg/kg/d) for 14 days; **CCR8 KO + Ang II**: CCR8 KO mice treated with Ang II (0.7mg/kg/d) for 14 days. **ACh**: acetylcholine; **DEA/NO**: diethylamine NONOate; **PE**: phenylephrine.

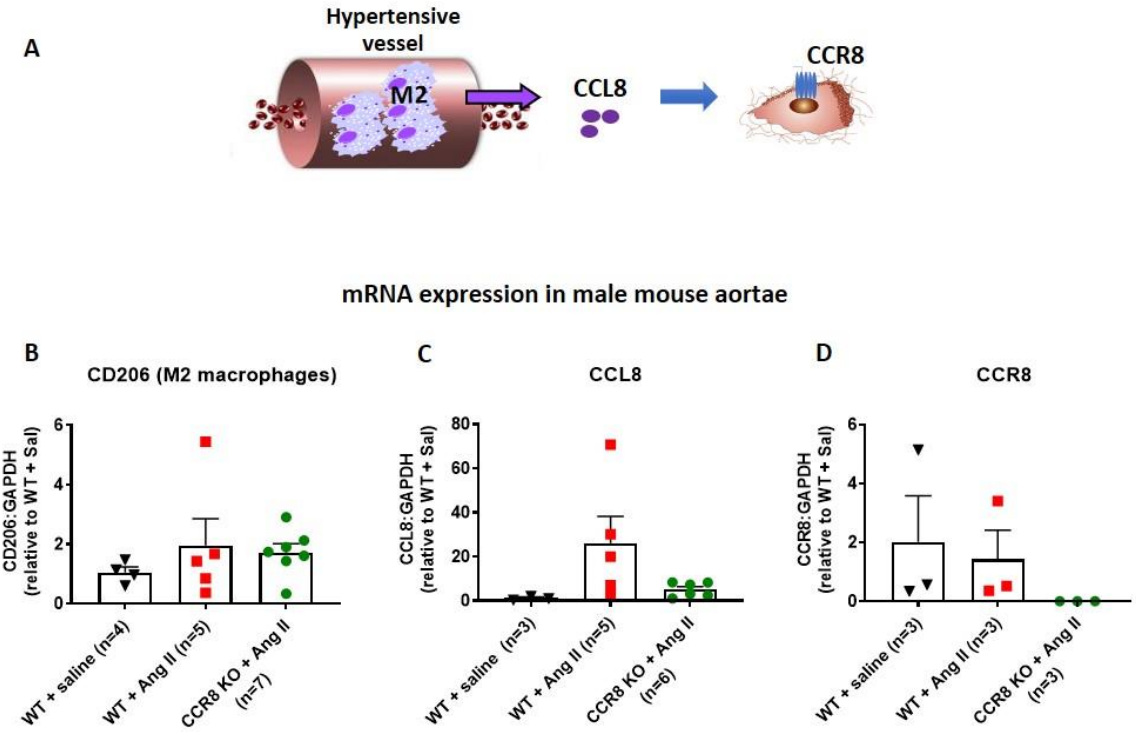

Figure 6. Effect of 14-day angiotensin II infusion on mRNA expression of CD206, CCL8 and CCR8 in the thoracic aorta of male wild-type and CCR8 KO mice. (A) Schema of the major cellular source and proposed actions of mouse CCL8. The expression of M2 macrophage-derived mouse CCL8 may be increased in the hypertensive vasculature, and CCL8 may target CCR8 to promote fibrosis and/or inflammation. **(B-D)** mRNA expression of CD206 (**B**), CCL8 (**C**) and CCR8 (**D**) in isolated thoracic aortae from male wildtype (WT) and CCR8 knockout (KO) mice treated with saline or Ang II (0.7 mg/kg/d) for 14 days.

Data represented as fold change relative to WT + Saline and presented as mean ± SEM, dots represent individual data points, n= number of animals. 1-way ANOVA, Tukey's post hoc test.

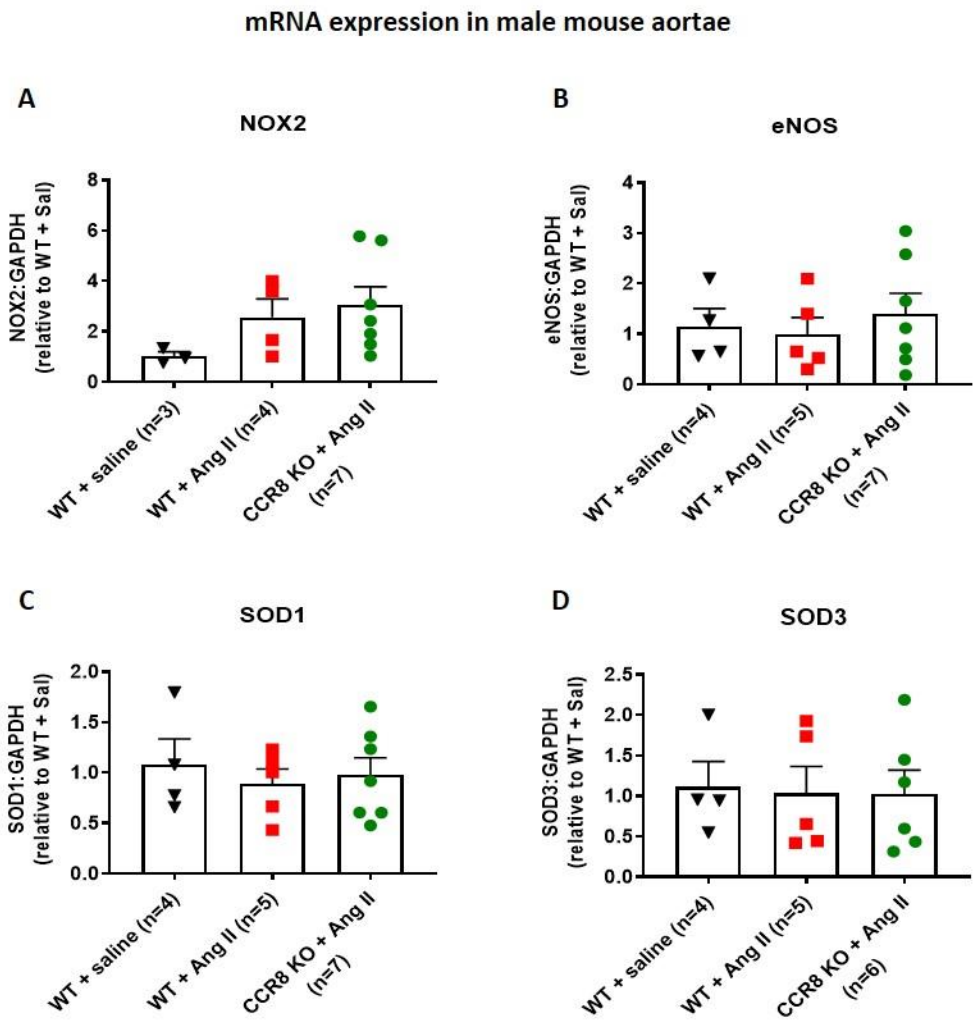

Figure 7. Effect of 14-day angiotensin II infusion on mRNA expression of oxidative stress markers in the thoracic aorta of male wild-type and CCR8 KO mice. mRNA expression of NOX2 (NADPH oxidase 2; **A**), eNOS (endothelial nitric oxide synthase; **B**), SOD1 (superoxide dismutase; **C**) and SOD3 (**D**) in isolated thoracic aortae from male wildtype (WT) and CCR8 knockout (KO) mice treated with saline or Ang II (0.7 mg/kg/d) for 14 days.

Data presented as mean ± SEM, dots represent individual data points, n= number of animals. 1-way ANOVA, Tukey's post hoc test.

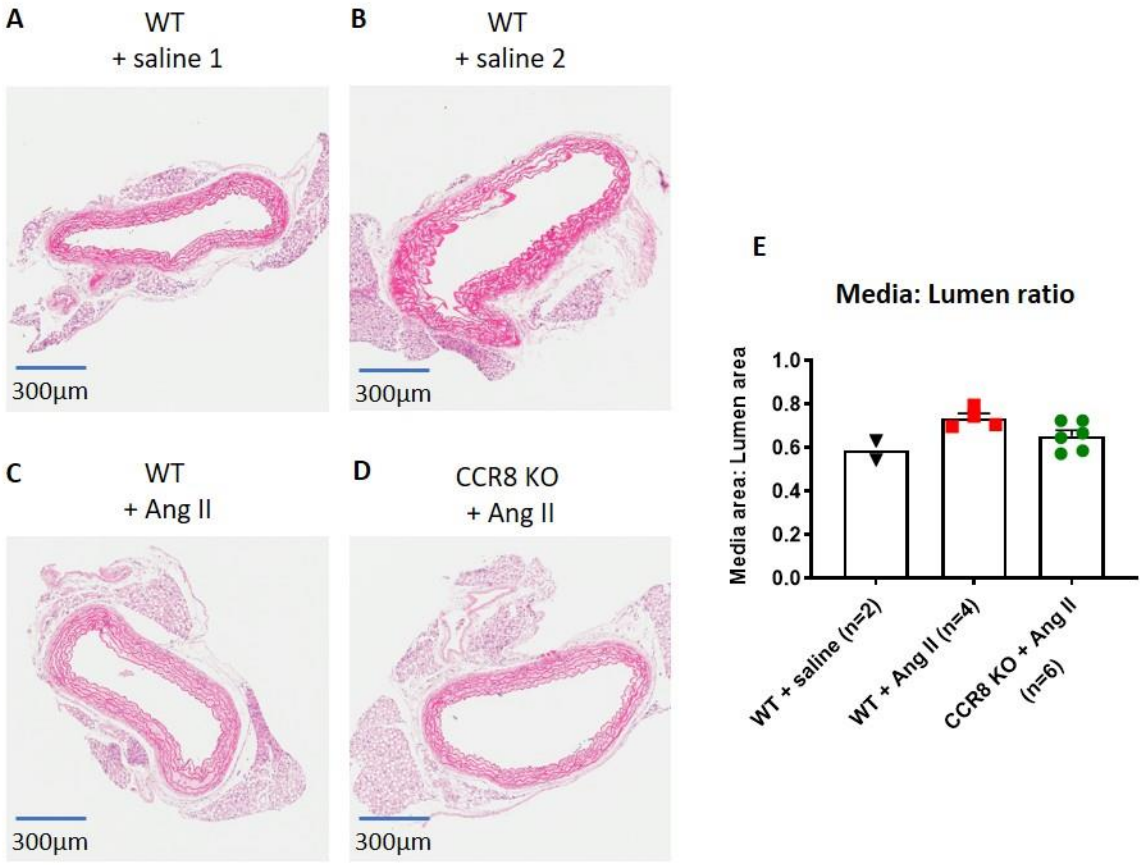

Figure 8. Effect of 14-day infusion of Ang II on the structure of the thoracic aorta from male wildtype and CCR8 KO mice. (A-D) Representative images of mouse aortic sections stained by hematoxylin and eosin (H&E). Wildtype (WT) and CCR8 knockout (KO) mice were treated with saline or Ang II (0.7 mg/kg/d) for 14 days. Images from both saline-treated WT mice (A-B) were shown as there was n=2 for this group. (**E**) Quantification of medial area: lumen area ratio. Data presented as mean ± SEM (when n> 2) or mean (when n= 2), n= number of animals.

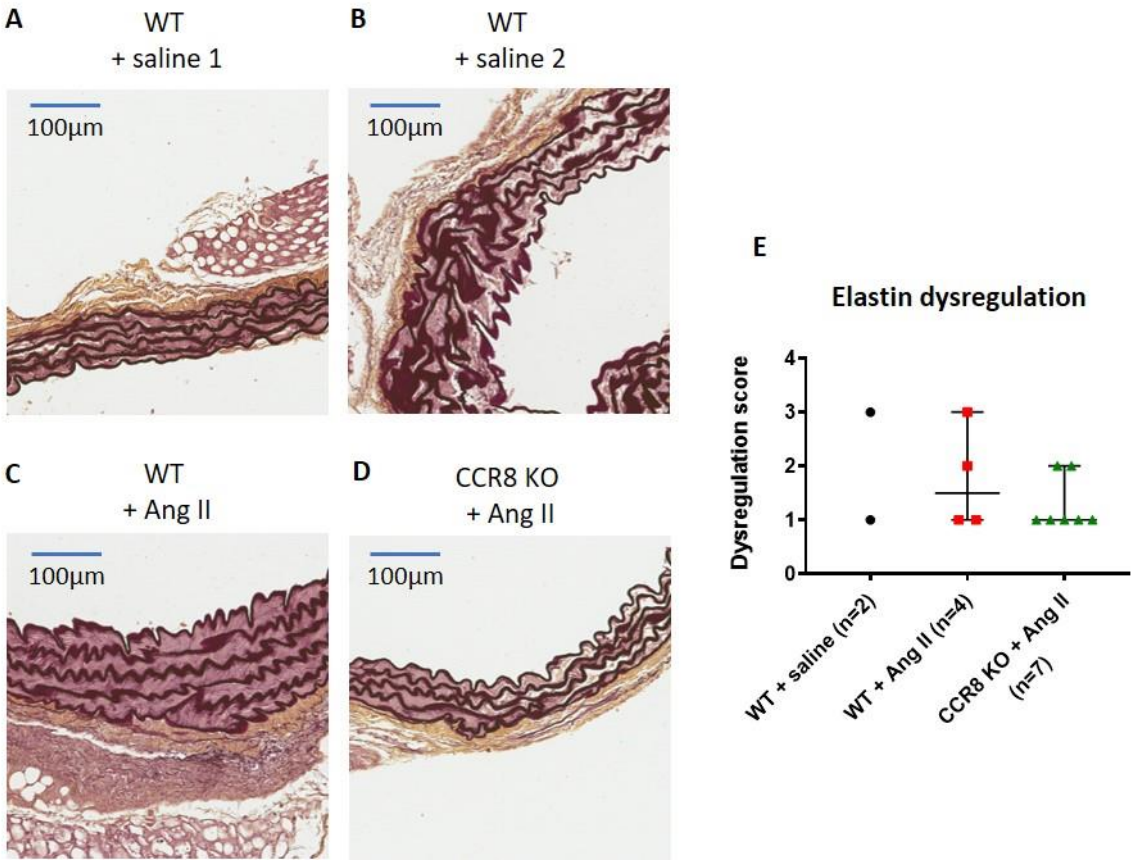

Figure 9. Effect of 14-day infusion of Ang II on elastin dysregulation of the thoracic aorta from male wildtype and CCR8 KO mice. (A-D) Representative images of mouse aortic sections stained by Verhoeff-Van Gieson (VVG). Wildtype (WT) and CCR8 knockout (KO) mice were treated with saline or Ang II (0.7 mg/kg/d) for 14 days. Images from both saline treated WT mice (A-B) were shown as there was n=2 for this group. (**E**) Scoring of the level of elastin dysregulation, where score= 1 represents normal elastin structure, and score= 4 represents severe elastin dysregulation. Data presented as median with 95% CI (when n> 2) or individual values (when n= 2), n= number of animals.

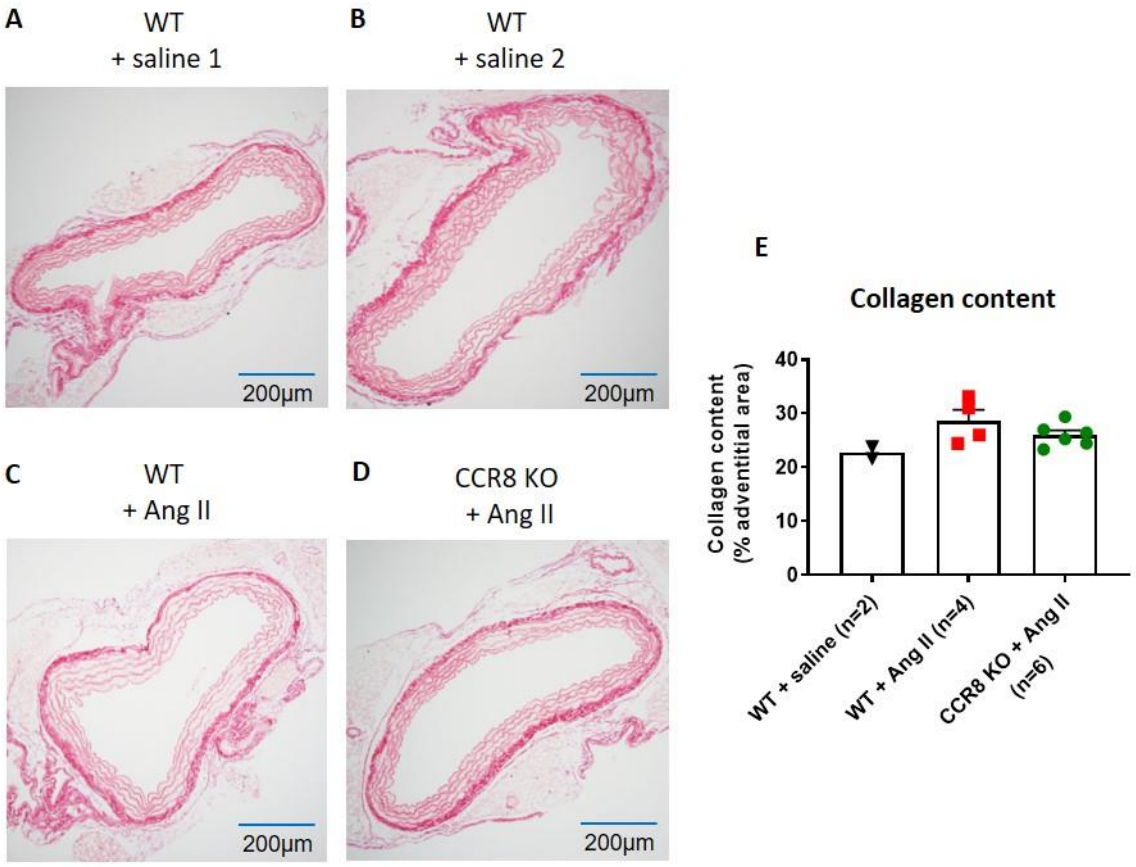

Figure 10. Effect of 14-day infusion of Ang II on the structure of the thoracic aorta from male wildtype and CCR8 KO mice. (A-D) Representative images of mouse aortic sections stained by picrosirius red. Wildtype (WT) and CCR8 knockout (KO) mice were treated with saline or Ang II (0.7 mg/kg/d) for 14 days. Images from both saline-treated WT mice (A-B) were shown as there was n=2 for this group. (**E**) Quantification of adventitial collagen expressed as % of adventitial area. Data presented as mean ± SEM (when n> 2) or mean (when n= 2), n= number of animals.

4.7 Discussion

M2 macrophage-derived pro-fibrotic chemokines, human CCL18 (hCCL18) and mouse CCL8 (mCCL8), are functional analogues and both signal via CCR8 (Islam et al., 2013). Given that M2 macrophages contribute to vascular fibrosis in hypertension (Moore et al., 2015), we conducted the first study that investigated the effects of global CCR8 knockout (KO) on the development of hypertension in male and female mice. Whilst genetic deletion of CCR8 did not impact the hypertensive response to angiotensin II (Ang II) or the associated vascular dysfunction and remodelling, it did limit the aortic expression of mCCL8. In addition, we have provided the first evidence that CCR8 KO male mice have improved endothelial function and augmented contractility to phenylephrine, both of which are effects independent of Ang II-induced hypertension. These findings suggest that the mCCL8-CCR8 signalling axis may not be a key contributor to the development of hypertension in this Ang II-induced disease model.

In this study, hypertension was induced by 2 weeks of Ang II infusion (0.7 mg/kg/d), which is a commonly utilised model to create a setting of well-established hypertension in mice. Thus, previous studies have demonstrated that 14d of Ang II treatment caused a robust elevation in systolic BP in both male (0.7 mg/kg/d Ang II) (Moore et al., 2015) and female (0.6 mg/kg/d Ang II) (Ebrahimian et al., 2008) mice. Our study has shown that the increase in systolic BP in response to Ang II is delayed in wild-type (WT) female mice as compared to WT male mice, with significant elevations observed at days 14 and 7, respectively. These findings are consistent with those of Ji et al. (2014) who measured changes in mean arterial pressure (MAP) in response to Ang II in male and female mice. It is proposed that the protection from hypertension in young female mice is provided by the abundance of estrogen and the lack of testosterone. Thus, ovariectomized female mice develop higher MAP as compared to intact females, and castrated male mice are protected from BP elevation compared to intact males (Xue et al., 2005). Of note, the genetic deletion of CCR8 did not confer protection against the rise in systolic BP in either female or male mice. Indeed, the hypertensive response to Ang II appeared to be accelerated in female mice, such that the time course of elevation in systolic BP was similar in female and male CCR8 KO mice. This observation requires further investigation since our study design did not control for the phases of the estrous cycle in female mice.

Hypertension is also associated with cardiac and renal hypertrophy as an adaptive response to the elevation in pressure (Brown et al., 1997; Kirchhoff et al., 2008), which can be quantified via measuring heart and kidney weights, relative to body weight, respectively. In this study, cardiac and renal hypertrophy was not evident in Ang II-treated male WT mice. This is consistent with data from a more severe model of Ang II-induced hypertension (2.2 mg/kg/d Ang II, 14-day), where the authors additionally reported mild cardiac fibrosis and a lack of kidney damage in their Ang II model of hypertension (Kirchhoff et al., 2008). By contrast, WT female hypertensive mice displayed cardiac, but not renal hypertrophy, which is also consistent with previous findings (Li et al., 2007). The observed gender difference may be explained by the different forms of cardiomyopathy evident in hypertension (Kessler et al., 2019). In hypertensive humans, males tend to develop eccentric cardiac hypertrophy, and females develop more concentric cardiac hypertrophy (Kessler et al., 2019). It is believed that concentric cardiac hypertrophy is associated with a greater left ventricular mass as compared to eccentric hypertrophy (de Simone, 2004) and whilst the underlying mechanism remains unclear, this may account for the cardiac hypertrophy observed in female versus male mice. The cardiac hypertrophy observed in hypertensive female mice was not ameliorated following genetic deletion of CCR8 which is in agreement with our finding that the magnitude of the hypertensive response to Ang II was similar in female WT and CCR8 KO mice.

Chronic hypertension is also associated with vascular dysfunction and remodelling, particularly in large conduit arteries, such as the aorta (Oparil et al., 2003). Aortae from Ang II infused mice have been observed to have impaired endothelium-dependent relaxation (Guzik et al., 2007), loss of endogenous NO (Al-Magableh et al., 2015) and augmented contractility (Seto et al., 2013). The aortic dysfunction can lead to vascular remodelling and stiffening, which can in turn cause end-organ damage and exacerbate hypertension (Drummond et al., 2019). Consistent with published data (Seto et al., 2013), contractile responses to the α_1-adrenoceptor agonist, phenylephrine (PE) were increased in the abdominal aorta from hypertensive WT male mice. It is well recognised that PE-induced contraction is modulated by endogenous nitric oxide (NO), such that NO synthase (NOS) inhibitors (e.g. L-NAME) augment PE contraction. It is generally assumed that enhanced PE contractility in hypertension is due to endothelial dysfunction and a loss in endogenous NO (Al-Magableh et al., 2015). However, this did not appear to be the case in the current study.

Thus, we found that ACh-induced relaxation and L-NAME-induced contraction (marker of endogenous NO bioavailability) were preserved in aortae from Ang II infused male mice, along with unchanged contractility to U46619. Whilst many studies have reported endothelial dysfunction following Ang II infusion (Barhoumi et al., 2011; Guzik et al., 2007; Laursen et al., 1997; Madhur et al., 2010; Ryan Michael et al., 2004), unpublished data from other studies in our laboratory and from our collaborators at La Trobe University, consistently demonstrate intact endothelium-dependent vasorelaxation in aorta from Ang II-treated mice. The inconsistency in the results of such experiments can be due to differences in the experimental protocols utilised, such as inconsistent resting tension and/or pre-contraction levels by U46619. Over-contraction of vessels with a vasoconstrictor, such as U46619, can damage the endothelium and blunt vasorelaxant responses (Lu & Kassab, 2011). As such, it is important to match the levels of pre-contraction to ensure vascular dysfunction does not reflect functional antagonism due to over-contraction. None of the above-mentioned publications which reported vascular dysfunction stated the level of pre-contraction when constructing vasorelaxation responses. However, in this study, the levels of pre-contraction were well matched by titrating the concentration of U46619 to achieve a level of pre-contraction of ≈65 % F_{max}, thereby facilitating valid comparisons of endothelial function between treatment groups.

Based on the current results and published literature, the mechanisms underlying the augmented contractility to PE in hypertension remain unknown. The observed augmented response in this study appears to be specific for PE, as the maximum contractions to U46619 do not differ in aortae from saline- or Ang II- treated mice. Possible causes for the enhanced contractility to PE (α_1-adrenoceptor agonist) include increased α_1-adrenoceptor expression/activities, and/or increased oxidative stress. Thus α_1-adrenoceptor expression has been shown to be increased in hypertension. Thus spontaneous hypertensive rats have higher expression of α_1-adrenoceptors in the aorta, as compared to normotensive rats (Rodríguez et al., 2020). In addition, it is suggested that reactive oxygen species (ROS) promotes α_1-adrenoceptor-dependent vascular smooth muscle contraction (Tsai & Jiang, 2010). Increased PE contraction in the hypertensive vasculature may also be due to a loss in regulatory inducible NOS (iNOS)-derived NO as a result of increased oxidative stress (Alvarez et al., 2008). Regardless of the underlying cause of augmented PE contractility in hypertension, our study has highlighted a positive correlation between the contractility of aortae to PE and systolic BP

of WT male mice. As such, PE may be a marker of hypertension-associated vascular damage, at least in WT male mice. It is also important to note that unlike male mice, the enhanced response to PE was not observed in hypertensive WT females. This finding, together with preserved endothelial function and endogenous NO bioavailability, suggest that females may be protected from hypertension associated vascular damage. To further support this hypothesis, Tatchum-Talom et al. (2005) reported vascular dysfunction (impaired endothelial function and enhanced contractility) in the mesenteric arteries of hypertensive male rats, but not in hypertensive female rats.

Although endothelial dysfunction was not evident in hypertensive male or female mice, it was interesting to note that genetic deletion of CCR8 lead to improved ACh-induced vasorelaxation in hypertensive male mice. Such an effect was not observed in female mice. Due to the impact of COVID-19, a group of 14d saline-treated male CCR8 KO mice were not included in this study design limiting the validity of the comparisons. However, extrapolation from data obtained in a cohort of 28d saline treated CCR8 KO mice (**Chapter 5**), indicate that endothelial function is preserved in hypertensive male CCR8 KO mice. The mechanisms underlying the augmented endothelial function in hypertensive CCR8 KO as compared to hypertensive WT mice remain to be elucidated. Thus, we have shown that ACh-induced vasorelaxation is largely inhibited by the NOS inhibitor L-NAME in naïve CCR8 KO mice, suggesting that such vasorelaxation is due predominantly to NO, so we could speculate that there is improved NO bioavailability following genetic deletion of CCR8. However, this is not supported by the finding that L-NAME contraction is similar between hypertensive CCR8 KO and WT mice. Moreover, the potency and efficacy of DEA/NO were similar between WT and CCR8 KO hypertensive mice, suggesting the improved vasorelaxation does not reflect increased responsiveness to NO at the level of vascular smooth muscle cells (VSMCs). The greater relaxation to ACh in the CCR8 KO vasculature may be due to upregulation of endothelium-derived vasodilators other than NO, such as prostacyclin (PGI_2) and endothelium-derived hyperpolarising factor (EDHF) (Jiang et al., 2016). Future studies can determine the relative contribution of these factors to ACh-induced vasorelaxation in WT and CCR8 KO mice. CCR8 KO may also improve vasorelaxation by limiting infiltration of inflammatory cells, considering the chemotactic actions of CCR8 (Connolly et al., 2012).

Interestingly, whilst genetic deletion of CCR8 led to an improvement in endothelial function in male hypertensive mice, it did not attenuate the augmented contractile response to PE. These findings further support the concept that PE responses are not modulated by endothelial function. Indeed, we observed that genetic deletion of CCR8 per se in untreated male, but not female mice, was associated with increased contractile efficacy to PE. Moreover, in the setting of hypertension PE contractility was not enhanced further in male CCR8 KO mice. Collectively, these findings suggest that under physiological conditions, CCR8 signalling may serve to limit vasoconstriction to PE. As discussed above, the mechanisms underlying the improved PE contraction in the mouse aorta remain unknown, but may relate to changes in the relative expression of α_1-adrenoceptors. Future experiments should interrogate the idea that there may be cross-talk between CCR8 and adrenoceptors. In particular, CCR8 is expressed on VSMCs and the endothelium (HUVECs) (Haque et al., 2004). As such, there is potential for an interaction between CCR8 and α_1-adrenoceptors on VSMCs (Ko et al., 1996). Of note, whilst PE contractility appeared to be enhanced in hypertensive CCR8 KO female mice as compared to their hypertensive WT counterparts, the findings are confounded by the limited sample size and variability in response in the saline-treated WT mice. Nevertheless, the current findings suggest that CCR8 signalling may serve to limit adrenoceptor-mediated contractile responses in both male and female mice.

It is well recognised that vascular inflammation and oxidative stress, are hallmarks of hypertension (Drummond et al., 2019). Indeed, hypertension is associated with infiltration of M2 macrophages into the vascular wall and elevated levels of mCCL8 (Moore et al., 2015). Studies in our lab have also shown co-localisation of mCCL8 to M2 macrophages in the vascular wall (Lewis, 2017). Based upon these findings, we wished to examine the impact of genetic deletion of the mCCL8 target, CCR8 on vascular inflammation and oxidative stress in the context of hypertension. These studies were conducted in male mice given the lack of vascular dysfunction observed in hypertensive WT females. Consistent with previous findings (Moore et al., 2015; Murdoch et al., 2011), we observed a trend for an increase in M2 macrophage, mCCL8 and NOX2 (NADPH oxidase 2, major source of vascular superoxide) expression in aortae from hypertensive mice. Although Murdoch et al. (2011) also reported changes in expression of the antioxidant enzyme, superoxide dismutase in Ang II-treated mice, specifically increased SOD1 and decreased SOD3 expression, we did not observe such changes.

Such differences may be related to the higher dose of Ang II used by Murdoch et al. (1.1mg/kg/d vs. our study: 0.7 mg/kg/d). Interestingly, M2 macrophage infiltration did not appear to be attenuated in hypertensive CCR8 KO mice, yet there was a trend for decrease in mCCL8 expression. One potential explanation for this observation is that CCR8 modulates the release of mCCL8 from M2 macrophages. Thus hCCL18 (functional analogue of mCCL8) is found to act on M2 macrophages to further promote hCCL18 generation in an autocrine or paracrine manner, creating a positive feedback loop (Schraufstatter et al., 2012), an effect which has been postulated to be mediated by CCR8. CCR8 KO may also dampen the chemotactic effects of mCCL8 (Islam et al., 2011), and therefore reduce mCCL8 production from cells other than macrophages, such as dendritic cells (Islam et al., 2011). In addition, CCR8 is expressed on Th2 cells (Connolly et al., 2012; Islam et al., 2011) which exacerbate inflammation in hypertension via infiltrating into the vasculature (Wu et al., 2016). As such, T cell infiltration may be reduced in the vasculature of hypertensive CCR8 KO mice, thereby limiting hypertension-associated vascular damage. Future studies can further investigate the role of mCCL8/ hCCL18 signalling on T cells in hypertension, using immunohistochemistry and/or flow cytometry, to confirm the population of inflammatory cells and the cellular source of mCCL8 within the vasculature of hypertensive WT and CCR8 KO mice. Relevant flow cytometric analysis has been utilised in **Chapter 5**.

Having demonstrated that genetic deletion of CCR8 may limit generation of the chemoattractant CCL8 and thus immune cell infiltration, we next investigated the impact of CCR8 deletion on vascular oxidative stress. Protein kinase C alpha (PKCα), a potent activator of NOX2 (Brandes et al., 2014), has been reported to mediate downstream signalling of CCL18 (Luzina et al., 2006). As such, CCR8 deletion may attenuate vascular oxidative stress. When CCR8 is genetically deleted in hypertensive mice, no change is observed in the expression of oxidative stress markers, suggesting that CCR8 may not modulate oxidative stress in the hypertensive vasculature. However, the measure of NOX2 expression (membrane subunit) in this study is not necessarily indicative of NOX2 activity and its ability to generate superoxide. Thus mCCL8-CCR8 signalling may lead to PKC-mediated phosphorylation of the NOX2 cytosolic subunit ($p47^{phox}$), its subsequent translocation to the membrane, and hence the activation of NOX2 followed by superoxide production (Paik et al., 2014). A superoxide assay, such as L-012- enhanced chemiluminescence assay, can be utilised in future studies to

investigate whether CCR8 global deletion reduces vascular NOX2 activity and/or superoxide generation in hypertension.

Hypertension is associated with vascular hypertrophy, stiffening as a consequence of increased collagen deposition and elastin dysregulation. Given the potential pro-fibrotic capacity of CCL8, and our finding that CCL8 expression was attenuated in the CCR8 KO hypertensive vasculature, we anticipated that genetic deletion of CCR8 may lead to reduced vascular remodelling and/or fibrosis. In this study, aortae from Ang II treated WT male mice appeared to have an increased media: lumen ratio and higher levels of collagen deposition. Although a larger sample size is required to ensure sufficient statistical power, these findings are consistent with other studies, suggesting that hypertension is associated with thickened medial area and vascular fibrosis (Nosalski et al., 2020; Williams et al., 2019). Whilst there was evidence for elastin dysregulation in the hypertensive vasculature, the low sample size and high degree of variability in measurements in the saline-treated WT group, limits interpretation. Of note, vascular elastin dysregulation has been reported following administration of Ang II at higher doses, predominantly in models of abdominal aortic aneurysm (e.g. 2.1 mg/kg/d Ang II, 14d) (Cui et al., 2016), or for longer periods (0.7 mg/kg/d Ang II, 28d) (Moore et al., 2015).

Genetic deletion of CCR8 did not appear to prevent the medial thickening, elastin dysregulation or increased collagen content in aortae of Ang II-treated mice. Considering the lack of comparable published studies and the small sample size in this study design, additional experiments are required to comprehensively assess the potential role of CCR8 in hypertension-associated vascular remodelling. Based upon the published findings that hCCL18 can signal to promote collagen generation in lung fibroblasts (Atamas et al., 2003) and our own data to suggest that hCCL18 can target aortic adventitial fibroblasts and endothelial cells to promote collagen generation and endothelial-mesenchymal transition, respectively (**Chapter 3**), the lack of impact of CCR8 deletion on aortic remodelling is somewhat unexpected. These findings may reflect differences between hCCL18 and mCCL8 signalling. It is also important to note that we do not have definitive evidence that CCR8 is the receptor responsible for the observed effects of hCCL18, due to poor CCR8 antibodies (presented in **Chapter 3**). Furthermore, the impact of CCR8 deletion may become more evident in a longer-term model of hypertension.

A number of limitations are associated with this study including the small sample sizes in some datasets due to the COVID-19 pandemic (as outlined in the COVID-19 impact statement; **Section 4.1**). As such, definitive conclusions could not be made such as the reduction in CCL8 expression in CCR8 KO hypertensive mice and elastin dysregulation in the WT hypertensive vasculature. Although littermates are used to control for genetic variations, our study lacks saline-treated CCR8 KO mice, and the phases of the estrous cycle in female mice are not controlled for. Furthermore, inconsistent with some published studies, endothelial dysfunction was not detected in the 14d Ang II model of hypertension. Future vascular function studies can focus on exploring the reasons why such inconsistency occurs, and/or investigating how changes in α_1-adrenoceptor expression or ROS generation modulate PE contraction. In the assessment of vascular damage, changes detected in mRNA expression requires confirmation by protein expression (western blotting), and the lack of changes in oxidative stress markers may be confirmed via measurement of superoxide release (e.g. using L-012 enhanced chemiluminescence). Lastly, together with other published studies using similar hypertension models (Kirchhoff et al., 2008), our data suggest that the 14d Ang II infusion model (0.7 mg/kg/d) causes little cardiac or renal damage. To further investigate the role of CCR8 in hypertension-associated organ damage, a model associated with more severe end organ dysfunction is required, either via infusion of Ang II at a higher dose or for a longer period (28d). Additionally, other agents such as deoxycorticosterone acetate and salt (DOCA-salt), alone or in combination with Ang II, may cause more robust organ damage (Kirchhoff et al., 2008).

In summary, genetic deletion of CCR8 does not limit the elevation in BP or associated cardiac hypertrophy in Ang II treated male and female mice. A loss in CCR8 was associated with improved endothelial function in hypertensive male mice, and an apparent reduction in expression of the chemoattractant chemokine, CCL8 suggesting that CCL8-CCR8 signalling may facilitate vascular inflammation and endothelial dysfunction in hypertension. However, a role for the CCL8-CCR8 axis in hypertension associated vascular remodelling was not apparent. In conclusion, the contribution of CCR8 signalling to hypertension-associated vascular dysfunction and remodelling is modest and targeting this pathway, at least in the early stages of hypertension, may not confer protection. Future experiments using more

chronic models of hypertension to investigate the contribution of CCR8 signalling to end-organ damage are warranted and presented in **Chapter 5**.

4.8 References

Al-Magableh MR, Kemp-Harper BK, & Hart JL (2015). Hydrogen sulfide treatment reduces blood pressure and oxidative stress in angiotensin II-induced hypertensive mice. Hypertens Res 38**:** 13-20.

Álvarez Y, Briones AM, Hernanz R, Pérez-Girón JV, Alonso MJ, & Salaices M (2008). Role of NADPH oxidase and iNOS in vasoconstrictor responses of vessels from hypertensive and normotensive rats. Br J Pharmacol 153: 926-935.

Atamas SP, Luzina IG, Choi J, Tsymbalyuk N, Carbonetti NH, Singh IS, Trojanowska M, Jimenez SA, & White B (2003). Pulmonary and Activation-Regulated Chemokine Stimulates Collagen Production in Lung Fibroblasts. Am J Respir Cell Mol Biol 29**:** 743-749.

Barhoumi T, Kasal Daniel A, Li Melissa W, Shbat L, Laurant P, Neves Mario F, Paradis P, & Schiffrin Ernesto L (2011). T Regulatory Lymphocytes Prevent Angiotensin II–Induced Hypertension and Vascular Injury. Hypertension 57**:** 469-476.

Brandes RP, Weissmann N, & Schröder K (2014). Nox family NADPH oxidases: Molecular mechanisms of activation. Free Radic Biol Med 76**:** 208-226.

Brown L, Passmore M, Duce B, & Sernia C (1997). Angiotensin Receptors in Cardiac and Renal Hypertrophy in Rats. J Mol Cell Cardiol 29**:** 2925-2929.

Connolly S, Skrinjar M, & Rosendahl A (2012). Orally bioavailable allosteric CCR8 antagonists inhibit dendritic cell, T cell and eosinophil migration. Biochem Pharmacol 83**:** 778-787.

Couto GK, Davel AP, Brum PC, & Rossoni LV (2014). Double disruption of α2A- and α2C-adrenoceptors induces endothelial dysfunction in mouse small arteries: role of nitric oxide synthase uncoupling. Exp Physiol 99**:** 1427-1438.

Cui M, Cai Z, Chu S, Sun Z, Wang X, Hu L, Yi J, Shen L, & He B (2016). Orphan Nuclear Receptor Nur77 Inhibits Angiotensin II-Induced Vascular Remodeling via Downregulation of β-Catenin. Hypertension 67**:** 153-162.

de Jager SCA, Bongaerts BWC, Weber M, Kraaijeveld AO, Rousch M, Dimmeler S, van Dieijen-Visser MP, Cleutjens KBJM, Nelemans PJ, van Berkel TJC, & Biessen EAL (2012). Chemokines CCL3/MIP1α, CCL5/RANTES and CCL18/PARC are Independent Risk Predictors of Short-Term Mortality in Patients with Acute Coronary Syndromes. PLoS One 7**:** e45804.

de Simone G (2004). Concentric or eccentric hypertrophy: how clinically relevant is the difference? Hypertension 43**:** 714-715.

Diez J (2007). Mechanisms of cardiac fibrosis in hypertension. J Clin Hypertens (Greenwich) 9**:** 546-550.

Drummond GR, Vinh A, Guzik TJ, & Sobey CG (2019). Immune mechanisms of hypertension. Nat Rev Immunol 19**:** 517-532.

Ebrahimian T, Sairam MR, Schiffrin EL, & Touyz RM (2008). Cardiac hypertrophy is associated with altered thioredoxin and ASK-1 signaling in a mouse model of menopause. Am J Physiol Heart Circ Physiol 295**:** H1481-1488.

Guzik TJ, Hoch NE, Brown KA, McCann LA, Rahman A, Dikalov S, Goronzy J, Weyand C, & Harrison DG (2007). Role of the T cell in the genesis of angiotensin II induced hypertension and vascular dysfunction. The Journal of experimental medicine 204**:** 2449-2460.

Haque NS, Fallon JT, Pan JJ, Taubman MB, & Harpel PC (2004). Chemokine receptor-8 (CCR8) mediates human vascular smooth muscle cell chemotaxis and metalloproteinase-2 secretion. Blood 103**:** 1296-1304.

Islam SA, Chang DS, Colvin RA, Byrne MH, McCully ML, Moser B, Lira SA, Charo IF, & Luster AD (2011). Mouse CCL8, a CCR8 agonist, promotes atopic dermatitis by recruiting IL-5+ TH2 cells. Nat Immunol 12**:** 167-177.

Islam SA, Ling MF, Leung J, Shreffler WG, & Luster AD (2013). Identification of human CCR8 as a CCL18 receptor. J Exp Med 210**:** 1889-1898.

Ji H, Zheng W, Li X, Liu J, Wu X, Zhang MA, Umans JG, Hay M, Speth RC, Dunn SE, & Sandberg K (2014). Sex-specific T-cell regulation of angiotensin II-dependent hypertension. Hypertension 64**:** 573-582.

Jiang J, Zheng JP, Li Y, Gan Z, Jiang Y, Huang D, Li H, Liu Z, & Ke Y (2016). Differential contribution of endothelium-derived relaxing factors to vascular reactivity in conduit and resistance arteries from normotensive and hypertensive rats. Clin Exp Hypertens 38**:** 393-398.

Kessler EL, Rivaud MR, Vos MA, & van Veen TAB (2019). Sex-specific influence on cardiac structural remodeling and therapy in cardiovascular disease. Biol Sex Differ 10**:** 7-7.

Kirchhoff F, Krebs C, Abdulhag UN, Meyer-Schwesinger C, Maas R, Helmchen U, Hilgers KF, Wolf G, Stahl RA, & Wenzel U (2008). Rapid development of severe end-organ damage in C57BL/6 mice by combining DOCA salt and angiotensin II. Kidney Int 73**:** 643-650.

Ko FN, Chang YL, Chen CM, & Teng CM (1996). (+/-)-Govadine and (+/-)-THP, two tetrahydroprotoberberine alkaloids, as selective alpha 1-adrenoceptor antagonists in vascular smooth muscle cells. J Pharm Pharmacol 48**:** 629-634.

Kraaijeveld AO, de Jager SC, de Jager WJ, Prakken BJ, McColl SR, Haspels I, Putter H, van Berkel TJ, Nagelkerken L, Jukema JW, & Biessen EA (2007). CC chemokine ligand-5 (CCL5/RANTES) and CC chemokine ligand-18 (CCL18/PARC) are specific markers of refractory unstable angina pectoris and are transiently raised during severe ischemic symptoms. Circulation 116**:** 1931-1941.

Laursen JB, Rajagopalan S, Galis Z, Tarpey M, Freeman BA, & Harrison DG (1997). Role of superoxide in angiotensin II-induced but not catecholamine-induced hypertension. Circulation 95**:** 588-593.

Lewis C (2017). Investigating the roles of distinct macrophage phenotypes in cardiovascular disease. PhD thesis: Monash University, Melbourne.

Li HL, She ZG, Li TB, Wang AB, Yang Q, Wei YS, Wang YG, & Liu DP (2007). Overexpression of myofibrillogenesis regulator-1 aggravates cardiac hypertrophy induced by angiotensin II in mice. Hypertension 49**:** 1399-1408.

Lu X, & Kassab GS (2011). Assessment of endothelial function of large, medium, and small vessels: a unified myograph. American journal of physiology Heart and circulatory physiology 300**:** H94-H100.

Luzina IG, Highsmith K, Pochetuhen K, Nacu N, Rao JN, & Atamas SP (2006). PKCα Mediates CCL18-Stimulated Collagen Production in Pulmonary Fibroblasts. Am J Respir Cell Mol Biol 35**:** 298-305.

Madhur MS, Lob HE, McCann LA, Iwakura Y, Blinder Y, Guzik TJ, & Harrison DG (2010). Interleukin 17 promotes angiotensin II-induced hypertension and vascular dysfunction. Hypertension 55**:** 500-507.

Moore JP, Vinh A, Tuck KL, Sakkal S, Krishnan SM, Chan CT, Lieu M, Samuel CS, Diep H, Kemp-Harper BK, Tare M, Ricardo SD, Guzik TJ, Sobey CG, & Drummond GR (2015). M2 macrophage accumulation in the aortic wall during angiotensin ii infusion in mice is associated with fibrosis, elastin loss, and elevated blood pressure. Am J Physiol Heart Circ Physiol 309**:** H906-H917.

Mui RK, Fernandes RN, Garver HG, Van Rooijen N, & Galligan JJ (2018). Macrophage-dependent impairment of α(2)-adrenergic autoreceptor inhibition of Ca(2+) channels in sympathetic neurons from DOCA-salt but not high-fat diet-induced hypertensive rats. American journal of physiology Heart and circulatory physiology 314**:** H863-H877.

Murdoch CE, Alom-Ruiz SP, Wang M, Zhang M, Walker S, Yu B, Brewer A, & Shah AM (2011). Role of endothelial Nox2 NADPH oxidase in angiotensin II-induced hypertension and vasomotor dysfunction. Basic Res Cardiol 106**:** 527-538.

Nosalski R, Siedlinski M, Denby L, McGinnigle E, Nowak M, Cat AND, Medina-Ruiz L, Cantini M, Skiba D, Wilk G, Osmenda G, Rodor J, Salmeron-Sanchez M, Graham G, Maffia P, Graham D, Baker AH, & Guzik TJ (2020). T-Cell-Derived miRNA-214 Mediates Perivascular Fibrosis in Hypertension. Circ Res 126**:** 988-1003.

Oparil S, Zaman MA, & Calhoun DA (2003). Pathogenesis of Hypertension. Ann Intern Med 139**:** 761-776.

Paik Y-H, Kim J, Aoyama T, De Minicis S, Bataller R, & Brenner DA (2014). Role of NADPH oxidases in liver fibrosis. Antioxid Redox Signal 20**:** 2854-2872.

Pochetuhen K, Luzina IG, Lockatell V, Choi J, Todd NW, & Atamas SP (2007). Complex regulation of pulmonary inflammation and fibrosis by CCL18. Am J Pathol 171**:** 428-437.

Rodríguez JE, Ruiz-Hernández A, Hernández-DíazCouder A, Huang F, Hong E, & Villafaña S (2020). Chronic diabetes and hypertension impair the in vivo functional response to phenylephrine independent of α1-adrenoceptor expression. Eur J Pharmacol 883: 173283.

Ryan Michael J, Didion Sean P, Mathur S, Faraci Frank M, & Sigmund Curt D (2004). Angiotensin II–Induced Vascular Dysfunction Is Mediated by the AT1A Receptor in Mice. Hypertension 43**:** 1074-1079.

Schmittgen TD, & Livak KJ (2008). Analyzing real-time PCR data by the comparative CT method. Nat Protocols 3**:** 1101-1108.

Schraufstatter IU, Zhao M, Khaldoyanidi SK, & Discipio RG (2012). The chemokine CCL18 causes maturation of cultured monocytes to macrophages in the M2 spectrum. Immunology 135**:** 287-298.

Schutyser E, Richmond A, & Van Damme J (2005). Involvement of CC chemokine ligand 18 (CCL18) in normal and pathological processes. J Leukoc Biol 78**:** 14-26.

Seto SW, Krishna SM, Yu H, Liu D, Khosla S, & Golledge J (2013). Impaired acetylcholine-induced endothelium-dependent aortic relaxation by caveolin-1 in angiotensin II-infused apolipoprotein-E (ApoE-/-) knockout mice. PLoS One 8**:** e58481-e58481.

Sunano S, Li-Bo Z, Matsuda K, Sekiguchi F, Watanabe H, & Shimamura K (1996). Endothelium-dependent relaxation by alpha 2-adrenoceptor agonists in spontaneously hypertensive rat aorta. J Cardiovasc Pharmacol 27**:** 733-739.

Tanaka Y, Funabiki M, Michikawa H, & Koike K (2006). Effects of aging on alpha1-adrenoceptor mechanisms in the isolated mouse aortic preparation. J Smooth Muscle Res 42**:** 131-138.

Tatchum-Talom R, Eyster KM, & Martin DS (2005). Sexual dimorphism in angiotensin II-induced hypertension and vascular alterations. Can J Physiol Pharmacol 83**:** 413-422.

Tsai MH, & Jiang MJ (2010). Reactive oxygen species are involved in regulating alpha1-adrenoceptor-activated vascular smooth muscle contraction. J Biomed Sci 17**:** 67.

Versteylen MO, Manca M, Joosen IA, Schmidt DE, Das M, Hofstra L, Crijns HJ, Biessen EA, & Kietselaer BL (2016). CC chemokine ligands in patients presenting with stable chest pain: association with atherosclerosis and future cardiovascular events. Netherlands heart journal : monthly journal of the Netherlands Society of Cardiology and the Netherlands Heart Foundation 24**:** 722-729.

Williams HC, Ma J, Weiss D, Lassègue B, Sutliff RL, & San Martín A (2019). The cofilin phosphatase slingshot homolog 1 restrains angiotensin II-induced vascular hypertrophy and fibrosis in vivo. Laboratory investigation; a journal of technical methods and pathology 99**:** 399-410.

Wu J, Montaniel KR, Saleh MA, Xiao L, Chen W, Owens GK, Humphrey JD, Majesky MW, Paik DT, Hatzopoulos AK, Madhur MS, & Harrison DG (2016). Origin of Matrix-Producing Cells That Contribute to Aortic Fibrosis in Hypertension. Hypertension 67**:** 461-468.

Wynn TA, & Ramalingam TR (2012). Mechanisms of fibrosis: therapeutic translation for fibrotic disease. Nat Med 18**:** 1028-1040.

Xue B, Pamidimukkala J, & Hay M (2005). Sex differences in the development of angiotensin II-induced hypertension in conscious mice. Am J Physiol Heart Circ Physiol 288**:** H2177-2184.

Yamamoto Y, & Koike K (2001). alpha(1)-Adrenoceptor subtypes in the mouse mesenteric artery and abdominal aorta. Br J Pharmacol 134**:** 1045-1054.

Zhao W, Chen SS, Chen Y, Ahokas RA, & Sun Y (2008). Kidney fibrosis in hypertensive rats: role of oxidative stress. Am J Nephrol 28**:** 548-554.

Zhu M (2016). CCL18 as a mediator of the pro-fibrotic actions of M2 macrophages in the vessel wall during hypertension. Honours thesis: Monash University, Melbourne.

4.9 Supplementary Figures

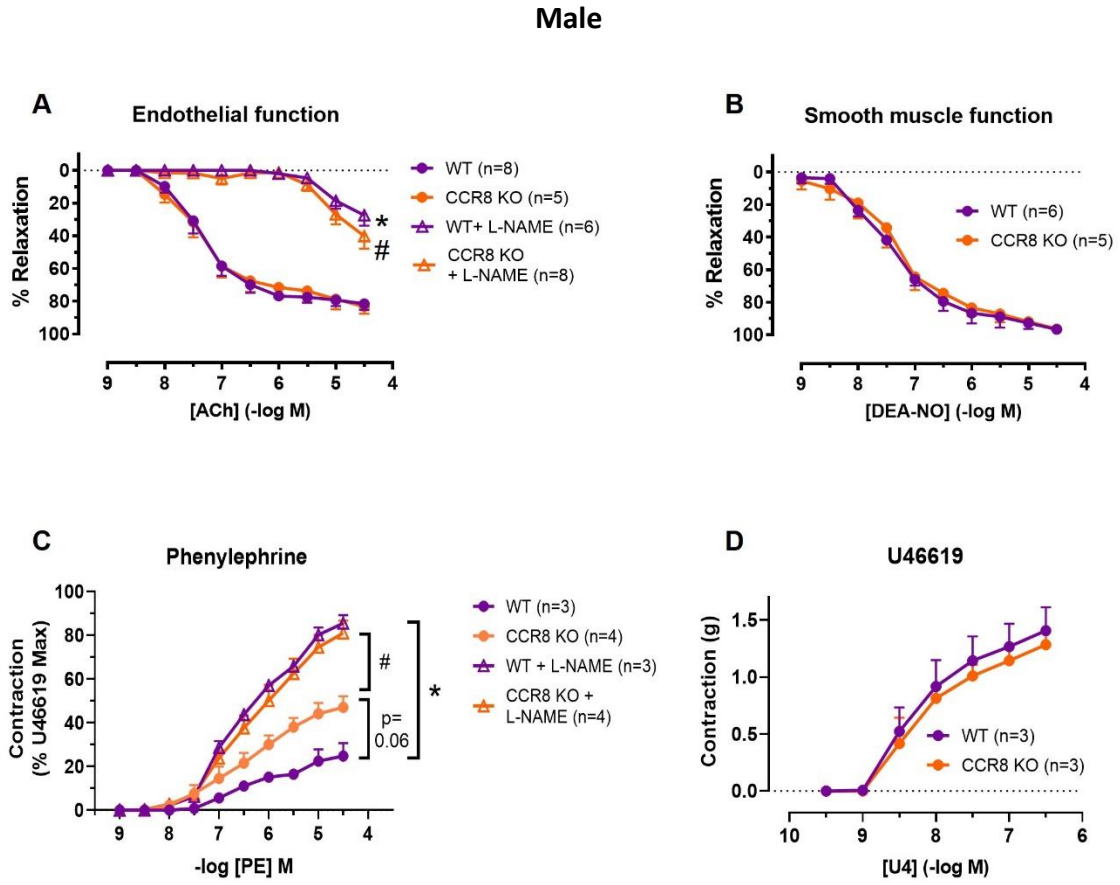

Supplementary Figure 1. Effect of genetic deletion of CCR8 on the function of the abdominal aorta in naïve male mice. Cumulative concentration-response curves to acetylcholine (ACh) (**A**), DEA-NO (**B**), phenylephrine (PE) (**C**), and U46619 (**D**) in isolated abdominal aortae from wildtype (WT) and CCR8 knockout (KO) mice. Responses to ACh and PE were obtained in the absence and presence of L-NAME (100 µM).

Data expressed as % reversal of pre-contraction to U46619 (A-B), % of the maximal U46619 contraction (C), or change in gram tension (D). Data presented as mean ± SEM, n= number of animals. *p<0.05 vs. WT, # p<0.05 vs. CCR8 KO (maximal contraction to PE or maximal relaxation to ACh), 1-way ANOVA, Tukey's post hoc test.

Female

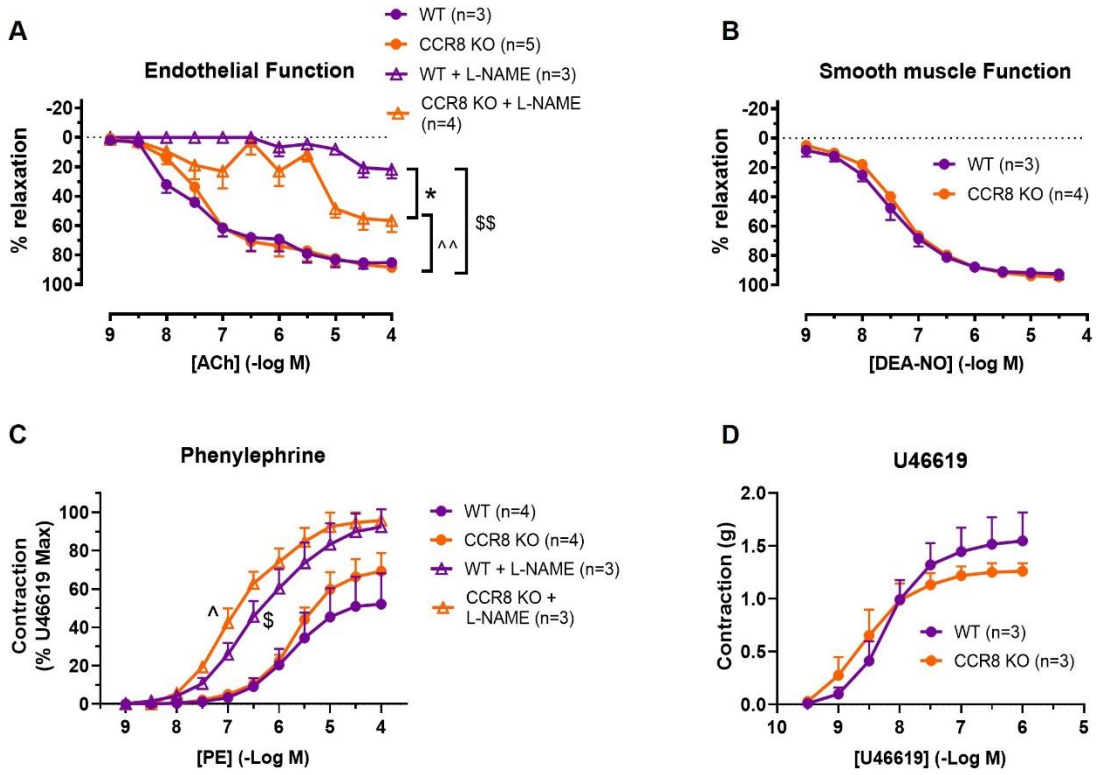

Supplementary Figure 2. Effect of genetic deletion of CCR8 on the function of abdominal aorta in naïve female mice. Cumulative concentration-response curves to acetylcholine (ACh) (**A**), DEA-NO (**B**), phenylephrine (PE) (**C**), and U46619 (**D**) in isolated abdominal aortae from wildtype (WT) and CCR8 knockout (KO) mice. Responses to ACh and PE were obtained in the absence and presence of L-NAME (100 µM).

Data expressed as % reversal of pre-contraction to U46619 (A-B), % of the maximal U46619 contraction (C), or change in gram tension (D). Data presented as mean ± SEM, n= number of animals. *p<0.05 vs. WT + L-NAME, $$ p<0.01 vs. WT, ^^ p<0.01 vs. CCR8 KO (maximal relaxation to ACh); $ p<0.05 vs. WT, ^ p<0.05 vs. CCR8 KO (pEC_{50} of contraction to PE); 1-way ANOVA, Tukey's post hoc test.

Male

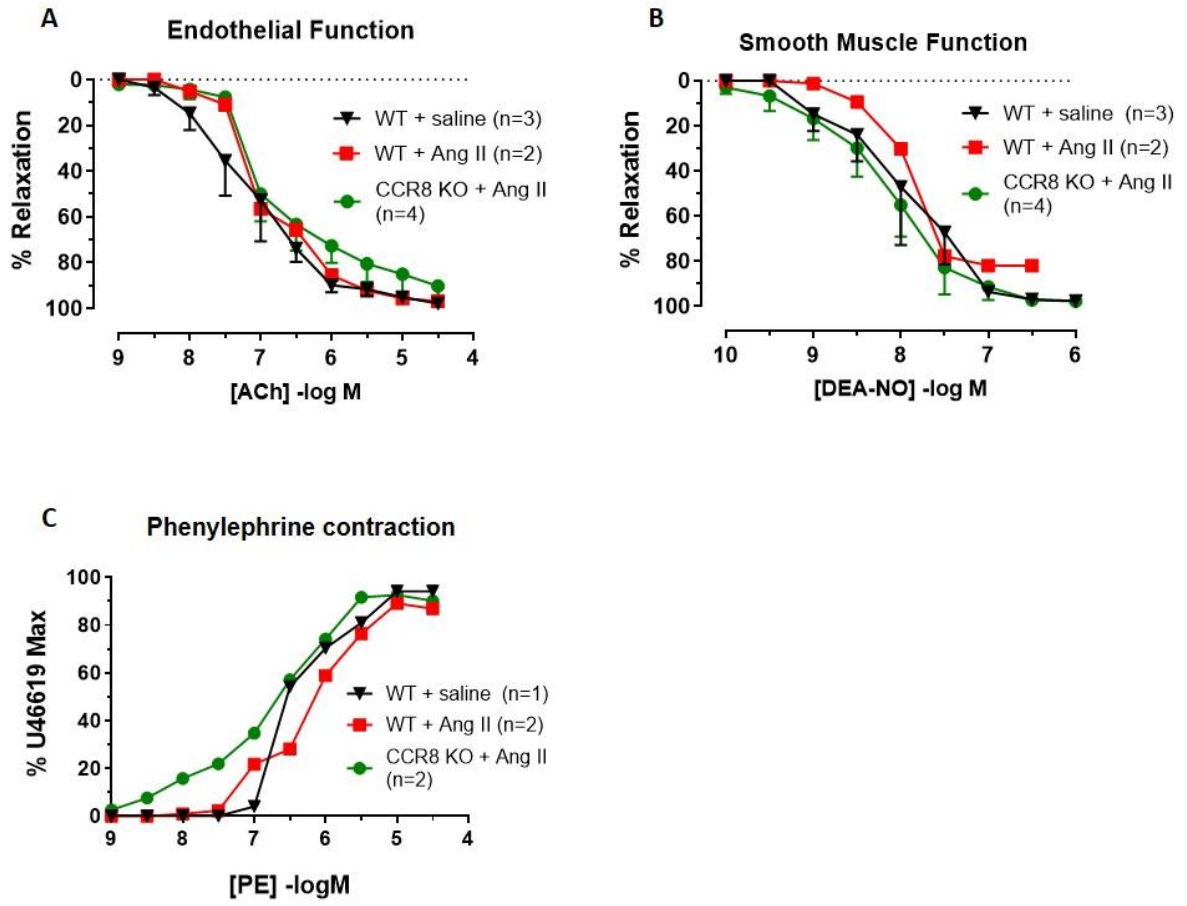

Supplementary Figure 3. Effect of 14-day angiotensin II infusion on the function of small mesenteric arteries from male WT and CCR8 KO mice. Cumulative concentration response curves to acetylcholine (ACh) (**A**), DEA-NO (**B**) and phenylephrine (PE) (**C**) in isolated small mesenteric arteries from wildtype (WT) and CCR8 knockout (KO) mice treated with either saline or Ang II (0.7 mg/kg/d) for 14 days.

Data expressed as % reversal of pre-contraction to U46619 (A-B) or % of the maximal U46619 contraction (C). Data presented as mean ± SEM (when n ≥3) or mean (when n<3), where n = number of animals. 1-way ANOVA, Tukey's post hoc test.

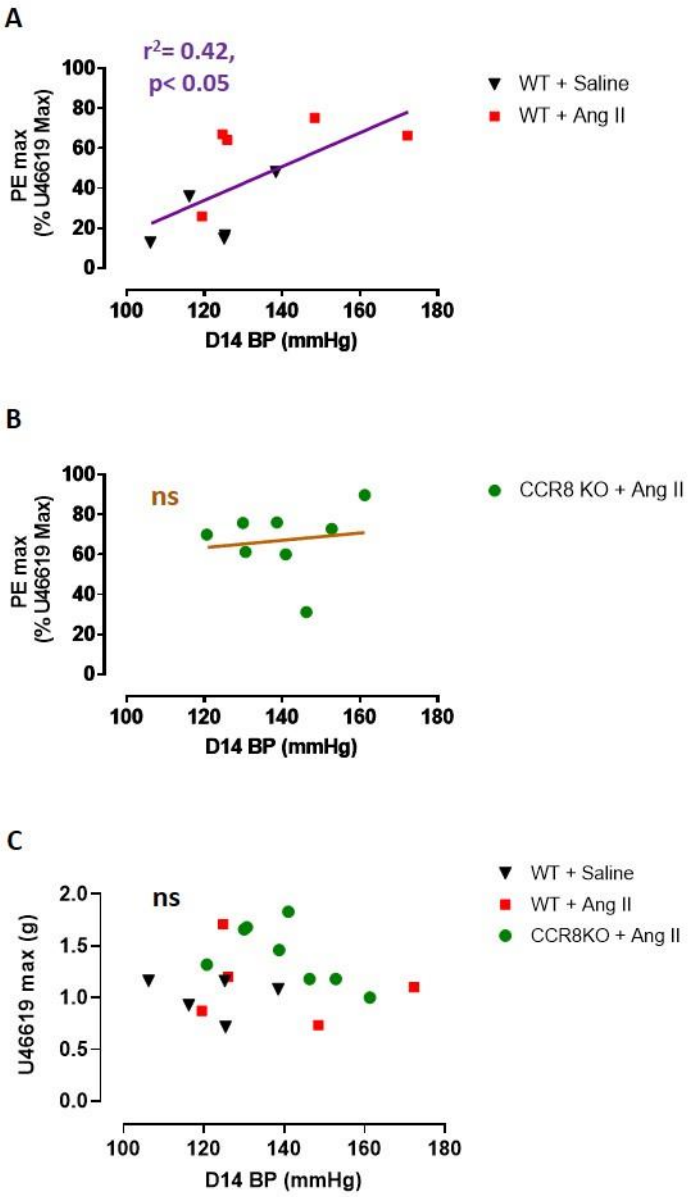

Supplementary Figure 4. Correlation of maximal phenylephrine contraction (PE max) with final day systolic BP (D14 BP) of male mice. Wildtype (WT; **A**) and CCR8 knockout (CCR8 KO; **B**) mice were treated with saline or Ang II (0.7 mg/kg/d) for 14 days, followed by the isolation of abdominal aortae for wire myography. (**C**) correlation of the maximal U46619 contraction (U4 max) with D14 BP.

PE max data were expressed as % of U4 max. Data presented as individual points, (A-B) n= 5-8, (C) n= 18. Linear regression analysis, ns = no statistical significance.

Chapter 5

Genetic or pharmacological targeting of CCR8 does not confer protection in an angiotensin II (28-day)-induced hypertension in mice

Genetic or pharmacological targeting of CCR8 does not confer protection in angiotensin II (28-day)-induced hypertension in mice

Authors:

Mingyu Zhu[1], Caitlin Lewis[1], Téa Christmas[1], Dorota Ferens[1], Yeong Hann Ling[1], Herman Lim[2], Antony Vinh[3], Alexander R. Pinto[4], Martin J. Stone[2], Grant R. Drummond[2], Barbara K. Kemp-Harper[1].

Affiliations:

[1] Biomedicine Discovery Institute, Department of Pharmacology, Monash University, Clayton, VIC, Australia.

[2] Biomedicine Discovery Institute, Department of Biochemistry and Molecular Biology, Monash University, Clayton, VIC, Australia.

[3] Department of Physiology, Anatomy & Microbiology, La Trobe University, Bundoora, VIC, Australia.

[4] Baker Heart and Diabetes Research Institute, Melbourne, VIC, Australia.

5.1 COVID-19 impact statement

Our CCR8 knockout (KO) mouse breeding colony was reduced in size in response to the first COVID-19 pandemic lockdown in Melbourne. Together with the COVID-19 relevant working restrictions, the ability to conduct chronic experiments on CCR8 KO mice was severely limited.

In Chapter 5, a small proportion of datasets involving the CCR8 KO mice require a larger number of animals than others, and hence have insufficient statistical power. These include histological studies (limited aortic samples for histological analysis due to use for myography and flow cytometric studies); and flow cytometry (due to the nature of this experimental approach which is associated with high data variability). The cohort of mice used for studying the effects of R243 (CCR8 antagonist) is also relatively small in size (n= 4-6), making it difficult to interpret the organ weight and vascular contraction data.

5.2 Abstract

Introduction: Hypertension is associated with end-organ damage in the vasculature, heart and kidneys. M2 macrophages contribute to vascular fibrosis and stiffening in hypertension, and such function may be mediated by the chemokine, C-C motif chemokine ligand 18 (CCL18). CCL18 activates its recently identified cognate receptor, C-C motif chemokine receptor 8 (CCR8). However, the role of the CCL18-CCR8 axis in chronic hypertension is yet to be investigated. This study aimed to explore the effects of genetic and pharmacological targeting of CCR8 on hypertension and its associated end-organ damage in mice.

Methods: CCR8 knockout (CCR8 KO; C57BL/6J background) male mice, and their wildtype (WT) controls were treated with angiotensin II (Ang II; 0.7 mg/kg/d, 28d, s.c) or saline. From Day 14, a separate cohort of WT mice were additionally treated with R243 (CCR8 antagonist, 1.1 mg/kg/d, s.c) or vehicle (DMSO with 20% HBC, s.c). Blood pressure was measured via tail cuff plethysmography, organs (including heart and kidneys) were weighed, and vascular function assessed by wire myography. The expression of mouse CCL8 (functional analogue of human CCL18) in plasma and aortae was measured via ELISA and single cell RNA-sequencing, respectively. Aortic structure, elastin regulation and adventitial fibrosis were assessed by staining with Haematoxylin and Eosin, Verhoeff–Van Gieson and picrosirius red, respectively. Leukocyte infiltration was measured in the aorta, kidney and spleen via flow cytometry. Bioluminescence Resonance Energy Transfer (BRET) assays were performed in CHO cells to confirm whether human CCL18 and mouse CCL8 signal via CCR8.

Results: Neither genetic deletion of CCR8 nor treatment with R243 attenuated the Ang II-induced increase in systolic blood pressure or cardiac hypertrophy. Mouse CCL8 was co-localised with M2 macrophages, whilst plasma levels of mouse CCL8 remained unchanged in hypertensive WT and CCR8 KO mice. The augmented contraction to phenylephrine in the aorta from hypertensive mice, was maintained in angiotensin II-treated CCR8 KO mice and following treatment with R243. By contrast, endothelium-dependent relaxation to ACh was enhanced in the aorta of hypertensive mice treated with R243. The hypertension associated vascular remodelling, elastin dysregulation and collagen deposition was not attenuated following genetic deletion of CCR8. In mouse kidneys, genetic deletion of CCR8 may limit CD4+

and CD8+ T cell infiltration, but this effect is independent of hypertension. Lastly, neither mouse CCL8 nor human CCL18 were found to activate CCR8 in CHO cells.

Discussion: Neither genetic deletion, nor pharmacological targeting, of CCR8 provides protection from the development of hypertension and the associated end-organ damage, in the 28d Ang II infusion model in mice. Although vascular expression of mouse CCL8 is elevated in hypertension, its target remains to be determined as both human CCL18 and mouse CCL8 were unable to activate CCR8. In conclusion, CCR8 signalling may not play a role in the development of hypertension and the contribution of CCL18, and its cognate receptor, to the pathophysiology of hypertension remains to be elucidated.

5.3 Introduction

Chronic hypertension is associated with end-organ damage, which includes aortic stiffening, heart failure and kidney disease (Diez, 2007; Oparil et al., 2003; Zhao et al., 2008). It has been hypothesized that such damage can be caused by systemic inflammation and the infiltration of leukocytes into target organs (Drummond et al., 2019). In particular, the M2 subtype of macrophages have been implicated in hypertensive aortic (Moore et al., 2015), myocardial (Falkenham et al., 2015) and kidney fibrosis and related dysfunction (Guiteras et al., 2016). Indeed, M2 macrophages accumulate in the hypertensive vasculature of Ang II treated mice, and the inhibition of macrophage infiltration has been reported to limit BP elevation and reverse hypertension-associated vascular fibrosis (Moore et al., 2015). Whilst M2 macrophages express factors such as TGF-β1 (Liu et al., 2018), which promote remodelling of the extracellular matrix (Liu et al., 2018), we have evidence that human, M2 macrophages express much higher levels of the pro-fibrotic chemokine, C-C motif chemokine ligand 18 (CCL18) (300-500-fold higher levels than TGF-β1) (Lewis, 2017).

CCL18 is released by, and serves as a marker of, M2 macrophages (Schutyser et al., 2005; Vrančić et al., 2012). CCL18 leads to chemotaxis of leukocytes, such as lymphocytes and immature dendritic cells, into the sites of inflammation (Schutyser et al., 2005). In addition, CCL18 has been found to be pro-fibrotic in the lungs (Atamas et al., 2003). Importantly, CCL18 has also been implicated in several cardiovascular diseases, such as acute coronary syndrome, angina, atherosclerosis and aneurysm (de Jager et al., 2012; Kraaijeveld et al., 2007; Versteylen et al., 2016). In the context of hypertension, we have shown that plasma levels of CCL18 are elevated in patients with resistant hypertension and have provided evidence in support of its pro-fibrotic effects in the vasculature (**Chapter 3**). As such, CCL18 may serve as a key mediator of the pro-fibrotic actions of M2 macrophages in hypertension.

Recently, CCL18 C-C motif chemokine receptor 8 (CCR8) has been identified by Islam et al. (2013) as a receptor of CCL18. CCL18 is reported to induce calcium mobilisation and chemotaxis of CCR8-expressing human Th2 cells and CCR8-transfected 4DE4 cells (mouse pre-B cell line) (Islam et al., 2013). CCR8 is suggested to be responsible for the chemotaxis of not only Th2 cells but also other inflammatory cells, such as monocytes/ macrophages, dendritic cells and eosinophils (Connolly et al., 2012; Haque et al., 2004). CCR8 is also expressed on

cardiovascular relevant cells types, including vascular smooth muscle cells (VSMCs) and human umbilical vein endothelial cells (HUVECs) (Haque et al., 2004). As such, M2 macrophage-derived CCL18 may signal via CCR8 to promote hypertension-associated end-organ damage. However, no studies have been published to explore the role of the CCL18-CCR8 axis in hypertension.

CCL18 is unique in that it is only found in primates. Whilst the absence of CCL18 in rodents raises challenges when studying the role of CCL18-CCR8 axis in animal models of hypertension, Islam et al. (2013) has suggested that mouse CCL8 (mCCL8) is a functional analogue of human CCL18 (hCCL18). Thus, both chemokines promote fibrosis (Atamas et al., 2003; Lim et al., 2017), and they are induced in human M2-like macrophages by M2-polarising cytokines (Islam et al., 2013). mCCL8 has also been reported to be an agonist of mouse CCR8 (mCCR8) and human CCR8 (hCCR8) (Islam et al., 2011). These lines of evidence suggest that the mCCL8-CCR8 axis may be targeted genetically or pharmacologically in mice, in order to investigate the role of hCCL18-CCR8 axis in hypertension.

Based on the above-mentioned evidence, it was hypothesized that targeting CCR8 limits the development of hypertension and the associated end-organ damage. In **Chapter 4**, the 14-day Ang II model of hypertension was found to be insufficient for establishing end-organ damage in male mice. Therefore, this chapter has utilised a 28-day Ang II infusion model of hypertension, and CCR8 is targeted by either global genetic deletion or a more clinically relevant pharmacological antagonist, R423. Bioluminescence resonance energy transfer (BRET) assays were also performed in CHO cells to confirm whether CCR8 is activated by mCCL8 and hCCL18.

5.4 Methods

Animals and genotyping

CCR8 knockout (CCR8 KO) and wildtype (WT) male mice were used in this study (all 10-12 weeks old, with a C57BL/6J background). CCR8 KO mice were generated via CRISPR/Cas9, by the Australian Phenomics Network, Monash University. Mice were bred and housed at the Animal Research Laboratories or Pharmacology Mouse Room (Monash University, Clayton, Australia), on a 12-hour light-dark cycle and provided with free access to chow diet and drinking water. A REDExtract-N-Amp™ Tissue PCR Kit (Sigma-Aldrich, Germany) was used to identify the genotype of each mouse, as per manufacturer's instructions (detailed in **Chapter 2, Section 2.2**). In this procedure, DNA was extracted from the tip of each mouse tail, and 100 ng DNA from each mouse was amplified with custom made primers for CCR8 (Sigma-Aldrich, Germany), followed by the loading of DNA into agarose gels for electrophoresis. All procedures were approved by the Monash Animal Research Platform Ethics Committee (Ethics Number: MARP/2017/104).

28-day model of hypertension and R243 treatment protocol

WT and CCR8 KO mice were randomly assigned to a saline or angiotensin II (Ang II, 0.7 mg/kg/d, GL Biochem, China) infusion group, with treatments administered via osmotic minipumps (Model 2004; Alzet, USA) for 28 days. A separate cohort of WT mice received either saline or Ang II (0.7 mg/kg/d) for 28 days via osmotic minipump (Model 2004), and after 14 days, saline-treated mice received vehicle (2:1 warm mixture of 30% hydroxypropyl-β-cyclodextrin: 100% DMSO) and Ang II mice received either vehicle or R243 (CCR8 antagonist, 1.1 mg/kg/d; Glixx Laboratories, USA), via osmotic minipump (Model 2002; Alzet, USA), for a subsequent 14 days.

All mice were under isoflurane anaesthesia (0.4 L/min, 2% inhaled with oxygen) during minipump implantation, where a lateral incision of ≈10 mm was made through the skin at the neck. A subcutaneous pouch was created through this incision, in which minipumps were inserted, followed by the closing of incision with monofilament sutures. After the surgery, mice were allowed to recover and then returned to home cages.

Tail cuff plethysmography

Systolic blood pressure (BP) was measured using tail cuff plethysmography (MC4000 multi-channel blood pressure analysis system; Hatteras Instruments, USA). After mice were acclimatised to the BP monitoring equipment, BP was recorded 3 days before surgeries, 1 day before surgeries, and just prior to surgeries (Day 0) to form an average baseline BP. During the 28-day treatment period, BP was measured on Days 3, 7, 10, 14, 17, 21, 24, 28. BP was recorded for 25-30 measurement cycles on each day of measurement, where mice were placed in restraints on a heated platform (40°C), with an inflatable cuff around the base of each tail. Systolic BP was recorded as the cuff inflation pressure required to fully occlude blood flow in the tail. At the end of the treatment period, mice were killed via overdose of CO2, with the plasma taken, organs (aorta, kidneys, heart, spleen, liver and lungs) of each mouse removed and weighed before being processed for end point measures.

Wire myography

To assess vascular function, abdominal aortae were isolated from CCR8 KO and WT mice, the fat and connective tissues removed and aortae cut into 2 mm sections. Aortic sections were mounted in a small vessel myograph (Danish Myo Technology A/S, Denmark) on pin mounts (200 µm diameter) and changes in isometric tension recorded (LabChart 8, ADI Instruments, New Zealand). Vessels were kept at a resting tension of 5mN at 37 °C in Kreb's solution (in mM: 118 NaCl, 4.5 KCl, 0.5 $MgSO_4$, 1 KH_2PO_4, 25 $NaHCO_3$, 11.1 glucose, 2.5 $CaCl_2$; pH 7.4), and bubbled with carbogen (5% CO_2, 95% oxygen). Arteries were contracted maximally with the thromboxane A_2 mimetic, U46619 (0.3 µM). Once the contraction had reached a plateau, vessels were washed, tension allowed to return to baseline and then arteries were rechallenged with U46619 (0.3 µM; F_{max}).

Endothelium-dependent and -independent vasorelaxation responses were assessed by constructing cumulative concentration-response (CR) curves to acetylcholine (ACh; 1 nM- 30 µM) and the NO donor, diethylamine NONOate (DEA-NO; 0.3 nM- 30 µM), respectively in aortae pre-contracted to ≈65 % F_{max} with titrated concentrations of U46619. In separate aortic

sections, cumulative CR curves to phenylephrine (PE; 1 nM-30 µM), were constructed. Arteries were then washed with Krebs', pre-contracted to ≈20-30 % F_{max} with U46619 prior to the addition of N(ω)-nitro-L-arginine methyl ester (L-NAME, 100 µM) to assess endogenous NO bioavailability.

Flow cytometry

Flow cytometry was performed to characterise the effects of genetic deletion of CCR8 on infiltration of inflammatory cells into target organs. Following euthanasia, mice were perfused through the left ventricle with phosphate-buffered saline (PBS) containing 0.2% Clexane (400 IU/ml; Sanofi Aventis, France). The thoracic aorta (with perivascular fat intact), left kidney (one half used), and spleen were then excised for flow cytometry. These samples were mechanically disrupted using scissors, where aortae and kidneys were further digested via the addition of 1 ml of digestion buffer for 45 minutes at 37 °C. The digestion buffer contained collagenase I-S (450 U/ml), collagenase XI (125 U/ml) and hyaluronidase (450 U/ml), which were dissolved in PBS containing calcium and magnesium (Sigma, USA).

Processed samples were passed through 70 µm filters (BD Bioscience, USA), followed by centrifugation (all centrifugation for flow cytometry was at 4 °C, 1500 rpm for 5 minutes unless otherwise specified). Cell pellets were resuspended in FACS buffer (PBS containing 1% bovine serum albumin) for aortae, 30% Percoll (GE Healthcare Life Science, UK) for kidneys, or Red Blood Cell Lysis Buffer (5-minute incubation on ice; BD Biosciences, USA) for spleens. Kidney samples were then under-laid with 70% Percoll and centrifuged at 25 °C, 2500 rpm for 25 minutes. The mononuclear cell layer between the Percoll gradients were collected, centrifuged and re-suspended in FACS buffer. For spleen samples, lysis buffer was neutralised with PBS after the incubation, followed by centrifugation and re-suspension in FACS buffer.

Single cell suspensions in FACS buffer were stained using an antibody cocktail (20 minutes on ice). The cocktail included AF-700 anti-CD45, BV 605 anti-CD11b, PE-Cy7 anti-F4/80, PE anti-CD206, APC anti-CD3, FITC anti-CD4, BV785 anti-CD8, all were of rat anti-mouse isotype (anti-CD11b from Invitrogen, USA; anti-CD3 from eBioscience, USA; others from BioLegend, USA). Each antibody was also individually incubated with UltraComp eBeads® (eBioscience, USA) for single-colour compensation.

Prior to sample running, CountBright counting beads (Invitrogen, USA) were added for data normalisation, and 7-AAD (BioLegend, USA) was used as a viability stain. Data from stained samples were obtained by a Fortessa X-20 instrument controlled by the FlowDiva software (BD Biosciences, USA), and processed using FlowJo software v10 (FlowJo, USA; relevant gating strategy as described in **Chapter 2, Section 2.6**).

Enzyme-linked immunosorbent assay (ELISA)

CCL8 levels from mouse plasma samples were measured using a CCL8 ELISA kit (Mouse CCL8/MCP-2 DuoSet ELISA; R&D Systems, USA) and an ancillary kit (DuoSet Ancillary Reagent Kit 2; R&D Systems, USA). ELISA was performed as per manufacturer's instructions, and plasma sample diluent was supplemented with 30% fetal bovine serum (FBS; Life technologies, USA) according to manufacturer's recommendation. Detailed procedures are described in **General Methods** (**Section 2.11**). CCL8 concentration was calculated by constructing a fitted standard curve of optical density against the concentrations of serially diluted CCL8.

Histological studies

A distal section (≈4 mm) of thoracic aorta, a transverse section of the heart (representing 1/3 of the heart taken near the basal region), and half a kidney were fixed in 10 % neutral buffered formalin for 3 days. Fixed tissues were then embedded in paraffin, and transverse sections of kidney and heart (4 µm) and cross sections of aortae (4-5 µm) were cut. 4 µm aortic sections were stained using Verhoeff-Van Gieson (VVG), and 5 µm sections were stained with hematoxylin and eosin (H&E) or Picrosirius red. Heart sections were stained with H&E and Picrosirius red, and kidney sections underwent Masson's Trichrome staining. The embedding, cutting and staining procedures were performed by Monash Histology Services (Monash University, Clayton, Australia).

VVG and H&E stains were performed to assess the structure of relevant tissues, whilst Picrosirius red and Masson's Trichrome were used to assess collagen deposition. The above-mentioned stains were performed as per protocols developed by Monash Histology Services (Monash University, Clayton, Australia) (**Appendices 1-3**). Aortic Picrosirius red slides were

imaged at x10 magnification using both bright-field and polarised microscopy (Olympus BX51, Olympus Life Science, Australia). Images for all other stains were captured at up to x40 magnification by a slide scanner (Aperio Scanscope AT Turbo, Leica Biosystems, Germany). Each section of the above-mentioned staining was analysed with 6-8 fields of view per animal (assessment of renal/ cardiac fibrosis), or as a whole with data averaged from 3 sections per animal averaged (all other measures).

Single-cell RNA sequencing (scRNA-Seq)

ScRNA-Seq and relevant analysis were performed by Dr. Antony Vinh, Prof. Grant Drummond and Dr. Alexander Pinto at La Trobe University, using the aortae of a cohort of WT saline- or Ang II-treated mice, as described by McLellan et al. (2020). In brief, metabolically active nucleated aortic cells were isolated by Fluorescence-Activated Cell Sorting (FACS) to form a single cell preparation. This preparation was processed by a Chromium controller with the Chromium Single Cell 3' v2 reagent kit (10X Genomics, USA), and then sequenced using HiSeq 4000 (Illumina, USA).

Bioluminescence resonance energy transfer (BRET) assays

BRET assays were performed by Dr. Herman Lim (Department of Biochemistry, Monash University). Briefly, Flp-In Chinese hamster ovary (CHO) cells were transfected by human CCR8 (hCCR8) or mouse CCR8 (mCCR8). CHO cells were then stimulated with human- or mouse-CCL1 (hCC1/ mCCL1; established CCR8 agonists), or hCC18/ mCCL8 (chemokines of interest). G-protein activation was assessed by measuring activation of different G-protein subunits: $G\alpha_{i2}$+ $G\beta_1$ tagged by $venus^{156-229}$, $G\gamma_2$ tagged by $venus^{1-155}$, GRKct tagged by Rluc, with CCR8 tagged by myc. cAMP inhibition assay was performed using 10μM forskolin, where CCR8 was tagged by myc. β-arrestin2 recruitment was measured with CCR8 tagged by Rluc and β-arrestin tagged by YFP.

Statistical analysis

All data were presented as mean ± standard error of the mean (SEM). Organ weights were expressed as % of body weight. Vasorelaxation responses to ACh or DEA-NO were expressed as % reversal of pre-contraction to U46619 (R_{max}), and vasoconstriction responses to PE or L-NAME were expressed as % of the maximum contraction to U46619 (F_{max}). Quantification of histological staining was performed in a blinded manner. Elastin dysregulation was assessed using a scoring system, with a score of 1= no dysregulation, 2=mild dysregulation, 3= moderate dysregulation, 4= severe dysregulation.

2-way ANOVA (with Tukey's post-hoc test) was used to compare systolic BP or body weight measurements in multiple treatment groups over the 28-day treatment period. scRNA data were analysed by principal component analysis (PCA), using Cell Ranger (version 2.1.1) and R (version 3.4 or 3.6) as described by McLellan et al. (2020). Other data were analysed by 1-way ANOVA with Tukey's post-hoc test. Statistical tests were performed using GraphPad Prism 8 (USA) unless otherwise specified, with $p< 0.05$ considered statistically significant.

5.5 Results

Genetic deletion of CCR8 does not affect systolic BP or organ weights in mice with Ang II (28d)-induced hypertension

In both wildtype (WT) and CCR8 knockout (KO) male mice, systolic BP was elevated to a similar level following 7 days of infusion of Angiotensin II (Ang II; 0.7 mg/kg/d) (WT + Ang II: 141 ± 4 mmHg vs CCR8 KO + Ang II: 139 ± 8 mmHg) (**Figure 1**). The elevation in systolic BP was maintained over the 28-day infusion period such that both hypertensive WT and CCR8 KO mice still had similar systolic BPs at the experimental endpoint (WT + Ang II: 150 ± 3 mmHg vs CCR8 KO + Ang II: 149 ± 5 mmHg) (**Figure 1**).

The starting body weights (BW) of WT and CCR8KO mice did not differ significantly, and all mice gained weight to a similar extent over the 28-day experimental period, independent of treatment or genotype (**Figure 2A**). 28-day Ang II infusion in male mice did not lead to changes in kidney, liver, lung or spleen weights. Cardiac hypertrophy was evident in Ang II-treated mice with a significant increase in ventricular weight: BW ratio (WT + saline: 0.42 ± 0.01 vs WT + Ang II: 0.57 ± 0.03 % BW; $p<0.05$). Genetic deletion of CCR8 did not attenuate the hypertension-associated cardiac hypertrophy (CCR8 KO + Ang II: 0.56 ± 0.02 % BW) (**Figure 2B**).

Ang II-induced hypertension is associated with an increase in vascular expression of macrophage-derived CCL8

CCL8 was detected in the plasma of saline-treated WT mice (841 ± 117 ng/ml), and did not change following the infusion of Ang II (848 ± 83 ng/ml). Similarly, plasma CCL8 did not differ between normotensive or hypertensive WT and CCR8 KO mice (**Figure 3A**). By contrast, single cell RNA (scRNA) sequencing showed an apparent increase in the expression of macrophage derived CCL8 in the hypertensive vasculature (aortae) from WT mice (**Figure 3B**).

Ang II infusion in both WT and CCR8 KO mice was not associated with a change in endothelium-dependent vasorelaxation to acetylcholine (ACh), endothelium-independent vasorelaxation to DEA-NO, or L-NAME induced contraction in isolated aortae (**Figure 4A-4C**).

For relaxation responses, pre-contraction levels with U46619 were well matched between treatment groups (**Table 1**). By contrast, the development of hypertension in WT mice was associated with an increase in the maximum contraction to phenylephrine (PE), (F_{max}: WT + saline, 29 ± 2 % vs WT + Ang II, 61 ± 5 %; $p<0.05$). As compared to normotensive WT mice, genetic deletion of CCR8 per se enhanced the PE response (F_{max} = 50 ± 3 %), an effect which was sustained following Ang II infusion (F_{max} = 60 ± 5 %) (**Figure 4D, Table 1**). The maximum contraction to PE was also positively correlated with Day 28 BP in WT (r^2= 0.24, $p< 0.05$) but not CCR8 KO mice (r^2= 0.14, p= 0.15) (**Supplementary Figure 1B-C**). Maximal aortic contraction to U46619 (F_{max}) did not differ among groups, with no correlation between U46619 maximum and Day 28 BP (**Supplementary Table 1, Supplementary Figure 1C**). Preliminary experiments indicated that contraction to PE was augmented in the presence of L-NAME in both normotensive WT and CCR8 KO mice, however this modulation by L-NAME appeared to be absent in aorta from hypertensive mice (**Supplementary Figure 2**).

<u>Vascular remodelling, elastin dysregulation and collagen deposition in hypertensive aortae are not improved in CCR8 KO mice</u>

Vascular remodelling, elastin structure and adventitial collagen deposition were also assessed using mouse aortae. Following treatment of WT mice with Ang II, the medial area of the aorta was increased by 44% (in $x10^4$ μm^2: 6.2 ± 0.5 vs WT + Saline 3.5 ± 0.4, $p< 0.01$; **Figure 5**). Medial area was also increased by 35% in Ang II treated CCR8 KO mice (in $x10^4$ μm^2: 5.5 ± 0.6 vs CCR8 KO + Saline 3.6 ± 0.3, $p< 0.05$; **Figure 5**). Ang II treatment increased the mean lumen area in both WT (in $x10^4$ μm^2: 9.7 ± 1.8 vs WT + Saline 4 ± 1.1) and CCR8 KO (in $x10^4$ μm^2: 8.5 ± 2.4 vs CCR8 KO + Saline 4.2 ± 1.3) mice, however these differences did not reach statistical significance (**Figure 5**). No significant difference was seen among groups with regard to the media: lumen ratio, and the overall vascular remodelling by Ang II did not differ between WT and CCR8 KO mice (**Figure 5)**.

Elastin dysregulation was not apparent in either saline-treated WT or CCR8 KO mice (score = 1). By contrast, Ang II treatment led to dysregulated elastin in WT mice (score = 2-3, $p<0.05$), with a trend for dysregulation in CCR8 KO mice (score = 1-3, p= 0.057) (**Figure 6**). Using picrosirius red staining, there was a trend for an increase in adventitial collagen content in

the aorta of Ang II-treated (in $x10^4$ μm^2: 5.2 ± 0.9) versus saline-treated WT (in $x10^4$ μm^2: 3.7 ± 0.9) mice. Genetic deletion of CCR8 lead to a significant increase in adventitial collagen content in hypertensive mice as compared to their normotensive controls (in $x10^4$ μm^2: 12 ± 3.6 vs CCR8 KO + Saline 3.1 ± 0.2, $p< 0.01$) (**Figure 7**). Of note, adventitial collagen content did not differ significantly between WT and CCR8 KO hypertensive mice (**Figure 7**).

Ang II infusion does not promote cardiac or renal collagen deposition

In addition to vascular fibrosis, cardiac and renal fibrosis were also assessed by measuring interstitial collagen by Picrosirius red staining (for the heart) or Masson's Trichrome staining (for kidneys). Treatment of WT mice with Ang II did not cause a change in collagen content in the heart (0.5 ± 0.1 %) or kidneys (0.82 ± 0.1 %) as compared to saline treated controls (heart: 0.68 ± 0.1 %; kidney 0.95 ± 0.1 %) (**Figures 8-9**). Similarly, collagen content in the heart and kidneys did not differ between saline- (heart: 0.69 ± 0.1 %; kidney: 0.75 ± 0.1 %) and Ang II-treated CCR8KO mice (heart: 0.72 ± 0.1 %; kidney: 0.85 ± 0.1 %) nor between the WT and CCR8 KO genotypes. (**Figures 8-9**).

Genetic deletion of CCR8 may limit T cell infiltration into the kidneys of saline- and Ang II-treated mice

Leukocyte infiltration into the target organs (aorta, kidney and spleen) was measured via flow cytometry. Kidneys from Ang II-treated WT mice showed no change in the infiltration of total leukocytes (CD45+), total T cells (CD3+) and CD4+ T cells, as compared to normotensive WT mice (**Figure 11**). Genetic deletion of CCR8 in normotensive mice appeared to be associated with a decrease in the total number of T cells (CD3+ cells; $x10^3$ cells per kidney: 3.3 ± 0.9 vs WT + Saline 9.6 ± 1.7), CD4+ T cells ($x10^3$ cells per kidney: 0.8 ± 0.2 vs WT + Saline 1.8 ± 0.5) and CD8+ T cells (cells per kidney: 455 ± 156 vs WT + Saline 1316 ± 483) in the kidney, although these differences failed to reach statistical significance. This decrease in T cell population in the kidney appeared to be sustained in hypertensive CCR8 KO mice (**Figure 11**). Infiltration of myeloid-linage cells (CD11+), macrophages (F4/80+) and M2 macrophages (CD206+) into the kidneys remained unchanged when mice were treated with Ang II and/or when CCR8 was

knocked out (**Figure 11 C-D**). In the aortae and spleens, no apparent difference in leukocyte infiltration was shown among treatment/ genotype groups (**Figures 10, 12**).

The CCR8 antagonist, R243, improves endothelial-dependent vasorelaxation in hypertensive mice

To evaluate the effects of pharmacologically targeting CCR8 on hypertension, hypertensive mice were treated with R243, a CCR8 antagonist. Consistent with our previous findings, infusion of Ang II led to a rise in systolic BP which was ≈40 mmHg above baseline at 14 days. Subsequent treatment of hypertensive mice with either vehicle or R243 for the following 14 days, did not have a significant effect on BP (by Day 28: 162 ± 10 mmHg Ang II + Vehicle, 139 ± 8 mmHg Ang II + R243, vs 110 ± 6 mmHg Saline + Vehicle, $p< 0.05$) (**Figure 13**).

The BW and organ weights (% BW) of this cohort of mice (10-12 weeks old on Day 0) did not differ among treatment groups (n= 4-6) (**Figure 14**). Although there was a trend for cardiac hypertrophy in the Ang II-treated WT mice, the study was not sufficiently powered for statistical comparison with a low number of samples in each group. Nevertheless, R243 did not appear to change the HW:BW ratio in hypertensive mice.

Although endothelial dysfunction was not apparent in Ang II infused mice, treatment of hypertensive mice with R243 lead to a significant 5-fold ($p<0.05$) increase in vasorelaxant potency to ACh in the isolated aorta (**Figure 15A, Table 2**). By contrast, R243 treatment did not alter vasorelaxation to DEA/NO or the contractile response to PE in hypertensive mice (**Figure 15 B-C**).

Neither mouse CCL8 (mCCL8) nor human CCL18 (hCCL18) activates CCR8

To confirm whether hCCL18 and mCCL8 activate CCR8, bioluminescence resonance energy transfer (BRET) assays were performed using mouse CCR8 (mCCR8) and human (hCCR8) expressing Chinese hamster ovary (CHO) cells. hCCL1 (an established agonist of CCR8) led to G-protein activation, cAMP inhibition and β-arrestin2 recruitment in human CCR8 (hCCR8)-expressing CHO cells, whereas none of these effects were observed when cells were stimulated with hCCL18 (**Figure 16A**). Similarly, mCCL1, but not mCCL8, caused G-protein

activation, cAMP inhibition and β-arrestin2 recruitment in mouse CCR8 (mCCR8)-expressing CHO cells (**Figure 16B**). Furthermore, scRNA data showed that CCR8 and its known ligand, CCL1 were both expressed at low levels in the normotensive and hypertensive mouse vasculature, predominantly on T cells (**Figure 17**).

5.6 Figures

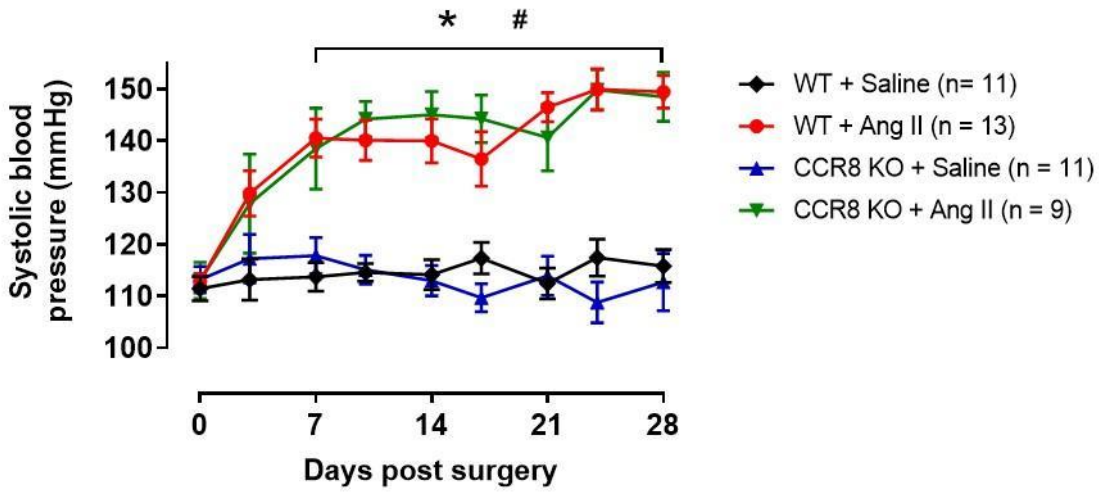

Figure 1. Effect of 28-day angiotensin II infusion on systolic blood pressure (BP) in male WT and CCR8 KO mice. Systolic BP over 28 days when wildtype (WT) and CCR8 knockout (KO) male mice were treated with saline or Ang II (0.7 mg/kg/d). BP was measured by tail cuff plethysmography.

Data presented as mean ± SEM, where n = number of animals. * $p < 0.05$ WT + Ang II vs. WT + Saline, # $p < 0.05$ CCR8 KO + Ang II vs. CCR8 KO + Saline; 2-way ANOVA, Tukey's post hoc test.

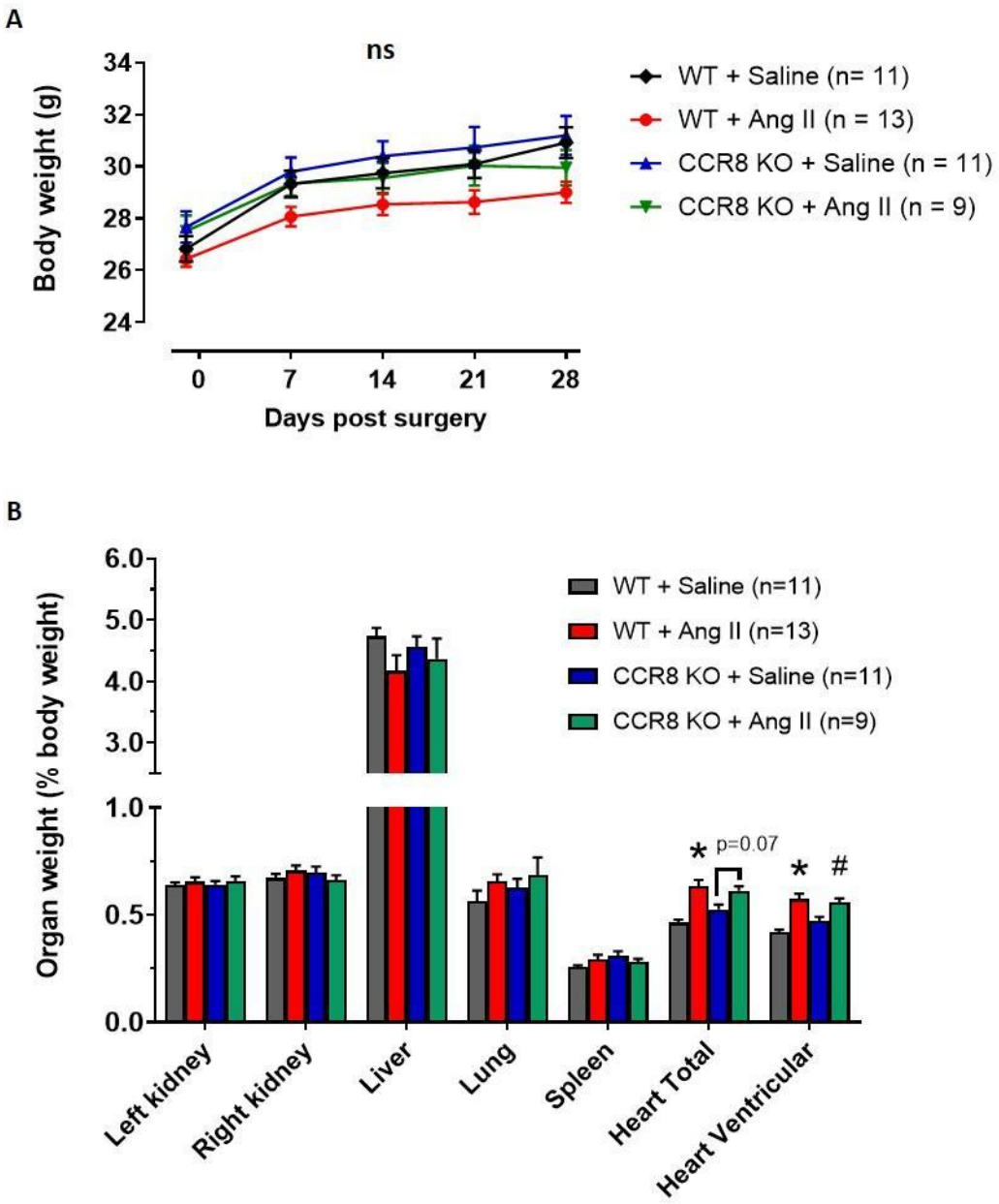

Figure 2. Effect of 28-day angiotensin II infusion on the body and organ weights of male WT and CCR8 KO mice. (**A**) Body weights of wildtype (WT) and CCR8 knockout (KO) mice over 28 days, when mice were treated with saline or Ang II (0.7 mg/kg/d). (**B**) Organ weights of WT and CCR8 KO mice (relative to body weights), at the end of their saline or Ang II (0.7 mg/kg/d) treatment. Data presented as mean ± SEM, n= number of animals. (A) 2-way ANOVA, ns= no statistical significance. (B) *p<0.05 vs. WT + Saline, #p<0.05 vs CCR8 KO + Saline; 1-way ANOVA, Tukey's post hoc test.

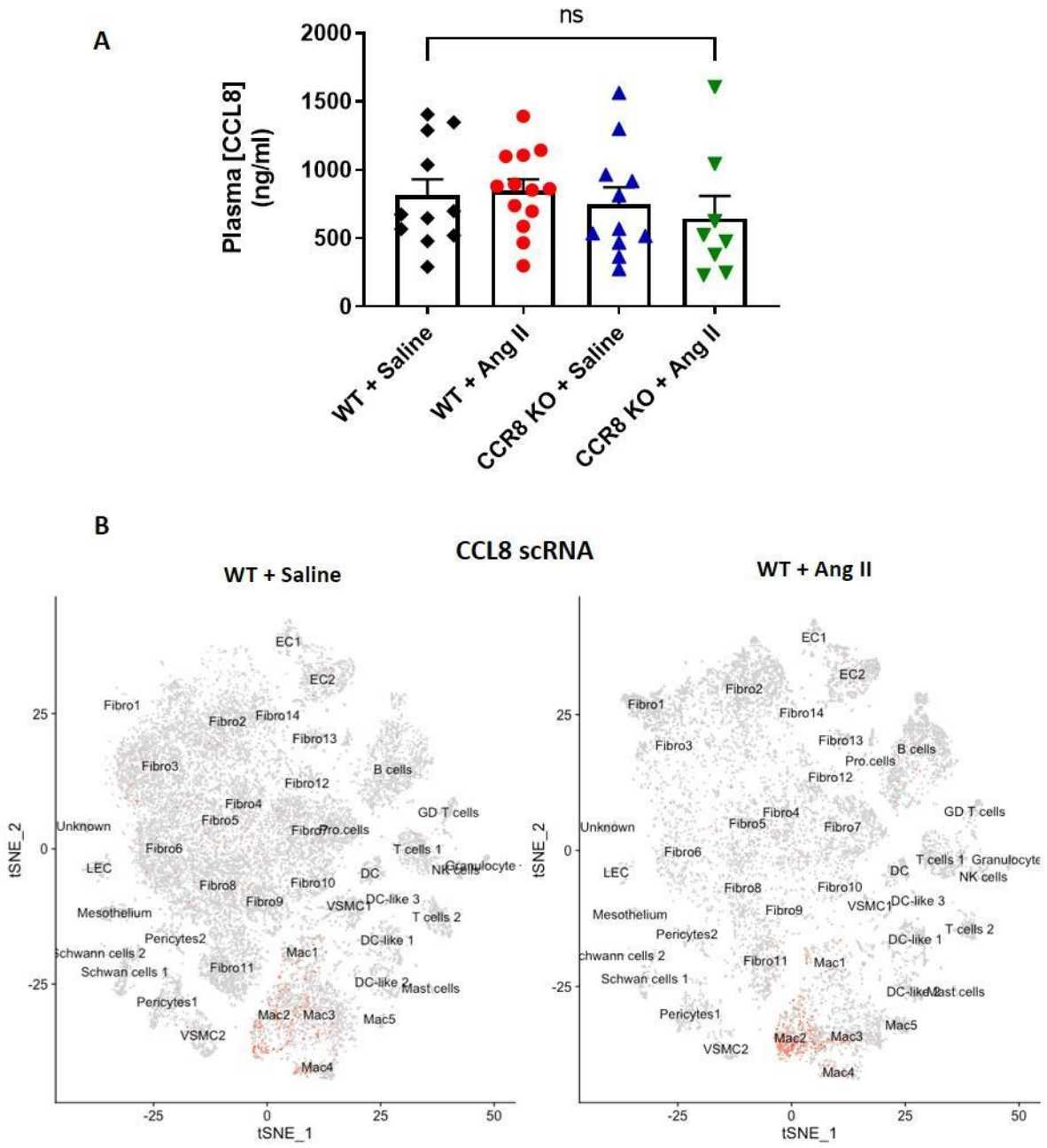

Figure 3. Plasma and aortic CCL8 expression in WT and hypertensive mice. (**A**) Plasma levels of CCL8 in saline- and Ang II-treated wildtype (WT) and CCR8 knockout (KO) mice, dots represent individual data points. (**B**) mRNA expression of CCL8 in aortae of saline- and Ang II-treated WT mice, measured via single cell RNA-sequencing (scRNA-Seq). All mice were treated with either saline or Ang II (0.7 mg/kg/d) for 28 days. (A) n= 8-13, 1-way ANOVA, ns= no statistical significance. (B) principal component analysis (PCA), positive expression highlighted in red, n= 4-6 pooled. Mac2= M2-like macrophages.

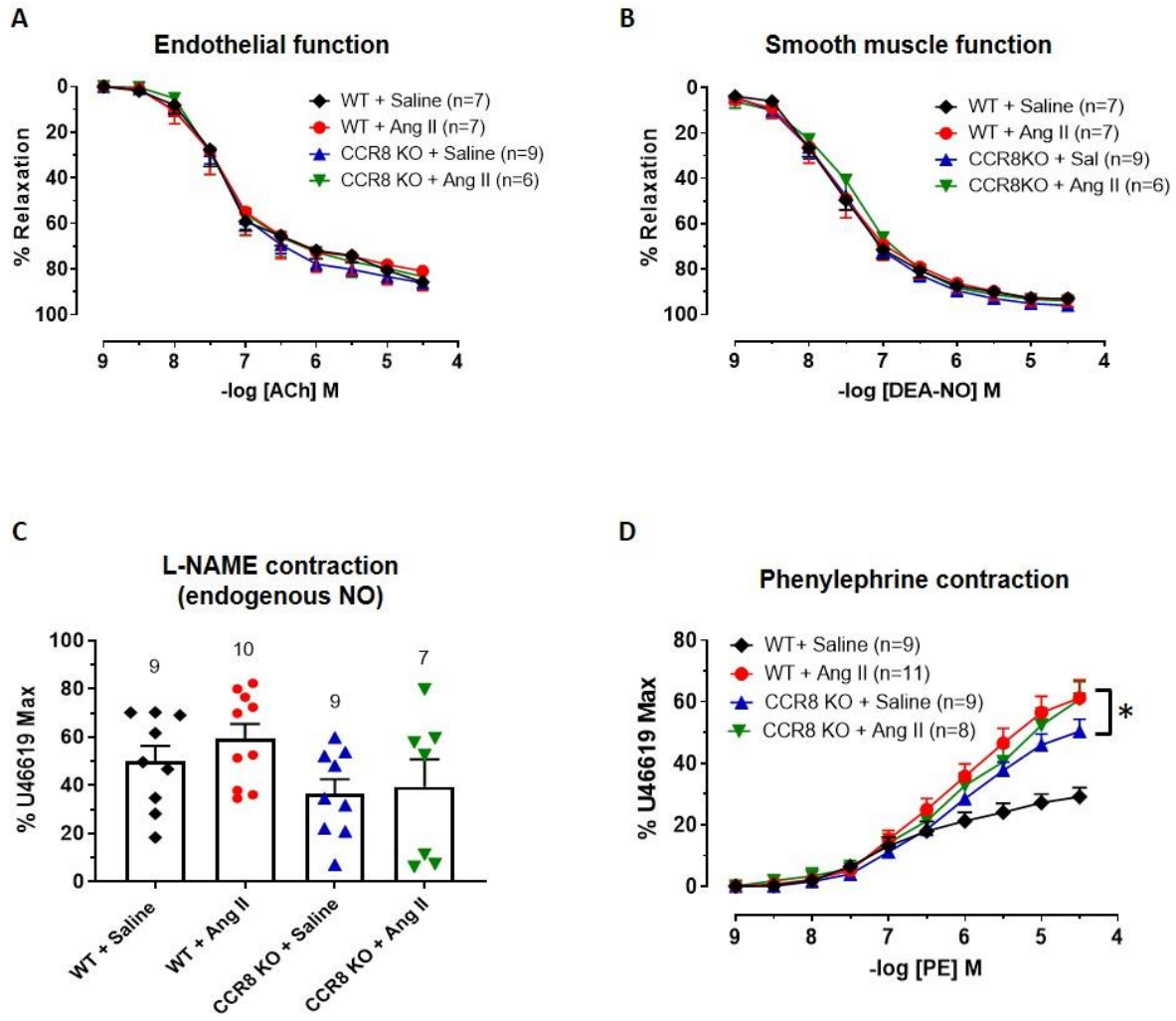

Figure 4. Effect of 28-day angiotensin II infusion on the function of the abdominal aorta in male WT and CCR8 KO mice. Cumulative concentration-response curves to acetylcholine (ACh) (**A**), DEA-NO (**B**) and phenylephrine (PE) (**D**) and L-NAME (100µM)-induced contraction (**C**) in isolated abdominal aorta from wildtype (WT) and CCR8 knockout (CCR8 KO) mice treated with either saline or Ang II (0.7 mg/kg/d) for 28 days.

Data expressed as % reversal of pre-contraction to U46619 (A-B) or % of the maximal U46619 contraction (C-D). Data presented as mean ± SEM, where n = number of animals. Dots represent individual data points (**C**). *p<0.05 vs. WT + Saline (maximal contraction to PE), 1-way ANOVA, Tukey's post hoc test.

Table 1. Effect of genetic deletion of CCR8 on relaxation to ACh and DEA/NO and contraction to PE in isolated aortae from saline- and Ang II-treated mice.

Group	Vasodilator/ Vasoconstrictor							
	ACh			**DEA-NO**			**PE**	
	pEC_{50} (-log M)	**R_{max} (%)**	**Pre-contraction (% U4 max)**	**pEC_{50} (-log M)**	**R_{max} (%)**	**Pre-contraction (% U4 max)**	**pEC_{50} (-log M)**	**F_{max} (%)**
WT + Saline	7.45 ± 0.14	85 ± 2	65 ± 2	7.55 ± 0.08	94 ± 2	60 ± 3	6.66 ± 0.21	29 ± 2
WT + Ang II	7.25 ± 0.16	80 ± 8	68 ± 2	7.57 ± 0.17	93 ± 3	64 ± 2	6.17 ± 0.16	61 ± 5 *
CCR8 KO + Saline	7.28 ± 0.07	86 ± 2	64 ± 2	7.55 ± 0.1	96 ± 1	58 ± 2	6.16 ± 0.11	50 ± 3 *
CCR8 KO + Ang II	7.12 ± 0.13	78 ± 6	64 ± 2	7.4 ± 0.11	92 ± 2	65 ± 3	5.75 ± 0.16	60 ± 5 *

pEC_{50} values expressed as -log M, R_{max} values as % reversal of the level of pre-contraction to U46619, and F_{max} values as % contraction to U46619 (0.3 µM). Values given as mean ± SEM. n= 7-11. *p<0.05 vs. WT + saline (maximal contraction to PE), 1-way ANOVA, Tukey's post hoc test.

WT + Saline: WT mice treated with saline for 28 days; **WT + Ang II**: WT mice treated with Ang II (0.7mg/kg/d) for 28 days; **CCR8 KO + Saline**: CCR8 KO mice treated with saline for 28 days; **CCR8 KO + Ang II**: CCR8 KO mice treated with Ang II (0.7mg/kg/d) for 28 days. **ACh**: acetylcholine; **DEA/NO**: diethylamine NONOate; **PE**: phenylephrine.

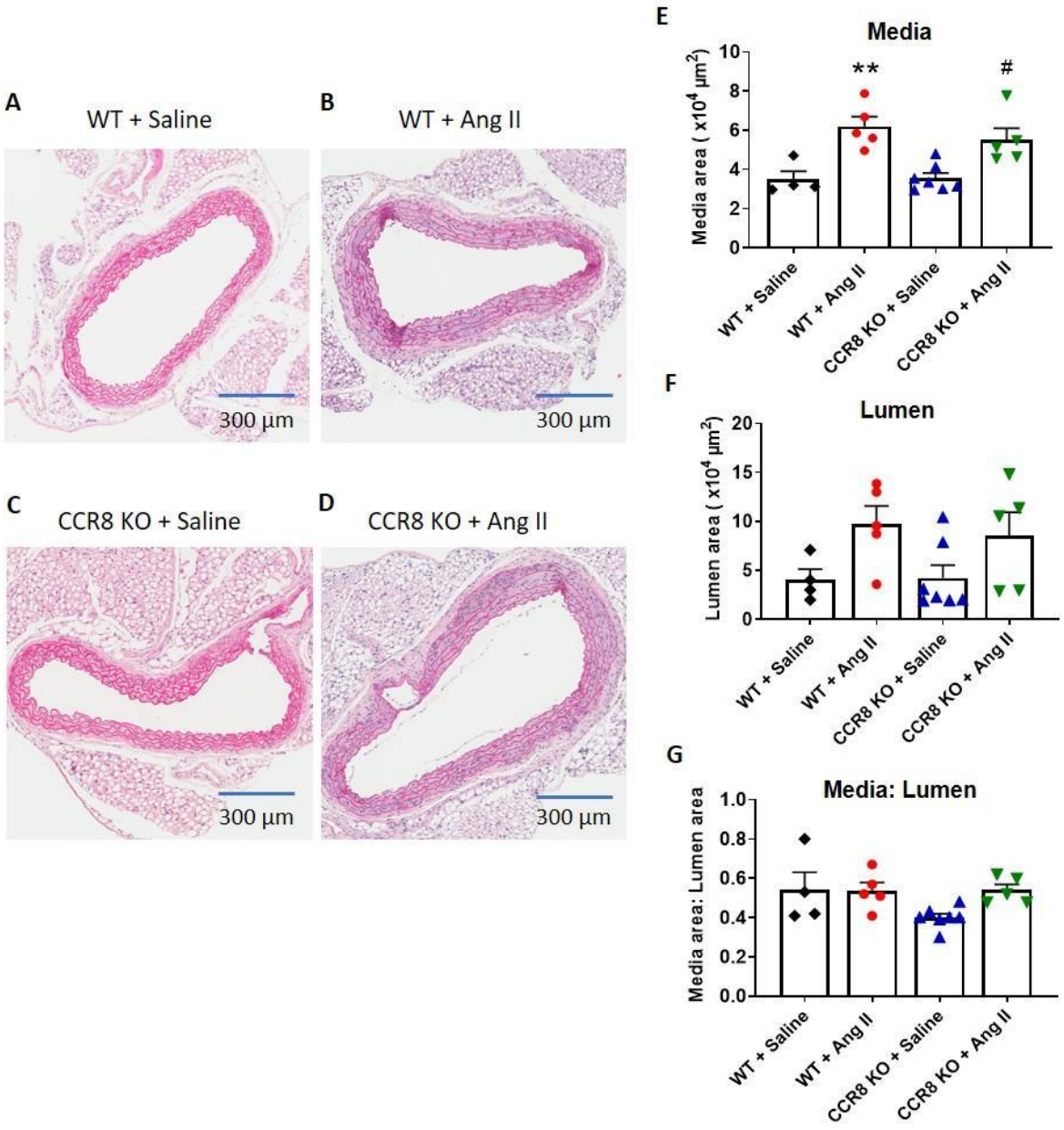

Figure 5. Effect of 28-day angiotensin II infusion on the structure of the thoracic aorta from male WT and CCR8 KO mice. (A-D) Representative images of mouse aortic sections stained by hematoxylin and eosin (H&E). Wildtype (WT) and CCR8 knockout (KO) mice were treated with saline or Ang II (0.7 mg/kg/d) for 28 days. (**E-G**) Quantification of medial area (**E**), lumen area (**F**), and medial: lumen area ratio (**G**). Data presented as mean ± SEM, dots represent individual data points, n= 4-7. **p<0.01 vs. WT + Saline, # p<0.05 vs. CCR8 KO + saline; 1-way ANOVA, Tukey's post hoc test.

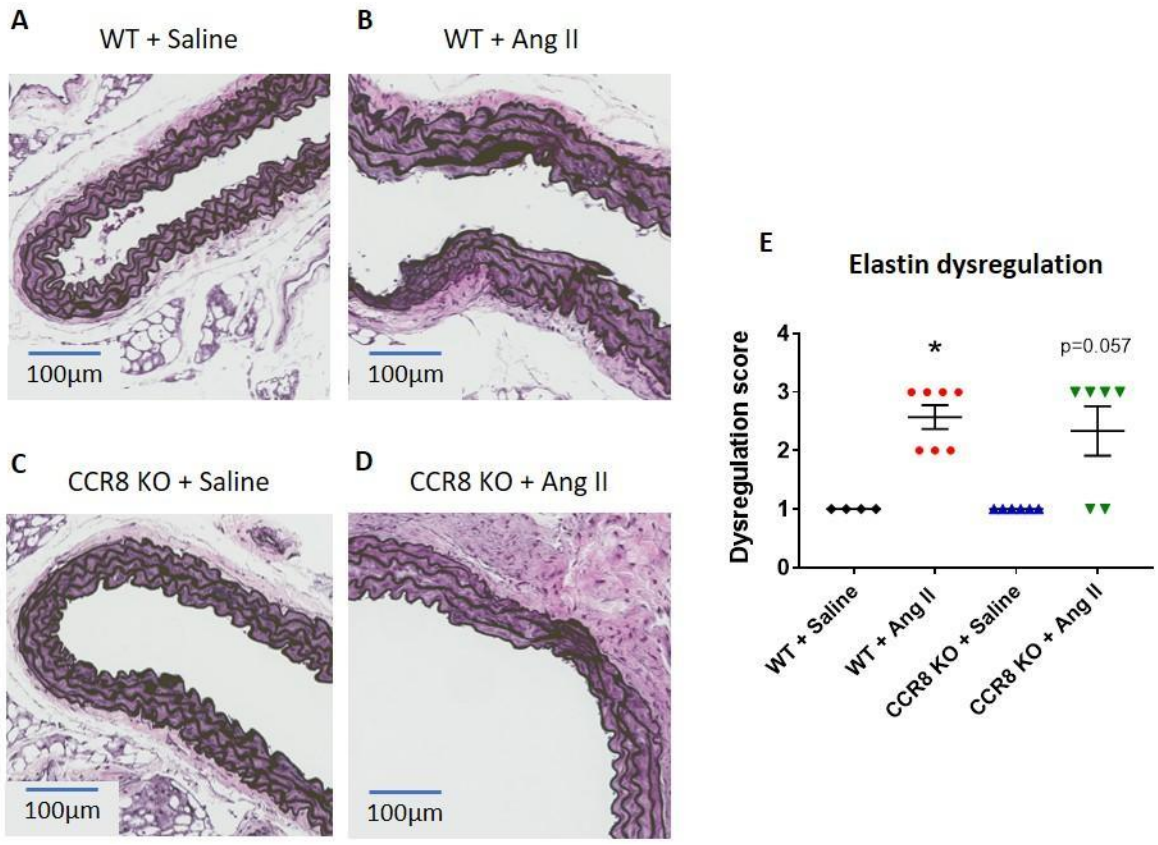

Figure 6. Effect of 28-day angiotensin II infusion on elastin dysregulation of the thoracic aorta from male WT and CCR8 KO mice. (A-D) Representative images of mouse aortic sections stained by Verhoeff-Van Gieson (VVG). Wildtype (WT) and CCR8 knockout (KO) mice were treated with saline or Ang II (0.7 mg/kg/d) for 28 days. (**E**) Scoring of the level of elastin dysregulation, where score= 1 represents normal elastin structure, and score= 4 represents severe elastin dysregulation. Data presented as median with 95% CI, dots represent individual data points, n= 4-7. *p<0.05 vs. WT + Saline, 1-way ANOVA, Kruskal-Wallis post hoc test.

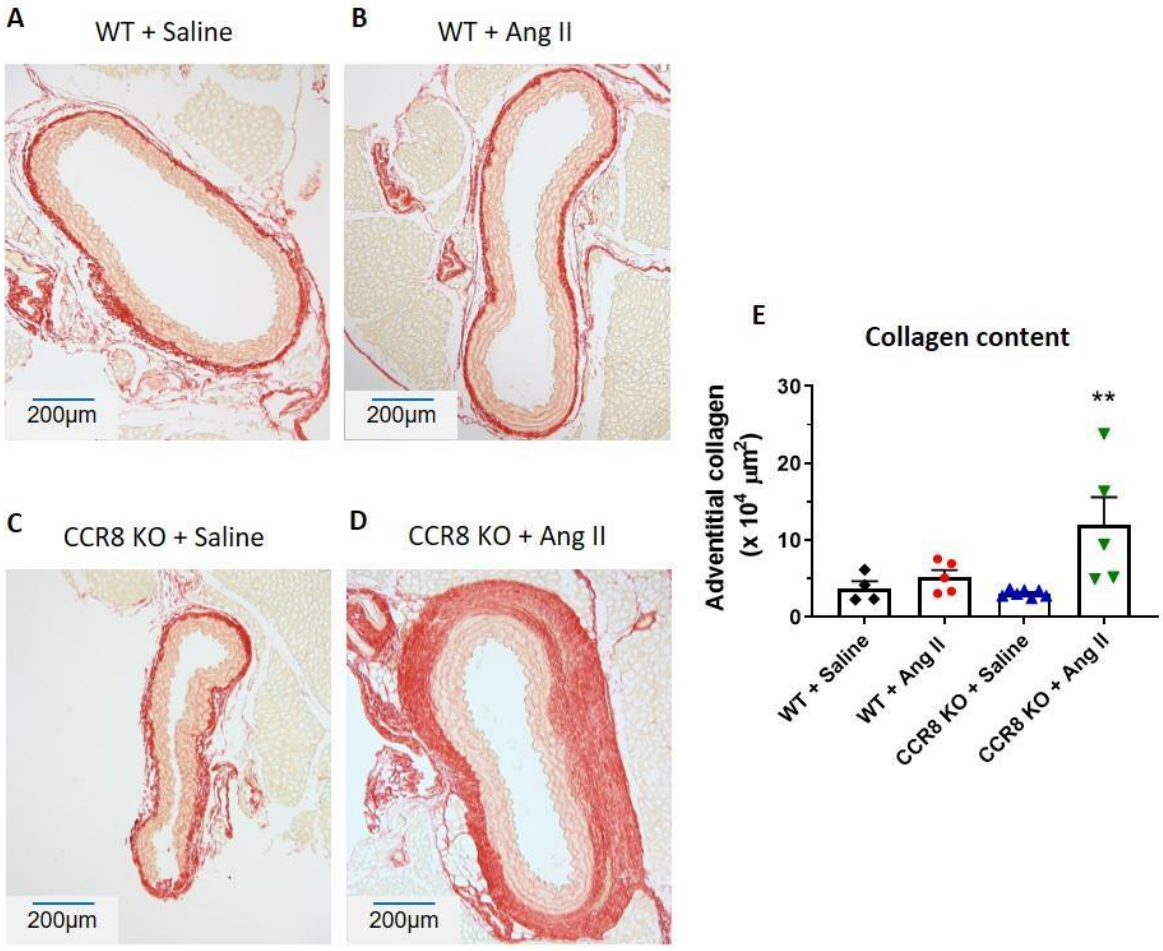

Figure 7. Effect of 28-day angiotensin II infusion on the collagen deposition of the thoracic aorta from male WT and CCR8 KO mice. (A-D) Representative images of mouse aortic sections stained by picrosirius red. Wildtype (WT) and CCR8 knockout (KO) mice were treated with saline or Ang II (0.7 mg/kg/d) for 28 days. (**E**) Quantification of adventitial collagen expressed as area of staining in the adventitia. Data presented as mean ± SEM, dots represent individual data points, n= 4-7 where n= number of animals. **p<0.01 vs. CCR8 KO + Saline, 1-way ANOVA, Tukey's post hoc test.

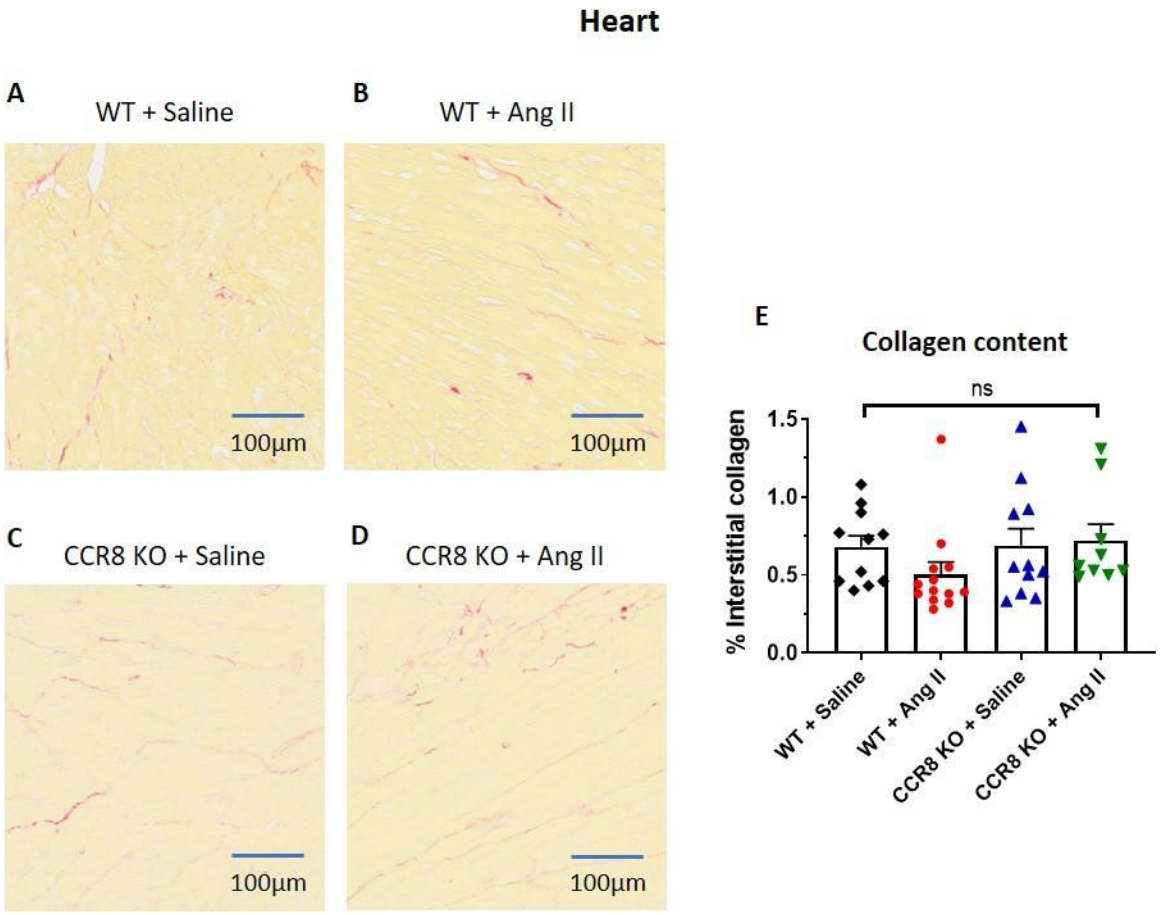

Figure 8. Effect of 28-day angiotensin II infusion on the collagen deposition of the heart from male WT and CCR8 KO mice. (A-D) Representative images of mouse heart sections stained by picrosirius red, where collagen was stained red. Wildtype (WT) and CCR8 knockout (KO) mice were treated with saline or Ang II (0.7 mg/kg/d) for 28 days. (**E**) Quantification of interstitial collagen expressed as % of image area. Data presented as mean ± SEM, dots represent individual data points, n= 9-13. 1-way ANOVA, ns= no statistical significance.

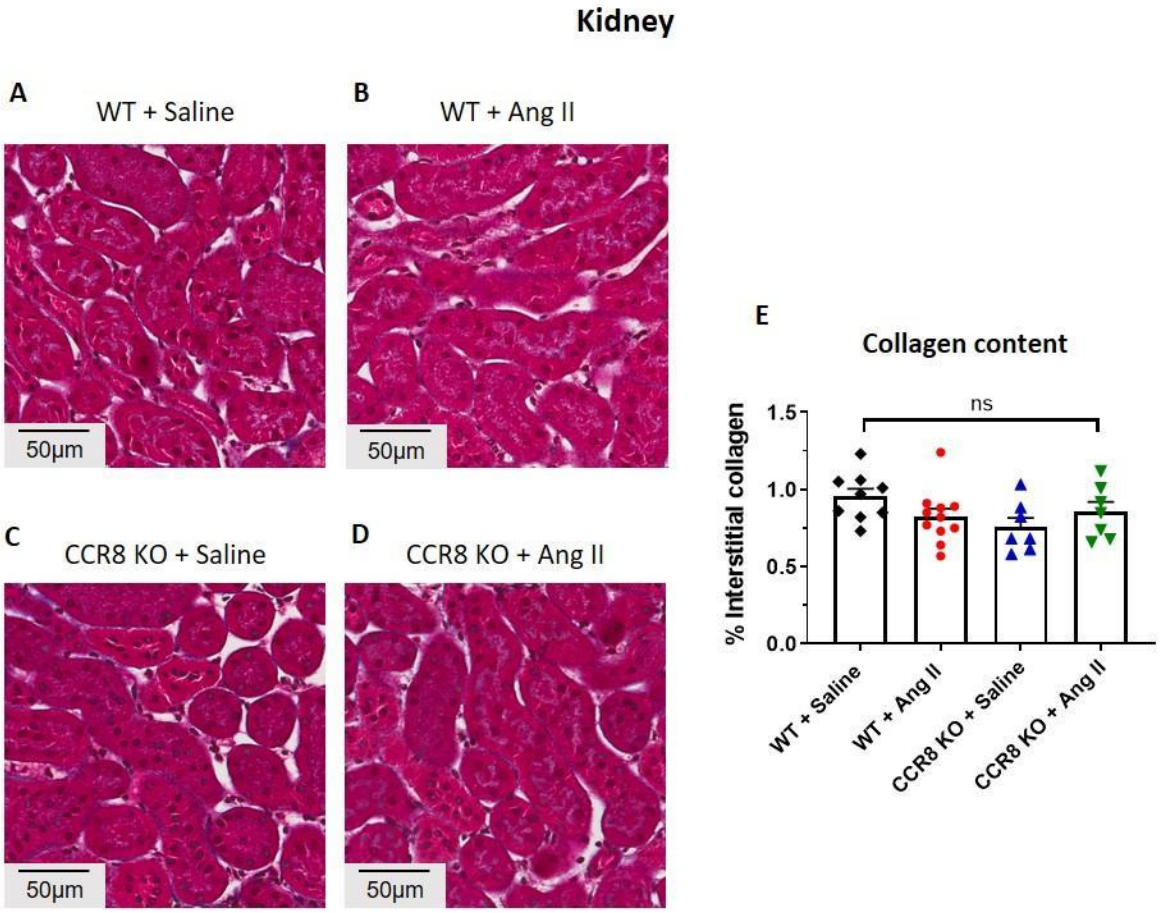

Figure 9. Effect of 28-day angiotensin II infusion on the collagen deposition of the kidney from male WT and CCR8 KO mice. (A-D) Representative images of mouse kidney sections stained by Masson's Trichrome, where collagen was stained blue. Wildtype (WT) and CCR8 knockout (KO) mice were treated with saline or Ang II (0.7 mg/kg/d) for 28 days. (**E**) Quantification of interstitial collagen expressed as % of image area. Data presented as mean ± SEM, dots represent individual data points, n= 7-11. 1-way ANOVA, ns= no statistical significance.

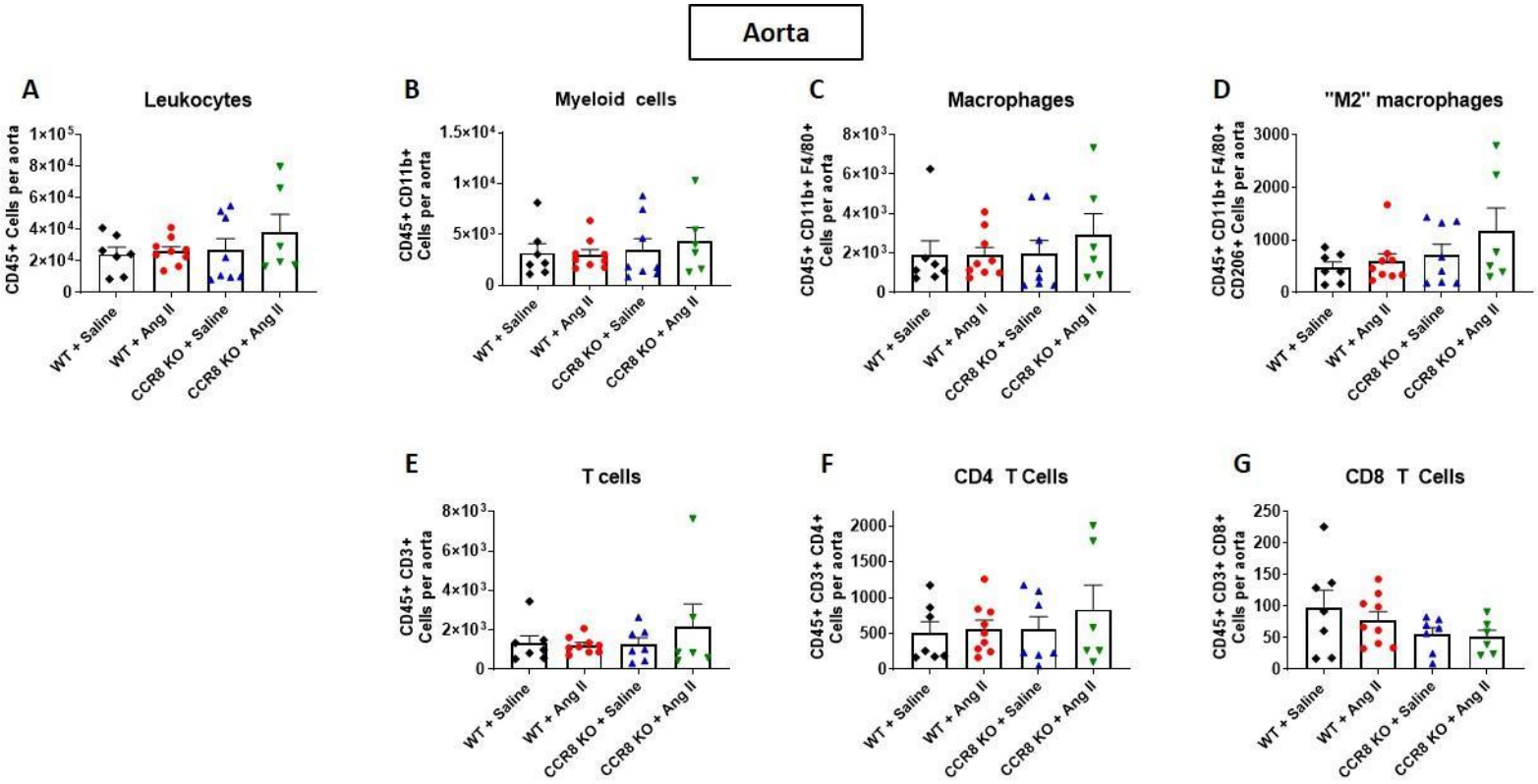

Figure 10. Effect of 28 days of angiotensin infusion on leukocyte infiltration into aortae from male WT and CCR8 KO mice. Cell numbers calculated via flow cytometric analysis, representing CD45+ leukocytes (**A**), CD11+ myeloid lineage cells (**B**), F4/80+ total macrophages (**C**), CD206+ "M2" macrophages (**D**), CD3+ total T cells (**E**), CD4+ T cells (**F**) and CD8+ T cells (**G**). Wildtype (WT) and CCR8 knockout (KO) mice were treated with saline or Ang II (0.7 mg/kg/d) for 28 days. Data presented as mean ± SEM, dots represent individual data points, n= 6-9. 1-way ANOVA.

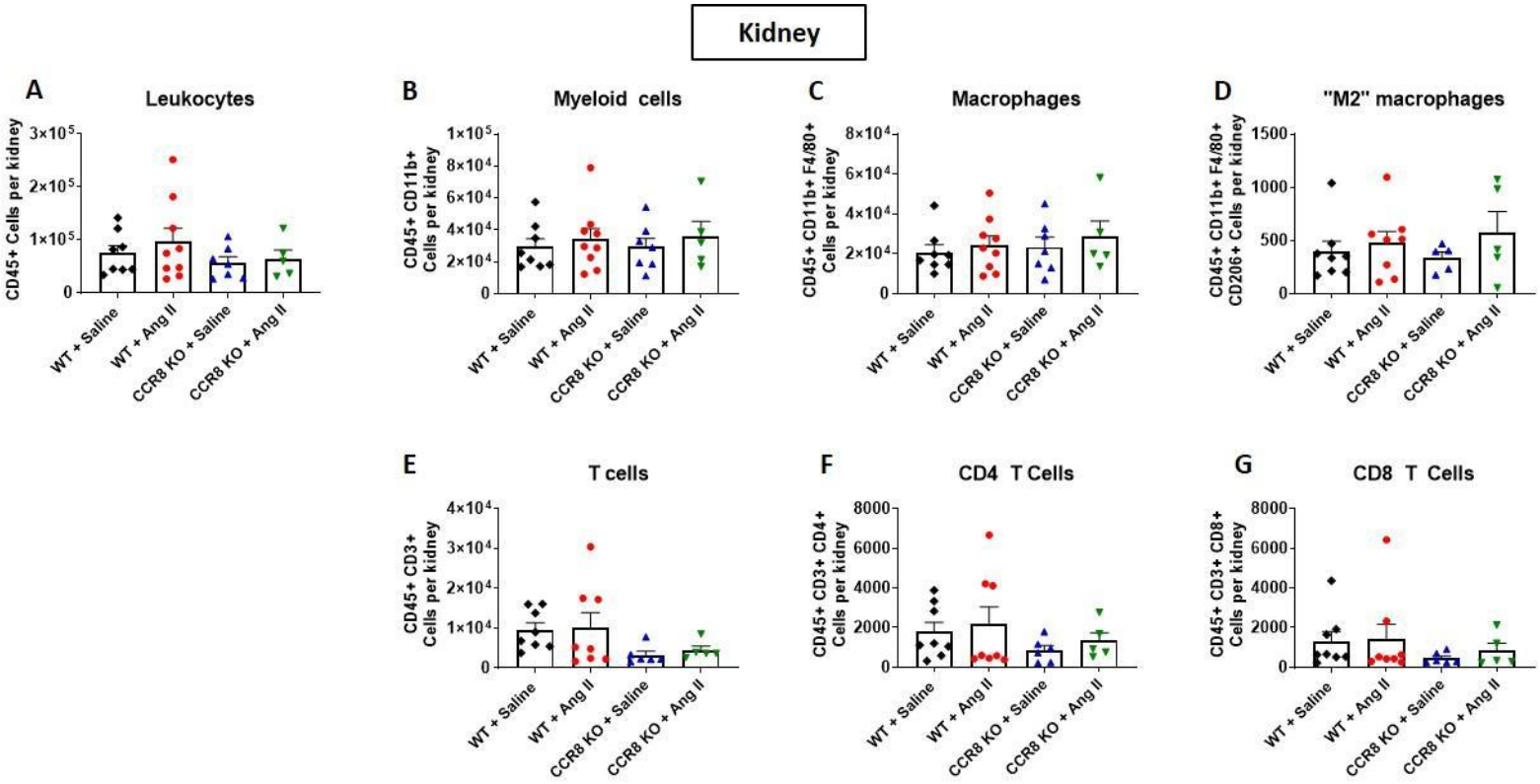

Figure 11. Effect of 28 days of angiotensin infusion on leukocyte infiltration into kidneys from male WT and CCR8 KO mice. Cell numbers calculated via flow cytometric analysis, representing CD45+ leukocytes (**A**), CD11+ myeloid lineage cells (**B**), F4/80+ total macrophages (**C**), CD206+ "M2" macrophages (**D**), CD3+ total T cells (**E**), CD4+ T cells (**F**) and CD8+ T cells (**G**). Wildtype (WT) and CCR8 knockout (KO) mice were treated with saline or Ang II (0.7 mg/kg/d) for 28 days. Data presented as mean ± SEM, dots represent individual data points, n= 5-9. 1-way ANOVA.

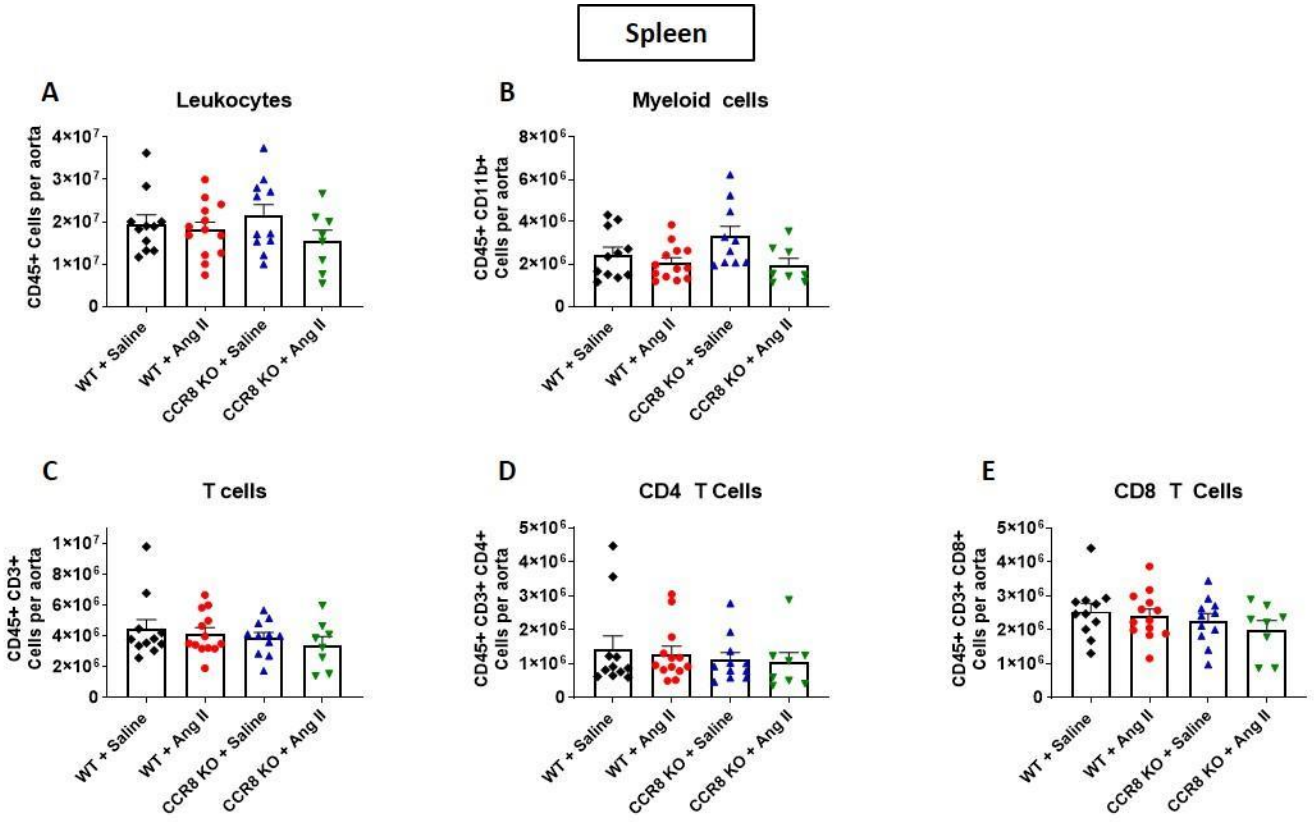

Figure 12. Effect of 28 days of angiotensin infusion on leukocyte infiltration into spleen from male WT and CCR8 KO mice. Cell numbers calculated via flow cytometric analysis, representing CD45+ leukocytes (**A**), CD11+ myeloid lineage cells (**B**), CD3+ total T cells (**C**), CD4+ T cells (**D**) and CD8+ T cells (**E**). Wildtype (WT) and CCR8 knockout (KO) mice were treated with saline or Ang II (0.7 mg/kg/d) for 28 days. Data presented as mean ± SEM, dots represent individual data points, n= 8-13. 1-way ANOVA.

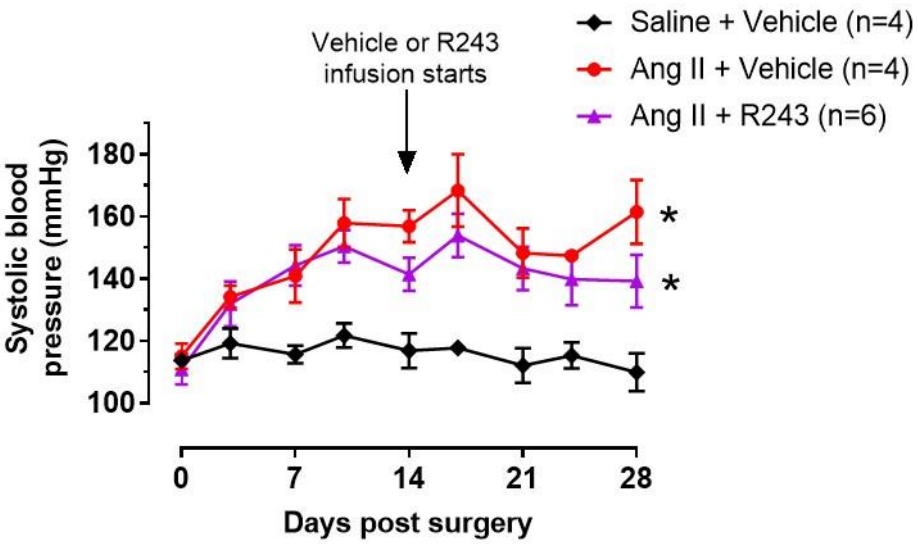

Figure 13. Effect of the CCR8 antagonist, R243 on the systolic BP in WT mice with angiotensin II-induced hypertension. Mice were treated with Ang II (0.7 mg/kg/d) for 28 days and received either R243 (1.1 mg/kg/d; CCR8 antagonist) or vehicle (2:1 warm mixture of 30% hydroxypropyl-β-cyclodextrin: 100% DMSO) for the final 14 days. Systolic BP was measured by tail cuff plethysmography over the 28-day experimental period. Data presented as mean ± SEM, n= number of animals. *p< 0.05 vs. Saline + Vehicle, 2-way ANOVA, Tukey's post hoc test.

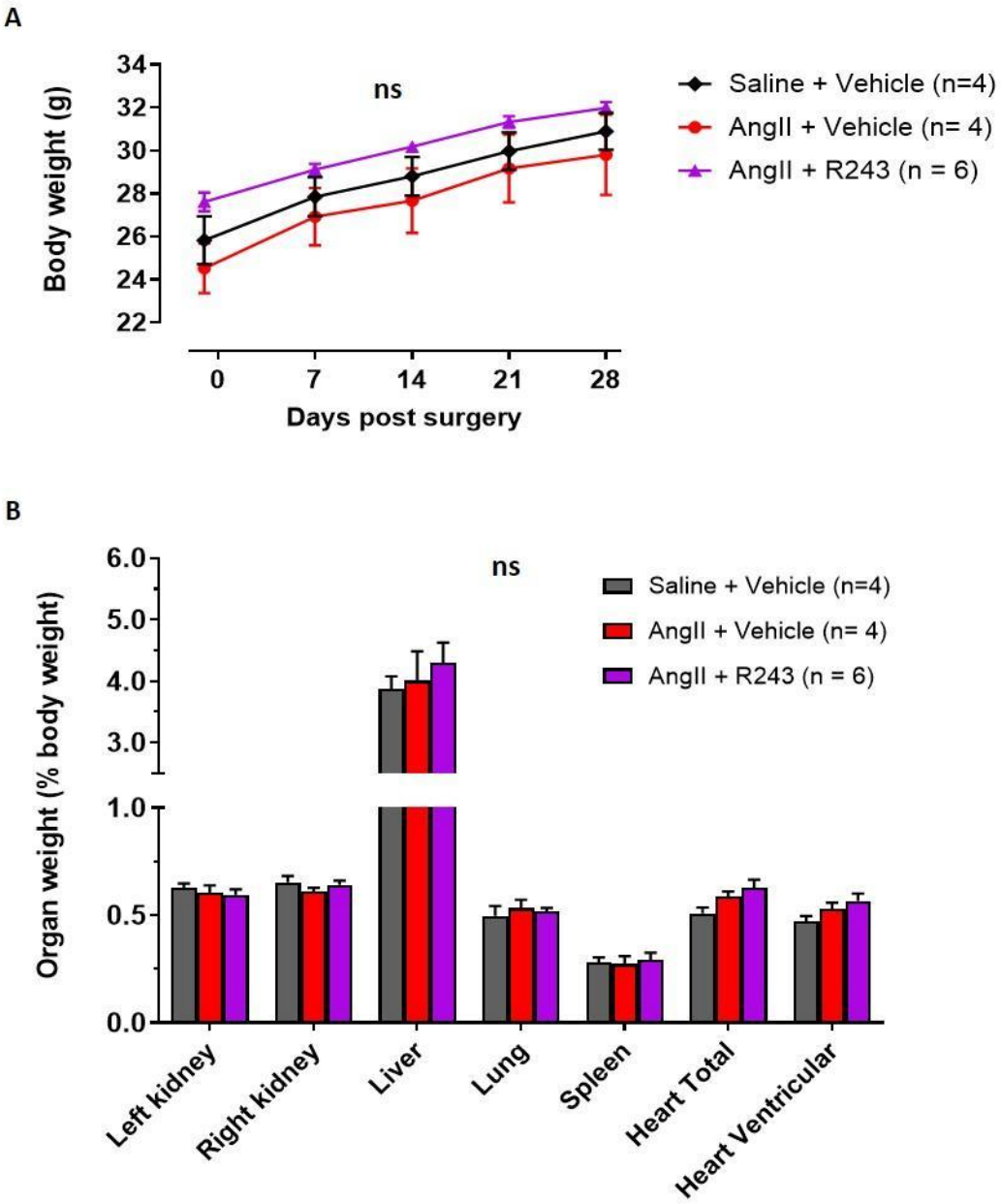

Figure 14. Effect of the CCR8 antagonist, R243 on body and organ weights of male hypertensive WT mice. (**A**) Body weights of mice over 28 days, when treated with saline or Ang II (0.7 mg/kg/d), with or without R243 administration from Day 14 (1.1 mg/kg/d; CCR8 antagonist). (**B**) Organ weights of mice (relative to body weight) at the end of the treatment period. Data presented as mean ± SEM, n= number of animals. (A) 2-way ANOVA, ns= no statistical significance. (B) 1-way ANOVA, ns= no statistical significance.

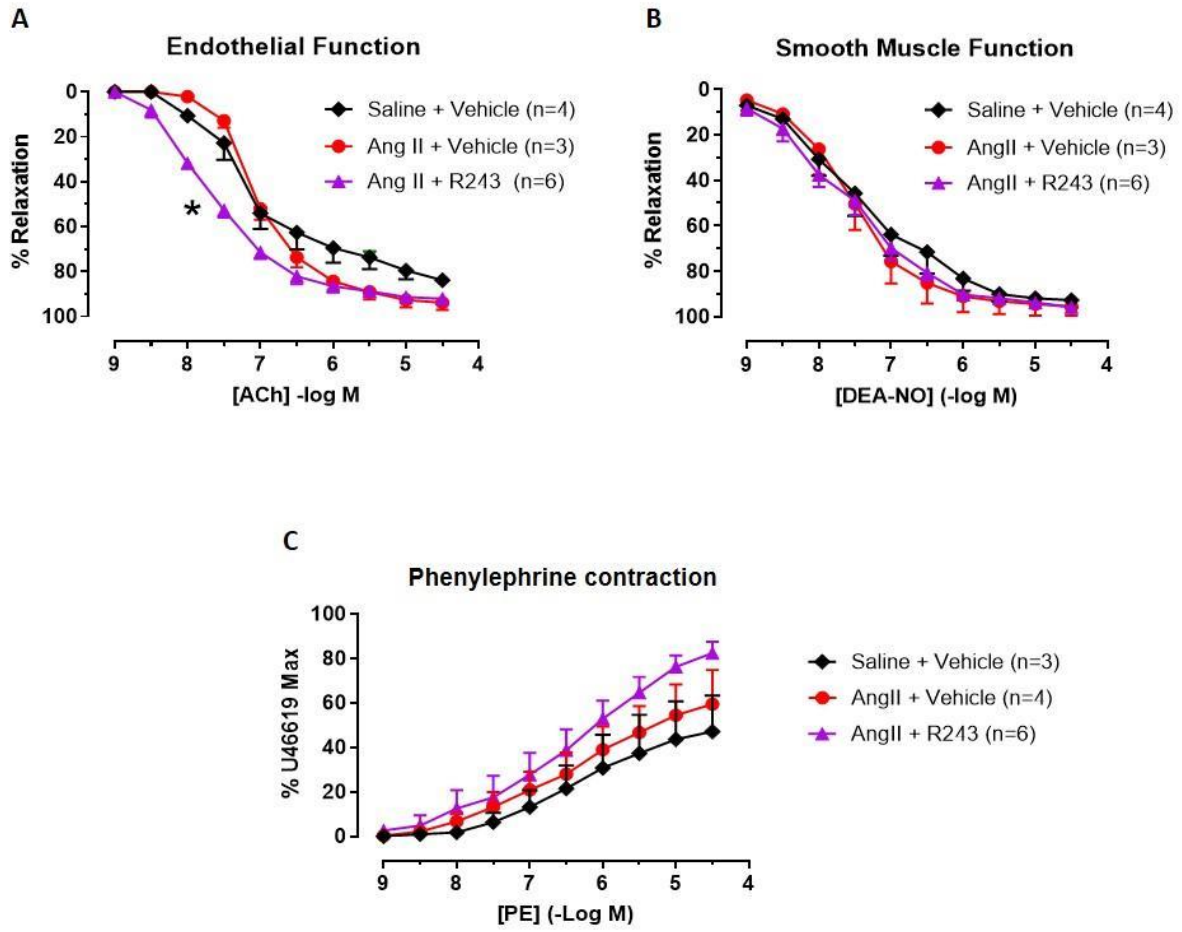

Figure 15. Effect of the CCR8 antagonist, R243 on the function of the abdominal aorta in hypertensive mice. Cumulative concentration-response curves to acetylcholine (ACh) (**A**), DEA-NO (**B**) and phenylephrine (PE) (**C**) in isolated abdominal aorta. C57BL/6J male mice were treated with saline or Ang II (0.7 mg/kg/d) for 28 days, with either vehicle (2:1 warm mixture of 30% hydroxypropyl-β-cyclodextrin: 100% DMSO) or R243 administered (1.1 mg/kg/d; CCR8 antagonist) from Day 14 onwards.

Data expressed as % reversal of pre-contraction to U46619 (A-B) or % of the maximal U46619 contraction (C). Data presented as mean ± SEM, n= number of animals. * $p<0.05$, pEC_{50} vs. Ang II + Vehicle and Saline + Vehicle, 1-way ANOVA, Tukey's post hoc test.

Table 2. Effect of the CCR8 antagonist, R243 on relaxation to ACh and DEA/NO and contraction to PE in isolated aortae from Ang II-treated mice.

Group	Vasodilator/ Vasoconstrictor							
	ACh			**DEA-NO**			**PE**	
	pEC_{50} (-log M)	**R_{max} (%)**	**Pre-contraction (% U4 max)**	**pEC_{50} (-log M)**	**R_{max} (%)**	**Pre-contraction (% U4 max)**	**pEC_{50} (-log M)**	**F_{max} (%)**
Saline + Vehicle	7.19 ± 0.14	83 ± 3	69 ± 1	7.44 ± 0.27	92 ± 2.7	66 ± 2	5.77 ± 0.65	47 ± 16
Ang II + Vehicle	7.13 ± 0.1	88 ± 5	68 ± 1	7.6 ± 0.22	95 ± 4	71 ± 6	6.62 ± 0.36	59 ± 15
Ang II + R243	7.83 ± 0.11 *	92 ± 2	63 ± 1	7.68 ± 0.16	95 ± 1	60 ± 2	7 ± 0.66	82 ± 5

pEC_{50} values expressed as -log M, R_{max} values as % reversal of the level of pre-contraction to U46619, and F_{max} values as % contraction to U46619 (0.3 µM). Values given as mean ± SEM. n= 3-6. *p<0.05 vs. Ang II + Vehicle and Saline + Vehicle (maximal contraction to PE), 1-way ANOVA, Tukey's post hoc test.

Saline + Vehicle: mice treated with saline for 28 days, with vehicle administered from Day 14 onwards; **Ang II + Vehicle**: mice treated with Ang II (0.7mg/kg/d) for 28 days, with vehicle administered from Day 14 onwards; **Ang II + R243**: mice treated with Ang II (0.7mg/kg/d) for 28 days, with R243 (1.1 mg/kg/d) administered from Day 14 onwards. **ACh**, acetylcholine; **DEA/NO**, diethylamine NONOate; **PE**, phenylephrine.

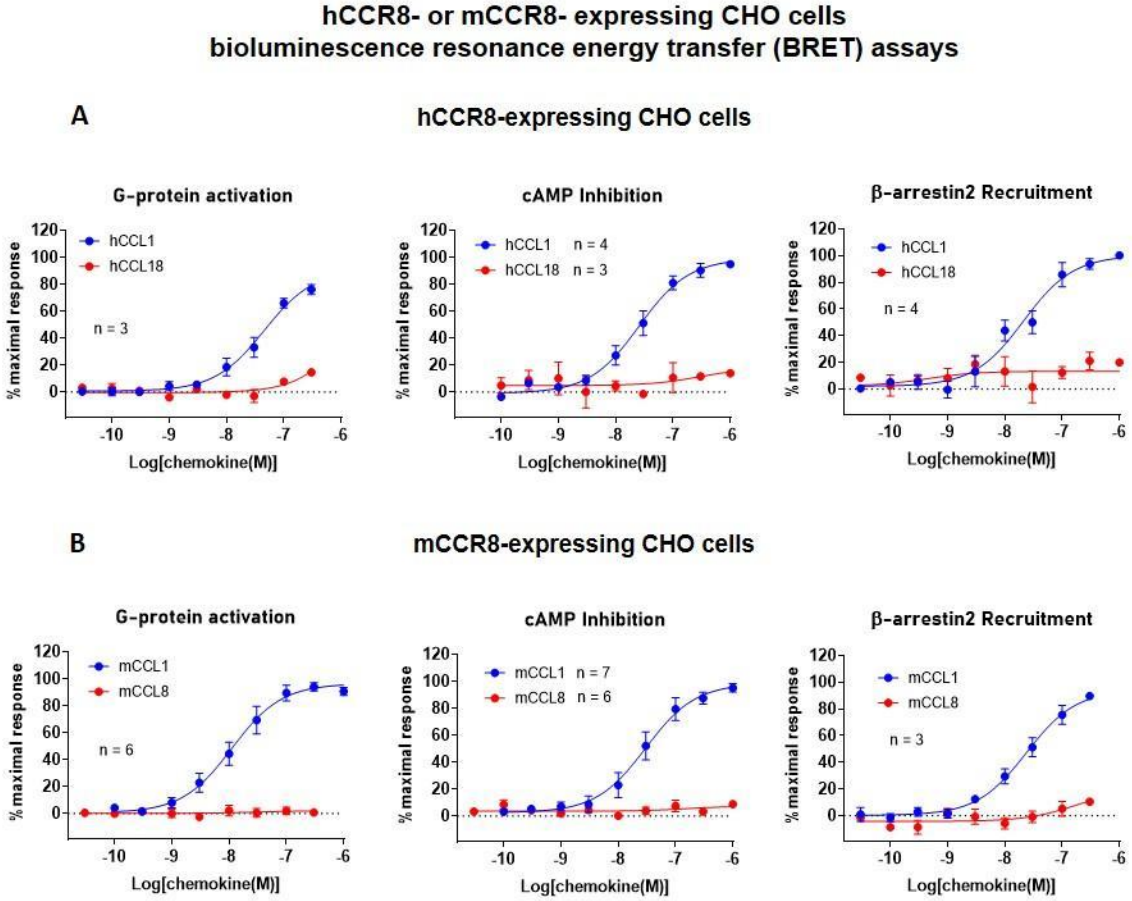

Figure 16. Assessment of CCR8 activation by human CCL18 (hCCL18) and mouse CCL8 (mCCL8) via bioluminescence resonance energy transfer (BRET) assays. Flp-In Chinese hamster ovary (CHO) cells were transfected with mouse CCR8 (mCCR8; **A**) or human CCR8 (hCCR8; **B**). **Left panel**: G-protein activation, $G\alpha_{i2}$+ $G\beta_1$ tagged by venus$^{156\text{-}229}$, $G\gamma_2$ tagged by venus$^{1\text{-}155}$, GRKct tagged by Rluc; CCR8 tagged by myc. **Middle panel**: cAMP inhibition assay using 10µM forskolin, CCR8 tagged by myc. **Right panel**: β-arrestin2 recruitment, CCR8 tagged by Rluc, β-arrestin tagged by YFP. The well-established CCR8 agonists, human- and mouse-CCL1 (hCC1 and mCCL1), were used as positive controls. Data expressed as % of the maximal response and presented as mean ± SEM; n= 3-7.

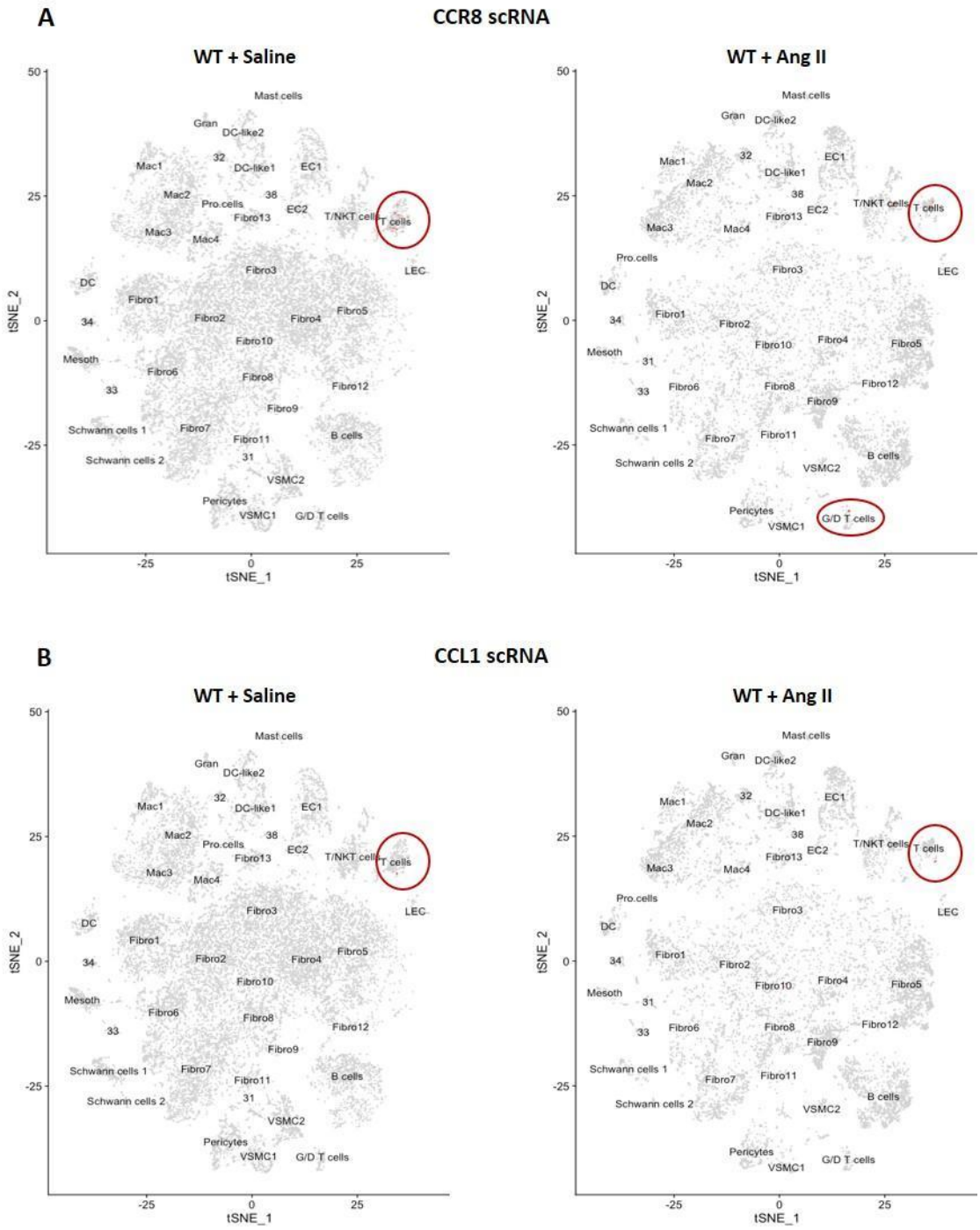

Figure 17. Aortic CCR8 and CCL1 expression in hypertensive mice. RNA expression of CCR8 (**A**) and CCL1 (**B**) in aortae of saline- and Ang II-treated wildtype mice, using single cell RNA (scRNA) sequencing. Mice were treated with saline or Ang II (0.7 mg/kg/d) for 28 days. Principal component analysis (PCA), positive expression highlighted in red, n= 4-6 pooled. G/D T cells= Gamma delta T cells.

5.7 Discussion

M2 macrophages contribute to hypertension-associated fibrosis in the aorta (Oparil et al., 2003), kidney (Zhao et al., 2008) and heart disease (Diez, 2007), and are the predominant source of the pro-fibrotic chemokines, human CCL18 (hCCL18) and mouse CCL8 (mCCL8) (Islam et al., 2011; Schutyser et al., 2005). Based on the study of (Islam et al., 2013), which identified these two chemokines as functional analogues and as agonists of CCR8, we sought to investigate the role of the mCCL8-CCR8 axis in the development of hypertension in mice using genetic deletion and pharmacological inhibition of CCR8. Extending our previous findings in a 14-day model of Ang II-induced hypertension (**Chapter 4**), we have utilised a more chronic model of hypertension (28-day Ang II infusion) in this study. We confirmed that M2 macrophages are a key source of mCCL8 in the hypertensive vasculature. Whilst genetic deletion of CCR8 did not confer protection against the hypertensive response to Ang II or the associated end-organ remodelling, it was noted that T cell infiltration into the kidneys of CCR8 KO mice had a trend towards attenuation. Moreover, we have provided the first evidence that the CCR8 antagonist, R243 improves endothelial-dependent vasorelaxation in the hypertensive vasculature, independently of a change in BP. Whilst mCCL8 was elevated in hypertension, our findings in CCR8 expressing CHO cells challenge the idea that hCCL18/mCCL8 signal via CCR8. As such, the lack of protection against hypertension and its associated end-organ damage, following genetic or therapeutic targeting of CCR8, may be indicative of the inability of M2 macrophage-derived mCCL8 to activate CCR8.

We chose to investigate the role of the mCCL8-CCR8 axis in the 28-day Ang II (0.7 mg/kg/d) infusion model of hypertension in mice. Like the 14-day Ang II model of hypertension used in **Chapter 4**, 28 days of Ang II infusion leads to a rapid elevation in systolic BP, however the associated end-organ damage may be more extensive as a result of the prolonged hypertension. Thus a 14-day Ang II (2.2 mg/kg/d) infusion model does not cause cardiac damage (Kirchhoff et al., 2008), whereas 28 days of Ang II (0.7 mg/kg/d) infusion leads to development of cardiac hypertrophy (Moore et al., 2015). Consistent with previous studies (Moore et al., 2015), Ang II infusion in WT mice caused a significant increase in systolic BP by 7 days which was maintained over the 28 day experimental period and was associated with cardiac hypertrophy.

It is well recognised that hypertension is associated with vascular inflammation and previous studies have shown that following Ang II infusion in mice, M2 macrophages accumulate in the vessel wall and aortic mCCL8 expression is increased (Moore et al., 2015) (**Chapter 4**). Moreover, using immunohistochemical approaches, we have previously shown that mCCL8 is co-localised with M2 macrophages in the aortae of 28-day Ang II treated mice (Zhu, 2016). We have now extended these studies, using a scRNA-Seq approach to confirm colocalization of mCCL8 with a population of macrophages in the aortic wall and a hypertension-associated increase in this subset of mCCL8-expressing macrophages. Whilst we observed elevated plasma levels of hCCL18 in patients with resistant hypertension (**Chapter 3**), plasma levels of mCCL8 were unchanged following Ang II infusion in mice. However, it is important to note that the murine Ang II infusion model is not a model of resistant hypertension and as such spillover of CCL8 from tissues into plasma may only arise after prolonged periods of sustained hypertension.

Having established a murine model of hypertension associated with cardiac remodelling and vascular inflammation (elevated aortic mCCL8), we next sought to delineate the role of the hCCL18/mCCL8 cognate receptor, CCR8 (Islam et al., 2013) on the development of hypertension. The global deletion of CCR8 did not protect mice from either the elevation in BP or cardiac hypertrophy. These findings are perhaps not so surprising, when considering the key immune cells reported to be involved in BP elevation. Thus, previous studies have shown that inhibition of monocyte trafficking and accumulation of M2 macrophages in the vascular wall leads to an antihypertensive effect (Moore et al., 2015). Whilst CCL8-CCR8 signalling is reported to promote chemoattraction, this is likely to reflect an action on T cells rather than macrophages themselves. As such, we would not anticipate that a loss of CCR8 would reduce macrophage accumulation in the vascular wall and lower BP. Indeed, as will be discussed in further detail later, our flow cytometric analysis did not detect changes in macrophage content in either WT or Ang II-treated CCR8 KO mice.

Although the hypertensive response to Ang II was not blunted in CCR8 KO mice, we wished to determine if CCR8 signalling modulated vascular function in the setting of hypertension. Chronic hypertension is associated with vascular dysfunction in large conduit arteries (Oparil et al., 2003), which can lead to fibrosis and stiffening (Drummond et al., 2019). Although endothelial dysfunction in commonly reported in pre-clinical models of hypertension (Al-

Magableh et al., 2015; Madhur et al., 2010), in the current study endothelium-dependent relaxation to ACh and the contractility to L-NAME (measure of endogenous NO bioavailability) were preserved in the abdominal aorta of WT hypertensive mice. As discussed in **Chapter 4** (**Section 4.7**), the observed inconsistency with published data may be caused by differences in experimental design, such as baseline tension and pre-contraction levels. By contrast, our finding of increased contractile responses to PE in the aorta of hypertensive WT mice is consistent with previous reports (Madhur et al., 2010). Moreover, we clearly demonstrated that the contractile response to PE in WT normotensive mice is modulated by endogenous NO (enhanced by L-NAME), yet this modulation appeared to be lost in WT hypertensive mice. Collectively this data suggests that a hypertension-associated loss in vasodilatory NO may contribute to enhanced contractility to PE, yet this concept is difficult to reconcile with our finding that endothelial function was preserved in hypertensive aortae. However, we have not confirmed that ACh-mediated relaxation in hypertensive aortae is mediated by NO, and an upregulation of other endothelium-derived relaxing factors, such as prostacyclin (PGI_2) or endothelium-derived hyperpolarising factor (EDHF) (Jiang et al., 2016), may serve to compensate for a potential loss in endogenous NO. Future experiments should explore this concept. As discussed in **Chapter 4**, we suggest that augmented contractility to PE may be related to factors such as changes in expression of α1- adrenoceptors (Rodríguez et al., 2020), and/or oxidative stress (Mui et al., 2018; Tsai & Jiang, 2010).

It is interesting to note that genetic deletion of CCR8 did not affect endothelial function, endogenous NO availability (assessed by L-NAME, high variability in response) or smooth muscle vasodilator function in this 28-day Ang II infusion model of hypertension. In addition, the augmented contractile response to PE in Ang II treated mice was maintained in CCR8 KO mice. Indeed, as discussed in **Chapter 4**, genetic deletion of CCR8 per se led to increased contractile efficacy to PE, independent of hypertension. Whilst CCR8 signalling limits adrenoceptor-mediated contractile responses, we also noted that endogenous NO appears to attenuate PE-induced contraction in WT but not hypertensive CCR8 KO mice. At this point it is worth considering the use of the contractile response to the NOS inhibitor, L-NAME as a measure of endogenous NO bioavailability. Prior to addition of L-NAME, care was taken to match the level of pre-contraction with U46619 to ≈25-30 % $F_{max.}$ Nevertheless, we observed a high degree of variability in L-NAME-induced contraction within experimental groups,

despite consistent ACh-induced vasorelaxation. These observations raise concerns with regard to the reliability of the use of L-NAME to assess endogenous vascular NO and in the future more sensitive measures of NO should be adopted. Such measures may include NO staining by 4-amino-5-methylamino-2', 7'-difluorofluorescein (DAF-FM) diacetate and diaminorhodamine (DAR)-4M, or quantification of nitrites and nitrates by a NO quantification kit (Oller et al., 2017). Collectively, our data suggests that CCL8-CCR8 signalling does not contribute to any hypertension-dependent changes in vascular function in the 28d Ang II model in mice.

A key feature of chronic hypertension is the remodelling, fibrosis and stiffening of large elastic arteries. Stiffened arteries do not effectively buffer pulse pressure, leading to higher pulse pressures in the periphery (Briet et al., 2012), and hence the subsequent end-organ damage (Oparil et al., 2003). Relevant mechanical changes in the artery are contributed to by both the thickening of the vessel wall and also the composition of the extracellular matrix. In the current study, Ang II treatment leads to medial thickening and lumen enlargement in the aorta, with unchanged media: lumen ratio. The enlarged and thickened vascular structure indicates outward hypertrophic remodelling (Van Varik et al., 2012), and hypertrophic remodelling of large conductive arteries is very commonly seen in hypertension (Brown et al., 2018). We have also found elastin dysregulation in the vasculature of Ang II treated WT mice, which is consistent with published data (Xu et al., 2019). Other published studies have reported increased adventitial collagen in the same model of hypertension (0.7 mg/kg/d Ang II, 28 days) (Bersi et al., 2016; Chan et al., 2015). As such, our inability to observe a statistically significant increase in collagen deposition in WT hypertensive mice is likely due to small sample sizes, which represents a limitation of the current study. Furthermore, the accumulation of M2 macrophages in the aortic wall has been shown to led to medial thickening, elastin loss and collagen deposition (Moore et al., 2015). Our finding that M2 macrophages express the pro-fibrotic chemokine mCCL8, and the expression of its cognate receptor CCR8 on vascular cell types (endothelial cells and VSMCs) (Haque et al., 2004), led us to hypothesise that the mCCL8-CCR8 axis may play a key role in the large elastic artery remodelling associated with hypertension. However, our study has shown that the genetic deletion of CCR8 does not impact the hypertension-associated hypertrophic remodelling and elastin dysregulation in the aorta and tended to increase, rather than decrease, adventitial

collagen deposition. Whilst these findings were unexpected, they raise a number of considerations with regard to the role of CCR8 signalling in vascular remodelling in hypertension. Thus, whilst CCR8 receptor expression has been reported in vascular cell types (Haque et al., 2004), the current study did not confirm, via immunohistochemical techniques, the expression of CCR8 in the aortic wall or its cellular localisation. Moreover, as will be discussed in further detail later, confirmation that mCCL8 targets CCR8 in collagen generating cells is lacking and given that mCCL1 is also a CCR8 ligand (Haskell et al., 2006), the function of this chemokine may also be impacted in CCR8 KO mice. As such the enhanced collagen deposition in the hypertensive vasculature following genetic deletion of CCR8, may reflect a loss in CCL1-CCR8 signalling. Although we are currently unaware of an anti-fibrotic action of CCL1 in the setting of hypertension, this concept warrants further investigation.

In the setting of hypertension, M2 macrophages are also likely to accumulate in other organs, such as the heart and kidney and contribute to cardiac and renal fibrosis and inflammation (Drummond et al., 2019). In the current study, neither cardiac nor renal fibrosis was evident following 28-day Ang II infusion, and genetic deletion of CCR8 had no impact on these measures. For comparison, there are previous studies that reported increased interstitial collagen in the heart or kidneys using 28-day Ang II treatments in mice, but to our knowledge, they all used higher doses of Ang II (typically above 2.1 mg/kg/d) than that of the current study (0.7 mg/kg/d) (Yu et al., 2018; Zhao et al., 2018). As noted previously, cardiac hypertrophy (increase in heart weight) was evident in WT hypertensive mice suggesting that heart damage may still have occurred. To confirm this, future studies can investigate the expression of cardiac hypertrophic markers, such as atrial natriuretic peptide and osteopontin (Ellmers et al., 2002; Singh et al., 2014). Alternatively, a different pre-clinical model of hypertension may be used to induce more overt cardiac or renal fibrosis and assess the impact of CCR8 deletion. For example, deoxycorticosterone acetate and salt (DOCA-salt) treatment on uninephrectomized mice, alone or in combination with Ang II, can cause severe damage to the heart and kidneys including substantial collagen deposition (Kirchhoff et al., 2008).

As discussed, the infiltration of immune cells, such as monocytes/macrophages, into target organs that play key roles in BP control (e.g. kidney), contribute to the pathophysiology of hypertension (Drummond et al., 2019). Given the chemoattractant properties of hCCL18/mCCL8 (Islam et al., 2011; Schutyser et al., 2005), we wished to determine if negating

mCCL8-CCR8 signalling, via genetic deletion of CCR8, modulated immune cell populations in the aorta, kidney and spleen. Using flow cytometry to measure various types of leukocytes in target organs, we demonstrated no significant change in immune cell populations (total macrophages, M2 macrophages, T cells) in the kidneys of hypertensive WT as compared to normotensive WT mice. The T cell data are consistent with the findings of a published study that used the same 28-day Ang II-induced hypertension model (Chan et al., 2015). Of note, a DOCA-salt mouse model of hypertension, which leads to more severe renal damage than the Ang II models (Kirchhoff et al., 2008), has been reported to cause increased infiltration of total and M2 macrophages in hypertensive kidneys (Krishnan et al., 2016; Krishnan et al., 2019). However, to our knowledge, studies using the Ang II-infusion mouse models of hypertension have not reported total or M2 macrophage cell counts in the kidneys. Interestingly, both normotensive and hypertensive CCR8 KO mice appeared to have ≈65% fewer T cells in their kidneys as compared to their WT counterparts, which may be due to a reduction in the number of CD4+ T cells. CCR8 is expressed on CD4+ T cells (Lim et al., 2017), and is found to mediate the chemotactic effects on these cells in response to CCL1 (Haque et al., 2004). In the kidney, CD4+ T cells produce increased amounts of inflammatory cytokines in response to Ang II treatment, contributing to hypertension-associated renal damage (Wei et al., 2014). Trott et al. (2014) also found that CD8 KO limits sodium and water retention in the mouse kidney, and hence protects mice from hypertension. However, to our knowledge, no published studies have confirmed CCR8 expression on CD8+ T cells in the kidney. In fact, Kremer et al. (2001) reported no detectable CCR8 on CD8+ thymocytes (precursor of CD8 T cells) in mouse thymus. Researchers (McCully et al., 2018) have also reported a much lower (≈30 %) proportion of CCR8+ cells among CD8+ T lymphocytes in human skin, compared to ≈60-80 % among CD4+ T cells. As such, potential effects of CCR8 KO on kidney inflammation/ function are likely to reflect an impact on CD4+ T cells. Nevertheless, together with our data showing that CD4+ and CD8+ T cell counts remain unchanged in the spleen (i.e. unchanged T cell production), it is suggested that CCR8 KO mice have limited T cell infiltration into the kidneys, independent of hypertension.

In mouse aorta, another key target organ of hypertension, published studies have found that Ang II treatment leads to the accumulation of macrophages (especially M2 macrophages) and T lymphocytes (especially CD4+ T cells) (Guzik et al., 2007; Moore et al., 2015). M2

macrophages and CD4+ T cells contribute to hypertension-associated vascular fibrosis and remodelling (Moore et al., 2015), yet the role of CD4+ T cells in hypertension-associated vascular damage remains to be elucidated (Drummond et al., 2019; Guzik et al., 2007). Surprisingly, Ang II infusion in the current study did not lead to an increase in the number of macrophages or T cells in the aorta. Moreover, both normotensive and hypertensive CCR8 KO mice appeared to have an unchanged leukocyte infiltration profile in the aortae as compared to WT mice. When compared to previous studies, the inconsistency of the flow cytometric data we obtained in WT normotensive and hypertensive mice may be explained by limitations in the experimental approach. Thus, only a quarter of the length of the thoracic aorta was stained for cell counting, limiting the number of cells available for assay and possibly accounting for the higher variability and/or lower accuracy of the relevant data. Future studies can overcome this limitation by running the whole length of thoracic aorta for flow cytometric analysis. The insufficient statistical power (due to COVID-19 as explained in **Section 5.1**) for the aorta and kidney data has also increased the difficulty of data interpretation.

To further investigate the role of CCR8 in hypertension, the pharmacological inhibitor, R243 was used. R243 was the only commercially available CCR8 antagonist when relevant experiments were commenced. It has been used previously to assess the pro-metastatic and inflammatory/ chemotactic effects of CCR8 in bladder cancer (Liu et al., 2019) and acute colitis (Oshio et al., 2014), respectively. However, R243 has not been studied in the context of hypertension or other cardiovascular diseases. This study has found that, similar to the genetic deletion of CCR8, R243 does not attenuate the Ang II induced increase in systolic BP in WT mice or change the heart weight/body weight measurements in Ang II treated mice. Endothelial dysfunction was again not observed in this cohort of hypertensive mice, yet R243 treatment of hypertensive mice lead to an improvement in endothelial function. Interestingly, in this 28-day Ang II infusion model, we saw improved endothelial function in R243 treated mice but not in CCR8 KO mice. Such findings may be attributed to the upregulation of compensatory mechanisms in response to the global deletion of CCR8, or to the fact that R243 antagonises not only CCR8 but also CCR2 (Oshio et al., 2014). Since CCR2 may also contribute to hypertension-associated vascular damage by inducing macrophage infiltration into the vasculature (Chan et al., 2012; Moore et al., 2015), a more specific antagonist is required to

study the effects of CCR8 blockade on hypertension. Recently another small molecule antagonist, AZ084, has become commercially available and is highly selective to CCR8 (Connolly et al., 2012). In addition, the lack of statistical power of the organ weight and PE-induced vessel contraction data has prevented us from drawing relevant conclusions (due to COVID-19 as explained in **Section 5.1**). In the future, R243 may be given to CCR8 KO mice so that we can identify whether the observed effects are mediated by CCR8 or CCR2. AZ084 will also be a useful pharmacological tool to selectively antagonise CCR8.

The concept that hCCL18/mCCL8 signal via CCR8 was predicated on the study by Islam et al. (2013) in which it was reported that CCR8 is the CCL18 receptor and that mCCL8 is a functional analogue of hCCL18. Of note, data from the current study suggest otherwise. Islam et al. (2013) observed CCL18-induced calcium mobilisation and chemotaxis of CCR8-expressing human Th2 cells, which, to our knowledge, has not been replicated to date. Our new data using BRET assays in CCR8-expressing CHO cells, provide evidence in support of CCR8 activation by the established agonist, CCL1 (Haskell et al., 2006). By contrast, both hCCL18 and mCCL8 failed to activate CCR8. Moreover, naïve T cells do not express CCR8, but they represent the immune cell population with the highest ability to migrate in response to hCCL18 (Chenivesse & Tsicopoulos, 2018). Collectively these data suggest that hCCL18/mCCL8 may activate receptors other than CCR8, and that targeting CCR8 may not negate the effects of these chemokines in the setting of hypertension, as we had assumed. The lack of CCL18 expression in rodents has made interpretation of relevant results difficult, but when considering hCCL18 per se, relevant receptors may include CCR1, 2, 3, 5, and PITPNM3. Thus, hCCL18 has been reported to antagonise CCR3 and inhibit the actions of CCR1, 2, 5 via displacement of bound agonists (Krohn et al., 2013). However, it is important to note that such actions would confer an anti-inflammatory and/or anti-fibrotic capacity of hCCL18. For example, CCR1 and CCR2 on VSMCs exert pro-fibrotic mechanisms (Seki et al., 2009a; Seki et al., 2009b), and CCR5 expressed on monocytes/ macrophages promotes chemotaxis and fibrosis (Seki et al., 2009a). Another study (Chen et al., 2011) has found that hCCL18 activates PITPNM3, a tumour-associated transmembrane receptor, on breast cancer cells. Whilst PITPNM3, to our knowledge, has not been identified in cardiovascular cell types, it still represents a target which should be considered. Future studies are required to identify the receptors responsible for the actions of hCCL18 in the setting of hypertension. Ultimately, the

use of a binding protein to negate the actions of mCCL8 will also help to delineate its role in hypertension.

In conclusion, genetic deletion of CCR8 does not confer protection against the development of hypertension or the associated end-organ damage, despite a trend towards a reduction in T cell infiltration in the kidney, a key BP controlling organ. Whilst pharmacological targeting of CCR8 (with R243) leads to a modest improvement in endothelial function, it does not impact on BP per se and its effects on end-organ remodelling remain to be determined. Moreover, the lack of selectivity of R243 and our data to indicate that neither hCCL18 nor mCCL8 activate CCR8, raise the possibility that targeting CCR8 does not represent an effective strategy to negate the actions of CCL18 in hypertension. Future studies should focus on identifying the relevant receptor(s) for CCL18 and/or directly studying the role of hCCL18 itself in hypertension. These concepts will be explored further in the General Discussion (**Chapter 6**).

5.8 References

Al-Magableh MR, Kemp-Harper BK, & Hart JL (2015). Hydrogen sulfide treatment reduces blood pressure and oxidative stress in angiotensin II-induced hypertensive mice. Hypertens Res 38**:** 13-20.

Atamas SP, Luzina IG, Choi J, Tsymbalyuk N, Carbonetti NH, Singh IS, Trojanowska M, Jimenez SA, & White B (2003). Pulmonary and Activation-Regulated Chemokine Stimulates Collagen Production in Lung Fibroblasts. Am J Respir Cell Mol Biol 29**:** 743-749.

Bersi MR, Bellini C, Wu J, Montaniel KRC, Harrison DG, & Humphrey JD (2016). Excessive Adventitial Remodeling Leads to Early Aortic Maladaptation in Angiotensin-Induced Hypertension. Hypertension (Dallas, Tex : 1979) 67**:** 890-896.

Briet M, Boutouyrie P, Laurent S, & London GM (2012). Arterial stiffness and pulse pressure in CKD and ESRD. Kidney Int 82**:** 388-400.

Brown IAM, Diederich L, Good ME, DeLalio LJ, Murphy SA, Cortese-Krott MM, Hall JL, Le TH, & Isakson BE (2018). Vascular Smooth Muscle Remodeling in Conductive and Resistance Arteries in Hypertension. Arterioscler Thromb Vasc Biol 38**:** 1969-1985.

Chan CT, Moore JP, Budzyn K, Guida E, Diep H, Vinh A, Jones ES, Widdop RE, Armitage JA, Sakkal S, Ricardo SD, Sobey CG, & Drummond GR (2012). Reversal of vascular macrophage accumulation and hypertension by a CCR2 antagonist in deoxycorticosterone/salt-treated mice. Hypertension 60**:** 1207-1212.

Chan CT, Sobey CG, Lieu M, Ferens D, Kett MM, Diep H, Kim HA, Krishnan SM, Lewis CV, Salimova E, Tipping P, Vinh A, Samuel CS, Peter K, Guzik TJ, Kyaw TS, Toh BH, Bobik A, & Drummond GR (2015). Obligatory Role for B Cells in the Development of Angiotensin II-Dependent Hypertension. Hypertension 66**:** 1023-1033.

Chen J, Yao Y, Gong C, Yu F, Su S, Chen J, Liu B, Deng H, Wang F, Lin L, Yao H, Su F, Anderson Karen S, Liu Q, Ewen Mark E, Yao X, & Song E (2011). CCL18 from Tumor-Associated Macrophages Promotes Breast Cancer Metastasis via PITPNM3. Cancer Cell 19**:** 541-555.

Chenivesse C, & Tsicopoulos A (2018). CCL18 - Beyond chemotaxis. Cytokine 109**:** 52-56.

Connolly S, Skrinjar M, & Rosendahl A (2012). Orally bioavailable allosteric CCR8 antagonists inhibit dendritic cell, T cell and eosinophil migration. Biochem Pharmacol 83**:** 778-787.

Couto GK, Davel AP, Brum PC, & Rossoni LV (2014). Double disruption of α2A- and α2C-adrenoceptors induces endothelial dysfunction in mouse small arteries: role of nitric oxide synthase uncoupling. Exp Physiol 99**:** 1427-1438.

de Jager SCA, Bongaerts BWC, Weber M, Kraaijeveld AO, Rousch M, Dimmeler S, van Dieijen-Visser MP, Cleutjens KBJM, Nelemans PJ, van Berkel TJC, & Biessen EAL (2012). Chemokines CCL3/MIP1α, CCL5/RANTES and CCL18/PARC are Independent Risk Predictors of Short-Term Mortality in Patients with Acute Coronary Syndromes. PLoS One 7**:** e45804.

Diez J (2007). Mechanisms of cardiac fibrosis in hypertension. J Clin Hypertens (Greenwich) 9**:** 546-550.

Drummond GR, Vinh A, Guzik TJ, & Sobey CG (2019). Immune mechanisms of hypertension. Nat Rev Immunol 19**:** 517-532.

Ellmers LJ, Knowles JW, Kim HS, Smithies O, Maeda N, & Cameron VA (2002). Ventricular expression of natriuretic peptides in Npr1(-/-) mice with cardiac hypertrophy and fibrosis. American journal of physiology Heart and circulatory physiology 283**:** H707-H714.

Falkenham A, de Antueno R, Rosin N, Betsch D, Lee TDG, Duncan R, & Légaré J-F (2015). Nonclassical Resident Macrophages Are Important Determinants in the Development of Myocardial Fibrosis. The American Journal of Pathology 185**:** 927-942.

Guiteras R, Flaquer M, & Cruzado JM (2016). Macrophage in chronic kidney disease. Clin Kidney J 9**:** 765-771.

Guzik TJ, Hoch NE, Brown KA, McCann LA, Rahman A, Dikalov S, Goronzy J, Weyand C, & Harrison DG (2007). Role of the T cell in the genesis of angiotensin II induced hypertension and vascular dysfunction. The Journal of experimental medicine 204**:** 2449-2460.

Haque NS, Fallon JT, Pan JJ, Taubman MB, & Harpel PC (2004). Chemokine receptor-8 (CCR8) mediates human vascular smooth muscle cell chemotaxis and metalloproteinase-2 secretion. Blood 103**:** 1296-1304.

Haskell CA, Horuk R, Liang M, Rosser M, Dunning L, Islam I, Kremer L, Gutiérrez J, Marquez G, Martinez-A C, Biscone MJ, Doms RW, & Ribeiro S (2006). Identification and Characterization of a Potent, Selective Nonpeptide Agonist of the CC Chemokine Receptor CCR8. Mol Pharmacol 69**:** 309.

Islam SA, Chang DS, Colvin RA, Byrne MH, McCully ML, Moser B, Lira SA, Charo IF, & Luster AD (2011). Mouse CCL8, a CCR8 agonist, promotes atopic dermatitis by recruiting IL-5+ TH2 cells. Nat Immunol 12**:** 167-177.

Islam SA, Ling MF, Leung J, Shreffler WG, & Luster AD (2013). Identification of human CCR8 as a CCL18 receptor. J Exp Med 210**:** 1889-1898.

Jiang J, Zheng JP, Li Y, Gan Z, Jiang Y, Huang D, Li H, Liu Z, & Ke Y (2016). Differential contribution of endothelium-derived relaxing factors to vascular reactivity in conduit and resistance arteries from normotensive and hypertensive rats. Clin Exp Hypertens 38**:** 393-398.

Kirchhoff F, Krebs C, Abdulhag UN, Meyer-Schwesinger C, Maas R, Helmchen U, Hilgers KF, Wolf G, Stahl RA, & Wenzel U (2008). Rapid development of severe end-organ damage in C57BL/6 mice by combining DOCA salt and angiotensin II. Kidney Int 73**:** 643-650.

Kraaijeveld AO, de Jager SC, de Jager WJ, Prakken BJ, McColl SR, Haspels I, Putter H, van Berkel TJ, Nagelkerken L, Jukema JW, & Biessen EA (2007). CC chemokine ligand-5 (CCL5/RANTES) and CC chemokine ligand-18 (CCL18/PARC) are specific markers of refractory unstable angina pectoris and are transiently raised during severe ischemic symptoms. Circulation 116**:** 1931-1941.

Kremer L, Carramolino L, Goya I, Zaballos A, Gutiérrez J, Moreno-Ortiz MdC, Martínez AC, & Márquez G (2001). The transient expression of C-C chemokine receptor 8 in thymus identifies a thymocyte subset committed to become CD4+ single-positive T cells. J Immunol 166**:** 218-225.

Krishnan SM, Dowling JK, Ling YH, Diep H, Chan CT, Ferens D, Kett MM, Pinar A, Samuel CS, Vinh A, Arumugam TV, Hewitson TD, Kemp-Harper BK, Robertson AAB, Cooper MA, Latz E, Mansell A, Sobey CG, & Drummond GR (2016). Inflammasome activity is essential for one kidney/deoxycorticosterone acetate/salt-induced hypertension in mice. Br J Pharmacol 173**:** 752-765.

Krishnan SM, Ling YH, Huuskes BM, Ferens DM, Saini N, Chan CT, Diep H, Kett MM, Samuel CS, Kemp-Harper BK, Robertson AAB, Cooper MA, Peter K, Latz E, Mansell AS, Sobey CG, Drummond GR, & Vinh A (2019). Pharmacological inhibition of the NLRP3 inflammasome reduces blood pressure, renal damage, and dysfunction in salt-sensitive hypertension. Cardiovasc Res 115**:** 776-787.

Krohn SC, Bonvin P, & Proudfoot AE (2013). CCL18 exhibits a regulatory role through inhibition of receptor and glycosaminoglycan binding. PLoS One 8**:** e72321.

Lewis C (2017). Investigating the roles of distinct macrophage phenotypes in cardiovascular disease. PhD thesis: Monash University, Melbourne.

Lim JY, Ryu DB, Lee SE, Park G, & Min CK (2017). Mesenchymal Stem Cells (MSCs) Attenuate Cutaneous Sclerodermatous Graft-Versus-Host Disease (Scl-GVHD) through Inhibition of Immune Cell Infiltration in a Mouse Model. J Invest Dermatol 137**:** 1895-1904.

Liu X, Xu X, Deng W, Huang M, Wu Y, Zhou Z, Zhu K, Wang Y, Cheng X, Zhou X, Chen L, Li Y, Wang G, & Fu B (2019). CCL18 enhances migration, invasion and EMT by binding CCR8 in bladder cancer cells. Mol Med Report 19**:** 1678-1686.

Liu Z, Kuang W, Zhou Q, & Zhang Y (2018). TGF-β1 secreted by M2 phenotype macrophages enhances the stemness and migration of glioma cells via the SMAD2/3 signalling pathway. Int J Mol Med 42**:** 3395-3403.

Madhur MS, Lob HE, McCann LA, Iwakura Y, Blinder Y, Guzik TJ, & Harrison DG (2010). Interleukin 17 promotes angiotensin II-induced hypertension and vascular dysfunction. Hypertension 55**:** 500-507.

McCully ML, Ladell K, Andrews R, Jones RE, Miners KL, Roger L, Baird DM, Cameron MJ, Jessop ZM, Whitaker IS, Davies EL, Price DA, & Moser B (2018). CCR8 Expression Defines Tissue-Resident Memory T Cells in Human Skin. Journal of immunology (Baltimore, Md : 1950) 200**:** 1639-1650.

McLellan MA, Skelly DA, Dona MSI, Squiers GT, Farrugia GE, Gaynor TL, Cohen CD, Pandey R, Diep H, Vinh A, Rosenthal NA, & Pinto AR (2020). High-Resolution Transcriptomic Profiling of the Heart During Chronic Stress Reveals Cellular Drivers of Cardiac Fibrosis and Hypertrophy. Circulation.

Moore JP, Vinh A, Tuck KL, Sakkal S, Krishnan SM, Chan CT, Lieu M, Samuel CS, Diep H, Kemp-Harper BK, Tare M, Ricardo SD, Guzik TJ, Sobey CG, & Drummond GR (2015). M2 macrophage accumulation in the aortic wall during angiotensin ii infusion in mice is associated with fibrosis, elastin loss, and elevated blood pressure. Am J Physiol Heart Circ Physiol 309**:** H906-H917.

Mui RK, Fernandes RN, Garver HG, Van Rooijen N, & Galligan JJ (2018). Macrophage-dependent impairment of α(2)-adrenergic autoreceptor inhibition of Ca(2+) channels in sympathetic neurons from DOCA-salt but not high-fat diet-induced hypertensive rats. American journal of physiology Heart and circulatory physiology 314**:** H863-H877.

Oller J, Méndez-Barbero N, Ruiz EJ, Villahoz S, Renard M, Canelas LI, Briones AM, Alberca R, Lozano-Vidal N, Hurlé MA, Milewicz D, Evangelista A, Salaices M, Nistal JF, Jiménez-Borreguero LJ, De Backer J, Campanero MR, & Redondo JM (2017). Nitric oxide mediates aortic disease in mice deficient in the metalloprotease Adamts1 and in a mouse model of Marfan syndrome. Nat Med 23**:** 200-212.

Oparil S, Zaman MA, & Calhoun DA (2003). Pathogenesis of Hypertension. Ann Intern Med 139**:** 761-776.

Oshio T, Kawashima R, Kawamura YI, Hagiwara T, Mizutani N, Okada T, Otsubo T, Inagaki-Ohara K, Matsukawa A, Haga T, Kakuta S, Iwakura Y, Hosokawa S, & Dohi T (2014). Chemokine receptor CCR8 is required for lipopolysaccharide-triggered cytokine production in mouse peritoneal macrophages. PLoS One 9**:** e94445.

Rodríguez JE, Ruiz-Hernández A, Hernández-DíazCouder A, Huang F, Hong E, & Villafaña S (2020). Chronic diabetes and hypertension impair the in vivo functional response to phenylephrine independent of α1-adrenoceptor expression. Eur J Pharmacol 883: 173283.

Schutyser E, Richmond A, & Van Damme J (2005). Involvement of CC chemokine ligand 18 (CCL18) in normal and pathological processes. J Leukoc Biol 78**:** 14-26.

Seki E, De Minicis S, Gwak GY, Kluwe J, Inokuchi S, Bursill CA, Llovet JM, Brenner DA, & Schwabe RF (2009a). CCR1 and CCR5 promote hepatic fibrosis in mice. J Clin Invest 119**:** 1858-1870.

Seki E, de Minicis S, Inokuchi S, Taura K, Miyai K, van Rooijen N, Schwabe RF, & Brenner DA (2009b). CCR2 promotes hepatic fibrosis in mice. Hepatology 50**:** 185-197.

Singh M, Dalal S, & Singh K (2014). Osteopontin: At the cross-roads of myocyte survival and myocardial function. Life Sci 118**:** 1-6.

Tanaka Y, Funabiki M, Michikawa H, & Koike K (2006). Effects of aging on alpha1-adrenoceptor mechanisms in the isolated mouse aortic preparation. J Smooth Muscle Res 42**:** 131-138.

Trott DW, Thabet SR, Kirabo A, Saleh MA, Itani H, Norlander AE, Wu J, Goldstein A, Arendshorst WJ, Madhur MS, Chen W, Li C-I, Shyr Y, & Harrison DG (2014). Oligoclonal CD8+ T cells play a critical role in the development of hypertension. Hypertension (Dallas, Tex : 1979) 64**:** 1108-1115.

Tsai MH, & Jiang MJ (2010). Reactive oxygen species are involved in regulating alpha1-adrenoceptor-activated vascular smooth muscle contraction. J Biomed Sci 17**:** 67.

Van Varik B, Rennenberg R, Reutelingsperger C, Kroon A, de Leeuw P, & Schurgers L (2012). Mechanisms of arterial remodeling: lessons from genetic diseases. Frontiers in Genetics 3.

Versteylen MO, Manca M, Joosen IA, Schmidt DE, Das M, Hofstra L, Crijns HJ, Biessen EA, & Kietselaer BL (2016). CC chemokine ligands in patients presenting with stable chest pain: association with atherosclerosis and future cardiovascular events. Netherlands heart journal : monthly journal of the Netherlands Society of Cardiology and the Netherlands Heart Foundation 24**:** 722-729.

Vrančić M, Banjanac M, Nujić K, Bosnar M, Murati T, Munić V, Stupin Polančec D, Belamarić D, Parnham MJ, & Eraković Haber V (2012). Azithromycin distinctively modulates classical activation of human monocytes in vitro. Br J Pharmacol 165**:** 1348-1360.

Wei Z, Spizzo I, Diep H, Drummond GR, Widdop RE, & Vinh A (2014). Differential Phenotypes of Tissue-Infiltrating T Cells during Angiotensin II-Induced Hypertension in Mice. PLoS One 9**:** e114895.

Xu H, Du S, Fang B, Li C, Jia X, Zheng S, Wang S, Li Q, Su W, Wang N, Zheng F, Chen L, Zhang X, Gustafsson J-Å, & Guan Y (2019). VSMC-specific EP4 deletion exacerbates angiotensin II-induced aortic dissection by increasing vascular inflammation and blood pressure. Proceedings of the National Academy of Sciences 116**:** 8457.

Yamamoto Y, & Koike K (2001). alpha(1)-Adrenoceptor subtypes in the mouse mesenteric artery and abdominal aorta. Br J Pharmacol 134**:** 1045-1054.

Yu X, Xia Y, Zeng L, Zhang X, Chen L, Yan S, Zhang R, Zhao C, Zeng Z, Shu Y, Huang S, Lei J, Yuan C, Zhang L, Feng Y, Liu W, Huang B, Zhang B, Luo W, Wang X, Zhang H, Haydon RC, Luu HH, He TC, & Gan H (2018). A blockade of PI3Kγ signaling effectively mitigates angiotensin II-induced renal injury and fibrosis in a mouse model. Sci Rep 8**:** 10988.

Zhao W, Chen SS, Chen Y, Ahokas RA, & Sun Y (2008). Kidney fibrosis in hypertensive rats: role of oxidative stress. Am J Nephrol 28**:** 548-554.

Zhao W, Zhao T, Chen Y, Bhattacharya SK, Lu L, & Sun Y (2018). Differential Expression of Hypertensive Phenotypes in BXD Mouse Strains in Response to Angiotensin II. Am J Hypertens 31**:** 108-114.

Zhu M (2016). CCL18 as a mediator of the pro-fibrotic actions of M2 macrophages in the vessel wall during hypertension. Honours thesis: Monash University, Melbourne.

5.9 Supplementary figures

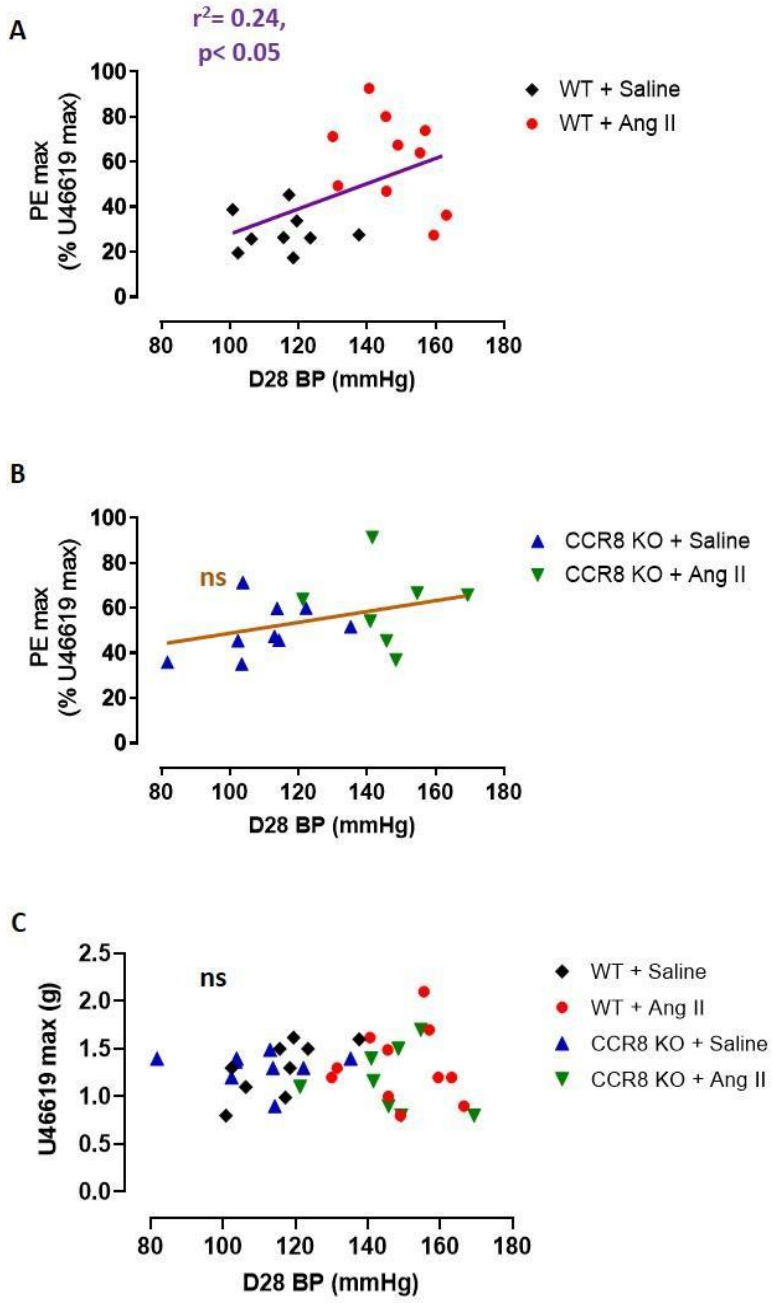

Supplementary Figure 1. Correlation of maximal phenylephrine contraction (PE max) with final day systolic BP (D28 BP) in WT and CCR8 KO mice. Wildtype (WT; **A**) and CCR8 knockout (CCR8 KO; **B**) mice were treated with saline or Ang II (0.7 mg/kg/d) for 28 days, and the maximum contraction to PE in the isolated abdominal aorta correlated with the D28 BP reading. (**C**) Correlation of the maximal U46619 contraction (U4 max) with D28 BP. PE max data were expressed as % of U46619 max. Data presented as individual points, (A-B) n= 7-10, (C) n= 37. Linear regression analysis, ns = no statistical significance.

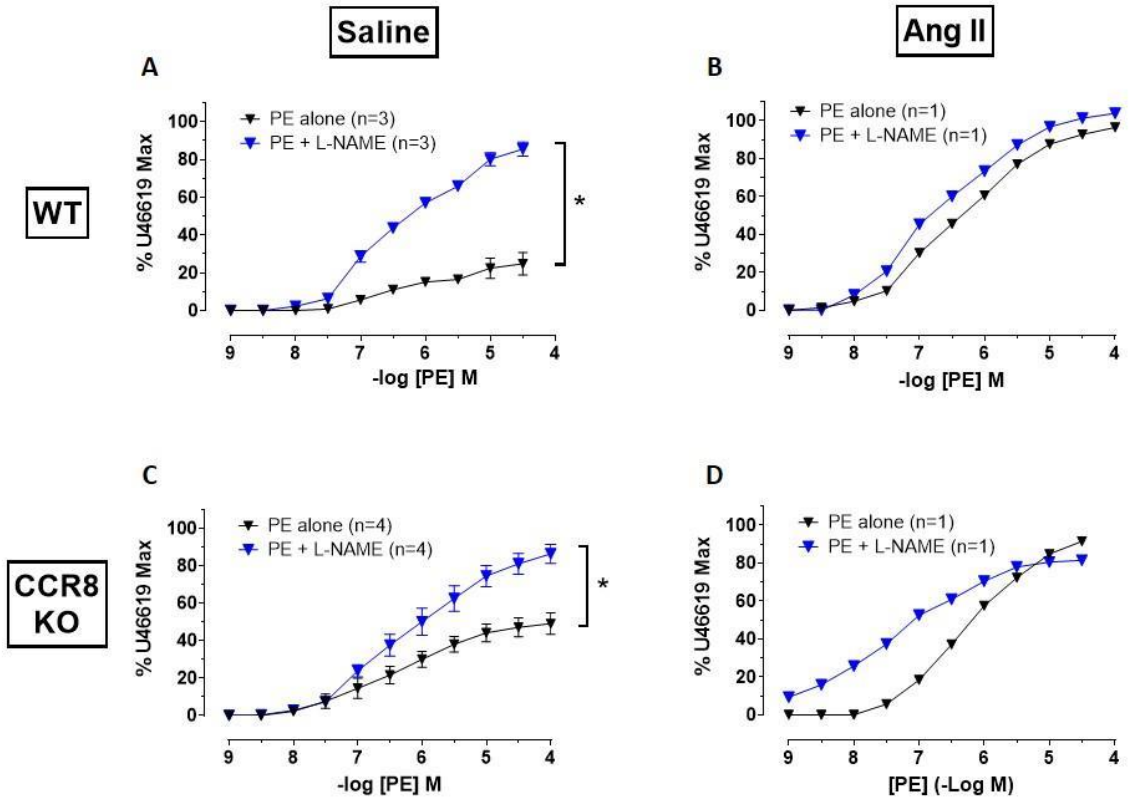

Supplementary Figure 2. Effects of L-NAME and genetic deletion of CCR8 on PE-induced contraction in the abdominal aorta of saline- and Ang II-treated mice. Cumulative concentration-response curves to phenylephrine (PE), in the absence or presence of L-NAME (100 µM), in saline- and Ang II-treated WT (**A-B**) and CCR8 KO (**C-D**) male mice. WT and CCR8 KO mice were treated with saline (left panel) or Ang II (0.7 mg/kg/d; right panel) for 28 days. Data expressed as % of the maximal U46619 contraction. Data presented as mean ± SEM (when n ≥3) or mean (when n<3). * p<0.05 vs. PE alone, Student's unpaired t-test.

Chapter 6

General Discussion

6.1 Summary of key findings

Hypertension is associated with fibrosis and damage of end-organs such as the heart, kidneys, and the vasculature (Diez, 2007; Oparil et al., 2003; Zhao et al., 2008). Such organ damage puts patients, especially those with resistant hypertension, at significantly increased risk of major cardiovascular events (Daugherty et al., 2012). It has been found that M2 macrophages play a crucial role in hypertension and its associated end-organ damage (Drummond et al., 2019), and preliminary data from our laboratory suggest that CCL18 is the mediator of the profibrotic functions of M2 macrophages in hypertension. As such, this thesis investigates the role of CCL18, and its recently identified receptor CCR8 (Islam et al., 2013), in hypertension. **Chapter 3** provides the first evidence that CCL18 is elevated in the plasma of resistant hypertensive patients, and can promote vascular fibrosis via targeting human aortic adventitial fibroblasts (AoAFs) and aortic endothelial cells (HAECs). Genetic deletion, or pharmacological inhibition, of CCR8 in mice does not modulate the development of chronic hypertension (induced by 14 or 28 days of Ang II treatment) (**Chapters 4-5**). Based upon the lack of impact of CCR8 deletion on the pathogenesis of hypertension and CCR8 signalling assays (Bioluminescence Resonance Energy Transfer assays; BRET assays), we suggest that CCR8 may not be the cognate receptor of CCL18 (**Chapter 5**). These findings have provided novel information with regard to the role of CCL18 and CCR8 in hypertension, which lead to implications on future research directions with high relevance to the clinical management of hypertension (**detailed in sections 6.2-6.4**).

6.2 Effects of genetic or pharmacological targeting of CCR8 on hypertensive male and female mice

To explore the potential contribution of the CCL18-CCR8 axis in hypertension, two time-courses of Ang II induced hypertension (0.7 mg/kg/d, 14-day or 28-day treatment; **Chapters 3-4**) were utilised in wild-type (WT) and CCR8 knockout (KO) mice. The prolonged Ang II treatment (28-day) is associated with more extensive end-organ damage than the 14-day Ang II treatment. In addition, pharmacological inhibition of CCR8 in hypertensive WT mice was

achieved via treatment with the CCR8 antagonist, R243 (1.1 mg/kg/d; **Chapter 4**), given as an intervention in the 28-day Ang II treatment period. Systolic blood pressure (BP) and hypertension-associated organ damage (aorta, kidneys and heart) were assessed. To date, these are the first studies to investigate the role of CCR8 in hypertension.

6.2.1 Effects of genetic deletion of CCR8 on Ang II-induced hypertension in mice (14-day and 28-day)

BP elevation

Ang II infusion in both male and female mice caused a robust increase in BP. Whilst the increase of BP in females at the end of the 14-day period was the same as males, the BP elevation was delayed in females. This suggests there is a degree of protection against the development of hypertension in female mice. In fact, until the sixth decade of life, men have higher BP than females (Mozaffarian et al., 2015), whereas the relevant mechanisms underlying this protection remain unclear. In animal models of hypertension, studies have reported that T cells in male mice have a higher ability to migrate and infiltrate into target organs, as compared to female mice (Ji et al., 2014; Pollow Dennis et al., 2014). Hypertensive female rats also have a higher proportion of regulatory T cells in the kidneys than their male counterparts (Zimmerman et al., 2014), which may also be protective due to the anti-inflammatory property of regulatory T cells. As such, the observed delay of BP elevation in female mice may be related to sex differences in immune mechanisms of hypertension. However, the genetic deletion of CCR8 did not impact the pressor response to Ang II in either male or female mice.

Renal damage

Although we found that the genetic deletion of CCR8 did not limit the BP elevation in response to Ang II treatment in mice in both the 14-day and the 28-day hypertension models, it was important to explore the effects of global deletion of CCR8 on hypertension-associated organ damage. To achieve this objective, hypertension was established in mice over a shorter-term (14-day) and more prolonged (28-day) period, with damage to the aorta, heart and kidney assessed. Our finding that kidney damage, assessed via a change in weight or collagen

deposition, was not evident in the Ang II-induced models of hypertension used, is consistent with published literature. Kidney damage was not observed in mice treated with 14 days of Ang II infusion at a higher dose (2.16 mg/kg/d) (Kirchhoff et al., 2008). Moreover, to our knowledge, studies that report kidney fibrosis in mice treated with 28 days of Ang II all use higher doses of Ang II (typically >2.1 mg/kg/d) as compared to the current study (0.7 mg/kg/d) (Yu et al., 2018; Zhao et al., 2018). Indeed, the Ang II infusion model of hypertension has been used primarily to study hypertension-associated vascular damage. As such, to interrogate the impact of a loss of CCR8 on kidney damage and function, a different hypertension model, such as the deoxycorticosterone acetate (DOCA)-salt rodent model that is known to cause kidney damage (Basting & Lazartigues, 2017), together with markers of renal injury (e.g. kidney-injury molecule-1) and function (glomerular filtration rate), should be used in future studies.

The immune system plays a key role in hypertension. Indeed, immune cell infiltration into BP controlling organs such as the kidney can lead to chronic inflammation and disrupt their ability to regulate BP (Drummond et al., 2019; Sierra-Filardi et al., 2014). Thus, although kidney damage was not clearly evident, we wished to determine if immune cell infiltration was evident in the hypertension models. In line with the kidney weight and fibrosis data, flow cytometric analysis revealed no change in leukocyte infiltration into hypertensive kidneys following 28 days treatment with Ang II, which is again consistent with published data (Chan et al., 2015). However, it is important to note that flow cytometry experiments were only performed for our 28-day model of hypertension, but not the 14-day model. In fact, some published studies have shown an increase in total T cell (CD3+) accumulation in the hypertensive kidneys, using a 14-day mouse model of hypertension (0.7 mg/kg/d Ang II treatment) (Wei et al., 2014). This leads to the hypothesis that T cell infiltration into kidneys occurs at earlier stages of hypertension. Effector T cells can subsequently attract other immune cells (e.g. monocytes/macrophages) into the kidney as well as directly influencing renal sodium and water reabsorption via the release of cytokines such as interferon-ϒ (IFN-γ) (Drummond et al., 2019). When considering T cell subsets, studies using the 14-day Ang II hypertension model have also found that CD4+ T cells accumulate in the kidneys, as well as aortae, to a larger extent than CD8+ T cells (Guzik et al., 2007; Wei et al., 2014). However, the role of CD4+ T cells in hypertension remains controversial, such that mice deficient in total T and B lymphocytes ($Rag1^{-/-}$ mice) are protected from Ang II-induced (14 days) hypertension,

yet adoptive transfer of CD4+ T cells fails to restore hypertension in Rag1$^{-/-}$ mice (Trott et al. (2014)). By contrast CD8+ T cells are thought to play a key role, being antigenically activated and their deficiency conferring protection against Ang II-induced BP elevation and vascular remodelling in the kidney in mice (Trott et al. (2014). As such, based upon our finding that global deletion of CCR8 in male mice, was associated with reduced infiltration of T cells, especially CD8+ T cells, into the kidney of both normotensive and hypertensive mice, we may have anticipated that CCR8 KO mice would be protected to an extent, from Ang II-induced hypertension and kidney damage. The apparent reduction in kidney T cell infiltration in normotensive CCR8 KO mice, is not surprising given the known ability of CCR8 to mediate the infiltration of T cells into sites of inflammation (Connolly et al., 2012). Future studies should use flow cytometric analysis to confirm, in the 14-day Ang II-infusion model, an elevation in T cells in the kidney and a reduction in CCR8 KO mice. Moreover, investigating the impact of genetic deletion of CCR8 on the associated vascular remodelling (vascular rarefaction) in the kidney may provide a more comprehensive insight into the role of CCR8 signalling in the pathogenesis of hypertension.

Vascular damage

It is well recognised that chronic hypertension is associated with stiffening of large elastic arteries (e.g. aorta), which is determined by both the mechanical properties of the vessel wall (e.g. thickness vessel wall, extracellular matrix composition) and smooth muscle tone (Brown et al., 2018; Cocciolone et al., 2018). Such stiffening reduces the capacity to buffer pulse pressure leading to damage to the microvasculature and end-organs (Briet et al., 2012). As such a key focus of this thesis was hypertension-associated vascular damage. Although the 14-day Ang II hypertension model may be more appropriate to study renal inflammation, hypertension-associated vascular damage appears to be more prominent at later stages of the disease. Specifically, 28 days of Ang II treatment caused more apparent medial thickening and elastin dysregulation in the aortae of WT male mice, as compared to those treated with Ang II for 14 days. Published studies have reported medial thickening induced by both 14 and 28 days of Ang II infusion (Moore et al., 2015; Williams et al., 2019). However, to our knowledge, elastin dysregulation (with Verhoeff-Van Gieson staining) has only been associated with the use of higher doses of Ang II (e.g. 2.1 mg/kg/d, 14d-day) (Cui et al., 2016) or following longer treatment periods (> 14 days, e.g. 0.7 mg/kg/d, 28-day) (Moore et al.,

2015). A key contributor to aortic stiffening is the increased deposition of collagen within the vascular wall (Cocciolone et al., 2018). Aortic collagen content was assessed using picrosirius red staining, and it should be noted that the quantification methods used in the 14- and 28-day Ang II infusion models differed slightly. Thus the % staining of adventitial area was measured for the 14-day model, whilst the area of adventitial collagen was quantified for the 28-day model, due to the apparent medial thickening caused by 28 days of Ang II treatment. Both quantification methods revealed a trend for vascular fibrosis in hypertensive WT mice, which failed to reach statistical significance. The 14-day and 28-day Ang II models utilised in our studies are well known to cause increased adventitial collagen deposition (Bersi et al., 2016; Nosalski et al., 2020), whilst it is important to note that both picrosirius red and Masson's Trichrome staining are commonly used to assess vascular collagen content (Chen et al., 2011a). It is likely that the failure to observe a significant increase in collagen content in aortae from Ang II treated mice, was due to low sample sizes and insufficient statistical power due to the impacts of COVID-19 (detailed in **Sections 4.1 and 5.1**). We anticipate that the 28-day Ang II model of hypertension would lead to more robust vascular remodelling in male mice than the 14-day model, and future studies using larger sample sizes and/or using Masson's Trichrome to stain for collagen are required. Of note, the above-mentioned end-point measures were not performed in female mice, as they have been found to be protected from Ang II-induced vascular dysfunction (detailed in the following paragraph).

As highlighted, smooth muscle tone is central to arterial compliance/stiffness. An increase in smooth muscle tone, in large conduit arteries, as a consequence of vascular dysfunction (endothelial dysfunction and/or increased vascular smooth muscle contractility), is associated with hypertension (Oparil et al., 2003). In the current studies, WT male and female mice did not develop significant endothelial dysfunction after a 14- or 28-day Ang II treatment (0.7 mg/kg/d). As discussed in Chapters 4-5, although this finding is inconsistent with published literature (Al-Magableh et al., 2015; Madhur et al., 2010), other unpublished studies from our laboratory or our collaborators have also observed a lack of endothelial dysfunction. Such inconsistencies may be due to differences in experimental design, such as baseline tension and precontraction levels prior to the construction of relaxation curves to the endothelium-dependent dilator, acetylcholine (ACh). On the other hand, contractility to the α_1-adrenoceptor agonist, phenylephrine (PE) was augmented in the aortae of WT hypertensive

male mice (in both the 14-day and 28-day models) as compared to their normotensive counterparts. These findings were consistent with published data in the same pre-clinical model of hypertension (Madhur et al., 2010; Seto et al., 2013). Increased responsiveness to PE in the setting of hypertension, is often indicative of a loss in the modulatory actions of endogenous nitric oxide (NO) (Al-Magableh et al., 2015). Indeed, our findings provided evidence for an ability of NO to modulate PE-induced contraction, such that the contractility to PE was increased in the presence of L-NAME (NO synthase inhibitor) in the normotensive, but not hypertensive, vasculature. However, whether the enhanced contractility to PE in the Ang II infusion model of hypertension is due to a loss in endogenous NO remains unclear. Thus, we did not have direct evidence of either endothelial dysfunction (maintained ACh vasorelaxation) or a reduction in endogenous NO generation (ascertained via contraction to L-NAME) in aortae from hypertensive WT mice. Given contractile responses of aortae to L-NAME alone do not differ between treatment groups, we suggest that L-NAME alone may not be an adequate indicator of endogenous NO. On this basis, L-NAME was not used to investigate the effects of R243 (CCR8 antagonist) on hypertension-associated vascular damage. Collectively, our findings do not support endothelial dysfunction in either the 14 day or 28-day Ang II infusion models of hypertension, and the augmented response to PE may be related to changes in the expression and/or receptor-effector coupling of α_1-adrenoceptors (Rodríguez et al., 2020). Regardless of the mechanisms underlying the enhanced contractility of hypertensive aortae to PE, we have shown that the PE response is positively correlated with systolic BP in WT male mice, in both the 14-day and the 28-day hypertension models. We propose that aortic PE contraction may serve as an indicator of systolic BP in WT male mice. On the contrary, female mice are found to be protected from enhanced PE contractility caused by Ang II treatment, hence other end-point measurements on vascular damage have been mainly performed on male mice. Of note, the absence of the increase in PE contractility in females may be due to the fact that over the 14 days of Ang II infusion, BP was elevated for a shorter period of time in females as compared to males.

A growing body of evidence suggests that vascular inflammation may underpin the vascular remodelling, fibrosis and dysfunction that occurs in chronic hypertension (Drummond et al., 2019). There is evidence that monocytes and macrophages contribute to vascular damage in hypertension. In brief, during the early stages of hypertension (e.g. first 7 days), M1

macrophages in the vascular wall play a role in recruiting pro-inflammatory natural killer cells, and promoting oxidative stress and endothelial dysfunction (Kossmann et al., 2014). During the later stages of hypertension (2-4 weeks Ang II infusion), the M2 subset of macrophages contribute to vascular fibrosis and stiffening (Moore et al., 2015). In this thesis, we have provided evidence for the presence of vascular inflammation in both the 14- and 28-day Ang II models of hypertension in WT mice. Specifically, the expression of murine CCL8 (mCCL8), the functional analogue of human CCL18 (hCCL8) (Islam et al., 2013), was increased in the vasculature of hypertensive mice following both 14 (measured via PCR) and 28 (scRNA-sequencing) days of Ang II treatment. mCCL8 is a M2 macrophage-derived pro-inflammatory chemokine (Islam et al., 2011) and based upon the scRNA-sequencing data, we propose that M2 macrophages are the predominant source of this chemokine in hypertension. This concept is further supported by a published study in which an elevation in both mCCL8 and M2 macrophages was observed in the hypertensive mouse vasculature (Moore et al., 2015). Unexpectedly, our flow cytometric analysis of aortic samples from 28-day Ang II treated mice did not show increased leukocyte (CD45+), macrophage (F480+) or M2 macrophage (CD206+) infiltration into the hypertensive vasculature. **As discussed in Chapter 5**, this flow cytometric data is inconsistent with published literature (Moore et al., 2015). Such a discrepancy may be due to the lack of statistical power and/or a small number of aortic cells processed in each sample, which can cause higher data variability and/or lower data accuracy.

Having characterised the vascular changes associated with shorter-term and more prolonged hypertension, we sought to assess the impact of genetic deletion of CCR8 on aortic function and remodelling. In this regard, genetic deletion of CCR8 led to several vascular changes that were primarily independent of hypertension. Though we proposed that a loss in CCR8 would limit vascular dysfunction, we observed an augmented contractility to PE in aortae from normotensive CCR8 KO male mice as compared to their WT counterparts, an effect which was sustained in hypertension. A similar trend was observed in female CCR8 KO mice. As discussed in **Chapter 4**, the underlying reasons for this modulation of α_1-adrenoceptor signalling by CCR8 are currently unknown but such an interaction may explain why PE contractility is positively correlated with BP in WT but not CCR8 KO mice (in both the 14-day and the 28-day model). Unexpectedly, following 14 days of Ang II infusion, we observed an improvement in ACh-induced vasorelaxation in the aorta of male hypertensive CCR8 KO mice, as compared to

hypertensive WT mice. Such an improvement was not apparent in female mice or following 28 days of Ang II treatment. Such observations may indicate that in males CCR8 signalling attenuates endothelial function early in the development of hypertension and such an impact is lost in the later stages of the disease. However, it remains possible that the apparent time-dependent differences observed reflect the distinct cohorts of WT and CCR8 KO mice used. It is important to note that the CCR8 KO and WT mice used in the 14-day Ang II model were littermates, whilst the 28-day Ang II model did not use littermates due to time constraints and the limited number of CCR8 KO mice generated via heterozygous ($CCR8^{+/-}$) x heterozygous ($CCR8^{+/-}$) breeding. Consequently, the data generated using the 14-day Ang II-infusion model, may be more robust and provide evidence to support targeting of CCR8 to improve endothelial function in hypertension. Future studies should confirm these findings and include a saline treated CCR8 KO group for comparison in the 14-day Ang II model and use WT and CCR8 KO littermates in the 28-day Ang II treatment groups.

In relation to vascular inflammation, we made the interesting observation that a loss in CCR8 attenuated the hypertension-associated (14-day Ang II) increase in aortic mCCL8 expression. Such a finding may be indicative of a decrease in M2 macrophages in the vascular wall and/or reduced generation of mCCL8 from this macrophage subtype. Given M2 macrophage content was not decreased in hypertensive CCR8 KO mice, at least following 28 days of Ang II infusion, we propose that, like hCCL18 (Schraufstatter et al., 2012), mCCL8 act on M2 macrophages to further promote mCCL8 generation in an autocrine or paracrine manner, creating a positive feedback loop. It remains to be determined if aortic mCCL8 levels are modulated similarly, following genetic deletion of CCR8, in the later stages of hypertension. Collectively our findings suggest that in the hypertensive vasculature negating CCR8 signalling may improve endothelial function and limit the impact of the chemoattractant and pro-fibrotic chemokine, mCCL8.

Cardiac damage

Similar to the findings with regard to vascular damage, the 28-day hypertension model seems to be better suited than the 14-day model to study hypertension-associated cardiac damage. Thus, whilst cardiac hypertrophy (increase heart weight) was evident in female mice following 14 days of Ang II treatment, a consistent increase in heart weight was only observed following

28 days of Ang II treatment in male mice. The data from female mice (14-day model) and male mice (14- and 28-day models) are all consistent with published findings (Kirchhoff et al., 2008; Li et al., 2007; Moore et al., 2015). As discussed in **Chapter 4**, the observed sex difference may be due to the different types of cardiac hypertrophy present in hypertensive males and females. Hypertensive male patients tend to develop eccentric cardiac hypertrophy, whereas female patients with systemic hypertension most commonly develop concentric cardiac hypertrophy (Kessler et al., 2019). Compared to eccentric hypertrophy, concentric cardiac hypertrophy is associated with a greater left ventricular mass (de Simone, 2004), and may thereby contribute to the early-stage heart weight increase in female hypertensive mice. Eccentric cardiac hypertrophy in men is also associated with heart failure with reduced ejection fraction (HFrEF), as opposed to concentric cardiac hypertrophy in females being associated with heart failure with preserved ejection fraction (HFpEF) (de Simone, 2004). Importantly, hypertension is a risk factor for both types of heart failure (Dunlay et al., 2017), and patients who develop HFrEF have a higher mortality rate than those who develop HFpEF (Chioncel et al., 2017), which may place male hypertensive patients under a greater risk of fatal cardiovascular events than females. The underlying mechanisms leading to these sex differences are currently under investigation, where researchers have suggested that estrogen and estrogen receptor-beta (ER-β) may protect pre-menopausal women from cardiac damage (Kessler et al., 2019).

Whilst cardiac hypertrophy was evident in the current study, cardiac fibrosis was not detected in hypertensive WT mice (28-day model). These findings contrast a previous study in the 28-day Ang II infusion model, which reported interstitial collagen deposition in the heart, albeit using a higher dose of Ang II than ourselves (Yu et al., 2018). Therefore, whilst our 28-day Ang II model causes more robust cardiac hypertrophy than the 14-day model, other hypertension models may still be required to assess the associated cardiac fibrosis. Indeed, in combination with Ang II, a DOCA-salt rodent model can cause substantial cardiac damage including fibrosis (Kirchhoff et al., 2008).

Cardiac hypertrophy and fibrosis, in the setting of hypertension, have been associated with inflammation. Moreover, toll-like receptor 3 (TLR-3) and TLR-4, key components of the innate immune system, have recently been shown to mediate Ang II-induced cardiac hypertrophy in mice (Singh et al., 2019). Although the profile of infiltrating leukocytes into the heart following

Ang II infusion was not examined, based upon our findings in the hypertensive kidney we anticipate that genetic deletion of CCR8 would modulate T cell infiltration/ functioning, rather than the innate immune cell (macrophage) populations. As such, the finding that cardiac hypertrophy was sustained in hypertensive CCR8 KO mice, may reflect the more prominent role of monocytes/macrophages in cardiac hypertrophy and an inability of CCR8 signalling to modulate infiltration of this immune cell population.

Summarising the effects of CCR8 genetic deletion

In the setting of hypertension, the modest effects of genetic deletion of CCR8 on end-organ function, remodelling and inflammation, and lack of modulation of the pressor response to Ang II, suggest that CCR8 deficiency does not afford protection against Ang II-dependent hypertension. Whilst CCR8 expression has been reported on immune cells and cardiovascular cell types including VSMCs and endothelial cells (Haque et al., 2004), the lack of impact of global CCR8 deletion on hypertension may be attributed to the low expression of CCR8 in the mouse vasculature and our finding that CCR8 was only co-localised with T cells (scRNA-sequencing data). In addition, we propose that contrary to previous reports (Islam et al., 2013), mCCL8 does not target CCR8 (further discussed in **Section 6.2.2**). Thus the chemokine CCL1, rather than hCCL18 or mCCL8, is recognised as the endogenous ligand of CCR8 in both mice and humans (Haskell et al., 2006). To our knowledge, the CCL1-CCR8 axis has not been studied in the setting of hypertension, yet this axis may be protective in atherosclerosis, facilitating the recruitment of regulatory T cells (Vila-Caballer et al., 2019). Importantly, hypertension is associated with a reduction in regulatory T cell activity, and selective depletion of these cells exacerbates experimental hypertension (Barhoumi et al., 2011; Kvakan et al., 2009). As such, a loss in CCR8 may not protect against hypertension associated-end organ damage, due to disruption of the CCL1-CCR8 axis and a potential reduction in protective regulatory T cells. Of note, this thesis has shown a low level of CCL1 expression in the normotensive and hypertensive mouse vasculature (via scRNA-sequencing). As such, future studies should measure CCL1 levels in other end-organs and examine the impact of CCR8 KO on regulatory T cells. Although our findings suggest that CCR8 signalling does not play a crucial role in hypertension, global deletion of CCR8 in mice may lead to compensatory mechanisms to counteract the loss of CCR8. As such, pharmacological inhibition of CCR8 may help us draw more valid conclusions.

6.2.2 Effects of R243, a CCR8 antagonist

As discussed in **Section 6.1.1**, experiments that pharmacologically target CCR8 can complement the findings in CCR8 KO mice, and are more clinically relevant. Therefore, the CCR8 antagonist, R243 (Oshio et al., 2014), was administered as an intervention, in Ang II treated hypertensive mice. These studies were performed concurrently with our CCR8 KO studies. Like genetic deletion of CCR8, R243 had little effect on the Ang II-induced pressor response, cardiac hypertrophy or vascular dysfunction. In line with findings in the 14-day Ang II treated CCR8 KO mice, R243 appeared to augment contractility to PE in the aorta and improve endothelial function. Given R243-treated normotensive WT mice were not included in the study design, it is unclear if this effect of R243 is only apparent in hypertensive mice. It is important to note that R243 lacks selectivity and can also antagonise CCR2 (Oshio et al., 2014), a chemokine receptor which has been shown to contribute to the pathogenesis of hypertension (Chan et al., 2012). Thus researchers have found that the inhibition of CCR2 prevents monocyte recruitment and macrophage accumulation into the vasculature, which in turn reverse vascular fibrosis in Ang II- (Moore et al., 2015) as well as DOCA-salt- (Chan et al., 2012) induced hypertension. CCR8 independent actions of R243 could be ascertained by administering R243 to hypertensive CCR8 KO mice to determine if the antagonist confers any additional beneficial actions. Alternatively, a new antagonist that is highly selective for CCR8, AZ084 (Connolly et al., 2012), has recently become commercially available and may be used to further study the effects of pharmacological inhibition of CCR8 on hypertension.

In this thesis, CCR8 KO mice and the CCR8 antagonist, R243 were used to negate the actions of the hCCL18/mCCL8-CCR8 axis in the setting of hypertension. These experiments were designed based on the findings of a reputable research group, which suggested that CCR8 is the cognate receptor of hCCL18, and that mCCL8 is a functional analogue of hCCL18 (Islam et al., 2011; Islam et al., 2013). However, we now have evidence that neither mCCL8 nor hCCL18 activate CCR8. Using BRET assays in CCR8-expressing CHO cells, we have demonstrated that the well-recognised CCR8 agonist CCL1 (Haskell et al., 2006), but not mCCL8 or hCCL18 activates CCR8. By contrast, Islam et al. (2013) has shown that hCCL18 causes chemotaxis and calcium influx in CCR8 transfected 4DE4 cells (pre-B cell line), as well as CCR8-expressing type 2 T helper (Th2) cells. Whilst our study has used hCCL18 from the same source as Islam et al. (2013), CCR8 activation could not be detected in CCR8 transfected CHO cells. A possible

explanation for the observed differences may be related to potential receptor crosstalk. For example, CCL18 may activate an unidentified receptor leading to the subsequent stimulation of the chemotactic function of CCR8. If this novel CCL18 receptor is naturally expressed on 4DE4 cells and Th2 cells, but not on CHO cells, then CCL18 will activate the cells used by Islam et al. (2013), but not CHO cells. Therefore, future studies should repeat the relevant BRET assays using 4DE4 cells and/or Th2 cells to confirm the above-mentioned hypothesis, followed by the identification of the CCL18 cognate receptor using molecular and proteomic approaches.

A further limitation to the research area, is that CCL18 is only found in primates. Islam et al. (2013), however concluded that murine CCL8 was a functional analogue of hCCL18, based on their observations that these two chemokines are regulated similarly in M2 macrophages and both target CCR8. We now provide evidence to suggest that like hCCL18, mCCL8 does not activate CCR8. As such, whether mCCL8 is a functional analogue of hCCL18 requires further confirmation. These two chemokines are indeed only 31 % identical according to the online Basic Local Alignment Search Tool (BLAST) (National Library of Medicine (US), 2006; National Library of Medicine (US), 2015), whereas proteins with >40% identity are generally considered likely to have functional similarities (Pearson, 2013). Therefore, regarding the mouse functional analogue of hCCL18, its existence and/or identity remains unclear. Nonetheless, as detailed in **Section 6.2.1**, independent of the identity of the endogenous ligand, our studies, using CCR8 KO mice and pharmacological inhibition of CCR8, have shown that CCR8 signalling may not contribute to the development of hypertension. Without identification of the cognate receptor or mouse functional analogue of CCL18, the most appropriate approach to investigate the role of CCL18 in hypertension is to use human cells or patient samples.

6.2.3 Study limitations and future directions

Although the genetic or pharmacological targeting of CCR8 failed to significantly impact the development of hypertension and associated end-organ damage, our studies provide valuable information about the 14-day and 28-day Ang II models (0.7 mg/kg/d) and challenge the idea that CCR8 is the cognate receptor of CCL18. The limitations and future directions of these studies are mostly discussed in **Chapters 4-5**, as well as **Sections 6.2.1 and 6.2.2** of this

chapter. In brief, no robust renal or cardiac damage is observed in our hypertension models, which suggests that the use of a different hypertension model (e.g. the DOCA-salt model) (Kirchhoff et al., 2008) to study relevant end-organ damage would be appropriate. A number of experiments, particularly the flow cytometric analysis in the kidney and aorta, generated inconclusive data due to the low sample size and lack of statistical power (under the impact of COVID-19). Future studies should obtain larger sample sizes to confirm our findings. Furthermore, the use of a highly selective CCR8 antagonist (AZ084) (Connolly et al., 2012), or the inclusion of a R243 treated group of CCR8 KO mice will allow further confirmation of the effects of pharmacological CCR8 inhibition on hypertension. In addition, the potential implication of PE contractility in aortae as a predictor of systolic BP in WT male mice is to be further explored. As discussed in **Chapter 4 (Section 4.7)**, changes in expression or receptor-effector coupling of α1- adrenoceptors (Couto et al., 2014; Tanaka et al., 2006; Yamamoto & Koike, 2001) and/or oxidative stress (Mui et al., 2018; Tsai & Jiang, 2010) may contribute to the enhancement of vascular contraction in response to PE in the setting of hypertension.

To thoroughly interrogate the role of CCL18 in hypertension, it is essential to identify its cognate receptor. Two complementary approaches could be taken to achieve this aim including i) screening against known chemokine receptors and ii) cross-linking/pulldown together with proteomics. Thus, CCL18 has only moderate (29%) sequence identity to CCL1, the only validated CCR8 ligand, but much higher (up to 62%) identity to numerous other human CC chemokines that are agonists or antagonists of other receptors (CCR1-5 and CCR7) (National Library of Medicine (US), 1988). Indeed, studies have found that CCL18 antagonises CCR3 (Nibbs et al., 2000), and inhibits CCR2, 4, 5 by displacing receptor-bound chemokines (Krohn et al., 2013). Whilst CCL18 does not activate CCR1-5, studies have identified CCL18 as an agonist of PITPNM3 (Chen et al., 2011b) and GPR30 (Catusse et al., 2010). CCL18 can activate PITPNM3 on tumour-associated macrophages to promote tumour cell migration and metastasis (Chen et al., 2011b). On the contrary, GPR30 on acute lymphocytic leukemia B cells is activated by CCL18 to inhibit chemotaxis and cell proliferation (Catusse et al., 2010). To date, the biphasic functions of CCL18 mediated by PITPNM3 and GPR30 have only been studied in the setting of cancer (Chenivesse & Tsicopoulos, 2018), and the role of these receptors in hypertension remains to be investigated. The potential receptors of CCL18 and their characteristics are summarised in **Table 1** below. Future experiments, using CHO cells

expressing these receptors coupled with BRET assays for downstream signalling, could test the ability of CCL18 to activate these targets and antagonise activation of these receptors by known agonists. The second approach, would aim to directly identify CCL18 receptors on primary monocytes/macrophages, T cells, and fibroblasts using cross-linking/pulldown together with proteomics. In brief, biotinylated CCL18 could be bound to these cells, cross-linked to adjacent proteins, extracted and then the bound target identified by proteomics.

Looking ahead, with the absence of a validated rodent functional analogue of CCL18, human samples, such as cells and plasma, are most likely to be the main study focus in the near future.

Table 1. Potential receptors of CCL18 other than CCR8.

Receptors	Stimulated/ Inhibited by CCL18	Cell types expressing receptors	Actions of receptors	References
PITPNM3	Stimulated (agonism)	Tumour cells, tumour associated macrophages	Metastasis	(Chen et al., 2011b)
GPR30	Stimulated (agonism)	Acute lymphocytic leukemia B cells	Inhibition of chemotaxis and cell proliferation	(Catusse et al., 2010)
CCR3	Inhibited (antagonism)	Mainly eosinophils, Th2 cells and fibroblasts	Chemotaxis, pro-fibrotic	(Huber et al., 2002; Komai et al., 2010; Krohn et al., 2013; Nibbs et al., 2000)
CCR 1, 2, 4, 5	Inhibited (via displacement of bound GAG chemokines)	• CCR1 and CCR2: monocytes, macrophages, VSMCs • CCR4: mainly T cells • CCR5: monocytes, macrophages	Chemotaxis, pro-fibrotic	(Krohn et al., 2013; Matsuo et al., 2016; Pignatti et al., 2006; Seki et al., 2009a; Seki et al., 2009b; Vestergaard et al., 2004)

VSMCs: vascular smooth muscle cells, HUVECs: human umbilical vein endothelial cells, Th2 cells: type 2 T helper cells, GAG: glycosaminoglycan.

6.3 Role of CCL18 in resistant hypertension

Despite the lack of involvement of CCR8 in experimental models of hypertension, the role of its purported ligand, CCL18 in the pathogenesis of hypertension remains to be of interest. Indeed, CCL18 is elevated in a number of cardiovascular disease states (de Jager et al., 2012; Hägg et al., 2009; Versteylen et al., 2016), and it may mediate the pro-fibrotic actions of M2 macrophages in BP controlling organs in hypertension (Zhu, 2016). Expressed predominantly by monocytes and macrophages (Schraufstatter et al., 2012), CCL18 has a suite of actions including chemoattraction of T and B lymphocytes (Chenivesse & Tsicopoulos, 2018; Günther et al., 2014), stimulation of collagen generation from pulmonary fibroblasts (Atamas et al., 2003) and promotion of M2 polarisation (Schraufstatter et al., 2012). **Chapter 3** of this thesis presents the novel finding that CCL18 promotes vascular fibrosis, and is elevated in patients with resistant hypertension.

Using clinically relevant human vascular cells types, we have provided the first evidence that exogenous CCL18 promotes vascular fibrosis. Specifically, CCL18 directly targets aortic adventitial fibroblasts (AoAFs) to stimulate collagen generation, an effect which was independent of fibroblast to myofibroblast differentiation. In addition, using human aortic endothelial cells (HAECs), this thesis has demonstrated that CCL18 may also stimulate endothelial-mesenchymal transition (End-MT) to promote vascular fibrosis. Although additional experiments are required to confirm these observations, our findings are supported by the previously identified pro-fibrotic capacity of CCL18 in pulmonary fibroblasts (Atamas et al., 2003).

As discussed in **Chapter 3**, the pro-fibrotic function of CCL18 in the vasculature can be further studied by measuring the levels of pro-collagen I, collagen I, MMPs and TIMPs (tissue inhibitor of metalloproteinases) in the AoAF culture media. Additional End-MT markers, such as transcription factor SNAIL (Kokudo et al., 2008), may also be used to confirm the effects of CCL18 on End-MT. Furthermore, the effects of CCL18 on other collagen generating cells in the vascular wall are of interest. Specifically, it will be of interest to determine if CCL18 modulates collagen-producing VSMCs (Wanjare et al., 2015) and fibrocytes (Yeager et al., 2011). Fibrocytes are of particular interest given the recent report by Wu et al. (2016) which suggested that, rather than resident fibroblasts, collagen-producing leukocytes known as

"fibrocytes" are the predominant source of collagen in the aortic wall during hypertension. As such there is potential for CCL18 to additionally target fibrocytes to enhance their infiltration into the vessel wall and/or generation of collagen. Furthermore, fibrocytes themselves may be a source of CCL18. These concepts would be interesting to investigate in future studies in order to identify the key vascular targets of M2 macrophage-derived CCL18 and their role in mediating aortic stiffening. Given CCL18 is a chemoattractant, its pro-fibrotic capacity may also be dependent upon its ability to promote migration of T cells into the vascular wall and stimulate their capacity to generate ROS and IFN-Ɣ.

Collectively, our findings suggest that CCL18 may promote aortic stiffening. This is of particular relevance in the context of hypertension, as aortic stiffening promotes damage of other end-organs in hypertension (Oparil et al., 2003), and can further exacerbate the elevation of BP (Kaess et al., 2012). Importantly, the pro-fibrotic actions of CCL18 may extend beyond the vasculature. Indeed, our laboratory has demonstrated an ability of CCL18 to increase collagen generation from human cardiac fibroblasts (Lewis, 2017) and future studies will investigate the effects of CCL18 on renal fibroblasts.

Based upon our findings, there is clear rationale for suppressing CCL18 activity to limit cardiovascular fibrosis. Given chemokine receptors are G-protein coupled receptors, which are highly druggable, it would be appropriate to target the CCL18 receptor itself. However, in **Chapter 5** we have challenged the idea that CCR8 is the cognate receptor of CCL18**.** In further support of this concept, in **Chapter 3** we were unable to detect CCR8 expression, at the level of mRNA or protein, in either human AoAFs or HAECs. As such, the receptor responsible for the pro-fibrotic actions of CCL18 remains unknown (detailed in **Section 6.2**). The future identification of the CCL18 receptor, will facilitate the use of siRNA or small molecule antagonists directed at the receptor, to further explore the mechanisms of CCL18-induced cardiovascular fibrosis. Our studies suggest that CCL18 may represent a novel therapeutic target for hypertension-associated fibrosis. Since current anti-hypertensive treatments do not directly target fibrosis, anti-fibrotic medications targeting CCL18 or its cognate receptor may be used alone or in combination with current therapies, to improve the clinical outcome of hypertension.

Targeting CCL18 to prevent hypertension-induced organ damage may be of particular benefit in patients with resistant hypertension. Resistant hypertensive patients have uncontrolled blood pressure (BP) ((≥ 140/90 mmHg) despite treatment with ≥ 3 different classes of anti-hypertensives (de la Sierra et al., 2011). Prolonged exposure to uncontrolled BP results in measurable end-organ damage (e.g. aortic stiffening, heart failure and kidney disease), and patients with resistant hypertension are ~50% more likely to experience cardiovascular events than patients with controlled hypertension (Daugherty et al., 2012). Moreover, there are currently no available biomarkers to identify patients who will be resistant to anti-hypertensive therapies, leaving them at high cardiovascular risk while attempting to optimize conventional therapies often over prolonged periods of time. This thesis presents the novel hypothesis that CCL18 can serve as a biomarker of resistant hypertension and a therapeutic target for the treatment of hypertension-associated end-organ damage. We have shown, for the first time, that plasma levels of CCL18 are elevated in patients with resistant, but not essential (untreated), hypertension. Correlational studies described in **Chapter 3** suggest that the association between CCL18 and resistant hypertension is not confounded by age, BMI, heart rate, or the amplitude of BP per se. Thus, the use of CCL18 as a biomarker may provide a unique opportunity to improve the clinical management of resistant hypertension.

To validate CCL18 as a biomarker and therapeutic target, it is critical that future studies determine the cause-effect relationship between CCL18 and resistant hypertension. This will be achieved via a longitudinal assessment of resistant hypertensive patients, in which plasma CCL18 levels and end-organ damage (LV hypertrophy, aortic stiffness, renal function) will be measured pre- and post- renal denervation, a surgical process recently found to effectively decrease BP in resistant hypertension (Azizi et al., 2018; Townsend et al., 2017). If CCL18 is elevated as a consequence of resistant hypertension, reduced BP following renal denervation will lead to a decrease in plasma CCL18 levels. Conversely, if CCL18 plays a casual role in resistant hypertension then a reduction in plasma levels of CCL18 may proceed the fall in BP. Potential identification of a causal role of CCL18 in patients with resistant hypertension will provide a stronger rationale for the development of pharmacotherapies targeting CCL18 to treat the disease.

To further understand cause-effect relationship of CCL18 and hypertension, it is also important to determine the primary source of human plasma CCL18. According to the Human

Protein Atlas (proteinatlas.org, 2020; Uhlén et al., 2015), macrophages express much higher levels of CCL18 than circulating monocytes. As such, CCL18 is likely to be synthesized by macrophages residing in tissues and released into the circulation. The proposed major organ/tissue sources of CCL18 include the lungs, lymph nodes, thymus, heart, adipose tissue and tonsils (proteinatlas.org, 2020). Among these organs/tissues, the role of the lungs in systemic hypertension remains unclear, although a study has demonstrated a positive association between systemic hypertension and an accelerated decline in lung function (Miele et al., 2018). On the other hand, in the setting of hypertension generation of CCL18 from the heart is feasible given cardiac inflammation and damage is commonly seen in chronic hypertension (Drummond et al., 2019). Similarly, adipose tissue may modulate the development of hypertension (Das et al., 2018), and lymphoid organs of the immune system have a clear role in the pathogenesis of hypertension (Drummond et al., 2019). In addition, CCL18 is a marker of the M2 subtype of macrophages (Vrančić et al., 2012). M2 macrophages play a key role in hypertension-associated vascular fibrosis (Moore et al., 2015), and are implicated in renal fibrosis (Guiteras et al., 2016). As such, it is possible that M2 macrophages in the vasculature or kidneys may generate substantially higher levels of CCL18 in hypertension-associated pathological conditions. Collectively, if CCL18 is the cause of resistant hypertension, M2 macrophages from one or more of the above-mentioned tissues may synthesize abnormally high amounts of CCL18 contributing to the development of resistant hypertension and associated end-organ damage.

Regardless of whether CCL18 has a causal role in resistant hypertension, it remains as a potential biomarker of resistant hypertension. This concept is supported by findings in other cardiovascular pathologies such as atherosclerosis (Hägg et al., 2009), acute coronary syndrome (ACS) (de Jager et al., 2012) and unstable angina pectoris (Kraaijeveld et al., 2007). The prognostic value of CCL18 is further supported by the finding that ACS patients with high serum CCL18 levels (66.9 [43.3–104.8] ng/ml) are at a three times greater risk of having a future fatal cardiovascular event (de Jager et al., 2012). As discussed in **Chapter 3,** future studies are required to confirm the predictive value of CCL18 as a biomarker for resistant hypertension. In particular, more female patients are to be recruited for the investigation of a potential sex difference in the utility of CCL18 as a biomarker. Thus, our study has shown that CCL18 may serve as a better marker for resistant hypertension in females than males.

Moreover, patients in the "essential hypertension" cohort were newly diagnosed and untreated in our study. As such, future identification and exclusion of patients resistant to treatments in this cohort will provide a clearer distinction between essential and resistant hypertension. Further correlational studies may also be utilised to assess the predictive value of CCL18 in hypertension-associated clinical outcomes, such as pulse wave velocity, ventricular hypertrophy, and glomerular filtration rate. In addition, plasma CCL18 may serve as a more selective marker of resistant hypertension, when combined with measures of systemic inflammation markers, such as C-reactive protein (CRP) (de Jager et al., 2012), tumour necrosis factor-α and IL-1β (Dörffel et al., 1999) (detailed in **Chapter 3, Section 3.7**).

Establishing CCL18 as a biomarker of resistant hypertension will allow earlier identification of these patients and facilitate more aggressive and earlier use of multi-combination conventional anti-hypertensive therapies. Interventional approaches, such as renal denervation (Azizi et al., 2018), may also be considered upon early diagnosis of resistant hypertension to significantly lower BP. In addition, longitudinal monitoring of CCL18 plasma levels in resistant hypertensive patients following renal denervation, may provide a robust indicator of the effectiveness of the intervention as opposed to the more invasive measures. For example, the level of renal noradrenaline spillover, measured via catheterisation, is a current indicator of renal denervation effectiveness (Schlaich et al., 2004). The early diagnosis of resistant hypertension, and the subsequent treatment and BP monitoring strategies, will lead to improved clinical outcomes via prevention of end-organ damage and reduction of cardiovascular event risk.

The findings of **Chapter 4** collectively suggest that CCL18 is a potential biomarker of resistant hypertension, and may promote hypertension-associated vascular fibrosis. The key findings of this thesis, in relation to the current literature are summarised in **Figure 1**. From a clinical context, this research program has identified a potential approach to improve the clinical management of patients with resistant hypertension. The early identification of resistant hypertensive patients, using plasma CCL18 measures, will allow clinicians to implement relevant treatments and BP monitoring strategies to prevent end-organ damage and reduce cardiovascular risk. Identification of a causal role of CCL18 in patient with resistant hypertension will also provide strong rationale for the development of pharmacotherapies targeting CCL18 to treat the disease.

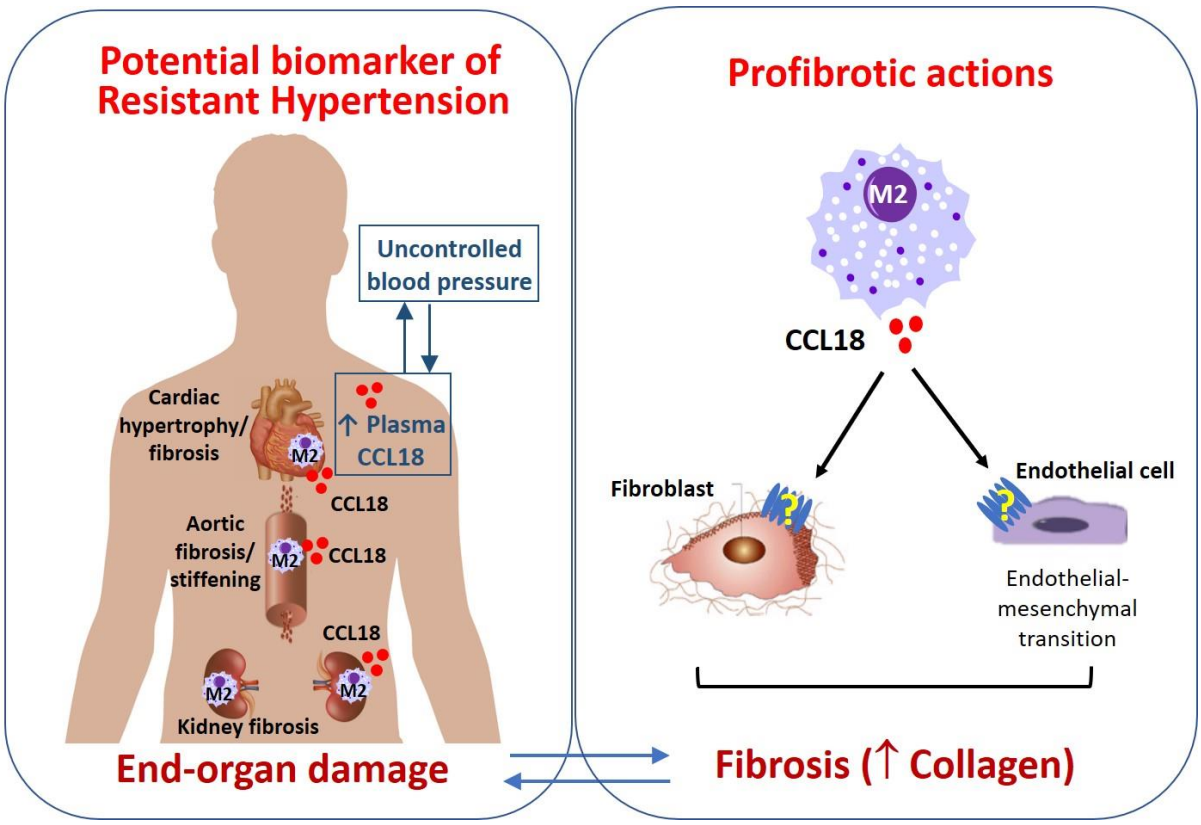

Figure 1. Summary of the role of CCL18 in hypertension, based on findings of this thesis and published literature. **Left panel**: hypertension is associated with damage in end-organs. M2 macrophages have been implicated in the fibrosis of these organs (Falkenham et al., 2015; Guiteras et al., 2016; Moore et al., 2015), and can generate high amounts of CCL18 (Guiteras et al., 2016). This thesis identifies plasma CCL18 as a potential biomarker of resistant hypertension, which may be a cause or an effect of resistant hypertension and/or the associated end-organ damage. **Right panel**: CCL18 promotes collagen generation from human cardiac fibroblasts (unpublished data from our laboratory) and human aortic fibroblasts (data from this thesis). We also have evidence that CCL18 induces endothelial-mesenchymal transition in human aortic endothelial cells. The receptor mediating CCL18 effects remains to be identified.

6.4 Conclusions

This thesis represents the first study to identify CCL18 as a potential biomarker of resistant hypertension, and to demonstrate pro-fibrotic effects of CCL18 in the human vasculature. We have also conducted the first studies to demonstrate that genetic or pharmacological targeting of CCR8 may not modulate the development of hypertension in mice, and subsequently challenge the idea (Islam et al., 2013) that CCR8 is the cognate receptor of CCL18. We suggest that future research should focus on confirming the predictive value of CCL18 as a biomarker of resistant hypertension, further exploring the role of CCL18 in target organs of hypertension, and identifying the CCL18 cognate receptor. In conclusion, CCL18 is a potential biomarker of resistant hypertension, and targeting CCL18 may represent a novel therapeutic strategy for resistant hypertension and/or hypertension-associated end-organ damage.

6.5 References

Al-Magableh MR, Kemp-Harper BK, & Hart JL (2015). Hydrogen sulfide treatment reduces blood pressure and oxidative stress in angiotensin II-induced hypertensive mice. Hypertens Res 38**:** 13-20.

Atamas SP, Luzina IG, Choi J, Tsymbalyuk N, Carbonetti NH, Singh IS, Trojanowska M, Jimenez SA, & White B (2003). Pulmonary and Activation-Regulated Chemokine Stimulates Collagen Production in Lung Fibroblasts. Am J Respir Cell Mol Biol 29**:** 743-749.

Azizi M, Schmieder RE, Mahfoud F, Weber MA, Daemen J, Davies J, Basile J, Kirtane AJ, Wang Y, Lobo MD, Saxena M, Feyz L, Rader F, Lurz P, Sayer J, Sapoval M, Levy T, Sanghvi K, Abraham J, Sharp ASP, Fisher NDL, Bloch MJ, Reeve-Stoffer H, Coleman L, Mullin C, & Mauri L (2018). Endovascular ultrasound renal denervation to treat hypertension (RADIANCE-HTN SOLO): a multicentre, international, single-blind, randomised, sham-controlled trial. Lancet 391**:** 2335-2345.

Barhoumi T, Kasal Daniel A, Li Melissa W, Shbat L, Laurant P, Neves Mario F, Paradis P, & Schiffrin Ernesto L (2011). T Regulatory Lymphocytes Prevent Angiotensin II–Induced Hypertension and Vascular Injury. Hypertension 57**:** 469-476.

Basting T, & Lazartigues E (2017). DOCA-Salt Hypertension: an Update. Curr Hypertens Rep 19**:** 32-32.

Bersi MR, Bellini C, Wu J, Montaniel KRC, Harrison DG, & Humphrey JD (2016). Excessive Adventitial Remodeling Leads to Early Aortic Maladaptation in Angiotensin-Induced Hypertension. Hypertension (Dallas, Tex : 1979) 67**:** 890-896.

Briet M, Boutouyrie P, Laurent S, & London GM (2012). Arterial stiffness and pulse pressure in CKD and ESRD. Kidney Int 82**:** 388-400.

Brown IAM, Diederich L, Good ME, DeLalio LJ, Murphy SA, Cortese-Krott MM, Hall JL, Le TH, & Isakson BE (2018). Vascular Smooth Muscle Remodeling in Conductive and Resistance Arteries in Hypertension. Arterioscler Thromb Vasc Biol 38**:** 1969-1985.

Catusse J, Wollner S, Leick M, Schröttner P, Schraufstätter I, & Burger M (2010). Attenuation of CXCR4 responses by CCL18 in acute lymphocytic leukemia B cells. J Cell Physiol 225**:** 792-800.

Chan CT, Moore JP, Budzyn K, Guida E, Diep H, Vinh A, Jones ES, Widdop RE, Armitage JA, Sakkal S, Ricardo SD, Sobey CG, & Drummond GR (2012). Reversal of vascular macrophage accumulation and hypertension by a CCR2 antagonist in deoxycorticosterone/salt-treated mice. Hypertension 60**:** 1207-1212.

Chan CT, Sobey CG, Lieu M, Ferens D, Kett MM, Diep H, Kim HA, Krishnan SM, Lewis CV, Salimova E, Tipping P, Vinh A, Samuel CS, Peter K, Guzik TJ, Kyaw TS, Toh BH, Bobik A, & Drummond GR (2015). Obligatory Role for B Cells in the Development of Angiotensin II-Dependent Hypertension. Hypertension 66**:** 1023-1033.

Chen J, Lee SK, Abd-Elgaliel WR, Liang L, Galende E-Y, Hajjar RJ, & Tung C-H (2011a). Assessment of Cardiovascular Fibrosis Using Novel Fluorescent Probes. PLoS One 6**:** e19097.

Chen J, Yao Y, Gong C, Yu F, Su S, Chen J, Liu B, Deng H, Wang F, Lin L, Yao H, Su F, Anderson Karen S, Liu Q, Ewen Mark E, Yao X, & Song E (2011b). CCL18 from Tumor-Associated Macrophages Promotes Breast Cancer Metastasis via PITPNM3. Cancer Cell 19**:** 541-555.

Chenivesse C, & Tsicopoulos A (2018). CCL18 - Beyond chemotaxis. Cytokine 109**:** 52-56.

Chioncel O, Lainscak M, Seferovic PM, Anker SD, Crespo-Leiro MG, Harjola V-P, Parissis J, Laroche C, Piepoli MF, Fonseca C, Mebazaa A, Lund L, Ambrosio GA, Coats AJ, Ferrari R, Ruschitzka F, Maggioni AP, & Filippatos G (2017). Epidemiology and one-year outcomes in patients with chronic heart failure and preserved, mid-range and reduced ejection fraction: an analysis of the ESC Heart Failure Long-Term Registry. Eur J Heart Fail 19**:** 1574-1585.

Cocciolone AJ, Hawes JZ, Staiculescu MC, Johnson EO, Murshed M, & Wagenseil JE (2018). Elastin, arterial mechanics, and cardiovascular disease. American Journal of Physiology-Heart and Circulatory Physiology 315**:** H189-H205.

Connolly S, Skrinjar M, & Rosendahl A (2012). Orally bioavailable allosteric CCR8 antagonists inhibit dendritic cell, T cell and eosinophil migration. Biochem Pharmacol 83**:** 778-787.

Couto GK, Davel AP, Brum PC, & Rossoni LV (2014). Double disruption of α2A- and α2C-adrenoceptors induces endothelial dysfunction in mouse small arteries: role of nitric oxide synthase uncoupling. Exp Physiol 99**:** 1427-1438.

Cui M, Cai Z, Chu S, Sun Z, Wang X, Hu L, Yi J, Shen L, & He B (2016). Orphan Nuclear Receptor Nur77 Inhibits Angiotensin II-Induced Vascular Remodeling via Downregulation of β-Catenin. Hypertension 67**:** 153-162.

Das E, Moon JH, Lee JH, Thakkar N, Pausova Z, & Sung HK (2018). Adipose Tissue and Modulation of Hypertension. Curr Hypertens Rep 20**:** 96.

Daugherty SL, Powers JD, Magid DJ, Tavel HM, Masoudi FA, Margolis KL, O'Connor PJ, Selby JV, & Ho PM (2012). Incidence and prognosis of resistant hypertension in hypertensive patients. Circulation 125**:** 1635-1642.

de Jager SCA, Bongaerts BWC, Weber M, Kraaijeveld AO, Rousch M, Dimmeler S, van Dieijen-Visser MP, Cleutjens KBJM, Nelemans PJ, van Berkel TJC, & Biessen EAL (2012). Chemokines CCL3/MIP1α, CCL5/RANTES and CCL18/PARC are Independent Risk Predictors of Short-Term Mortality in Patients with Acute Coronary Syndromes. PLoS One 7**:** e45804.

de la Sierra A, Segura J, Banegas JR, Gorostidi M, de la Cruz JJ, Armario P, Oliveras A, & Ruilope LM (2011). Clinical features of 8295 patients with resistant hypertension classified on the basis of ambulatory blood pressure monitoring. Hypertension 57**:** 898-902.

de Simone G (2004). Concentric or eccentric hypertrophy: how clinically relevant is the difference? Hypertension 43**:** 714-715.

Diez J (2007). Mechanisms of cardiac fibrosis in hypertension. J Clin Hypertens (Greenwich) 9**:** 546-550.

Dörffel Y, Lätsch C, Stuhlmüller B, Schreiber S, Scholze S, Burmester GR, & Scholze J (1999). Preactivated peripheral blood monocytes in patients with essential hypertension. Hypertension 34**:** 113-117.

Drummond GR, Vinh A, Guzik TJ, & Sobey CG (2019). Immune mechanisms of hypertension. Nat Rev Immunol 19**:** 517-532.

Dunlay SM, Roger VL, & Redfield MM (2017). Epidemiology of heart failure with preserved ejection fraction. Nature Reviews Cardiology 14**:** 591-602.

Falkenham A, de Antueno R, Rosin N, Betsch D, Lee TDG, Duncan R, & Légaré J-F (2015). Nonclassical Resident Macrophages Are Important Determinants in the Development of Myocardial Fibrosis. The American Journal of Pathology 185**:** 927-942.

Guiteras R, Flaquer M, & Cruzado JM (2016). Macrophage in chronic kidney disease. Clin Kidney J 9**:** 765-771.

Günther J, Kill A, Becker MO, Heidecke H, Rademacher J, Siegert E, Radić M, Burmester GR, Dragun D, & Riemekasten G (2014). Angiotensin receptor type 1 and endothelin receptor type A on immune cells mediate migration and the expression of IL-8 and CCL18 when stimulated by autoantibodies from systemic sclerosis patients. Arthritis Res Ther 16**:** R65.

Guzik TJ, Hoch NE, Brown KA, McCann LA, Rahman A, Dikalov S, Goronzy J, Weyand C, & Harrison DG (2007). Role of the T cell in the genesis of angiotensin II induced hypertension and vascular dysfunction. The Journal of experimental medicine 204**:** 2449-2460.

Hägg DA, Olson FJ, Kjelldahl J, Jernås M, Thelle DS, Carlsson LMS, Fagerberg B, & Svensson PA (2009). Expression of chemokine (C-C motif) ligand 18 in human macrophages and atherosclerotic plaques. Atherosclerosis 204**:** e15-e20.

Haque NS, Fallon JT, Pan JJ, Taubman MB, & Harpel PC (2004). Chemokine receptor-8 (CCR8) mediates human vascular smooth muscle cell chemotaxis and metalloproteinase-2 secretion. Blood 103**:** 1296-1304.

Haskell CA, Horuk R, Liang M, Rosser M, Dunning L, Islam I, Kremer L, Gutiérrez J, Marquez G, Martinez-A C, Biscone MJ, Doms RW, & Ribeiro S (2006). Identification and Characterization of a Potent, Selective Nonpeptide Agonist of the CC Chemokine Receptor CCR8. Mol Pharmacol 69**:** 309.

Huber MA, Denk A, Peter RU, Weber L, Kraut N, & Wirth T (2002). The IKK-2/Ikappa Balpha /NF-kappa B pathway plays a key role in the regulation of CCR3 and eotaxin-1 in fibroblasts. A critical link to dermatitis in Ikappa Balpha -deficient mice. J Biol Chem 277**:** 1268-1275.

Islam SA, Chang DS, Colvin RA, Byrne MH, McCully ML, Moser B, Lira SA, Charo IF, & Luster AD (2011). Mouse CCL8, a CCR8 agonist, promotes atopic dermatitis by recruiting IL-5+ TH2 cells. Nat Immunol 12**:** 167-177.

Islam SA, Ling MF, Leung J, Shreffler WG, & Luster AD (2013). Identification of human CCR8 as a CCL18 receptor. J Exp Med 210**:** 1889-1898.

Ji H, Zheng W, Li X, Liu J, Wu X, Zhang MA, Umans JG, Hay M, Speth RC, Dunn SE, & Sandberg K (2014). Sex-specific T-cell regulation of angiotensin II-dependent hypertension. Hypertension 64**:** 573-582.

Kaess BM, Rong J, Larson MG, Hamburg NM, Vita JA, Levy D, Benjamin EJ, Vasan RS, & Mitchell GF (2012). Aortic stiffness, blood pressure progression, and incident hypertension. JAMA 308**:** 875-881.

Kessler EL, Rivaud MR, Vos MA, & van Veen TAB (2019). Sex-specific influence on cardiac structural remodeling and therapy in cardiovascular disease. Biol Sex Differ 10**:** 7-7.

Kirchhoff F, Krebs C, Abdulhag UN, Meyer-Schwesinger C, Maas R, Helmchen U, Hilgers KF, Wolf G, Stahl RA, & Wenzel U (2008). Rapid development of severe end-organ damage in C57BL/6 mice by combining DOCA salt and angiotensin II. Kidney Int 73**:** 643-650.

Kokudo T, Suzuki Y, Yoshimatsu Y, Yamazaki T, Watabe T, & Miyazono K (2008). Snail is required for TGFbeta-induced endothelial-mesenchymal transition of embryonic stem cell-derived endothelial cells. J Cell Sci 121**:** 3317-3324.

Komai M, Tanaka H, Nagao K, Ishizaki M, Kajiwara D, Miura T, Ohashi H, Haba T, Kawakami K, Sawa E, Yoshie O, Inagaki N, & Nagai H (2010). A novel CC-chemokine receptor 3 antagonist, Ki19003, inhibits airway eosinophilia and subepithelial/peribronchial fibrosis induced by repeated antigen challenge in mice. J Pharmacol Sci 112**:** 203-213.

Kossmann S, Hu H, Steven S, Schonfelder T, Fraccarollo D, Mikhed Y, Brahler M, Knorr M, Brandt M, Karbach SH, Becker C, Oelze M, Bauersachs J, Widder J, Munzel T, Daiber A, & Wenzel P (2014). Inflammatory monocytes determine endothelial nitric-oxide synthase uncoupling and nitro-oxidative stress induced by angiotensin II. J Biol Chem 289**:** 27540-27550.

Kraaijeveld AO, de Jager SC, de Jager WJ, Prakken BJ, McColl SR, Haspels I, Putter H, van Berkel TJ, Nagelkerken L, Jukema JW, & Biessen EA (2007). CC chemokine ligand-5 (CCL5/RANTES) and CC

chemokine ligand-18 (CCL18/PARC) are specific markers of refractory unstable angina pectoris and are transiently raised during severe ischemic symptoms. Circulation 116**:** 1931-1941.

Krohn SC, Bonvin P, & Proudfoot AE (2013). CCL18 exhibits a regulatory role through inhibition of receptor and glycosaminoglycan binding. PLoS One 8**:** e72321.

Kvakan H, Kleinewietfeld M, Qadri F, Park J-K, Fischer R, Schwarz I, Rahn H-P, Plehm R, Wellner M, Elitok S, Gratze P, Dechend R, Luft Friedrich C, & Muller Dominik N (2009). Regulatory T Cells Ameliorate Angiotensin II–Induced Cardiac Damage. Circulation 119**:** 2904-2912.

Lewis C (2017). Investigating the roles of distinct macrophage phenotypes in cardiovascular disease. PhD thesis: Monash University, Melbourne.

Li HL, She ZG, Li TB, Wang AB, Yang Q, Wei YS, Wang YG, & Liu DP (2007). Overexpression of myofibrillogenesis regulator-1 aggravates cardiac hypertrophy induced by angiotensin II in mice. Hypertension 49**:** 1399-1408.

Madhur MS, Lob HE, McCann LA, Iwakura Y, Blinder Y, Guzik TJ, & Harrison DG (2010). Interleukin 17 promotes angiotensin II-induced hypertension and vascular dysfunction. Hypertension 55**:** 500-507.

Matsuo K, Itoh T, Koyama A, Imamura R, Kawai S, Nishiwaki K, Oiso N, Kawada A, Yoshie O, & Nakayama T (2016). CCR4 is critically involved in effective antitumor immunity in mice bearing intradermal B16 melanoma. Cancer Lett 378**:** 16-22.

Miele CH, Grigsby MR, Siddharthan T, Gilman RH, Miranda JJ, Bernabe-Ortiz A, Wise RA, & Checkley W (2018). Environmental exposures and systemic hypertension are risk factors for decline in lung function. Thorax 73**:** 1120-1127.

Moore JP, Vinh A, Tuck KL, Sakkal S, Krishnan SM, Chan CT, Lieu M, Samuel CS, Diep H, Kemp-Harper BK, Tare M, Ricardo SD, Guzik TJ, Sobey CG, & Drummond GR (2015). M2 macrophage accumulation in the aortic wall during angiotensin ii infusion in mice is associated with fibrosis, elastin loss, and elevated blood pressure. Am J Physiol Heart Circ Physiol 309**:** H906-H917.

Mozaffarian D, Benjamin EJ, Go AS, Arnett DK, Blaha MJ, Cushman M, de Ferranti S, Despres JP, Fullerton HJ, Howard VJ, Huffman MD, Judd SE, Kissela BM, Lackland DT, Lichtman JH, Lisabeth LD, Liu S, Mackey RH, Matchar DB, McGuire DK, Mohler ER, 3rd, Moy CS, Muntner P, Mussolino ME, Nasir K, Neumar RW, Nichol G, Palaniappan L, Pandey DK, Reeves MJ, Rodriguez CJ, Sorlie PD, Stein J, Towfighi A, Turan TN, Virani SS, Willey JZ, Woo D, Yeh RW, & Turner MB (2015). Heart disease and stroke statistics--2015 update: a report from the American Heart Association. Circulation 131**:** e29-322.

Mui RK, Fernandes RN, Garver HG, Van Rooijen N, & Galligan JJ (2018). Macrophage-dependent impairment of α(2)-adrenergic autoreceptor inhibition of Ca(2+) channels in sympathetic neurons from DOCA-salt but not high-fat diet-induced hypertensive rats. American journal of physiology Heart and circulatory physiology 314**:** H863-H877.

National Library of Medicine (US) NCfBI (1988). National Center for Biotechnology Information (NCBI): https://www.ncbi.nlm.nih.gov/.

National Library of Medicine (US) NCfBI (2006). Protein [Chemokine (C-C motif) ligand 8 [Mus musculus]]: Bethesda (MD).

National Library of Medicine (US) NCfBI (2015). Protein [chemokine (C-C motif) ligand 18 (pulmonary and activation-regulated) [Homo sapiens]]: Bethesda (MD).

Nibbs RJ, Salcedo TW, Campbell JD, Yao XT, Li Y, Nardelli B, Olsen HS, Morris TS, Proudfoot AE, Patel VP, & Graham GJ (2000). C-C chemokine receptor 3 antagonism by the beta-chemokine macrophage inflammatory protein 4, a property strongly enhanced by an amino-terminal alanine-methionine swap. J Immunol 164**:** 1488-1497.

Nosalski R, Siedlinski M, Denby L, McGinnigle E, Nowak M, Cat AND, Medina-Ruiz L, Cantini M, Skiba D, Wilk G, Osmenda G, Rodor J, Salmeron-Sanchez M, Graham G, Maffia P, Graham D, Baker AH, & Guzik TJ (2020). T-Cell-Derived miRNA-214 Mediates Perivascular Fibrosis in Hypertension. Circ Res 126**:** 988-1003.

Oparil S, Zaman MA, & Calhoun DA (2003). Pathogenesis of Hypertension. Ann Intern Med 139**:** 761-776.

Oshio T, Kawashima R, Kawamura YI, Hagiwara T, Mizutani N, Okada T, Otsubo T, Inagaki-Ohara K, Matsukawa A, Haga T, Kakuta S, Iwakura Y, Hosokawa S, & Dohi T (2014). Chemokine receptor CCR8 is required for lipopolysaccharide-triggered cytokine production in mouse peritoneal macrophages. PLoS One 9**:** e94445.

Pearson WR (2013). An introduction to sequence similarity ("homology") searching. Curr Protoc Bioinformatics Chapter 3**:** Unit3.1-Unit3.1.

Pignatti P, Brunetti G, Moretto D, Yacoub MR, Fiori M, Balbi B, Balestrino A, Cervio G, Nava S, & Moscato G (2006). Role of the chemokine receptors CXCR3 and CCR4 in human pulmonary fibrosis. Am J Respir Crit Care Med 173**:** 310-317.

Pollow Dennis P, Uhrlaub J, Romero-Aleshire Melissa J, Sandberg K, Nikolich-Zugich J, Brooks Heddwen L, & Hay M (2014). Sex Differences in T-Lymphocyte Tissue Infiltration and Development of Angiotensin II Hypertension. Hypertension 64**:** 384-390.

Cell type atlas - CCL18 - The Human Protein Atlas. [Online] Available from https://www.proteinatlas.org/ENSG00000275385-CCL18/celltype. [Accessed].

Rodríguez JE, Ruiz-Hernández A, Hernández-DíazCouder A, Huang F, Hong E, & Villafaña S (2020). Chronic diabetes and hypertension impair the in vivo functional response to phenylephrine independent of α1-adrenoceptor expression. Eur J Pharmacol 883: 173283.

Schlaich MP, Lambert E, Kaye DM, Krozowski Z, Campbell DJ, Lambert G, Hastings J, Aggarwal A, & Esler MD (2004). Sympathetic augmentation in hypertension: role of nerve firing, norepinephrine reuptake, and Angiotensin neuromodulation. Hypertension 43**:** 169-175.

Schraufstatter IU, Zhao M, Khaldoyanidi SK, & Discipio RG (2012). The chemokine CCL18 causes maturation of cultured monocytes to macrophages in the M2 spectrum. Immunology 135**:** 287-298.

Seki E, De Minicis S, Gwak GY, Kluwe J, Inokuchi S, Bursill CA, Llovet JM, Brenner DA, & Schwabe RF (2009a). CCR1 and CCR5 promote hepatic fibrosis in mice. J Clin Invest 119**:** 1858-1870.

Seki E, de Minicis S, Inokuchi S, Taura K, Miyai K, van Rooijen N, Schwabe RF, & Brenner DA (2009b). CCR2 promotes hepatic fibrosis in mice. Hepatology 50**:** 185-197.

Seto SW, Krishna SM, Yu H, Liu D, Khosla S, & Golledge J (2013). Impaired acetylcholine-induced endothelium-dependent aortic relaxation by caveolin-1 in angiotensin II-infused apolipoprotein-E (ApoE-/-) knockout mice. PLoS One 8**:** e58481-e58481.

Sierra-Filardi E, Nieto C, Dominguez-Soto A, Barroso R, Sanchez-Mateos P, Puig-Kroger A, Lopez-Bravo M, Joven J, Ardavin C, Rodriguez-Fernandez JL, Sanchez-Torres C, Mellado M, & Corbi AL (2014). CCL2 shapes macrophage polarization by GM-CSF and M-CSF: identification of CCL2/CCR2-dependent gene expression profile. J Immunol 192**:** 3858-3867.

Singh MV, Cicha MZ, Nunez S, Meyerholz DK, Chapleau MW, & Abboud FM (2019). Angiotensin II-induced hypertension and cardiac hypertrophy are differentially mediated by TLR3- and TLR4-dependent pathways. Am J Physiol Heart Circ Physiol 316**:** H1027-h1038.

Tanaka Y, Funabiki M, Michikawa H, & Koike K (2006). Effects of aging on alpha1-adrenoceptor mechanisms in the isolated mouse aortic preparation. J Smooth Muscle Res 42**:** 131-138.

Townsend RR, Mahfoud F, Kandzari DE, Kario K, Pocock S, Weber MA, Ewen S, Tsioufis K, Tousoulis D, Sharp ASP, Watkinson AF, Schmieder RE, Schmid A, Choi JW, East C, Walton A, Hopper I, Cohen DL, Wilensky R, Lee DP, Ma A, Devireddy CM, Lea JP, Lurz PC, Fengler K, Davies J, Chapman N, Cohen SA, DeBruin V, Fahy M, Jones DE, Rothman M, & Böhm M (2017). Catheter-based renal denervation in patients with uncontrolled hypertension in the absence of antihypertensive medications (SPYRAL HTN-OFF MED): a randomised, sham-controlled, proof-of-concept trial. Lancet 390**:** 2160-2170.

Trott DW, Thabet SR, Kirabo A, Saleh MA, Itani H, Norlander AE, Wu J, Goldstein A, Arendshorst WJ, Madhur MS, Chen W, Li C-I, Shyr Y, & Harrison DG (2014). Oligoclonal CD8+ T cells play a critical role in the development of hypertension. Hypertension (Dallas, Tex : 1979) 64**:** 1108-1115.

Tsai MH, & Jiang MJ (2010). Reactive oxygen species are involved in regulating alpha1-adrenoceptor-activated vascular smooth muscle contraction. J Biomed Sci 17**:** 67.

Uhlén M, Fagerberg L, Hallström BM, Lindskog C, Oksvold P, Mardinoglu A, Sivertsson Å, Kampf C, Sjöstedt E, Asplund A, Olsson I, Edlund K, Lundberg E, Navani S, Szigyarto CA, Odeberg J, Djureinovic

D, Takanen JO, Hober S, Alm T, Edqvist PH, Berling H, Tegel H, Mulder J, Rockberg J, Nilsson P, Schwenk JM, Hamsten M, von Feilitzen K, Forsberg M, Persson L, Johansson F, Zwahlen M, von Heijne G, Nielsen J, & Pontén F (2015). Proteomics. Tissue-based map of the human proteome. Science 347**:** 1260419.

Versteylen MO, Manca M, Joosen IA, Schmidt DE, Das M, Hofstra L, Crijns HJ, Biessen EA, & Kietselaer BL (2016). CC chemokine ligands in patients presenting with stable chest pain: association with atherosclerosis and future cardiovascular events. Netherlands heart journal : monthly journal of the Netherlands Society of Cardiology and the Netherlands Heart Foundation 24**:** 722-729.

Vestergaard C, Just H, Baumgartner Nielsen J, Thestrup-Pedersen K, & Deleuran M (2004). Expression of CCR2 on monocytes and macrophages in chronically inflamed skin in atopic dermatitis and psoriasis. Acta Derm Venereol 84**:** 353-358.

Vila-Caballer M, González-Granado JM, Zorita V, Abu Nabah YN, Silvestre-Roig C, del Monte-Monge A, Molina-Sánchez P, Ait-Oufella H, Andrés-Manzano MJ, Sanz MJ, Weber C, Kremer L, Gutiérrez J, Mallat Z, & Andrés V (2019). Disruption of the CCL1-CCR8 axis inhibits vascular Treg recruitment and function and promotes atherosclerosis in mice. J Mol Cell Cardiol 132**:** 154-163.

Vrančić M, Banjanac M, Nujić K, Bosnar M, Murati T, Munić V, Stupin Polančec D, Belamarić D, Parnham MJ, & Eraković Haber V (2012). Azithromycin distinctively modulates classical activation of human monocytes in vitro. Br J Pharmacol 165**:** 1348-1360.

Wanjare M, Agarwal N, & Gerecht S (2015). Biomechanical strain induces elastin and collagen production in human pluripotent stem cell-derived vascular smooth muscle cells. Am J Physiol Cell Physiol 309**:** C271-281.

Wei Z, Spizzo I, Diep H, Drummond GR, Widdop RE, & Vinh A (2014). Differential Phenotypes of Tissue-Infiltrating T Cells during Angiotensin II-Induced Hypertension in Mice. PLoS One 9**:** e114895.

Williams HC, Ma J, Weiss D, Lassègue B, Sutliff RL, & San Martín A (2019). The cofilin phosphatase slingshot homolog 1 restrains angiotensin II-induced vascular hypertrophy and fibrosis in vivo. Laboratory investigation; a journal of technical methods and pathology 99**:** 399-410.

Wu J, Montaniel KR, Saleh MA, Xiao L, Chen W, Owens GK, Humphrey JD, Majesky MW, Paik DT, Hatzopoulos AK, Madhur MS, & Harrison DG (2016). Origin of Matrix-Producing Cells That Contribute to Aortic Fibrosis in Hypertension. Hypertension 67**:** 461-468.

Yamamoto Y, & Koike K (2001). alpha(1)-Adrenoceptor subtypes in the mouse mesenteric artery and abdominal aorta. Br J Pharmacol 134**:** 1045-1054.

Yeager ME, Frid MG, & Stenmark KR (2011). Progenitor cells in pulmonary vascular remodeling. Pulmonary Circulation 1**:** 3-16.

Yu X, Xia Y, Zeng L, Zhang X, Chen L, Yan S, Zhang R, Zhao C, Zeng Z, Shu Y, Huang S, Lei J, Yuan C, Zhang L, Feng Y, Liu W, Huang B, Zhang B, Luo W, Wang X, Zhang H, Haydon RC, Luu HH, He TC, & Gan H

(2018). A blockade of PI3Kγ signaling effectively mitigates angiotensin II-induced renal injury and fibrosis in a mouse model. Sci Rep 8**:** 10988.

Zhao W, Chen SS, Chen Y, Ahokas RA, & Sun Y (2008). Kidney fibrosis in hypertensive rats: role of oxidative stress. Am J Nephrol 28**:** 548-554.

Zhao W, Zhao T, Chen Y, Bhattacharya SK, Lu L, & Sun Y (2018). Differential Expression of Hypertensive Phenotypes in BXD Mouse Strains in Response to Angiotensin II. Am J Hypertens 31**:** 108-114.

Zhu M (2016). CCL18 as a mediator of the pro-fibrotic actions of M2 macrophages in the vessel wall during hypertension. Honours thesis: Monash University, Melbourne.

Zimmerman MA, Baban B, Tipton AJ, O'Connor PM, & Sullivan JC (2014). Chronic ANG II infusion induces sex-specific increases in renal T cells in Sprague-Dawley rats. American Journal of Physiology-Renal Physiology 308**:** F706-F712.

Appendices

Appendix 1: Monash Histology Platform Verhoeff-Van Geison staining protocol

WORK INSTRUCTIONS FOR VERHOEFF'S ELASTIC STAIN FOR ELASTIC FIBRES
PQMS3-MHP-WIN-0088-V1

DOCUMENT AUTHORISATION		Date of Next Review: 36 months	
Prepared by: Sue Connell	Technical Officer	Signed: SC – refer hard copy	Date: 31/10/13
Reviewed by: Camilla Cohen	Platform Manager	Signed: CC – refer hard copy	Date: 03/10/18
Authorised by: Camilla Cohen	Platform Manager	Signed: CC – refer hard copy	Date: 03/10/18
Additional authorisation if required			

1. PURPOSE

To describe the procedure used for demonstrating elastic fibres in paraffin sections.

2. RESPONSIBILITIES

It is the responsibility of the Platform Manager to oversee the implementation and maintenance of this procedure. The Platform Manager must ensure that staff or clients have been adequately trained to perform this procedure.

It is the responsibility of staff and clients involved in performing this technique to ensure that the methodology is followed correctly.

3. HEALTH AND SAFETY CONSIDERATIONS

Gloves and Laboratory gowns should be worn when performing this procedure.

All clients must undergo a training program with a suitably qualified staff member prior to performing this technique.

Refer to Protocol for Staff Occupational Health and Safety PQMS3-MHP-SOP-0008. Refer to Protocol for Client Occupational Health and Safety PQMS3-MHP-SOP-0009. Refer http://www.monash.edu.au/ohs/ for general safety information

4. PROCEDURE

Refer to Protocol for Staining PQMS3-MHP-SOP-0026-V for general staining information. This is a useful contrast stain to the Van Gieson's Stain.

Fixation Requirements:

- 10%Neutral buffered formalin or
- Carnoy's solution or

- Bouin's fixative

Reagents:

- 1. Modified Verhoeff's Solution:

  5% alcoholic Haematoxylin (freshly prepared) 20ml

  10% aqueous Ferric chloride 8ml

  Lugol's Iodine solution (1gm iodine crystals, 2gm potassium iodide, 100ml dist. water) 7ml Add the above reagents in the order given.

  Prepare this solution immediately before use.

- 2. Van Gieson's Stain:

  1% Aqueous acid Fuchsin

  7ml Saturated aqueous Picric acid 93ml

- 3. 2% Aqueous Ferric chloride

Method:

1. Bring paraffin sections to water.
2. Stain in Verhoeff's solution 15 minutes
3. Wash in water.
4. Wipe off surplus lake from around the section.
5. Differentiate in 2% aqueous ferric chloride a few seconds at a time, stop the process in tap water and examine microscopically till elastin fibres are defined on a slightly overstained background.
6. Wash in water.
7. Rinse in 95% ethanol.
8. Wash in water
9. Counter stain in Van Gieson's stain 2 minutes.
10. Rinse briefly in water.
11. Blot section with No.1 Whatman filter paper
12. Dehydrate in absolute ethanol 10 seconds.
13. Clear in xylene and mount.

Comments:

An excellent stain which requires careful judgement in differentiating to show the finest fibrils. Prolonged staining in Van Gieson's solution removes the elastic stain.

Results:

Elastic fibres— intense black

Chromatin— Black

Collagen fibres— Red

Other elements— Yellow or brownish yellow

5. REFERENCES

5.1 Internal

Protocol for Staining PQMS3-MHP-SOP-0026-V

5.2 External

Bancroft, J.D. and Gamble, M., Theory and Practice of Histological Techniques, 6th Edition, 2008, Page 152-3.

Appendix 2: Monash Histology Platform haematoxylin and eosin staining protocol

WORK INSTRUCTIONS FOR HAEMATOXYLIN AND EOSIN STAIN AUTOMATED METHOD FOR ROUTINE HISTOLOGICAL STAINING

PQMS3-MHP-WIN-0098-V3

DOCUMENT AUTHORISATION		Date of Next Review: 36 months	
Prepared by: Sue Connell	Technical Officer	Signed: SC – refer hard copy	Date: 24/10/13
Reviewed by: Camilla Cohen	Platform Manager	Signed: CC – refer hard copy	Date: 13/07/17
Authorised by: Camilla Cohen	Platform Manager	Signed: CC – refer hard copy	Date: 13/07/17
Additional authorisation if required			

1. PURPOSE

To describe the procedure used for differentiating nuclei from other tissue components in paraffin sections.

2. RESPONSIBILITIES

It is the responsibility of the Platform Manager to oversee the implementation and maintenance of this procedure. The Platform Manager must ensure that staff or clients have been adequately trained to perform this procedure.

It is the responsibility of staff and clients involved in performing this technique to ensure that the methodology is followed correctly.

3. HEALTH AND SAFETY CONSIDERATIONS

Gloves and Laboratory gowns should be worn when performing this procedure.

All clients must undergo a training program with a suitably qualified staff member prior to performing this technique.

Refer to Protocol for Staff Occupational Health and Safety PQMS3-MHP-SOP-0008.

Refer to Protocol for Client Occupational Health and Safety PQMS3-MHP-SOP-0009.

Refer http://www.monash.edu.au/ohs/ for general safety information

Refer Monash Risk Assessments https://riskcloud.net/prod/?ccode=monash#skiplink Staining Risk Assessment Ref 387

4. PROCEDURE

Refer to Protocol for Staining PQMS3-MHP-SOP-0026-V for general staining information.

Fixation Requirements:

- 10%Neutral buffered formalin
- Carnoy's solution
- Bouin's fixative

Reagents:

- Harris's Haematoxylin
- Acid alcohol
- Scott's tap water substitute
- 1% Alcoholic Eosin

Method:

<u>Select Program 1 on Leica XL Autostainer</u>

1. Ovenise sections for 25 minutes at 65 degrees Celsius
2. Dewax in 3 xylene changes 2 minutes each
3. Absolute alcohol x 3 for 2 minutes each
4. Running tap water 1 minute
5. Rinse in running tap water for 30 seconds
6. Stain in Harris's Haematoxylin for 5 minutes
7. Rinse in running tap water for 30 seconds
8. Differentiate in Acid Alcohol for 1 second
9. Rinse in running tap water for 30 seconds
10. Blue in Scott's tap water substitute for 30 seconds
11. Rinse in running tap water for 30 seconds
12. Stain in Aqueous Eosin for 2 minutes 30 seconds
13. Dehydrate in absolute alcohol x3 for 2 minutes each
14. Clear in xylene x 3 for 2 minutes each
15. Transfer via transfer station into xylene bath
16. Coverslip with Leica CV Mount

Results:

Nuclei— Dark blue

Other tissue components— Varying shades of pink

5. REFERENCES

5.1 Internal

Protocol for Staining PQMS3-MHP-SOP-0026-V

5.2 External

Bancroft, J.D. and Gamble, M., Theory and Practice of Histological Techniques, 6th Edition, 2008, page 126-7.

Appendix 3: Monash Histology Platform Masson's Trichrome staining protocol

WORK INSTRUCTIONS FOR MASSON'S TRICHROME STAIN FOR COLLAGEN FIBRES

PQMS3-MHP-WIN-0052-V2

DOCUMENT AUTHORISATION		Date of Next Review: 12 months	
Prepared by: Jonathan Bensley	Technical Assistant	Signed: JB – refer hard copy	Date: 29/09/14
Authorised by: Camilla Cohen	Platform Manager	Signed: CC – refer hard copy	Date: 29/09/14
Additional authorisation if required			

1. PURPOSE

Masson's Trichrome is the most popular of the Trichrome stains and is a good stain for examining collagen deposition within tissue.

2. RESPONSIBILITIES

It is the responsibility of the Platform Manager to oversee the implementation and maintenance of this procedure. The Platform Manager must ensure that staff or clients have been adequately trained to perform this procedure.

It is the responsibility of staff and clients involved in performing this technique to ensure that the methodology is followed correctly.

3. HEALTH AND SAFETY CONSIDERATIONS

Gloves and Laboratory gowns should be worn when performing this procedure.

All clients must undergo a training program with a suitably qualified staff member prior to performing this technique.

Refer to Protocol for Staff Occupational Health and Safety PQMS3-MHP-SOP-0004. Refer to Protocol for Client Occupational Health and Safety PQMS3-MHP-SOP-0005. Refer http://www.monash.edu.au/ohs/ for general safety information

4. REAGENTS

i) Bouin's Fixative

(1) 250 mL of Formalin (37%)

(2) 750 mL of saturated aqueous picric acid

(3) 50 mL of glacial Acetic acid

ii) Weigert's Iron Haematoxylin

(1) Solution A

(a) 5 g of Haematoxylin powder

(b) 500 mL of absolute Ethanol

(2) Solution B

(a) Add 6 grams of ferric chloride to 520mL of distilled water, and then add 5mL of concentrated hydrochloric acid. Stir continuously until the ferric chloride is completely dissolved.

(3) Mix solution A and B in equal parts, does not keep beyond a day

iii) Celestin Blue R

(1) 25 grams of Ferric ammonium sulphate

(2) 500 mL of distilled water

(3) 2.5 grams of Celestin Blue

Bring to the boil on a hot plate. Cool rapidly using a magnetic stirrer. When cool, add 70 mL of glycerin

iv) Biebrich scarlet-acid fuchsin staining solution

(1) 9 grams of Biebrich scarlet in 900 mL of distilled water

(2) 1 gram of acid fuchsin in 100 mL of distilled water

(3) 10 mL of glacial acetic acid

v) 5% aqueous Tungstophosphoric acid

(1) 50 grams of Tungstophosphoric acid

(2) 1,000 mL of distilled water

vi) Aniline blue staining solution

(1) 25 grams of Aniline Blue

(2) 25 mL of glacial Acetic acid

(3) 1,000 mL of distilled water

vii) 0.5% acid alcohol

(1) 5 mL of concentrated hydrochloric acid

(2) 995 mL of 70% aqueous ethanol

viii) 1% aqueous acetic acid

(1) 1 mL of glacial Acetic acid

(2) 99 mL of distilled water

5. PROCEDURE

1. Bring sections to water

2. Place sections in Bouin's fixative either overnight at room temperature or 1 hour at 60°C

3. Wash the sections in running water

4. Stain sections in Celestin Blue for 5 minutes

5. Wash the sections in tap water
6. Place the section in Weigert's haematoxylin for 30 minutes
7. Wash the sections in running tap water
8. Differentiate briefly in acid alcohol
9. Wash in running tap water for 10 minutes
10. Stain with Biebrich scarlet-acid fuchsin for 5 minutes
11. Wash briefly in distilled water
12. Apply 5% tungstophosphoric acid for 5 minutes
13. Wash briefly in distilled water
14. Stain with Aniline blue staining solution for 5 minutes
15. Wash in 1% aqueous acetic acid for 3 minutes
16. Dehydrate through 3 changes of ethanol
17. Clear in 3 changes of xylene
18. Mount with DPX

6. RESULTS

Collagen— Blue

Cytoplasm and muscle— Red

Nuclei— Dark brown to Black

7. REFERENCES

7.1 Internal

Protocol for Staining PQMS3-MHP-SOP-0026-V

7.2 External

Masson PJ, 1929, J. Tech. Methods, 12 p 75-90

8. COMMENTS

The given method is representative of a large group of collagen fibre stains based on the original methods of Mallory and Heidenhain. The trend to introduce more complexity (*) into the method by additional differentiating steps limits many modifications to specialised laboratories.

Remarks made under Van Giesen's stain are relevant to these methods and the function of tungstophosphoric acid which has both an affinity for collagen fibres and NH2 groups of triphenylmethane dyes increases the selectivity of the fibre stain.

* Picro-Mallory stain, MacFarlane Stain Tech. V.19, p.29. 1944